THESIS

MOTORIZED WINTER RECREATION IMPACTS ON SNOWPACK PROPERTIES

Submitted by

Jared Tucker Heath

Department of Ecosystem Science and Sustainability

In partial fulfillment of the requirements

For the Degree of Master of Science

Colorado State University

Fort Collins, Colorado

Summer 2011

Master's Committee:

Advisor: Steven Fassnacht

Kelly Elder
John Stednick
Kenneth Wilson

ABSTRACT

MOTORIZED WINTER RECREATION IMPACTS ON SNOWPACK PROPERTIES

Winter recreation, consisting of snowshoeing, skiing, snowboarding, and snowmobiling, has been increasing annually in Colorado's forests. This increase in recreational activity creates direct and indirect wildlife interactions. Motorized winter recreation in the backcountry compacts the snow possibly influencing the physical and mechanical properties of the snowpack. Snow depth, density, stratigraphy and grain characteristics control to the insulating properties of the snowpack and create habitat for small non-hibernating mammals. Changes to these physical properties and compaction of the subnivean space may be detrimental to these species. Two hypotheses were formulated: (1) a snowpack compacted by motorized winter recreation will result in changes to physical and mechanical properties of the snowpack; and (2) the amount of motorized winter recreation and the depth of snow when motorized winter recreation begins affects the physical properties of the snowpack.

During the 2009-2010 winter season snow compaction plots near Rabbit Ears Pass and Fraser Experimental Forest, Colorado were manipulated with varying use of motorized winter recreation (low, medium and heavy use) beginning on different snow depths, shallow (30 cm) and deep (120 cm). Physical and mechanical properties of the snowpack, including snow density, temperature, snow depth, snow water equivalent, stratigraphy, hardness and ram resistance were measured and used to examine the statistical difference between no use and varying degrees of motorized winter recreation (low, medium and heavy use). The results were used to infer implications on changes to the insulative value of the subnivean space and the potential for movement by subnivean mammals.

The largest differences in snowpack properties were associated with motorized winter recreation beginning on a shallow snowpack. Compaction from motorized winter recreation that began on a shallow snowpack increased both mean and subnivean density, hardness, and ram resistance, which resulted in significant differences ($p<0.10$) between varying use of motorized winter recreation and no use. Snow depth and basal temperatures (ground/snow interface) decreased as a result of motorized winter recreation beginning on a shallow snowpack ($p<0.10$), while temperature gradients were unaffected throughout the duration of the winter season. Implications to changes in these snowpack properties could decrease the insulative value of the snowpack and make movement by small mammals that utilize the subnivean space more difficult. On the contrary, motorized winter recreation that began on a deep snowpack showed no significant difference suggesting later initiation of use minimizes changes to snowpack properties from compaction.

ACKNOWLEDGEMENTS

Appreciation goes Robert Skorkowsky, Kent Foster and Becky Jones of the Hahns Peak/Bears Ears Ranger District of the US Forest Service for their help and support on Rabbit Ears Pass, and Kelly Elder of the Rocky Mountain Research Station (US Forest Service) for his support at Fraser Experimental Forest. I would like to recognize the Colorado Mountain Club for their help supporting this project with a generous grant. Special gratitude is necessary to those who contributed their time and contribution to field data collection: Megan Maiolo, Adam Heath, Joel Murray and Amir Kashipazha. Additional gratefulness is extended to James zumBrunnen for his support on statistical analysis for this project. I would like to acknowledge members of my graduate committee, Dr. Steven Fassnacht, Dr. Kevin (Kelly) Elder, Dr. John Stednick and Dr. Kenneth Wilson, for their support and guidance throughout this project. Thank you to my family and friends as they have provided continuous support in my personal and academic pursuits.

TABLE OF CONTENTS

LIST OF FIGURES

LIST OF TABLES

1.0 INTRODUCTION

1.1 Introduction

The seasonal snowpack of Colorado is not only a major source of water to the semi-arid west (Wahl, 1992), but for small terrestrial mammals it offers an overwintering seasonal habitat known as the subnivean space (Pruitt, 1984). The subnivean space is contained within the snowpack and can be defined as the interface between the snow and the ground, or vegetation confined within the snowpack (Figures 1.1a and 1.1b). This seasonal microhabitat provides a space for movement and protection for small terrestrial mammals from predation and the extreme climate conditions of the winter season (Auerbach and Halfpenny, 1991). The presence of the subnivean space within the snowpack, and the ability of non-hibernating terrestrial small mammals to move within this space are important for these mammals' overwintering success (Formozov, 1946; Pruitt, 1984).

The Colorado snowpack also offers outdoor winter recreational opportunities in national and state forests, and the presence of human activities may influence these seasonally snow-covered environments. Winter recreational activity in forests includes snowshoeing, skiing, snowboarding, and snowmobiling. As the number of people participating in these activities increases annually (Cook and Borrie, 1995; Winter Wildlands Alliance, 2006), management practices have been implemented by land management agencies. These include establishing boundaries to decrease conflict between users and seasonal closures related to snow depth. Imposed boundaries typically separate non-motorized from motorized recreation.

Around Rabbit Ears Pass, located on U.S. Highway 40 in the Medicine Bow-Routt National Forest in Northern Colorado, non-motorized recreation is permitted west of the pass and motorized recreation is permitted east of the pass. The boundary designating winter recreational usage on Rabbit Ears Pass provides an opportunity to study the influence of motorized recreation on the physical properties of the snowpack in relation to the subnivean space. Small mammals of particular interest inhabiting the subnivean space, listed on the 2009 Regional Forester's Sensitive Species List for the Routt National Forest (USDA Forest Service Rocky Mountain Region), include the pygmy shrew (*Sorex hoyi*) and Wyoming pocket gopher (*Thomomys clusius*). Few studies have been implemented to examine the impacts of motorized winter recreation on the snowpack with respect to the subnivean space (Sanecki et al., 2006).

Motorized winter recreation in the backcountry compacts the snow, influencing the physical properties of the snowpack. Snow depth, density, and grain characteristics contribute to the insulating properties of the snowpack and provide a seasonal habitat for non-hibernating terrestrial mammals. Changes to these physical properties and compaction of the subnivean space may be detrimental to species depending on this seasonal habitat and their overwintering success. The United States Department of Agriculture (USDA) Forest Service managing the Routt National Forest has not only implemented boundary regulations, but they have also put into effect regulatory practices designating the start of the snowmobile season when the unpacked snow depth equals or exceeds 30 cm (12 inches) (USDA Forest Service, 2005). There have been limited studies regarding the effectiveness of the current management plan with respect to an adequate snow depth that would minimize the potential impact motorized winter recreationalists have on this seasonal habitat. The goal of this research was to assess the impact of motorized winter recreation on snowpack properties and the subnivean space.

1.2 Hypotheses

Two hypotheses were tested: (1) a snowpack compacted by motorized winter recreation will result in changes to physical and mechanical properties of the snowpack; and (2) the amount of motorized winter recreation and the depth of snow when motorized winter recreation begins affect the physical properties of the snowpack.

1.3 Objectives

The objectives of this research were: (1) to examine the effect of motorized winter recreation on the physical properties of the snowpack; (2) to analyze the change in the physical properties of a snowpack by varying use of motorized recreation; (3) to assess the effect of motorized winter recreation on the potential for subnivean movement by quantifying the force required to penetrate the subnivean space; and (4) to evaluate these effects based on the depth of snow when motorized winter recreation begins (30 cm and 120 cm) and the snowfall environment (shallow versus deep) where motorized winter recreational vehicles operate.

Figure 1.1a. An example of animal tunnelling near the subnivean space.

Figure 1.1b. An example of subnivean space around vegetation.

2.0 BACKGROUND

2.1 Motorized Winter Recreation

Winter backcountry recreation has been increasing due to the availability and accessibility to trail systems in our state and national forests. Technological advances in outdoor equipment, such as improvements to snowshoes and skis, the introduction of snowboards, and more powerful snowmobiles, have also contributed to this increase in usage. There are over two million cross-country and snowshoe visits and 1.3 million snowmobile visits to Colorado's National Forests annually (Winter Wildlands Alliance, 2006). These recent advances have allowed more individuals to access remote and backcountry terrain increasing human/animal interaction.

The winter season is a critical period for the survival of many species of mammals relying on seasonal snow habitats. Snowmobiles present disturbance in the backcountry that may directly and indirectly disrupt wildlife. In the case of non-hibernating burrowing mammals, the presence of snomobiles may alter the seasonal habitat essential for overwintering success. Snowmobiles compact the snow providing an area where animals can travel over the snow surface more efficiently compared to deep uncompacted snow. The presence of compacted snowmobile trails may indirectly influence the interaction between predators competing for prey. Although there are other winter recreational activities that compact the snow, snowmobiling often creates extensive trail systems that potentially influence predator communities. Research on the effect of snowmobile trails on coyote movements within a lynx habitat determined that coyotes tend to select compacted snow for efficient travel (Kolbe et al., 2007). Although coyotes used snow compacted trails created by snowmobiles, it is unlikely that snowmobile trails affect competitive interactions between coyotes and lynx.

Motorized winter recreation can influence wildlife populations directly, as snowmobile “noise” can result in a flight response by wildlife. A flight response consumes valuable energy reserved for the winter season. It was concluded that snowmobile traffic resulted in displacement of white-tailed deer populations, which was directly proportional to snowmobile usage (Dorrance et al., 1975).

2.2 Subnivean Space and Burrowing Wildlife

The winter snowpack provides a seasonal habitat for many non-hibernating burrowing animals, in particular, small mammals such as voles, lemmings and shrews. The subnivean space is located within the matrix of the basal winter snowpack, and this microhabitat is important for the overwintering success of these animals. A number of factors are associated with the protection of animals relying on the subnivean space in relation to their overwintering success, including the insulative value and ability to move under the snow.

Auerbach and Halfpenny (1991) studied the overwinter success of small burrowing mammals. They looked at the snowpack and subnivean environment in an open meadow and evaluated snowpack depth, ground and surface temperatures, and snow crystal characteristics on different aspects. These properties were associated with

Marchand's (1982) thermal index measurement, an insulative value for the snowpack calculated from layer characteristics (layer thickness divided by density). The thermal index is a useful tool for evaluating the variable thermal properties within the snowpack, specifically related to the subnivean environment (Marchand, 1982). Suitable thermal conditions for the subnivean space require a high thermal index directly related to a deep snowpack.

The snowpack is a porous material composed mostly of air acting as a reliable thermal insulator. Compaction of the snowpack occurs naturally over the duration of the winter season resulting in snowpack densification. This increase in density, subsequent to fresh snowfall, can be attributed to several processes, including gravitational settling, wind packing, melting, and re-crystallization (Dunne and Leopold, 1978). Compaction helps create rounder snow grains and initiates inter-granular particle bonds (sintering) that decrease the volumetric content of air within the snowpack. This process results in an increase in the snowpack density, indirectly decreasing the thermal insulation of the snowpack. Auerbach and Halfpenny (1991) also concluded that suitable snow conditions for the subnivean space require stable and warm ground/snow interface temperatures. The thermal energy emitted at the ground/snow interface results in the formation of subnivean space by means of snow metamorphism. Each of these characteristics plays a vital role in maintaining a subnivean habitat for non-hibernating burrowing mammals.

The snowpack is variable throughout the duration of the winter season, and burrowing animals may have a choice on where they spend the winter (Auerbach and Halfpenny, 1991). Courtin et al. (1991) studied the overwintering success in the meadow vole (*Microtus pennsylvanicus*) by investigating mortality prior to and during winter.

High mortality rates were associated with rain and subfreezing temperatures prior to winter and shallow snowpacks during winter (Courtin et al., 1991). Climate variability resulting in pre-winter frozen soils can prevent burrowing animals from seeking protection in the soil. Additionally, early season snowpacks are typically shallow, providing little thermal stability for subnivean animals. Snowmelt and rain events in the spring negatively affect the thermal properties of snow creating ice layers with low thermal stability. These ice layers contain little volumetric air content crucial to insulating the snowpack. These ice layers effectively decrease the thermal stability of the snowpack directly impacting subnivean animals (Courtin et al., 1991).

Courtin et al. (1991) defined the cold season relative to differing characteristics that are hazardous to the success of subnivean mammals by four periods: pre-nival, nival, thaw, and post-nival period. The establishment of an adequate snowpack is critical for the survival of small mammals due to their inability to survive severe climate fluctuations (Pruitt, 1960). Therefore, the most critical periods for subnivean mammals are the pre-nival, thaw and post-nival periods. Pruitt (1970) defined the critical snow depth required for the subnivean environment to reach the maximum insulative value as the “hiemal threshold.” The snow depth required to reach this maximum insulative value was determined to be 20 cm, although changes in snow density and grain characteristics influence thermal conductivity and the insulative value (Aitchison, 2001; Green, 1998). Climate and weather fluctuations during these periods, in addition to the presence of motorized winter recreation, may accentuate the changes in the physical properties of the snowpack that subnivean animals depend on for success.

2.3 Snowpack Properties

Snow is a porous material that varies over space and time. The formation of snow crystals begins in atmospheric clouds where they experience a variety of changing environmental conditions. These conditions continue to change as snow crystals travel through the atmosphere from the clouds to the ground. As snow accumulates over space and time, the snowpack experiences a variety of environmental stimuli throughout the winter season and these stimuli can have a large influence on the material properties of the snowpack.

Following the accumulation of snow over the ground surface, the snowpack is bound by the ground and the atmosphere. The basal layer of the snowpack is warmed by the ground to temperatures near $0^{o}C$ as a result of warm summer temperatures and geothermal heating, which generally remains relatively steady for the duration of the winter season. Conversely, the surface of the snowpack is exposed to cold atmospheric air temperatures, which fluctuate between the day and night causing diurnal fluctuations and at times can be extreme (McClung and Schaerer, 2006). Extremes in temperature between the insulated basal layer and the cooler snow surface can generate a temperature gradient measured by the change in temperature over the depth in which the temperature change occurs. The temperature gradient of the snowpack is expressed in degrees Celsius per meter and vertical bulk temperature gradients can exceed $50^{o}C\ m^{-1}$ especially in continental climates, such as Colorado, that experience shallow, high porosity early season snow cover and cold arctic air masses (Colbeck, 1987). Strong temperature gradients are the driving force behind metamorphic processes that occur within the snowpack directly influencing the microstructure of the snowpack.

Two different types of metamorphism can occur within the snowpack: (1) equilibrium metamorphism results in hexagonal crystals becoming rounded (smaller grains) over time, and (2) kinetic growth metamorphism results in the formation of large cohesionless crystals known as facets. These processes of metamorphism are strongly influenced by temperature gradients within the snowpack. When the temperature gradient is small, vapor diffusion is limited within the snowpack and growth rate of snow crystals is slow, tending to favor recrystalization of the hexagonal form and sintering of ice grains (Colbeck, 1982). Conversely, kinetic growth occurs when a large temperature gradient in the snowpack increases the vapor pressure gradient resulting in diffusion of vapor onto grains higher in the snowpack where temperatures are colder. This metamorphic process results in the growth of grains and, if the growth rate is sufficient, the formation of cohesionless, faceted crystals (Colbeck, 1982). "*The critical temperature gradient to produce faceted forms in alpine snow is about* $10^oC\ m^{-1}$*; below this value, rounded forms tend to appear* (McClung and Shaerer, 2006)." Formation of faceted crystals near the base of the snowpack, termed as depth hoar, is associated with structural weakness (DeWalle and Rango, 2008), which may be important for unimpeded mammalian movement near the subnivean space. Changes in the microstructure of the snowpack as a result of metamorphism indirectly influence the physical and mechanical properties of the snowpack including density, hardness and ram resistance.

The snowpack is a porous material composed of interconnected ice, water and air and this granular matrix is directly related to the physical and mechanical properties of the snowpack. Snow density is defined as the mass per unit volume of snow. The density of fresh snow is approximately 100 kg/m^3; however, the density of fresh snow can vary because fresh snow density is a function of atmospheric conditions including crystal characteristics (shape and size), air temperature and humidity between the clouds and the ground, and surface characteristics, such as wind. As a result, the density of fresh snow may range from as low as 40 kg/m^3 to as high as 200 kg/m^3 (Diamond and Lowry, 1953; Schmidt and Gluns, 1991; Fassnacht and Soulis, 2002). The snowpack begins to experience changes immediately following deposition on the ground through a process known as densification. Densification of the snowpack can occur as a result of several natural processes including crystal metamorphism, wind redistribution, gravitational force due to the weight of overlying snow, and snowmelt processes. Field observations prior to snowmelt have revealed maximum late season snowpack densities ranging from 290 kg/m^3 to 400 kg/m^3 with snow densities as high as 500 kg/m^3 during snowmelt (Gold, 1958; Longley, 1960). For comparison, the density of ice at 0^oC is approximately 917 kg/m^3 and the density of water at 0^oC is approximately 1000 kg/m^3. Therefore, it is the high porosity composed mostly of air that makes snow an effective thermal insulator; however, changes in snow density can have an effect on thermal properties of the snowpack.

Thermal conductivity can be defined as the amount of energy that passes through a medium (the snowpack) over a given temperature gradient (between the surface, or top and bottom of the snowpack) usually expressed in units of $W\ m^{-1}\ K^{-1}$. Heat transfer along this temperature gradient is driven by three processes, including conduction through the ice matrix, conduction through air space and latent heat exchange (DeWalle and Rango, 2008; Strum et al. 1997). Within the snowpack, the thermal conductivity is a function of the density, grain characteristics (size and bonding) and temperature, and its high insulative value is due to the presence of large amounts of air, since air has a very low thermal conductivity. The thermal conductivity of air at 0^oC with a density of 1.29 kg/m^3 is 0.02 W m^{-1} K^{-1}. In comparison, the thermal conductivity of ice at 0^oC with a density of 916 kg/m^3 is two orders of magnitude higher at 2.22 W m^{-1} K^{-1} (DeWalle and Rango, 2008). In addition, latent heat transfer occurs when a temperature gradient induces vapor diffusion within pore spaces resulting in sublimation and/or condensation of vapor and the exchange of latent heat. The rate of vapor diffusion within the snowpack is a function of the temperature gradient, pore space and temperature. (DeWalle and Rango, 2008). Compaction from motorized winter recreation may alter density and grain characteristics, decreasing pore space and increasing the rate of heat transfer through the more efficient ice matrix, thereby adversely impacting the insulative value.

Densification not only influences the thermal conductivity of the snowpack, but also the snow hardness and ram resistance due to changes in the arrangement of ice grains. Hardness can be defined as a measure of strength in compression expressed in force per unit area and as the density of the snowpack increases the snow hardness increases (McClung and Shaerer, 2006). Hardness measurements are of particular importance for avalanche science and can be measured by the Swiss rammsonde (ram penetrometer) or estimated by the hand hardness test. The hand hardness test is a subjective measure of hardness, however more quantitative measurements can be obtained using snow-hardness gauges and circular metal plates of known area (McClung and Shaerer, 2006; Höller and Fromm, 2010). The ram penetrometer is an instrument that can be used to measure the vertical resistance to penetration within the snowpack.

Ram penetrometer measurements for stratigraphic layers in the snowpack have been measured from 0 N to greater than 1000 N (Colbeck et al., 1990). Compaction of the snowpack results in deformation of the snowpack and relationships have been established between the density and mechanical properties; however, the most important factor behind changes in density, hardness and ram resistance is alterations in the ice matrix (bonding/grain contacts) (Shapiro et al., 1997).

3.0 STUDY SITES

3.1 Rabbit Ears Pass, Colorado

Rabbit Ears Pass is located in the Rocky Mountains of northern Colorado within the Medicine Bow-Routt National Forest along the boundary of Grand and Jackson counties (Figure 3.1a). The Medicine Bow-Routt National Forest is located along the Continental Divide encompassing the Yampa, Upper Colorado River and the North Platte River watersheds. The terrain consists primarily of open meadows, aspen stands and coniferous forests. The open meadows in this area are a characteristic habitat for a variety of non-hibernating terrestrial burrowing mammals and also offer parks for motorized recreationalists. Motorized and non-motorized recreational opportunities are easily accessed from U.S. Highway 40 on Rabbit Ears Pass. Non-motorized winter recreation is allowed west of Rabbit Ears Pass and motorized winter recreation is allowed east of the pass. For this research, four open meadows were chosen near the summit as study sites (Figure 3.1b). These sites were chosen in attempt to minimize environmental factors including, wind, solar radiation, elevation, aspect, and slope.

The Columbine SNOTEL (snowpack telemetry) site, managed by the Natural Resource Conservation Service (NRCS) National Water and Climate Center, was used to characterize the 2009-2010 winter on Rabbit Ears Pass. SNOTEL is an automated system that collects snowpack and climate data, specifically snow water equivalent

(SWE), air temperature, cumulative precipitation and snow depth. The Columbine SNOTEL is located at approximately 364222 m E (UTM), 4473384 m N (UTM) in Zone 13, at an elevation of 2,792 m.

Based on the Columbine SNOTEL data, Rabbit Ears Pass experienced below average SWE for the 2010 winter compared to the 29-year historical average (Figure 3.1c). A peak SWE of 556 mm was observed on 9 April, which was 93 percent of the historical average peak SWE. Late snowstorm events at the end of April and beginning of May increased the SWE to as much as 300 percent of the historical average, but extended periods of above average spring temperatures (Figure 3.1d) resulted in an earlier snowmelt and abrupt decrease in SWE (Figure 3.1c). Average daily temperatures on Rabbit Ears pass were generally colder than the 29-year historical average. The coldest average daily temperature was recorded on 4 December at -19.8^{o}C (Figure 3.1d). December and February were the coldest months and by April warmer than freezing temperatures were observed often (Figure 3.1d). Snow depth reached a maximum of 185 cm on 7 April, which was 92 percent of the eight-year historical average over the winter season. The snow depth recorded at the Columbine SNOTEL site was generally shallower than the historic average (Figure 3.1e).

3.1.1 Walton Creek

The Walton Creek trailhead was the non-motorized winter recreation study site, and was located at approximately 357172 m E (UTM), 4471909 m N (UTM) in Zone 13, at an elevation of 2,895 m (Figure 3.1b). Snowshoers, skiers, and snowboarders primarily use this area to access backcountry terrain, thus, the snowpack in this area was not influenced by motorized recreation. It was used as a control and was assumed that compaction from non-motorized recreation was negligible in comparison to compaction from motorized winter recreation.

3.1.2 Dumont Lakes

The Dumont Lakes trailhead is an access point for motorized recreationists. This study site is located at approximately 360879 m E (UTM), 4472356 m N (UTM) in Zone 13 at an elevation of 2,909 m (Figure 3.1b). Motorized winter recreation use in this area is heavy, especially on weekends and over holidays.

3.1.3 Muddy Creek

The Muddy Creek trailhead is an additional access point for motorized recreationists. This study site is located at approximately 363000 m E (UTM), 4472000 m N (UTM) in Zone 13 at an elevation of 2,900 m (Figure 3.1b). This area is an open meadow, heavily used by snowmobiles.

3.1.4 Snow Compaction Study Plots

Two experimental snow compaction study plots were located at approximately 354974 m E (UTM), 4472125 m N (UTM) in Zone 13 at an elevation of 3,059 m (Figure 3.1b). This area is an open meadow located in a non-motorized area. These plots were used for the snow compaction experiment.

3.2 Fraser Experimental Forest, Colorado

Another study site was established at Fraser Experimental Forest (FEF) near Fraser, Colorado. Fraser Experimental Forest is located in the Rocky Mountains of central Colorado in the Arapaho National Forest (Figure 3.1a), and is a research unit of the United States Forest Service (USFS) Rocky Mountain Research Station. The approximately 93 km^2 experimental forest is located within the Colorado headwaters basin and consists of a variety of terrain with elevations ranging from 2,680 to 3,900 m. The lower elevations are comprised of primarily lodgepole pine (*Pinus contorta*) forest and small-dispersed meadows. The Fraser Experimental Forest study site is located at approximately 422004 m E (UTM), 4411196 m N (UTM) in Zone 13 at an elevation of 2,851 m (Figure 3.1a).

The Berthoud Summit SNOTEL (snowpack telemetry) site, managed by the Natural Resource Conservation Service (NRCS) National Water and Climate Center, was used to characterize the 2009-2010 winter season at Fraser Experimental Forest. The Berthoud Summit SNOTEL is located at approximately 432940 m E (UTM), 4405853m N (UTM) in zone 13, at an elevation of 3,444 m.

Based on the Berthoud Summit SNOTEL, Berthoud Summit experienced above average SWE for the 2010 winter compared to the 29-year historical average (Figure 3.2a). A peak SWE of 622 mm was observed on 16 May, which was 115 percent of the historical average peak SWE. Late snowstorm events at the end of April and beginning of May resulted in peak SWE occurring ten days later to as much as 135 percent of the historical average, but extended periods of above average spring temperatures (Figure 3.2b) resulted in an earlier snowmelt and abrupt decrease in SWE (Figure 3.2a). Average daily temperatures at the Berthoud Summit SNOTEL were generally colder than the 29-year historical average. The coldest average daily temperature was recorded on 10 December at -22.2^{o}C (Figure 3.1d). December and February were the coldest months and by April warmer than freezing temperatures were observed often (Figure 3.2b). Snow depth reached a maximum of 185 cm on 15 May, which was 147 percent of the eight-year historical average over the winter season. The snow depth recorded at the Berthoud Summit SNOTEL site was generally shallower than the historic average (Figure 3.2c). Measured snow depth at Fraser Experimental Forest never exceeded 1 m.

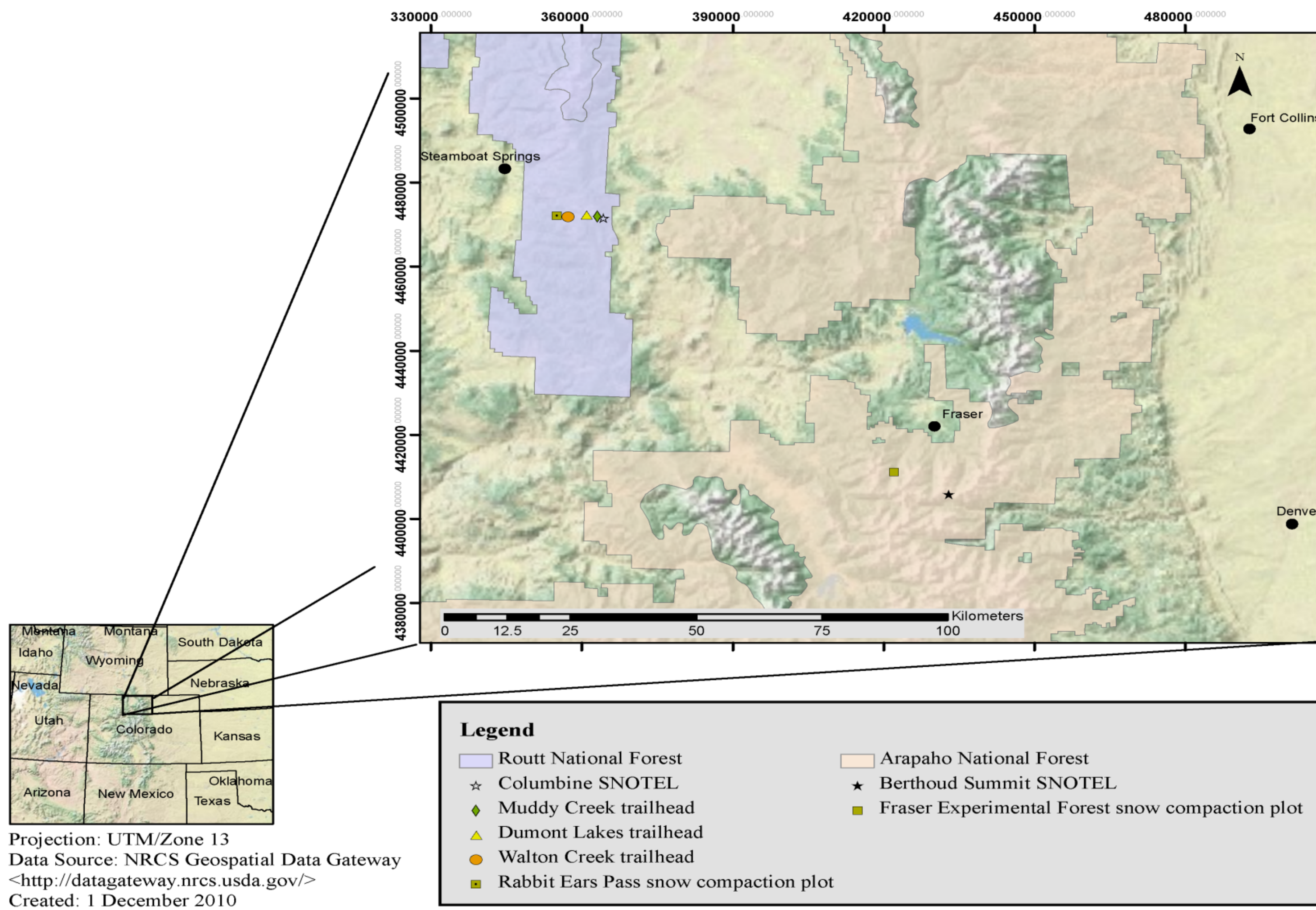

Figure 3.1a. The study sites are located on Rabbit Ears Pass in Routt National Forest and Fraser Experimental Forest in the Arapaho-Roosevelt National Forest, Colorado.

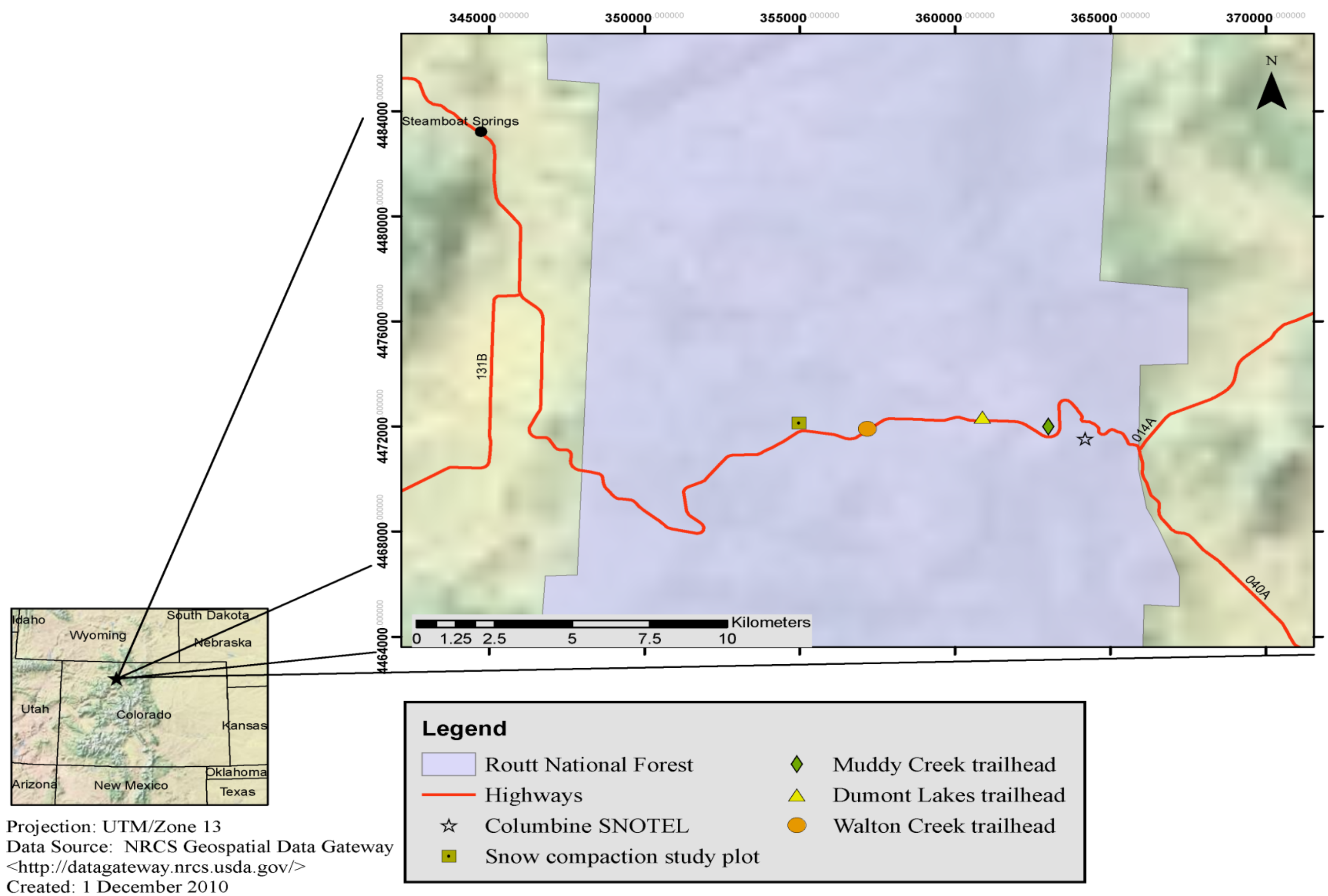

Figure 3.1b. Location of snow compaction plot and randomized snow pit analyses field sites on Rabbit Ears Pass, Colorado.

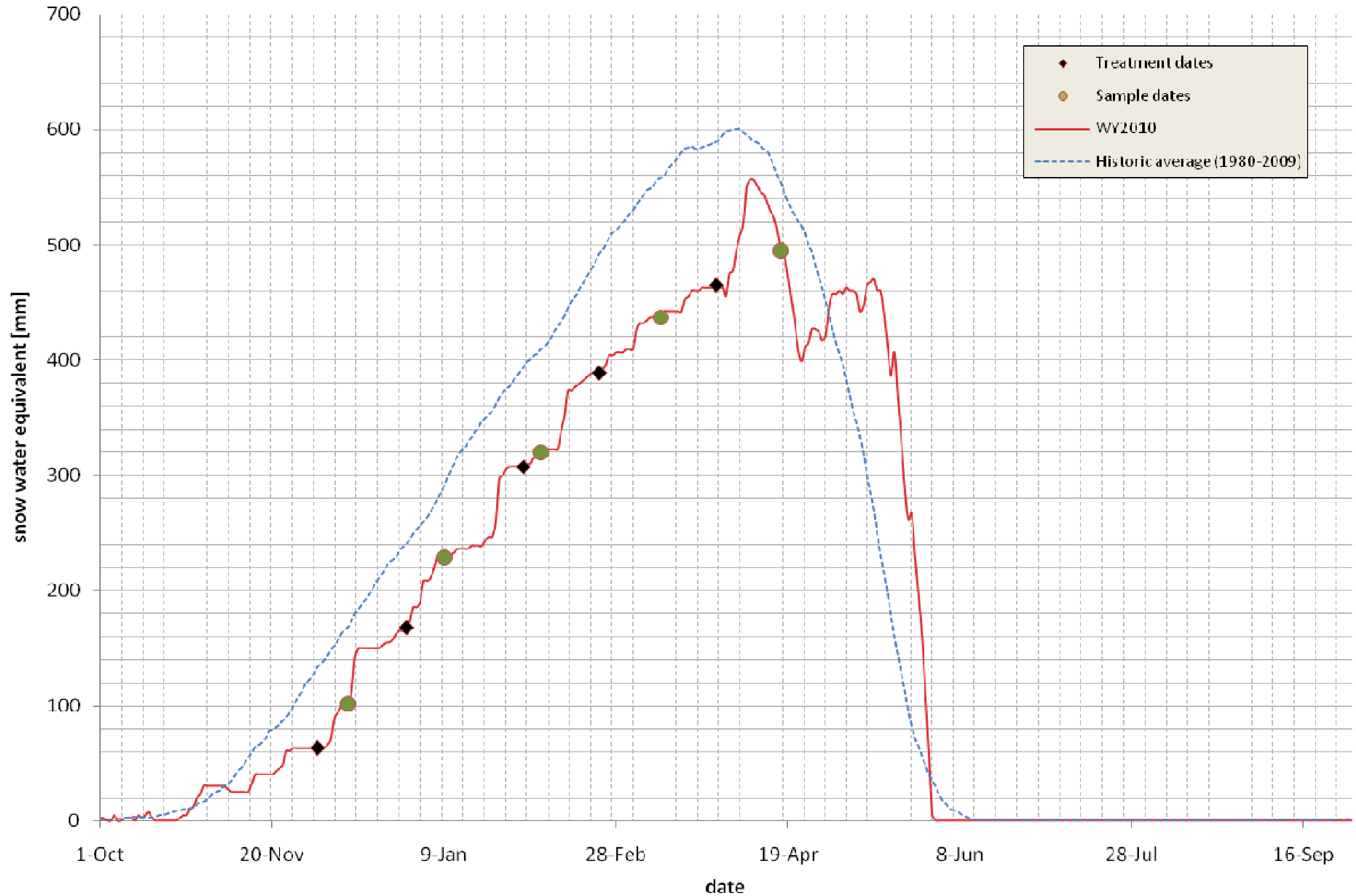

Figure 3.1c. Snow water equivalent for the 2010 water year (WY2010) and the 29-year historical average measured at the Columbine SNOTEL site near Rabbit Ears Pass, Colorado. Data was obtained online from the Natural Resource Conservation Service (NRCS) National Water and Climate Center (http://www.wcc.nrcs.usda.gov/; accessed 9/9/2010).

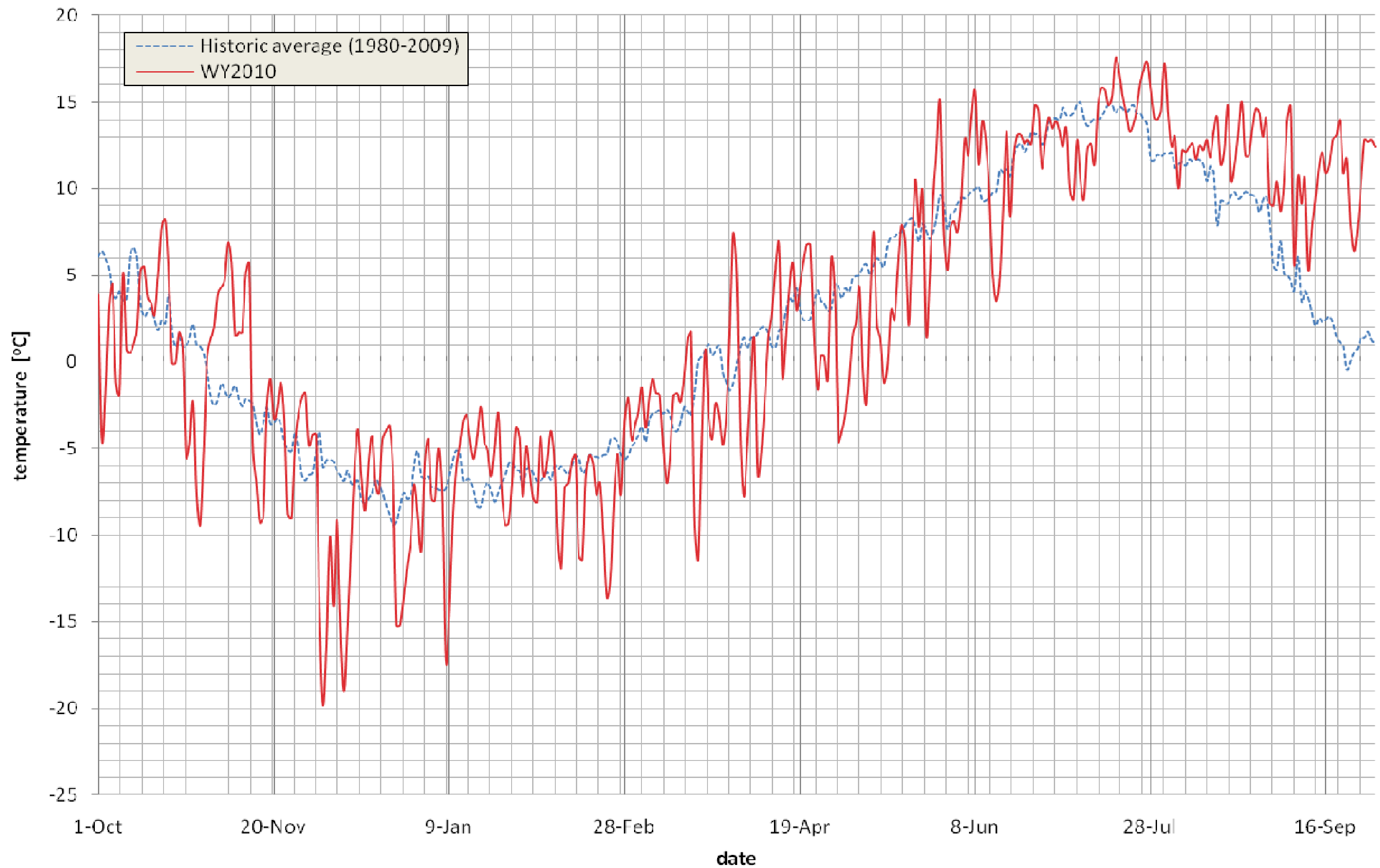

Figure 3.1d. Daily average air temperature for the 2010 water year (WY2010) and the 29-year historical average measured at the Columbine SNOTEL site near Rabbit Ears Pass, Colorado. Data was obtained online from the Natural Resource Conservation Service (NRCS) National Water and Climate Center (http://www.wcc.nrcs.usda.gov/; accessed 9/9/2010).

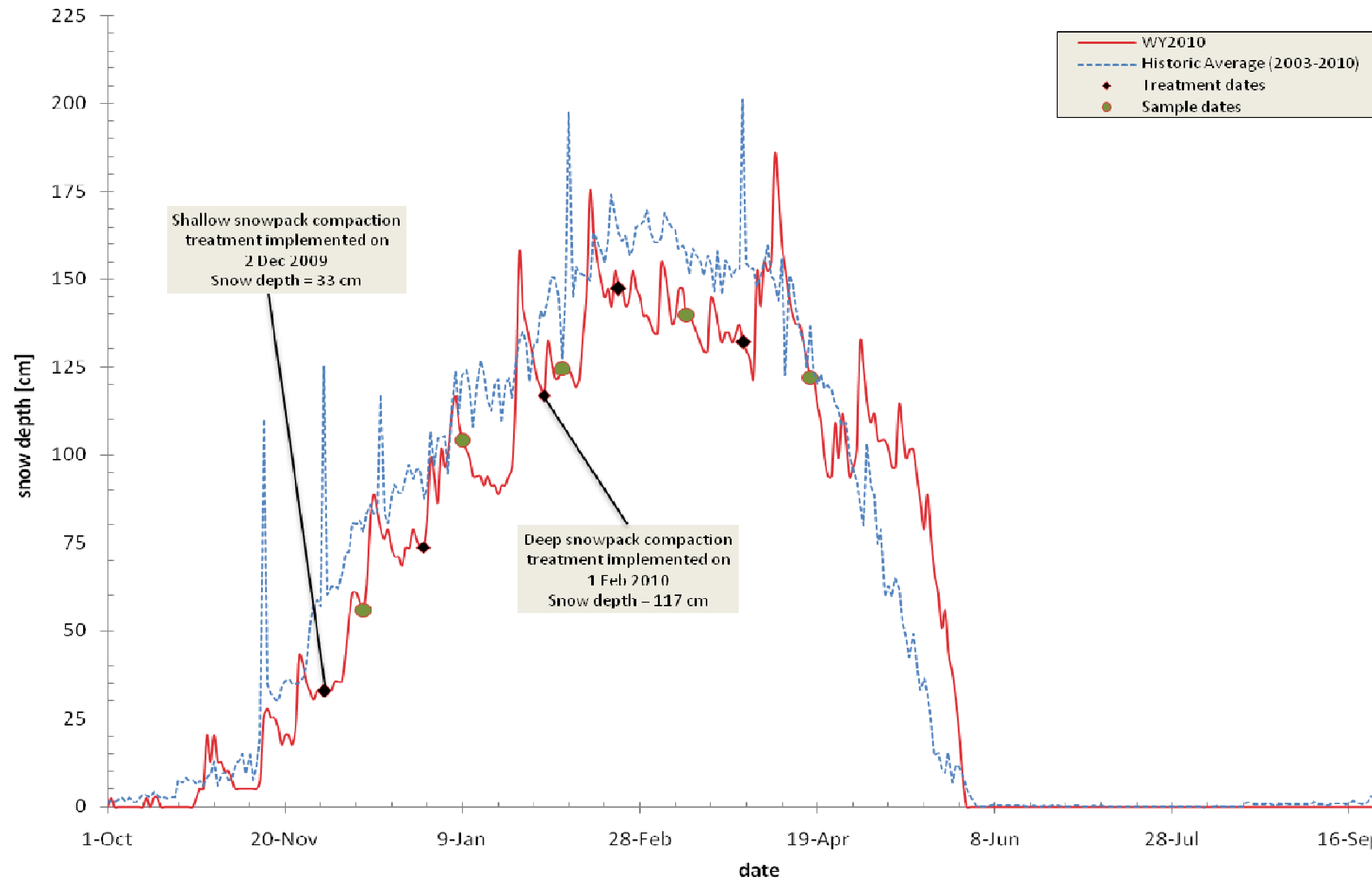

Figure 3.1e. Daily snow depth for the 2010 water year (WY2010) and the eight-year historical average measured at the Columbine SNOTEL site near Rabbit Ears Pass, Colorado. Data was obtained online from the Natural Resource Conservation Service (NRCS) National Water and Climate Center (<http://www.wcc.nrcs.usda.gov/>; accessed 9/9/2010).

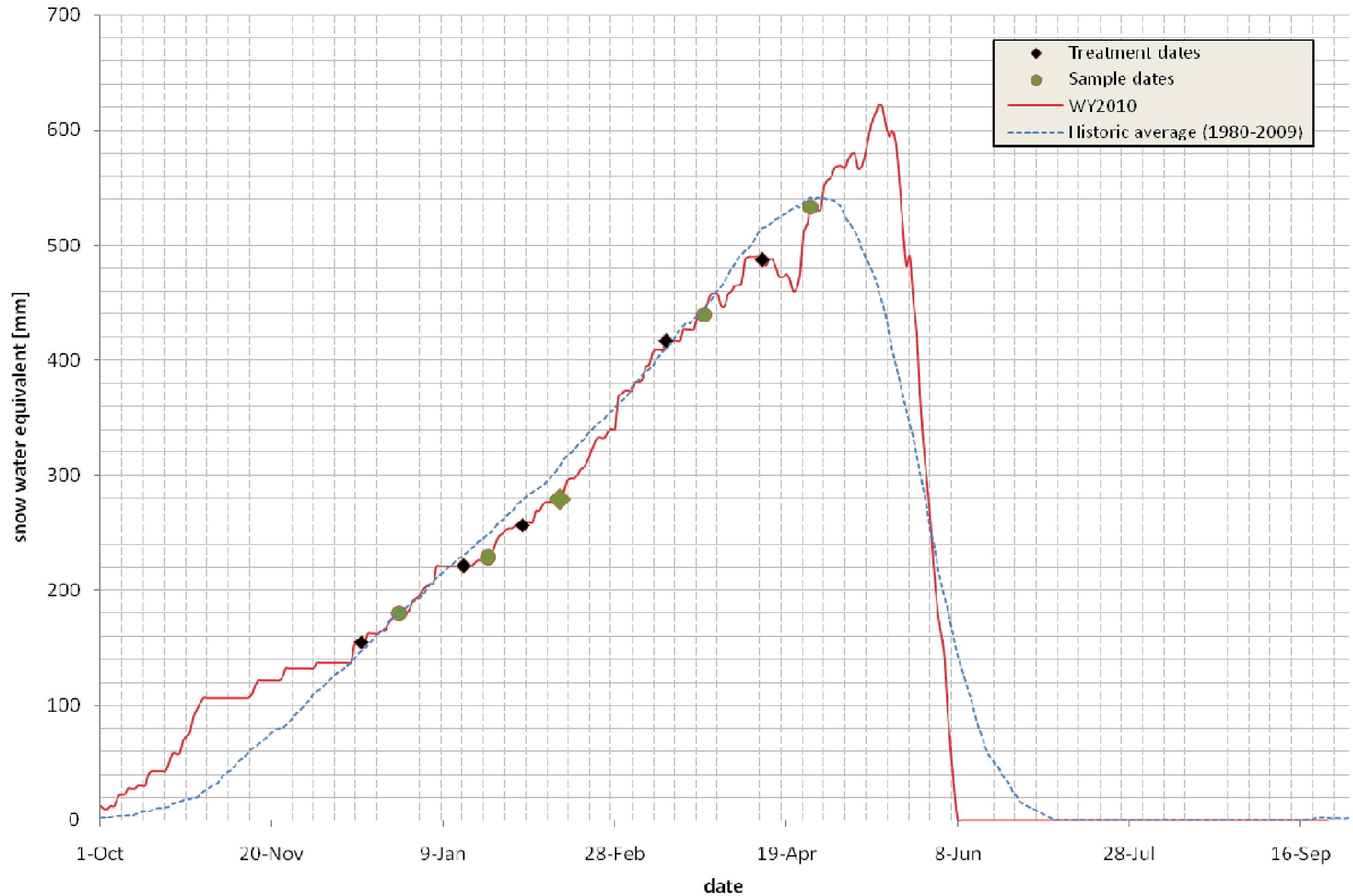

Figure 3.2a. Snow water equivalent for the 2010 water year (WY2010) and the 29-year historical average measured at the Berthoud Summit SNOTEL site near Fraser Experimental Forest, Colorado. Data was obtained online from the Natural Resource Conservation Service (NRCS) National Water and Climate Center (<http://www.wcc.nrcs.usda.gov/>; accessed 9/9/2010).

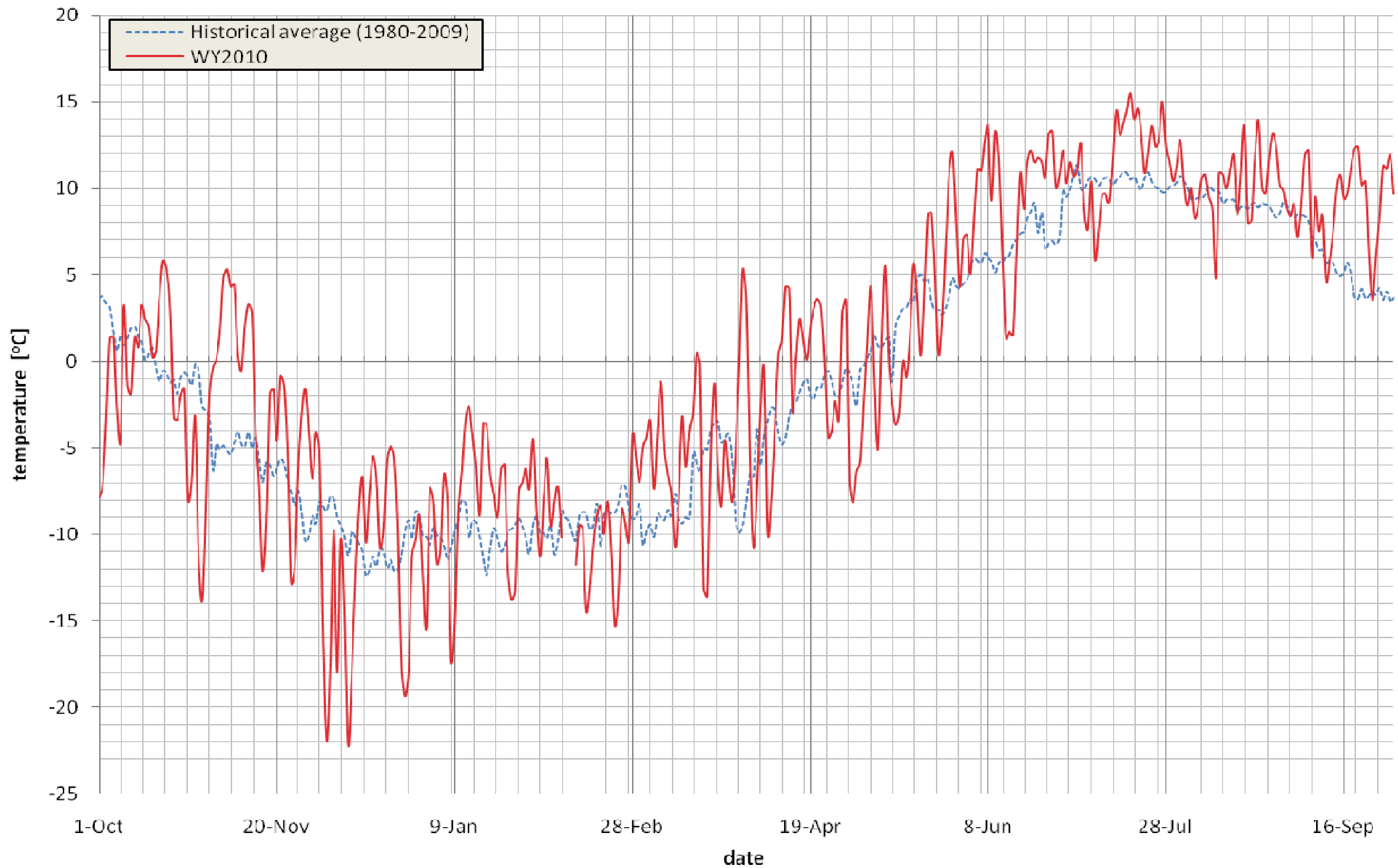

Figure 3.2b. Daily average air temperature for the 2010 water year (WY2010) and the 29-year historical average measured at the Berthoud Summit SNOTEL site near Fraser Experimental Forest, Colorado. Data was obtained online from the Natural Resource Conservation Service (NRCS) National Water and Climate Center (<http://www.wcc.nrcs.usda.gov/>; accessed 9/9/2010).

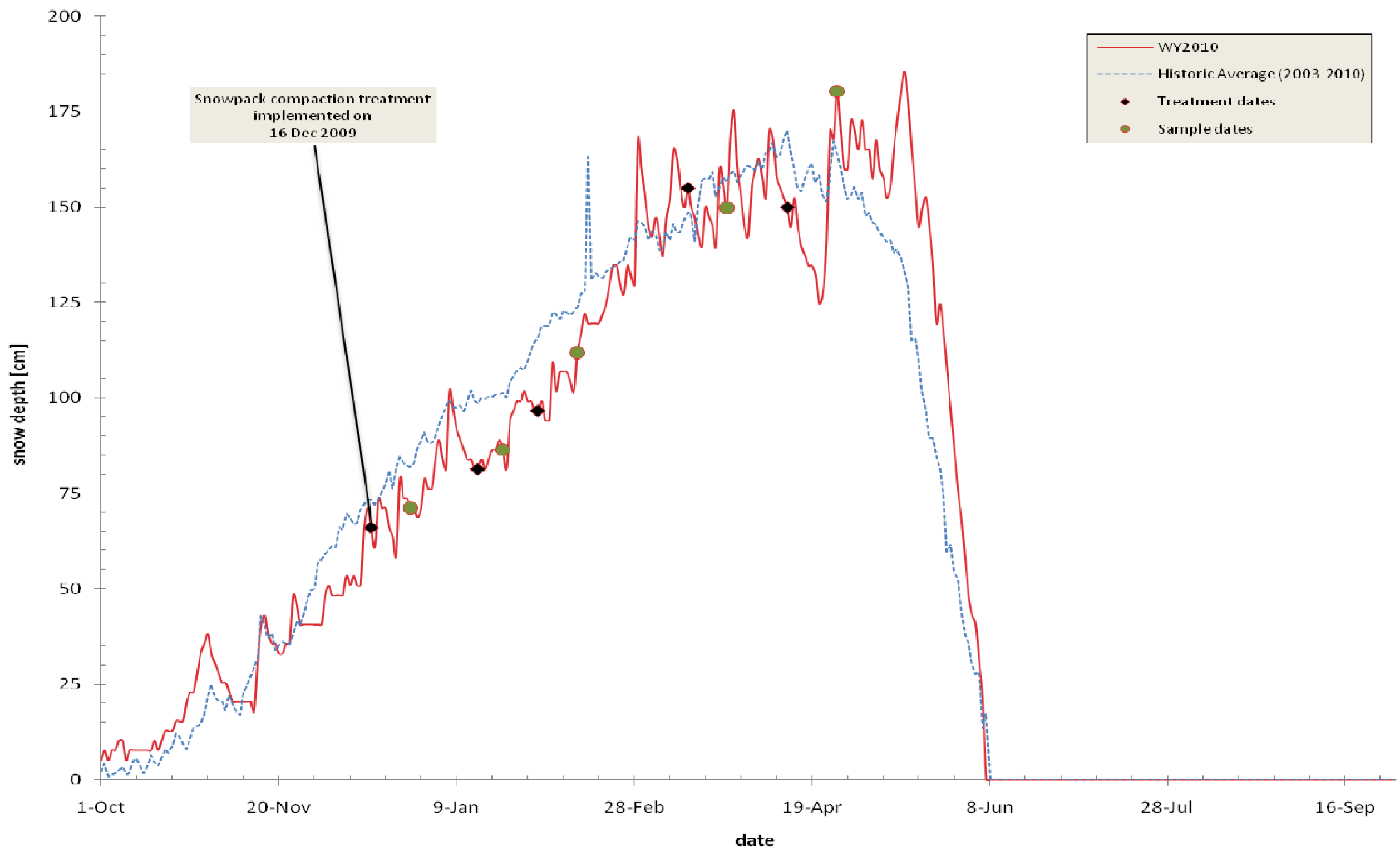

Figure 3.2c. Daily snow depth for the 2010 water year (WY2010) and the eight-year historical average measured at the Berthoud Summit SNOTEL site near Fraser Experimental Forest, Colorado. Data was obtained online from the Natural Resource Conservation Service (NRCS) National Water and Climate Center (<http://www.wcc.nrcs.usda.gov/>; accessed 9/9/2010).

4.0 METHODS

4.1 Snow Compaction Experimentation

4.1.1 Rabbit Ears Pass, Colorado

Two adjacent study plots were established in an undisturbed area on Rabbit Ears Pass. Each plot was 22 m wide and 15 m in length. The plots were divided into five equidistant transects (2 m) and treated with either low or heavy motorized use, including no treatment as a control transect representing an undisturbed snowpack. The locations of treatments and controls across the study plots were randomly selected. Each transect was separated by a 3 m buffer to eliminate the influence of compaction treatments to adjacent transects (Figure 4.1.1).

Transects were treated by driving a snowmobile over the length of each transect five or 50 times, representing low and high motorized winter recreational use, respectively (Figure 4.1.1). Treatments began when unpacked snow depths were approximately 30 cm (12 inches) and were implemented monthly thereafter (Figure 3.1e). This snow depth is the current management guideline for motorized winter recreation use designated in the Winter Recreation Management and Routt National Forest Plan Amendment (USDA Forest Service, 2005). Snow compaction treatments also began when unpacked snow depths equaled approximately 120 cm (48 inches) and were implemented monthly thereafter (Figure 3.1e) representing an alternative management strategy with respect to the start of the motorized winter recreation season. Snow pit measurements, described in the subsequent section, were undertaken once a month subsequent to each treatment.

4.1.2 Fraser Experimental Forest, Colorado

An additional study plot was located in Fraser Experimental Forest. This study plot was also 22 m wide and 15 m long. The plot was divided into equal width transects, which were treated with varying degrees of motorized winter recreation use: low, medium, and high (Figure 4.1.2). Two control transects were used to represent the undisturbed snowpack. Integrating two controls in the study plot allowed for replication and determination of experimental error. The location of treatments and controls across the study plot was randomly selected. Each transect was separated by a 3 m buffer to eliminate the influence of compaction treatments to adjacent transects (Figure 4.1.2).

Transects were treated by driving a snowmobile over the length of each transect. Transects were treated 5, 25 and 50 times, representing low, medium, and heavy motorized winter recreational use, respectively (Figure 4.1.2). The treatments were consistent with the Rabbit Ears study plots described above, with snow compaction treatments beginning when unpacked snow depths equaled 30 cm. Compaction treatments were implemented monthly thereafter (Figure 3.2c). Sampling was undertaken monthly after each treatment, and continued through the duration of the winter season (Figure 3.2c).

4.2 Snow Pit Analyses

Snow pit profiles were used to examine the physical and mechanical properties of the snowpack in all study areas. A vertical snow face was excavated by digging a pit from the snow surface to the ground and measurements of snow density, temperature, snow depth, stratigraphy, hardness and ram resistance were taken within the snowpack.

4.2.1 Density

Two snow density profiles were taken at 10 cm intervals, from the surface of the snowpack to the ground, by extracting a 250 mL or 1000 mL snow sample using a stainless steel wedge cutter and an electronic scale with a resolution of 1g. The density of the snow, ρ_s (g/cm^3), was determined by dividing the mass of the snow sample by the volume of the wedge cutter as follows:

$$\rho_s = \frac{\text{mass of snow sample (g)}}{\text{sample volume (cm}^3\text{)}} \qquad (4.1)$$

Snowpack density profiles, bulk snowpack density and the bottom 10 cm of the snowpack were compared. The bulk snowpack density was determined by averaging the depth integrated density measurements through the entire depth of the snowpack. The density measurements for the bottom 10 cm of the snowpack were averaged to obtain a mean density value for the subnivean space. Changes in this physical snowpack property and the difference between non-motorized and varying degrees of motorized winter recreation use were compared.

4.2.2 Temperature

Snowpack temperature measurements were obtained at 5 cm intervals from the top to the bottom of the snowpack using a dial stem thermometer with $\pm 1^{o}C$ accuracy, but repeatability for any given temperature is better and temperature gradients are well represented by this instrument (personal communication from K. Elder 2010). These measurements provided a temperature profile of the bulk snowpack, the temperature of the snow when the corresponding density was measured, and a representation of the temperature profile within the subnivean space. Snowpack temperature profiles and the corresponding bulk temperature gradient, the temperature gradient beginning at 10 cm and 5 cm, and the basal layer temperature (0 cm) of the snowpack were compared. The temperature gradient, T_G ($^{o}C/m$), was calculated as:

$$T_G = \Delta T/d \qquad (4.2)$$

where ΔT is the change in temperature (^{o}C) from the point of zero amplitude (upper boundary) (25-30 cm) and the temperature at 0 cm (lower boundary,) and d is the distance (m) over which the change in temperature occurs. For this study, the point of zero amplitude (25-30 cm) was used as the upper boundary to remove bias from diurnal fluctuations. The temperature gradient from 10 to 0 cm and 5 to 0 cm and the basal layer temperature (0 cm) were used to compare temperature changes near the subnivean space. Changes in this physical snowpack property and the difference between non-motorized and varying degrees of motorized winter recreation use were compared.

4.2.3 Snow Depth and Snow Water Equivalent

Snowpack depth measurements were obtained from each snow pit using a 2 m metric fiberglass folding ruler with 1 cm resolution. Snow water equivalent, *SWE* (mm), was computed from snow depth, d_s (cm) and snow density, ρ_s (g/cm^3), measurements as:

$$SWE\ (mm) = \rho_s/\rho_w \times d_s \tag{4.3}$$

where ρ_w is the density of water. Changes in these snowpack properties and the difference between non-motorized and varying degrees of motorized winter recreation use were compared.

4.2.4 Stratigraphic Analyses

Stratigraphic measurements illustrate the evolution of the snowpack over time by characterizing the shape and size of snow crystals within each stratified layer of the snowpack. Classification of grain morphology was based on *The International Classification for Seasonal Snow on the Ground* (Colbeck et al., 1990) and grain size was measured and recorded to the nearest 0.5 mm using a crystal card. Each layer of the snowpack had a corresponding density, hardness, and ram resistance and these parameters were used as surrogates for mammalian movement near the subnivean space.

4.2.5 Hardness

Hardness measurements were taken with a force gauge in each stratigraphic layer to quantify the bulk snowpack hardness and the hardness associated with the bottom stratigraphic layer. These hardness measurements were measured using Wagner Force Dials (Wagner Instruments, <http://wagnerinstruments.com>) with maximum force measurements of 25 and 100 N, and circular metal plate attachments of known area (McClung and Schaerer, 2006). The circular metal plate was pushed into the snow and the force required to penetrate the snow was recorded. The snow hardness, h_i (N/m^2), for each stratigraphic layer was calculated as:

$$h_i = F/A \tag{4.4}$$

where F is the force required to break the snow (N) and A is the area of the circular metal plate (m^2). The bulk snowpack hardness H_B (N/m^2) was determined by weighting each stratigraphic layer hardness measurement by stratigraphic layer thickness using the following formula:

$$H_B = \sum_{i=1}^{n} (d_i/d_s) \times h_i \tag{4.5}$$

where d_i is stratigraphic layer thickness (cm), d_s is the total snow depth (cm) and n is the total number of individual layers. The hardness associated with the bottom stratigraphic layer for each transect was used as a surrogate for mammalian movement within the subnivean space. Changes in this mechanical snowpack property and the difference between non-motorized and the varying degrees of motorized winter recreation use were compared.

4.2.6 Standard Ram Penetrometer

The standard ram penetrometer is an instrument used to measure the relative hardness or resistance of the snow layers (Greene et al., 2009). A ram profile measurement was taken subsequent to snow pit profile measurements and was taken 0.5 meters from the edge of the snow pit wall. These measurements were used to assess the change in ram resistance due to compaction through the duration of the winter season. The mean ram resistance, S_B (N), was determined by weighting each stratigraphic layer's ram resistance value obtained from the standard ram penetrometer measurement by layer thickness using the following formula:

$$S_B = \sum_{i=1}^{n} (d_i/d_s) \times RR \qquad (4.6)$$

where *RR* is the ram resistance (N). The ram resistance value associated with the bottom stratigraphic layer was measured and used as a surrogate for mammalian movement within the subnivean space. Changes in this mechanical snowpack property and the difference between non-motorized and the varying degrees of motorized winter recreation use were compared.

4.2.7 Heat Flow

One of the main attributes the snowpack yields to subnivean mammals attempting to survive over winter is the insulative value (Pruitt, 1960), which is a function of thermal conductivity. Thermal conductivity, k_{eff} (W m^{-1} K^{-1}), at Fraser Experimental Forest was estimated using the following model outlined by the US Army Cold Regions Research and Engineering Laboratory (2005):

$$k_{eff} = 0.138 - 1.01\rho_s + 3.233\rho_s^2 \qquad (4.7)$$

where ρ_s is the snow density (g/cm^3).

4.3 Mixed Model Analysis for Variance

A mixed model analysis for variance was used to determine the level of statistical significance between varying uses of motorized winter recreation for the snow compaction study plots at Rabbit Ears Pass and Fraser Experimental Forest and to determine statistical differences between Muddy Creek, Dumont Lakes and Walton Creek trailheads (personal communication from James zumBrunnen 2010). The mixed model procedure fits a variety of mixed linear models to data, which allows the user to make statistical inferences about the data. The differences of least squares means was used to infer statistical differences between the varying uses with respect to the probability distribution of the data (p-values). This model assumes that (1) the data are normally distributed; (2) the means (expected values) of the data are linear; and (3) the variance and covariance of the data are in terms of a different set of parameters (SAS Institute Inc., 2008). Logarithmic transformations were performed on data that were not normally distributed and the transformations better approximated a normal distribution.

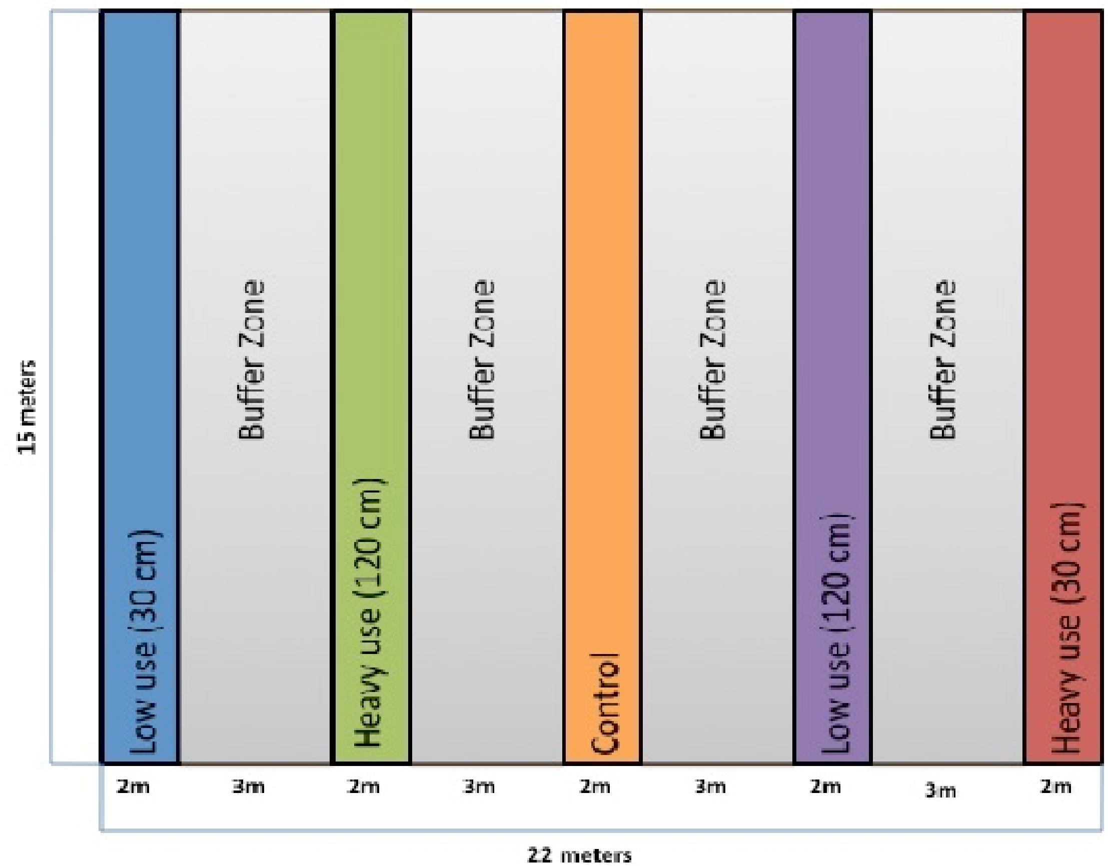

Figure 4.1.1. Snow compaction study plot design for the established two adjacent study plots on Rabbit Ears Pass, Colorado for the 2009/2010 winter.

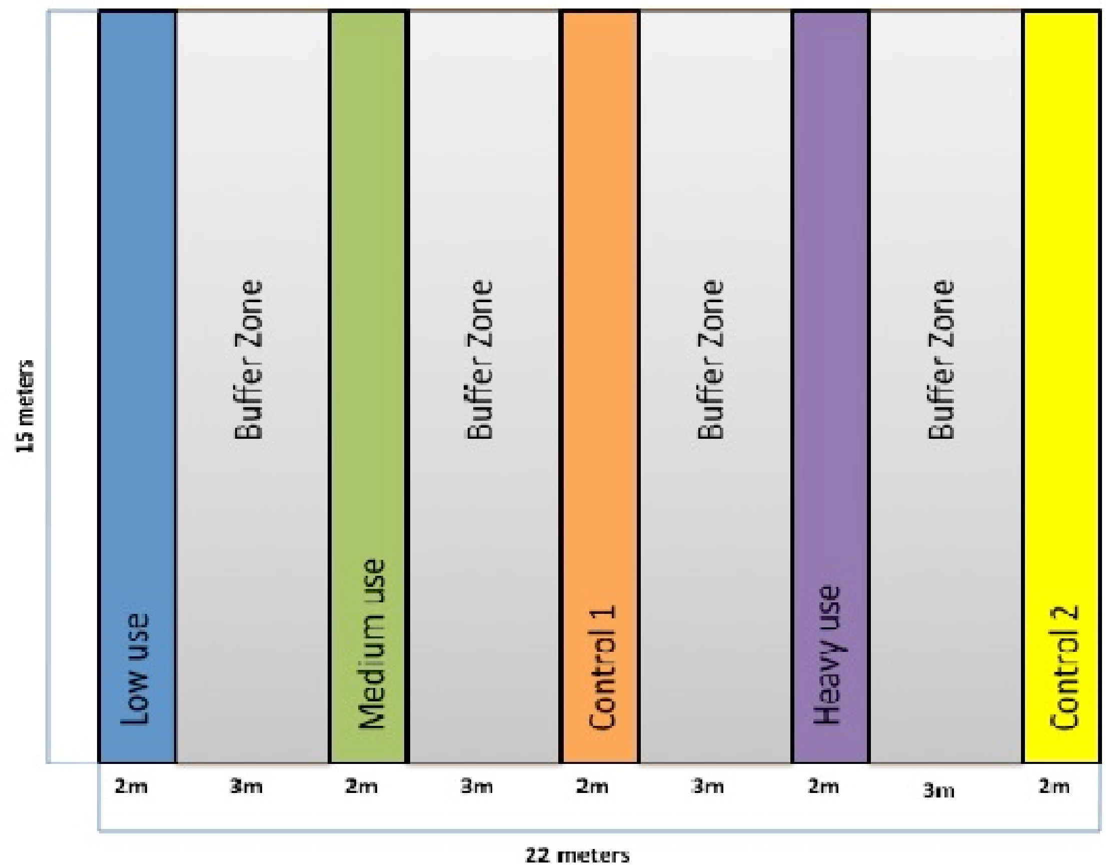

Figure 4.1.2. Snow compaction study plot design for the established study plot in Fraser Experimental Forest, Colorado for the 2009/2010 winter season.

5.0 RESULTS

5.1 Density

5.1.1 Shallow Snowpack Compaction Initiation (30 cm): Rabbit Ears Pass

Low and heavy use compaction treatments resulted in an increase in both bulk snowpack density and subnivean density following compaction treatments beginning on 30 cm of snow (Figure 5.1a). These results showed significant differences between the treatments and the control, and low and heavy use compaction treatments beginning on 120 cm of snow (Table 5.1a). Bulk snowpack density for low and heavy use compaction treatments had the greatest difference compared to the control on 6-7 February with densities of 284 kg/m^3 and 327 kg/m^3, respectively, compared to 248 kg/m^3 (Figure 5.1a), while the largest subnivean density differences were observed on 12 December with subnivean densities of 351 kg/m^3 and 377 kg/m^3, respectively, compared to 218 kg/m^3 (Figure 5.1a). The control bulk snowpack density and subnivean density increased throughout the duration of the season and by the last sampling date on 17 April there was little difference between the control and treatments (Figure 5.1a).

5.1.2 Deep Snowpack Compaction Initiation (120 cm): Rabbit Ears Pass

In contrast to the shallow initiation results above, low and heavy use compaction treatments did not result in a significant difference in bulk snowpack density or subnivean density when compaction treatments began on 120 cm of snow (Table 5.1a). Low and heavy use bulk snowpack densities were 260 kg/m^3 and 272 kg/m^3 on 6-7 February, respectively, compared to 248 kg/m^3 (Figure 5.1a), which was the largest difference observed through the winter season. Low and heavy use subnivean densities were 234 kg/m^3 and 268 kg/m^3 on 6-7 February, respectively (Figure 5.1a), compared to 229 kg/m^3, which was the largest difference observed during the winter season. Nonetheless, these small increases in both bulk snowpack density and subnivean density were not sufficient enough to result in significant differences compared to the control (Table 5.1a). Both bulk snowpack density and subnivean density were similar to the control by the end of the winter season on 17 April (Figure 5.1a).

5.1.3 Walton Creek, Dumont Lakes and Muddy Creek Trailheads: Rabbit Ears Pass

Mean snowpack density and subnivean density at Muddy Creek and Dumont Lakes were significantly different than measurements observed at Walton Creek (Table 5.2a). Mean snowpack densities at Muddy Creek and Dumont Lakes were 223 kg/m^3 and 228 kg/m^3 on 11 December, respectively, compared to 210 kg/m^3 measured at Walton Creek (Figure 5.1b). Subnivean densities measured on this date were 331 kg/m^3, 226 kg/m^3, and 235 kg/m^3, respectively, which was the largest difference observed between Muddy Creek and Walton Creek (Figure 5.1b). The largest difference in subnivean density between Dumont Lakes and Walton Creek was observed on 12 March with measurements of 336 kg/m^3 and 240 kg/m^3, respectively (Figure 5.1b) and the largest difference in bulk snowpack density was observed on 8 January with measurements of 297 kg/m^3 and 279 kg/m^3 at Muddy Creek and Dumont Lakes, respectively, compared to 213 kg/m^3 at Walton Creek (Figure 5.1b). Bulk snowpack density and subnivean density for Muddy Creek and Dumont Lakes was generally greater than Walton Creek throughout the winter; however, there was minimal difference by the end of the winter (Figure 5.1b).

5.1.4 Shallow Snowpack Compaction Initiation (30 cm): Fraser Experimental Forest

Low, medium and heavy use compaction treatments at the Fraser Experimental Forest compaction plot resulted in an increase in bulk snowpack density and subnivean density following the initial compaction treatment beginning on 30 cm of snow (Figure 5.1c). Significant differences were observed between treatments and the control; however, there were no significant differences between the varying treatments (Table 5.1a). The largest difference in bulk snowpack density between low and medium use was 119 kg/m^3 and 134 kg/m^3, respectively, greater than the average control observed on 12 February (Figure 5.1c), while heavy use bulk snowpack density had the largest difference from the control on 22 January varying by 149 kg/m^3 (Figure 5.1c). Low, medium, and heavy use subnivean densities were 288 kg/m^3, 336 kg/m^3, and 330 kg/m^3, respectively (Figure 5.1c), compared to 116 kg/m^3 on 27 December. These density measurements were the largest differences observed throughout the winter. The bulk snowpack density and subnivean density of all treatments generally increased during the study period; however, there were minimal differences between the controls and treated transects by the end of winter (Figure 5.1c).

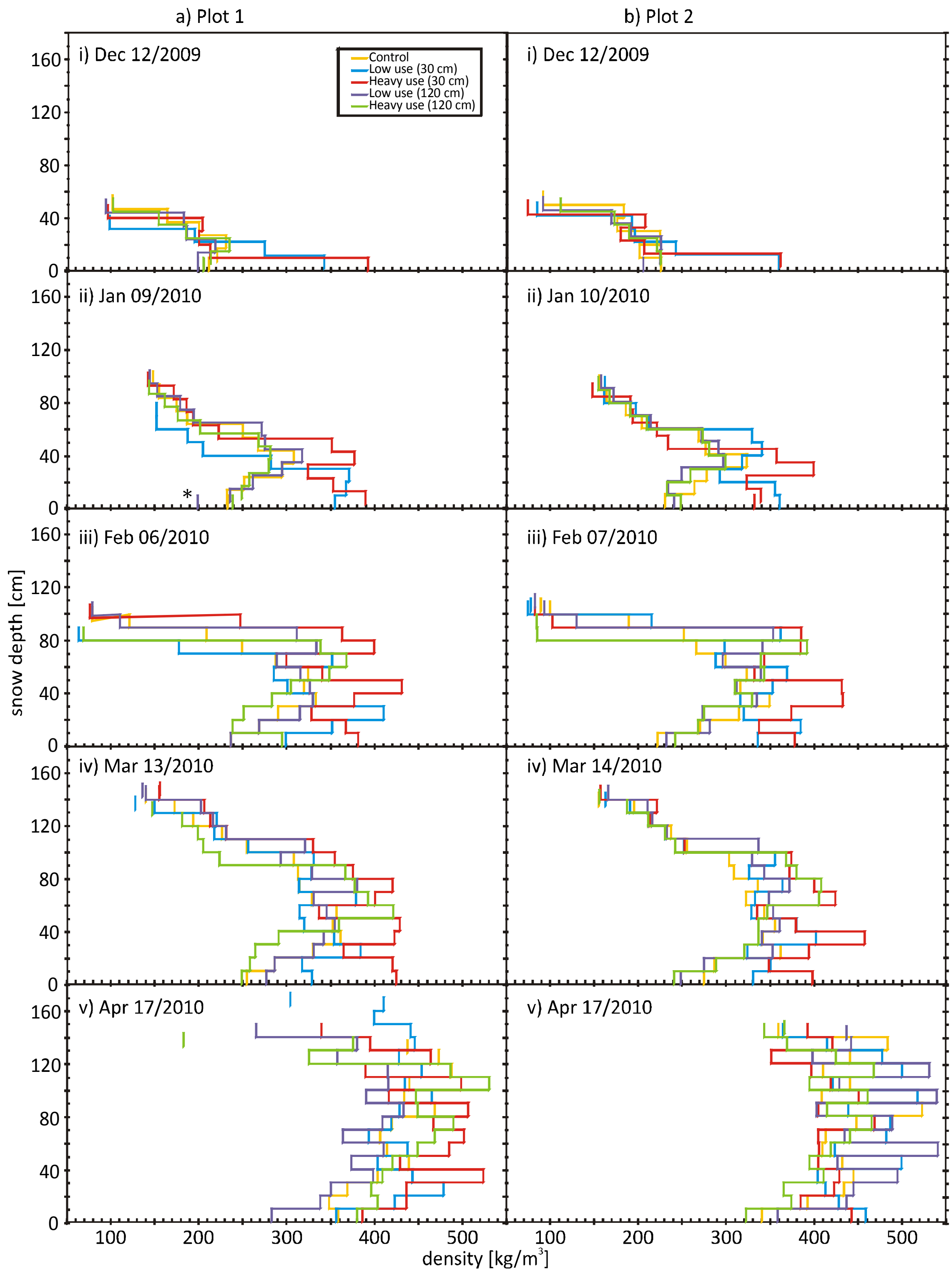

Figure 5.1a. Density profiles measured for no, low, medium, and heavy use snow compaction treatments beginning on 30 cm and 120 cm of snow at the snow compaction study plots located near Rabbit Ears Pass, Colorado during the 2009-2010 winter. (*Free floating measurements represent overlapping density measurements)

Table 5.1. Statistical difference (p-values) between varying snow compaction treatments on snowpack properties at the study plots located at Rabbit Ears Pass and Fraser Experimental Forest, Colorado during the 2009-2010 winter season. Slashes (/) separate mean and subnivean differences, respectively, for a) density, d) hardness and e) ram resistance; snow water equivalent and snow depth for b) snow water equivalent and snow depth; and bulk temperature gradient, temperature gradient from 0 to 10 cm, temperature gradient from 0 to 5 cm and basal layer temperature for b) temperature. P-values highlighted in red represent a statistical difference based on a confidence interval of 90% or greater.

a) Density			No use	*Shallow initiation depth (30 cm)*		
				Low	Medium	Heavy
Rabbit Ears Pass	*Shallow initiation depth (30 cm)*	Low	<0.001/<0.001			0.001/<0.001
		Heavy	<0.001/<0.001	0.001/<0.001		
	Deep initiation depth (120 cm)	Low	0.440/0.578	<0.001/<0.001		<0.001/<0.001
		Heavy	0.236/0.514	<0.001/<0.001		<0.001/<0.001
Fraser Experimental Forest	*Shallow initiation depth (30 cm)*	Low	<0.001/<0.001		0.289/0.206	0.302/0.798
		Medium	<0.001/<0.001	0.289/0.206		0.975/0.304
		Heavy	<0.001/<0.001	0.302/0.798	0.975/0.304	

b) Temperature			No use	*Shallow initiation depth (30 cm)*		
				Low	Medium	Heavy
Rabbit Ears Pass	*Shallow initiation depth (30 cm)*	Low	0.215/1.000/ 0.593/0.014			0.108/0.395/ 0.593/0.606
		Heavy	0.700/0.395/ 1.000/0.004	0.108/0.395/ 0.593/0.606		
	Deep initiation depth (120 cm)	Low	0.772/0.669/ 0.593/0.305	0.338/0.669/ 0.288/0.127		0.501/0.669/ 0.593/0.045
		Heavy	1.000/0.669/ 0.288/0.606	0.215/0.669/ 0.115/0.045		0.700/0.205/ 0.288/0.014
Fraser Experimental Forest	*Shallow initiation depth (30 cm)*	Low	0.115/1.000/ 1.000/0.081		0.894/1.000/ 0.742/0.642	0.103/0.098/ 0.203/1.000
		Medium	0.144/1.000/ 0.742/0.035	0.894/1.000/ 0.742/0.642		0.129/0.098/ 0.332/0.642
		Heavy	0.643/0.098/ 0.203/0.081	0.103/0.098/ 0.203/1.000	0.129/0.098/ 0.332/0.642	

c) SWE/Snow depth			No use	*Shallow initiation depth (30 cm)*		
				Low	Medium	Heavy
Rabbit Ears Pass	*Shallow initiation depth (30 cm)*	Low	0.074/0.004			0.001/0.024
		Heavy	0.002/0.480	0.136/0.024		
	Deep initiation depth (120 cm)	Low	0.528/0.658	0.238/0.001		0.010/0.254
		Heavy	0.236/0.033	0.015/0.402		<0.001/0.139
Fraser Experimental Forest	*Shallow initiation depth (30 cm)*	Low	0.314/<0.001		0.770/0.795	0.662/0.846
		Medium	0.481/<0.001	0.770/0.795		0.884/0.948
		Heavy	0.397/<0.001	0.662/0.846	0.884/0.948	

d) Hardness			No use	*Shallow initiation depth (30 cm)*		
				Low	Medium	Heavy
Rabbit Ears Pass	*Shallow initiation depth (30 cm)*	Low	0.001/<0.001			0.157/0.051
		Heavy	<0.001/<0.001	0.157/0.051		
	Deep initiation depth (120 cm)	Low	0.424/0.909	0.001/<0.001		<0.001/<0.001
		Heavy	0.061/0.700	0.022/<0.001		0.001/<0.001
Fraser Experimental Forest	*Shallow initiation depth (30 cm)*	Low	<0.001/<0.001		0.357/0.032	0.014/0.003
		Medium	<0.001/<0.001	0.357/0.032		0.081/0.200
		Heavy	<0.001/<0.001	0.014/0.001	0.081/0.200	

e) Ram resistance			No use	*Shallow initiation depth (30 cm)*		
				Low	Medium	Heavy
Rabbit Ears Pass	*Shallow initiation depth (30 cm)*	Low	<0.001/<0.001			0.079/0.060
		Heavy	<0.001/<0.001	0.079/0.060		
	Deep initiation depth (120 cm)	Low	0.320/0.133	<0.001/<0.001		<0.001/<0.001
		Heavy	0.065/0.886	0.006/<0.001		<0.001/<0.001
Fraser Experimental Forest	*Shallow initiation depth (30 cm)*	Low	<0.001/<0.001		0.332/0.928	<0.001/0.014
		Medium	<0.001/<0.001	0.332/0.928		0.002/0.016
		Heavy	<0.001/<0.001	<0.001/0.014	0.002/0.016	

Table 5.2. Statistical difference between Walton Creek and motorized winter recreation trailheads, Muddy Creek and Dumont Lakes, near Rabbit Ears Pass, Colorado during the 2009-2010 winter season. Slashes (/) separate mean and subnivean differences for a) density, d) hardness and e) ram resistance; and bulk temperature gradient, temperature gradient from 0 to 10 cm, temperature gradient from 0 to 5 cm and basal layer temperature differences for b) temperature. P-values highlighted in red represent a statistical difference based on a confidence interval of 90% or greater.

		Walton Creek
Muddy Creek	*a) Density*	0.007/0.025
	b) Temperature	0.287/0.267/0.267/0.506
	c) Depth	0.944
	d) SWE	0.009
	e) Hardness	0.009/0.002
	f) Ram Resistance	0.004/0.016
Dumont Lakes	*a) Density*	0.018/0.208
	b) Temperature	0.889/0.267/0.267/0.207
	c) Depth	0.624
	d) SWE	0.081
	e) Hardness	0.040/0.007
	f) Ram Resistance	0.093/0.096

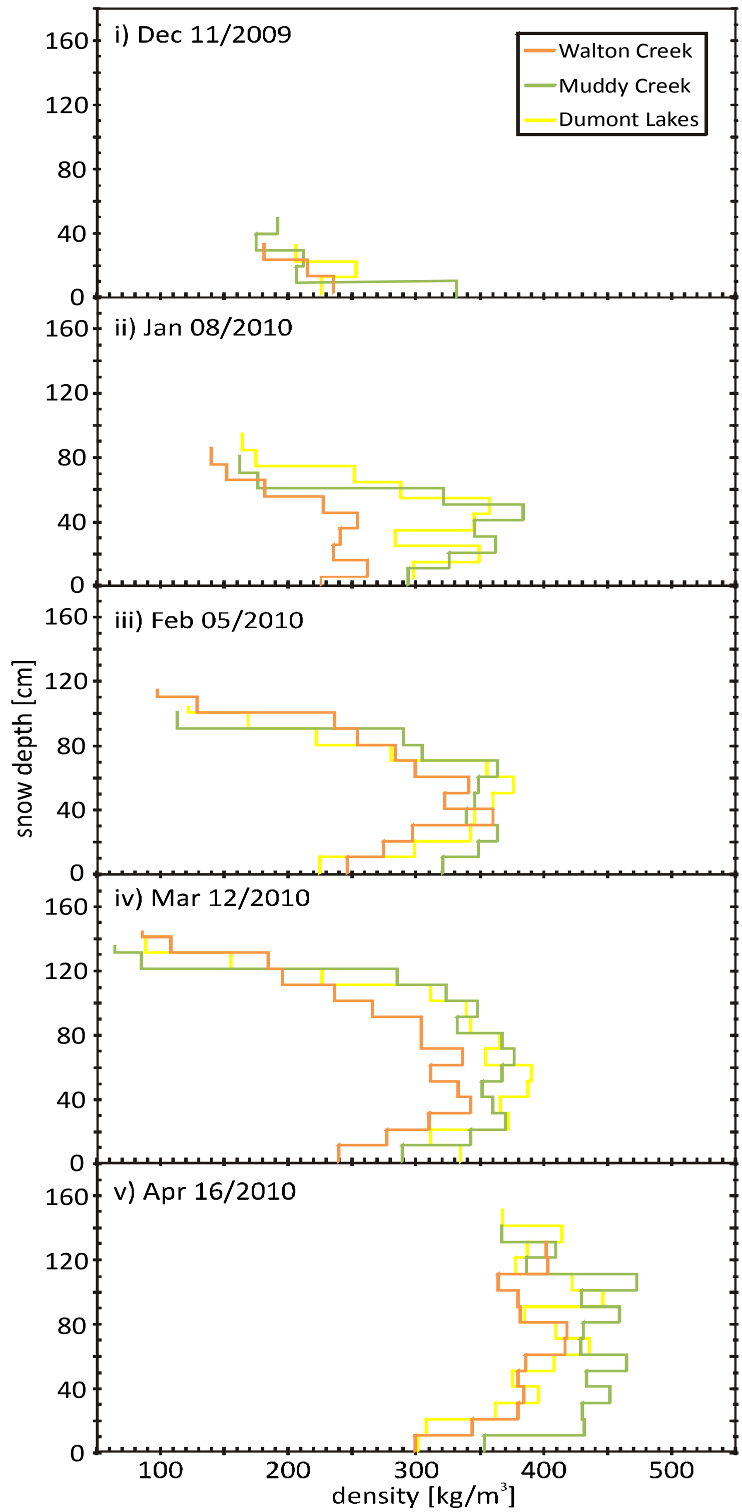

Figure 5.1b. Density profiles measured at Muddy Creek, Dumont Lakes, and Walton Creek trailheads on Rabbit Ears Pass, Colorado during the 2009-2010 winter.

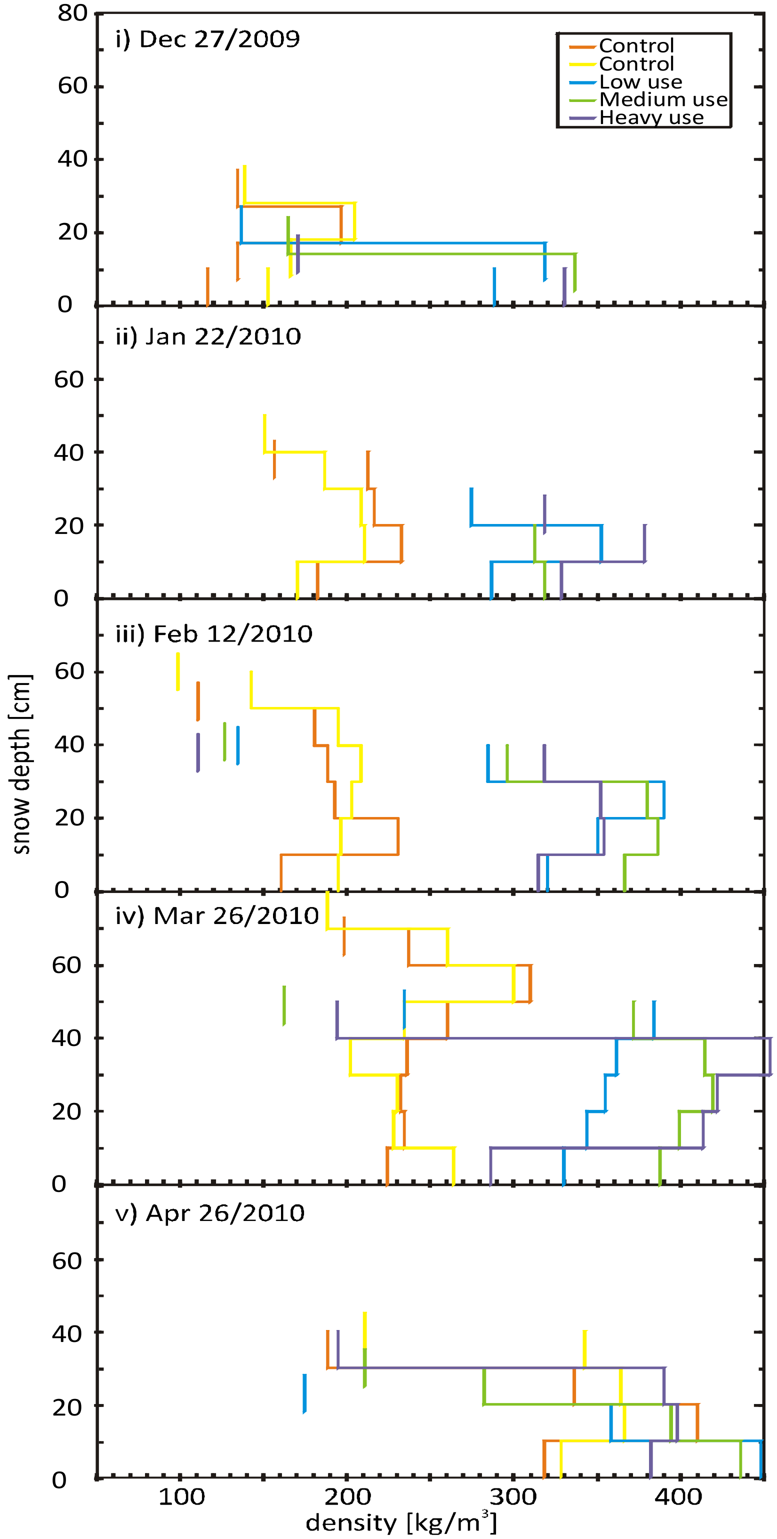

Figure 5.1c. Density profiles measured for no, low, medium, and heavy use snow compaction treatments beginning on 30 cm of snow at the snow compaction study plot located in Fraser Experimental Forest, Colorado during the 2009-2010 winter.

5.2 Temperature

5.2.1 Shallow Snowpack Compaction Initiation (30 cm): Rabbit Ears Pass

Low and heavy use compaction treatments that began on a shallow snowpack of 30 cm did not result in significant differences in temperature gradients (bulk, 10 to 0 cm and 5 to 0 cm) compared to the control, and compaction treatments that began on a deep snowpack of 120 cm of snow; however, significant differences were measured for temperatures at the basal layer (0 cm) between the heavy use treatment and the control, and compaction treatments that began on 120 cm of snow (Table 5.1b). No, low and heavy use bulk temperature gradients were at a maximum of 18^{o}C m^{-1}, 28^{o}C m^{-1} and 25^{o}C m^{-1} on 12 December, respectively, and decreased throughout the winter season until all uses exhibited a bulk temperature gradient near 0^{o}C m^{-1} by 17 April (Figure 5.2a). No, low and heavy use basal layer temperatures were at a minimum of -3^{o}C, -3^{o}C and -2^{o}C on 12 December, respectively, and increased throughout the winter season until all uses exhibited a basal layer temperature of -1^{o}C by 17 April (Figure 5.2a).

5.2.2 Deep Snowpack Compaction Initiation (120 cm): Rabbit Ears Pass

Low and heavy use compaction treatments that began on a deep snowpack of 120 cm did not result in significant differences in temperature gradients (bulk, 0 to 10 cm and 0 to 5 cm) compared to the control and low and heavy use compaction treatments that began on a shallow snowpack of 30 cm of snow; however, significant differences were observed for temperatures at the basal layer (0 cm) between low and heavy use compaction treatments and compaction treatments that began on 30 cm of snow (Table 5.1b). No, low and heavy use bulk temperature gradients were at a maximum of

$23^oC\ m^{-1}$, $23^oC\ m^{-1}$ and $25^oC\ m^{-1}$ on 12 December, respectively, and decreased throughout the winter season until all uses exhibited bulk temperature gradients near $0^oC\ m^{-1}$ by 17 April (Figure 5.2a). No, low and heavy use basal layer temperatures were at a minimum of -2^oC on 12 December and increased throughout the winter season until all uses exhibited a basal layer temperature of -1^oC by 17 April (Figure 5.2a).

5.2.3 Walton Creek, Dumont Lakes and Muddy Creek Trailheads: Rabbit Ears Pass

Temperature gradients (bulk, 0 to 10 cm and 0 to 5 cm) and basal layer temperatures at Muddy Creek and Dumont Lakes were not significantly different compared to measurements observed at Walton Creek (Table 5.2b). Bulk temperature gradients at Muddy Creek, Dumont Lakes and Walton Creek were at a maximum of $25^oC\ m^{-1}$, $33^oC\ m^{-1}$ and $33^oC\ m^{-1}$ on 11 December, respectively, and decreased to a minimum near $0^oC\ m^{-1}$ by 16 April (Figure 5.2b). Basal layer temperatures measured at Muddy Creek, Dumont Lakes and Walton Creek fluctuated between -2^oC and -1^oC through the season; all study sites exhibited a maximum basal layer temperature of -1^oC by 16 April (Figure 5.2b).

5.2.4 Shallow Snowpack Compaction Initiation (30 cm): Fraser Experimental Forest

Low, medium and heavy use compaction treatments did not result in significant differences in temperature gradients (bulk, 0 to 10 cm and 0 to 5 cm) compared to the control. Significant differences were observed between low, medium and heavy use basal layer temperatures (0 cm) and no use, and low and medium use temperature gradients from 0 to 10 cm compared to the heavy use (Table 5.1b). No, low medium and heavy use bulk temperature gradients were at a maximum of $30^oC\ m^{-1}$, $13^oC\ m^{-1}$, $20^oC\ m^{-1}$ and $20^oC\ m^{-1}$ on 27 December, respectively, and decreased throughout the winter season until all uses exhibited a bulk temperature gradient near $0^{o}C\ m^{-1}$ by 26 April (Figure 5.2c). No, low and heavy use basal layer temperatures were at a minimum of $-5^{o}C$ on 27 December, while medium use basal layer temperature was at a minimum of $-6^{o}C$ on 22 January; all increased throughout the winter season until basal layer temperatures were $-1^{o}C$ by 26 April (Figure 5.2c).

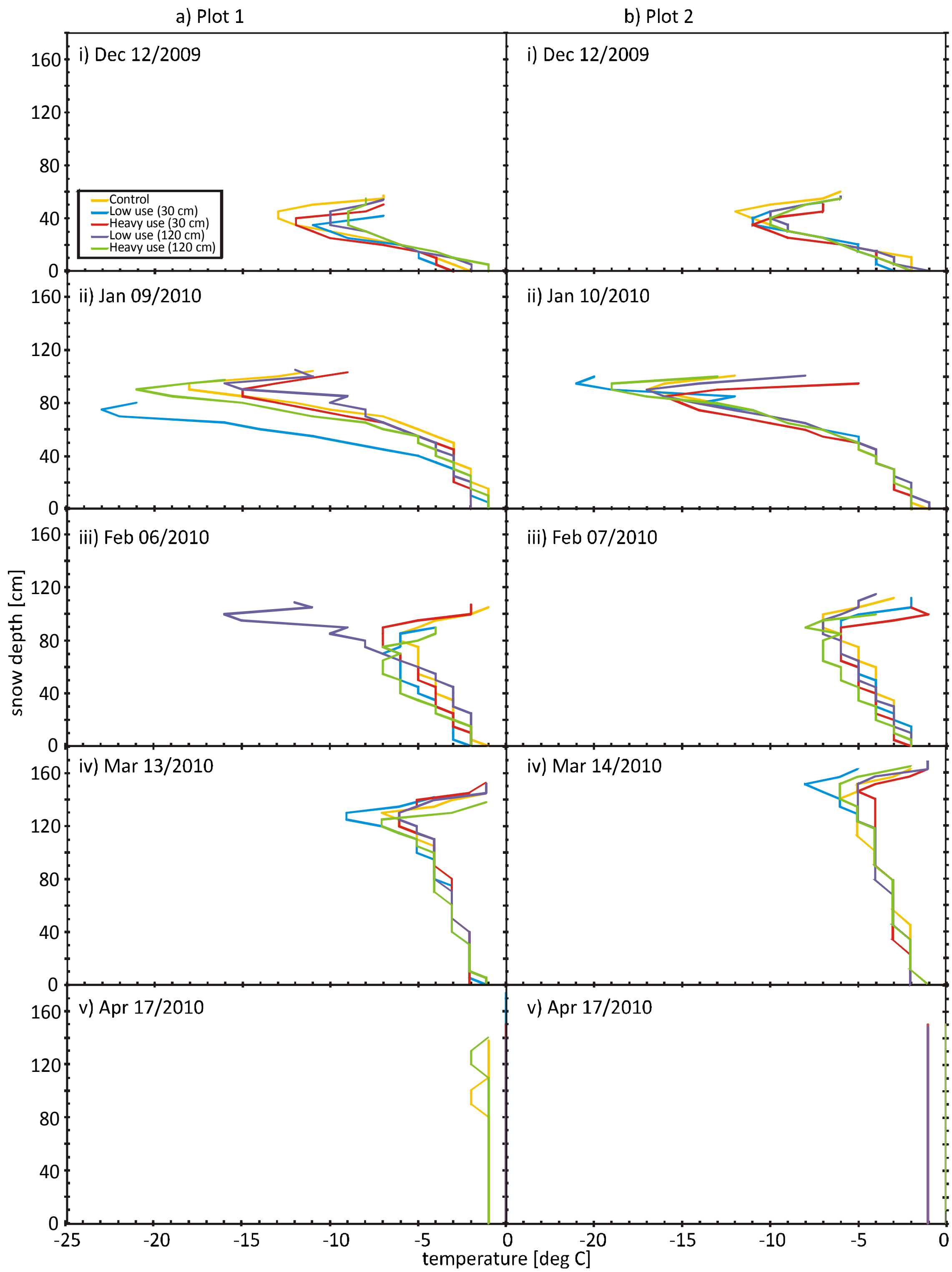

Figure 5.2a. Temperature profiles measured for no, low, medium, and heavy use snow compaction treatments beginning on 30 cm and 120 cm of snow at the snow compaction study plots located near Rabbit Ears Pass, Colorado during the 2009-2010 winter.

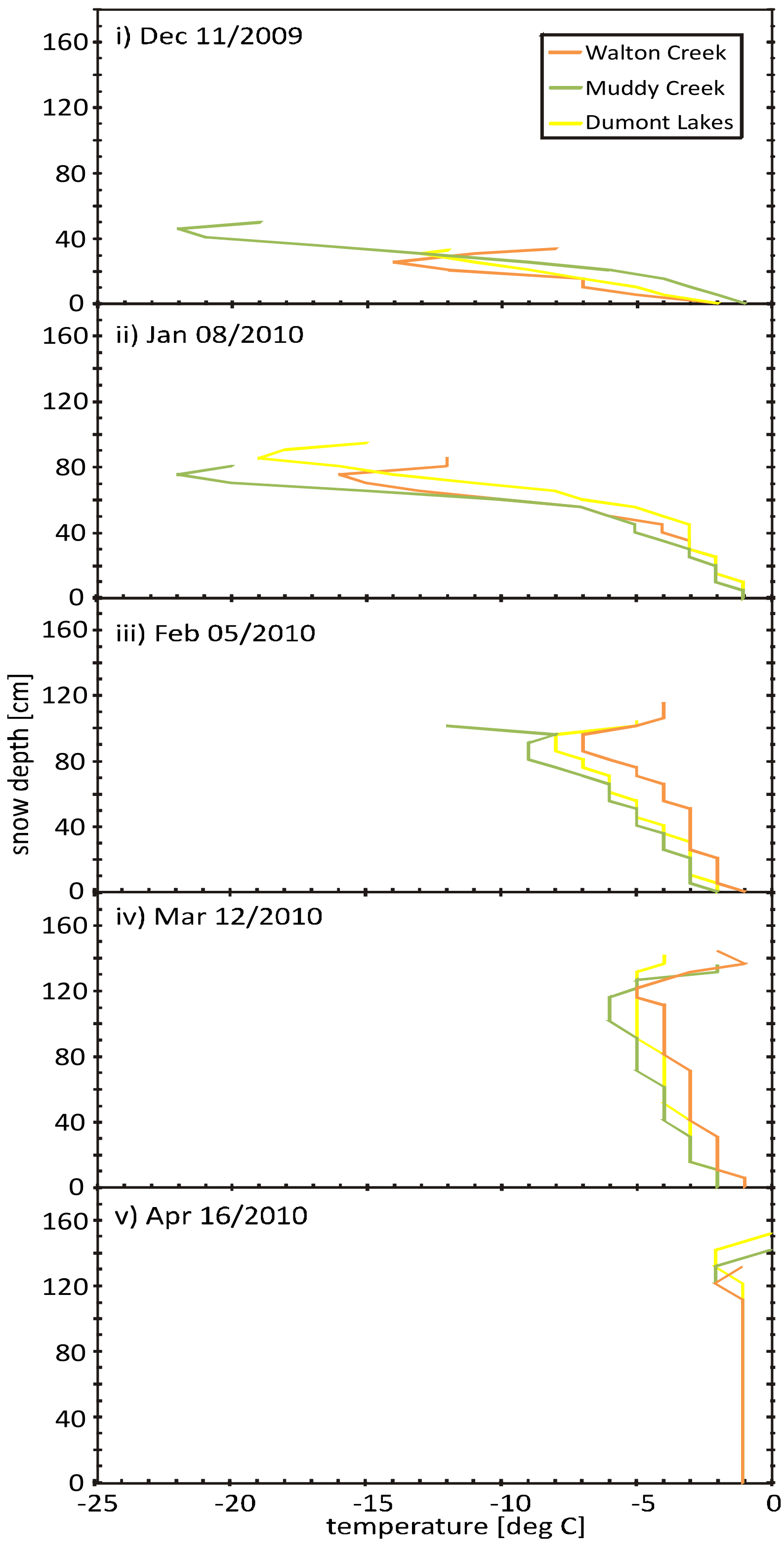

Figure 5.2b. Temperature profiles measured at Muddy Creek, Dumont Lakes, and Walton Creek trailheads on Rabbit Ears Pass, Colorado during the 2009-2010 winter.

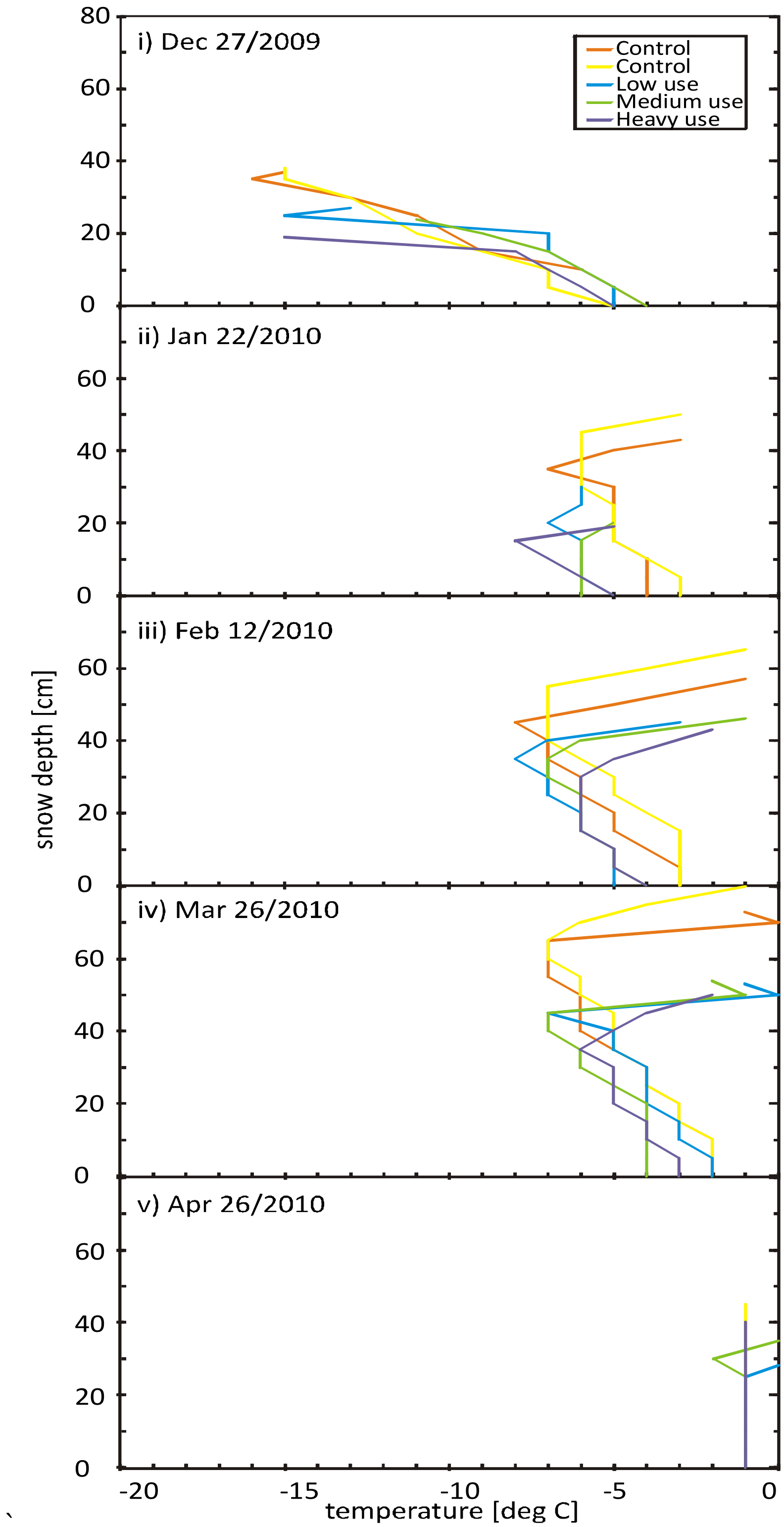

Figure 5.2c. Temperature profiles measured for no, low, medium, and heavy use snow compaction treatments beginning on 30 cm of snow at the snow compaction study plot located in Fraser Experimental Forest, Colorado during the 2009-2010 winter.

5.3 Snow Depth and Snow Water Equivalent

5.3.1 Shallow Snowpack Compaction Initiation (30 cm): Rabbit Ears Pass

Low and heavy use compaction treatments resulted in shallower snow depths compared to the control when snow compaction treatments began on 30 cm of snow at the Rabbit Ears Pass study plots (Figure 5.3a). Low and heavy use reached a maximum snow depth of 147 cm, 162 cm, 152 cm, on 13-14 March, 17 April, and 13-14 March, respectively (Figure 5.3a). The difference between low and heavy use snow depth and the control decreased as the winter season progressed, and by the end of the winter, low and heavy use snow depths were deeper than the control (Figure 5.3a). The low use snow depth was less than heavy use snow depth for the first three sampling dates (Figure 5.3a), which resulted in a significant difference compared to the control, while no significant differences were observed between no use and heavy use snow depths (Table 5.1c).

Snow water equivalent was greater for low and heavy use compaction treatments, which resulted in a significant difference in snow water equivalent compared to the control (Table 5.1c). Low and heavy use reached a maximum snow water equivalent of 703 mm and 643 mm on 17 April, respectively, compared to 609 mm for the control (Figure 5.3b).

5.3.2 Deep Snowpack Compaction Initiation (120 cm): Rabbit Ears Pass

Low and heavy use compaction treatments resulted in shallower snow depths compared to the control when snow compaction treatments began on 120 cm of snow at the Rabbit Ears Pass study plots (Figure 5.3a). Low use and heavy use reached a maximum snow depth of 147 cm and 151 cm on 13-14 March, respectively, compared to a maximum of 148 cm for the control on 17 April (Figure 5.3a). Low use snow depth was greater than the control for the majority of the winter season with no significant difference; however, a significant difference was observed between the control and heavy use treatment (Table 5.1c).

There were no significant differences in snow water equivalent between the treatments and the control (Table 5.1c). Low and heavy use reached a maximum snow water equivalent of 615 mm and 608 mm on 17 April, respectively, compared to 609 mm for the control (Figure 5.3b).

5.3.3 Walton Creek, Dumont Lakes and Muddy Creek Trailheads: Rabbit Ears Pass

Snow depth at Muddy Creek and Dumont Lakes was generally shallower compared to the snow depth at Walton Creek; however, these differences were not very large. Muddy Creek, Dumont Lakes, and Walton Creek reached maximum snow depths of 140 cm, 150 cm and 143 cm observed on 16 April, 16 April, and 12 March, respectively (Figure 5.3c). The difference between Muddy Creek and Dumont Lakes compared to Walton Creek decreased as the winter season progressed and by 16 April the snow depths at Muddy Creek and Dumont Lakes were 140 cm and 150 cm, respectively, compared to 130 cm measured at Walton Creek (Figure 5.3c).

Snow water equivalent measurements at Muddy Creek and Dumont Lakes were greater compared to Walton Creek for the entire winter and this increase in snow water equivalent resulted in a significant difference between the motorized winter recreation study areas and the non-motorized winter recreation study area (Table 5.2d). Muddy Creek and Dumont Lakes reached a maximum measured snow water equivalent of 593 mm and 578 mm on 16 April, respectively, compared to 492 mm measured at Walton Creek (Figure 5.3d).

5.3.4 Shallow Snowpack Compaction Initiation (30 cm): Fraser Experimental Forest

Low, medium, and heavy use compaction treatments resulted in a decrease in snow depth when compaction treatments began on 30 cm of snow at the Fraser Experimental Forest study plot (Figure 5.3e), which resulted in a significant differences between the treatments and the control (Table 5.1c). Low, medium, and heavy use snow depth was 27 cm, 24 cm and 19 cm on 27 December, respectively, compared to 38 cm observed for the control (Figure 5.3e). Maximum snow depths of 53 cm, 54 cm, and 50 cm for low, medium and heavy use treatments was observed on 14 March, respectively, compared to 77 cm measured for the control (Figure 5.3e). Snow depths for low, medium and heavy use began to approach snow depths similar to the control by 26 April (Figure 5.3e).

Low, medium, and heavy use compaction treatments did not result in a significant difference with respect to snow water equivalent (Table 5.1c). Low, medium, and heavy use snow water equivalent measurements were 65 mm, 50 mm and 48 mm on 27 December, respectively, compared to 59 mm observed for the control (Figure 5.3f). Low, medium and heavy use reached a maximum snow water equivalent of 177 mm, 197 mm and 175 mm on 14 March, respectively, compared to 181 mm for the control (Figure 5.3f).

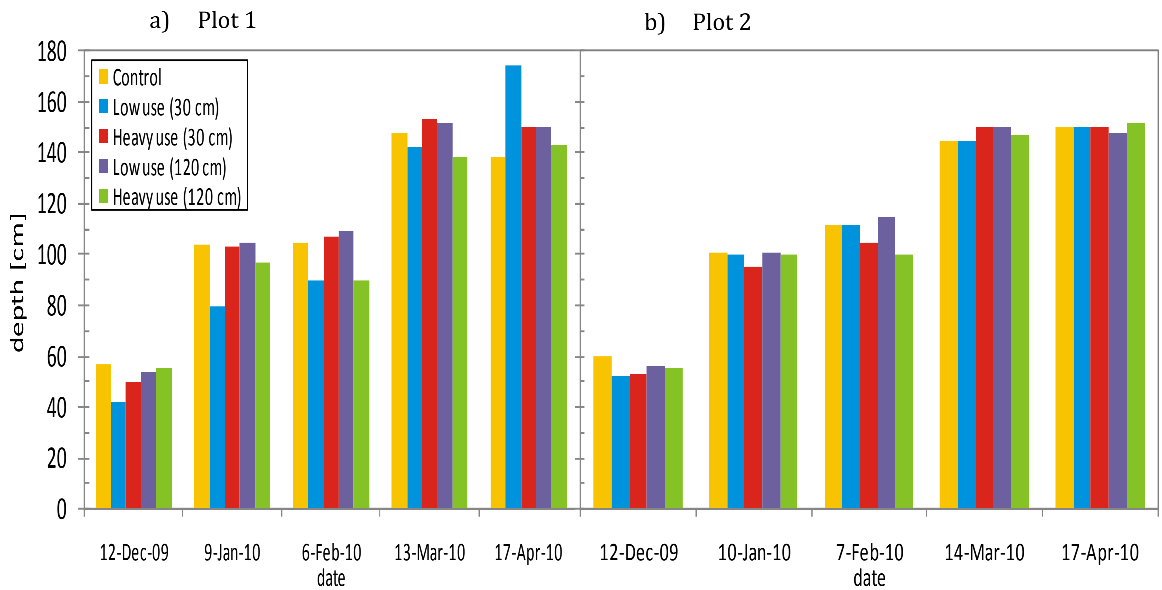

Figure 5.3a. Snow depth measured for no, low and heavy use snow compaction treatments beginning on 30 cm and 120 cm of snow at the snow compaction study plots located near Rabbit Ears Pass, Colorado during the 2009-2010 winter.

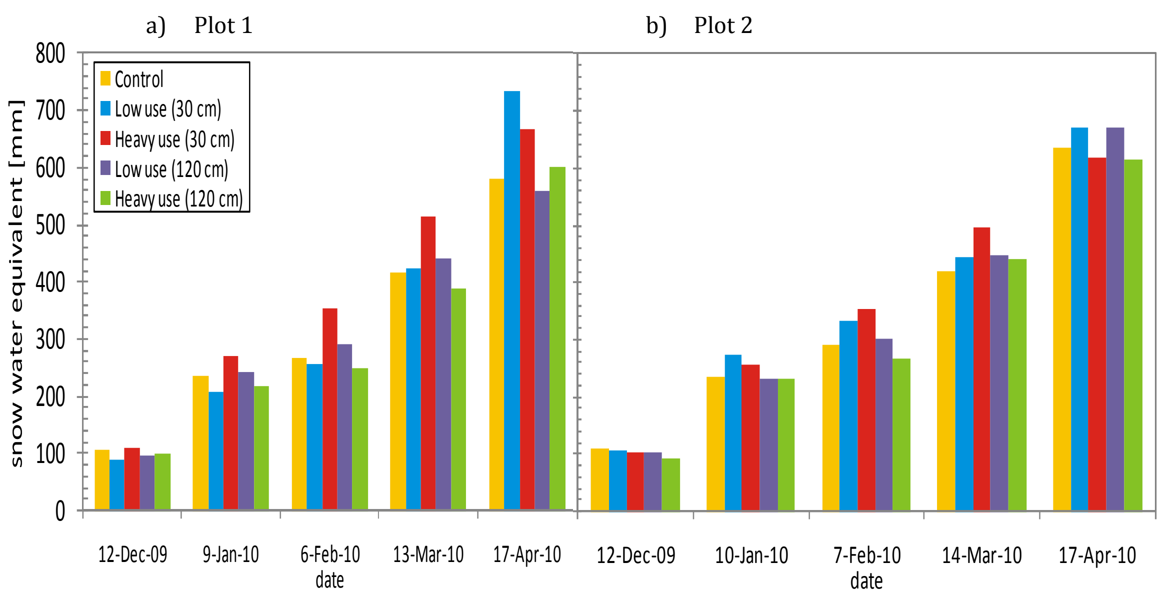

Figure 5.3b. Snow water equivalent measured for no, low and heavy use snow compaction treatments beginning on 30 cm and 120 cm of snow at the snow compaction study plots located near Rabbit Ears Pass, Colorado during the 2009-2010 winter.

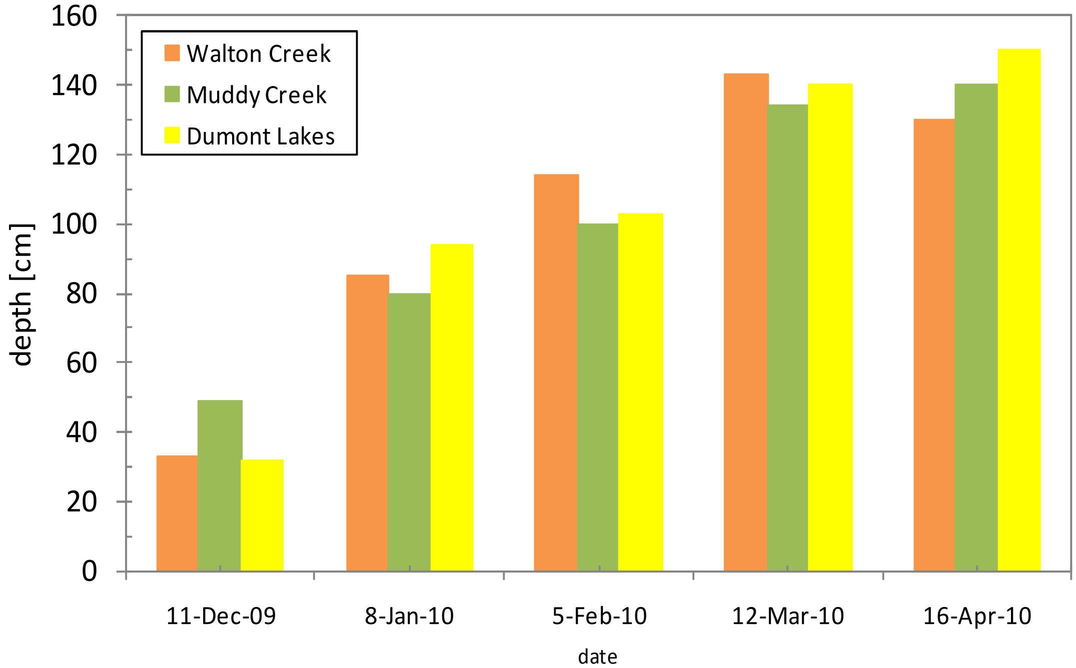

Figure 5.3c. Snow depth measured at Muddy Creek, Dumont Lakes, and Walton Creek trailheads on Rabbit Ears Pass, Colorado during the 2009-2010 winter.

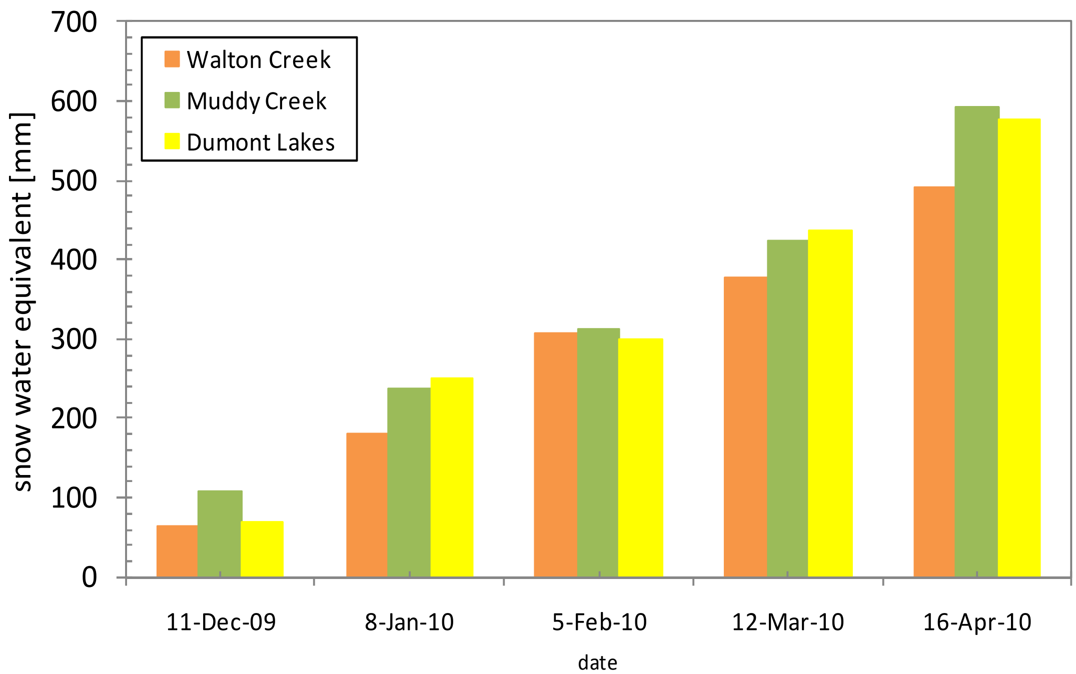

Figure 5.3d. Snow water equivalent measured at Muddy Creek, Dumont Lakes, and Walton Creek trailheads on Rabbit Ears Pass, Colorado during the 2009-2010 winter.

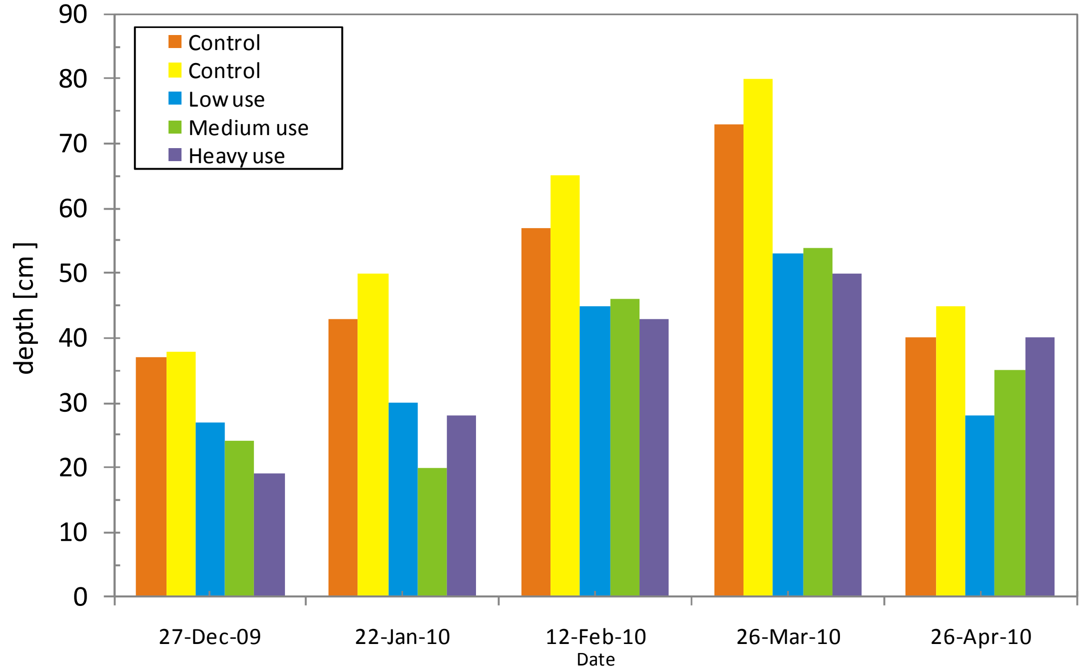

Figure 5.3e. Snow depth measured for no, low, medium, and heavy use snow compaction treatments beginning on 30 cm of snow at the snow compaction study plot located in Fraser Experimental Forest, Colorado during the 2009-2010 winter.

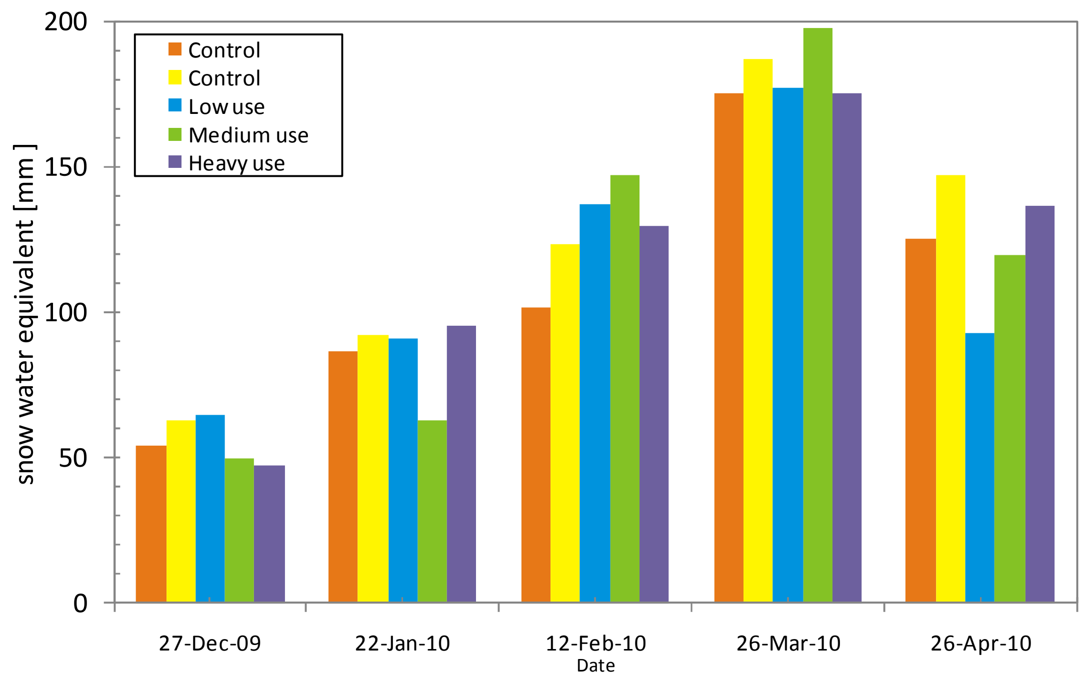

Figure 5.3f. Snow water equivalent measured for no, low, medium, and heavy use snow compaction treatments beginning on 30 cm of snow at the snow compaction study plot located in Fraser Experimental Forest, Colorado during the 2009-2010 winter.

5.4 Stratigraphy

Compaction from motorized winter recreation decreased crystal size (Table 5.3) near the subnivean space. For example, depth hoar crystals for the controls at Fraser Experimental Forest reached a maximum average size of 9.0 mm (Table 5.3), while low, medium and heavy use resulted in average crystal sizes of 1.3 mm, 2.5 mm and 1.5 mm, respectively (Table 5.3). Depth hoar crystal size at Fraser Experimental Forest for low, medium and heavy use remained smaller than the control for the entire winter season following the initial snow compaction treatment. Similarly, this trend was observed on Rabbit Ears Pass, although the deeper snow regime allowed growth of depth hoar and the difference in depth hoar crystal sizes between the treatments and control was not as prominent as was observed at Fraser Experimental Forest (Table 5.3).

Table 5.3. Grain size near measured near the subnivean space at the snow compaction study plots located at Rabbit Ears Pass and Fraser Experimental Forest, Colorado during the 2009-2010 winter season. Slashes (/) separate grain sizes differences between plot 1 and plot 2 near Rabbit Ears Pass.

		date	subnivean grain size [mm]			
			Control	*Low use*	*Medium use*	*Heavy use*
Rabbit Ears Pass	*Shallow initiation depth (30 cm)*	12-Dec-09	3.0/2.5	1.0/1.0		<0.5/<0.5
		9/10-Jan-10	2.0/3.5	3.0/3.0		1.0/1.0
		6/7-Feb-10	3.0/3.0	1.5/2.0		1.0/1.0
		13/14 Mar-10	3.0/3.0	3.0/2.5		1.0/1.0
		17-Apr-10	1.5/1.5	1.5/1.5		1.0/1.0
	Deep initiation depth (30 cm)	12-Dec-09	3.0/2.5	3.0/3.0		3.0/2.5
		9/10-Jan-10	2.0/3.5	3.0/3.0		1.5/3.0
		6/7-Feb-10	3.0/3.0	3.5/3.0		3.0/3.0
		13/14 Mar-10	3.0/3.0	3.0/3.0		3.5/3.0
		17-Apr-10	1.5/1.5	1.5/1.5		1.5/2.0
Fraser Experimental Forest	*Shallow initiation depth (30 cm)*	27-Dec-09	4.0	3.0	1.0	1.0
		22-Jan-10	3.0	1.0	2.0	1.5
		12-Feb-10	4.5	2.0	2.0	1.5
		26-Mar-10	9.0	1.0	2.5	1.5
		26-Apr-10	5.0	1.5	3.0	3.0

5.5 Hardness

5.5.1 Shallow Snowpack Compaction Initiation (30 cm): Rabbit Ears Pass

Low and heavy use compaction treatments resulted in an increase in both mean snowpack hardness and subnivean hardness following compaction treatments beginning on 30 cm of snow at the Rabbit Ears Pass study plot (Figure 5.5a). These increases in hardness were large enough to result in significant differences between treatments and the control, and compaction treatments that began on 120 cm of snow (Table 5.1d). Mean snowpack hardness for low and heavy use treatments increased to a maximum of 188 kPa and 425 kPa on 12 December and 6-7 February, respectively, compared to 59 kPa for the control on 17 April (Figure 5.5a). Low and heavy use treatments resulted in a maximum subnivean hardness of 188 kPa and 158 kPa measured on 12 December and 6-7 February, respectively, compared to 6 kPa for the control on 13-14 March (Figure 5.5a). Low and heavy use mean snowpack hardness and subnivean hardness measurements were greater than the control throughout the winter; however, there were minimal differences by the end of winter (Figure 5.5a).

5.5.2 Deep Snowpack Compaction Initiation (120 cm): Rabbit Ears Pass

Both low and heavy use mean snowpack hardness and subnivean hardness did not experience a significant change compared to the control following snow compaction treatments beginning on 120 cm of snow at the Rabbit Ears Pass study plot (Table 5.1d). Similar values were observed prior to the initial snow compaction treatments. After, low and heavy mean snowpack hardness increased, but the following compaction treatments did not seem to have a large effect (Table 5.1d). Mean snowpack hardness increased to a maximum of 77 kPa and 280 kPa on 17 April and 6-7 February for low and heavy use treatments, respectively, compared to 59 kPa for the control on 17 April (Figure 5.5a). Low and heavy use subnivean hardness increased to a maximum of 6 kPa and 5 kPa on 13-14 March, respectively (Figure 5.5a). Comparably, the control subnivean hardness reached a maximum of 6 kPa on 13-14 March (Figure 5.5a). Low and heavy use mean snowpack hardness were greater than the control for the entire winter following the initial treatment; however, the difference was not significant (Table 5.1d). The control, low, and heavy use treatments exhibited similar subnivean hardness values throughout the winter (Figure 5.5a).

5.5.3 Walton Creek, Dumont Lakes and Muddy Creek Trailheads: Rabbit Ears Pass

Mean snowpack hardness and subnivean hardness at Muddy Creek and Dumont Lakes were significantly different than Walton Creek (Table 5.2e). Mean snowpack hardness and subnivean hardness at Muddy Creek and Dumont Lakes showed no difference compared to Walton Creek at the beginning of the motorized winter recreation season on 11 December (Figure 5.5b). Subsequent to this sampling date mean snowpack hardness at Muddy Creek and Dumont Lakes were greater than Walton Creek throughout the winter (Figure 5.5b). Mean snowpack hardness at Muddy Creek and Dumont Lakes increased to a maximum of 138 kPa and 68 kPa on 5 February and 12 March, respectively, compared 42 kPa observed at Walton Creek on 12 March (Figure 5.5b). Subnivean hardness reached a maximum of 56 kPa and 24 kPa at Muddy Creek and Dumont Lakes on 5 February, respectively, compared to 6 kPa measured at Walton Creek (Figure 5.5b). The mean snowpack hardness and subnivean hardness at Walton Creek remained low throughout the winter season and by 16 April mean snowpack hardness and subnivean hardness at Muddy Creek and Dumont Lakes approached subnivean hardness measurements comparable to Walton (Figure 5.4b).

5.5.4 Shallow Snowpack Compaction Initiation (30 cm): Fraser Experimental Forest

Low, medium, and heavy use compaction treatments resulted in an increase in mean snowpack and subnivean hardness following snow compaction treatments beginning on 30 cm of snow at the Fraser Experimental Forest study plot (Figure 5.5c), which was significantly different than the control (Table 5.1d). Low use mean snowpack hardness increased to a maximum of 395 kPa on 22 January, while medium and heavy use mean snowpack hardness reached a maximum of 780 kPa and 4,627 kPa on 26 March, respectively (Figure 5.5c). In comparison, the maximum mean snowpack hardness for the control was 25 kPa on 26 March (Figure 5.4c). Low use subnivean hardness increased to a maximum of 138 kPa on 22 January, while medium and heavy use subnivean hardness increased to a maximum of 352 kPa and 728 kPa on 26 March, respectively, compared to 4 kPa for the control on 26 March (Figure 5.5c).

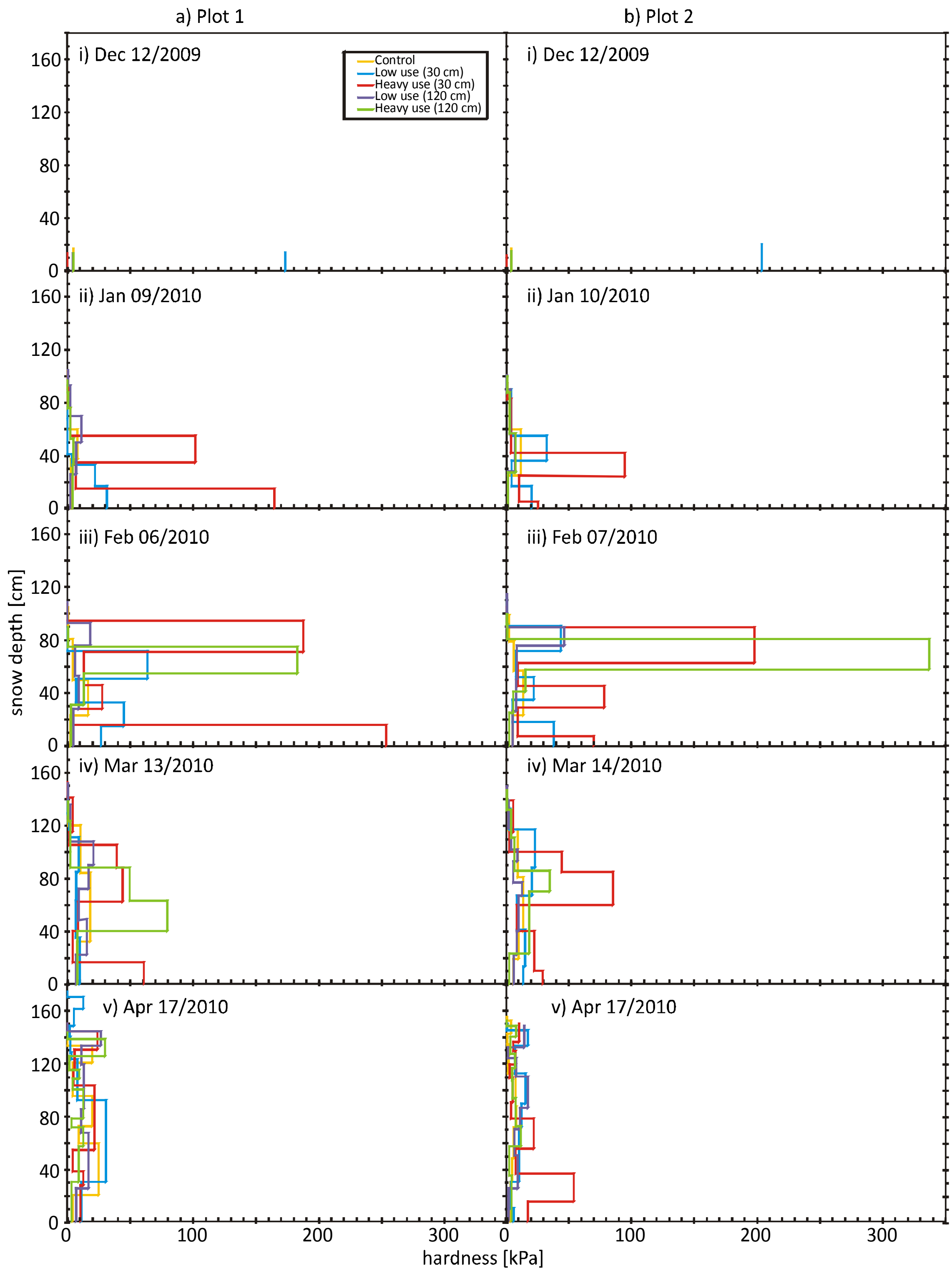

Figure 5.5a. Hardness profiles measured for no, low, medium, and heavy use snow compaction treatments beginning on 30 cm and 120 cm of snow at the snow compaction study plots located near Rabbit Ears Pass, Colorado during the 2009-2010 winter.

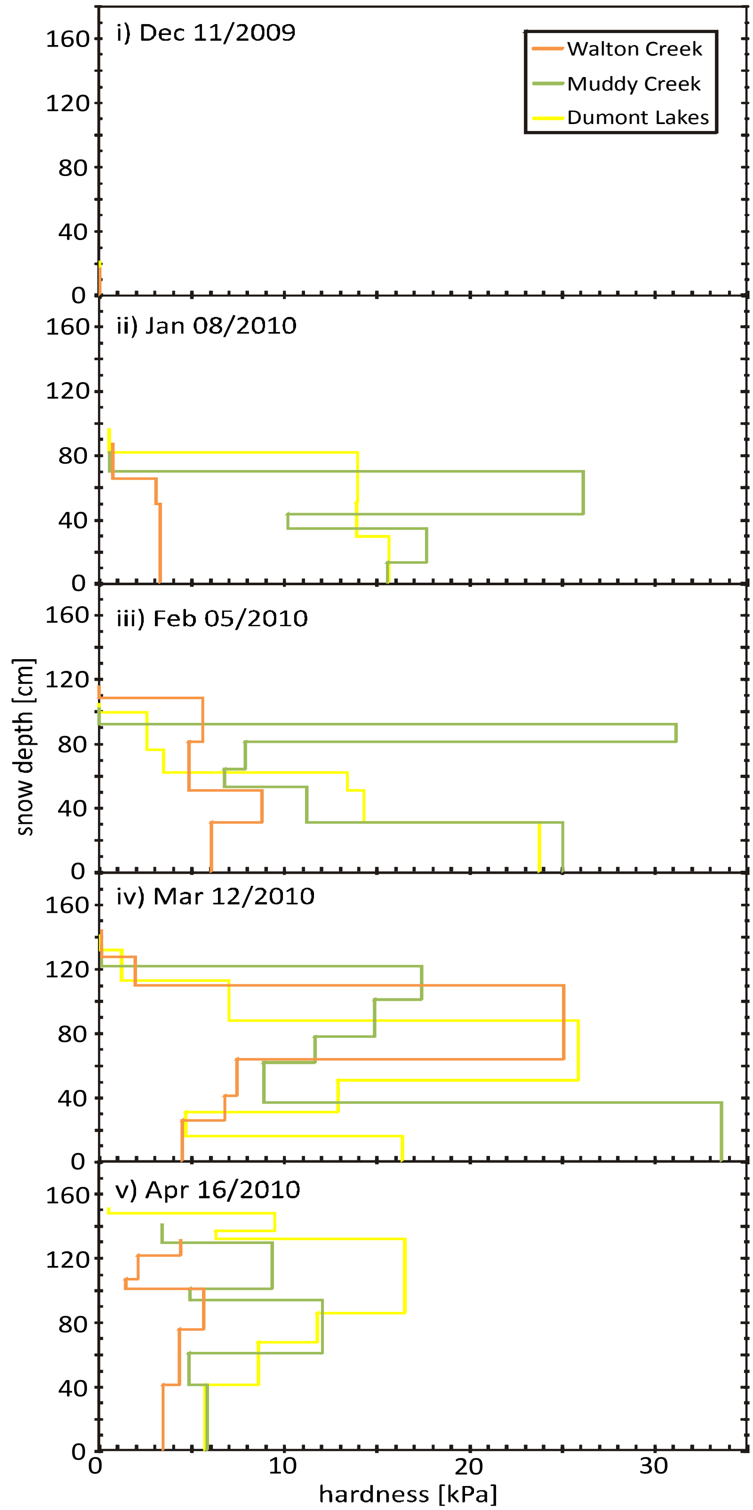

Figure 5.5b. Hardness profiles measured at Muddy Creek, Dumont Lakes, and Walton Creek trailheads on Rabbit Ears Pass, Colorado during the 2009-2010 winter.

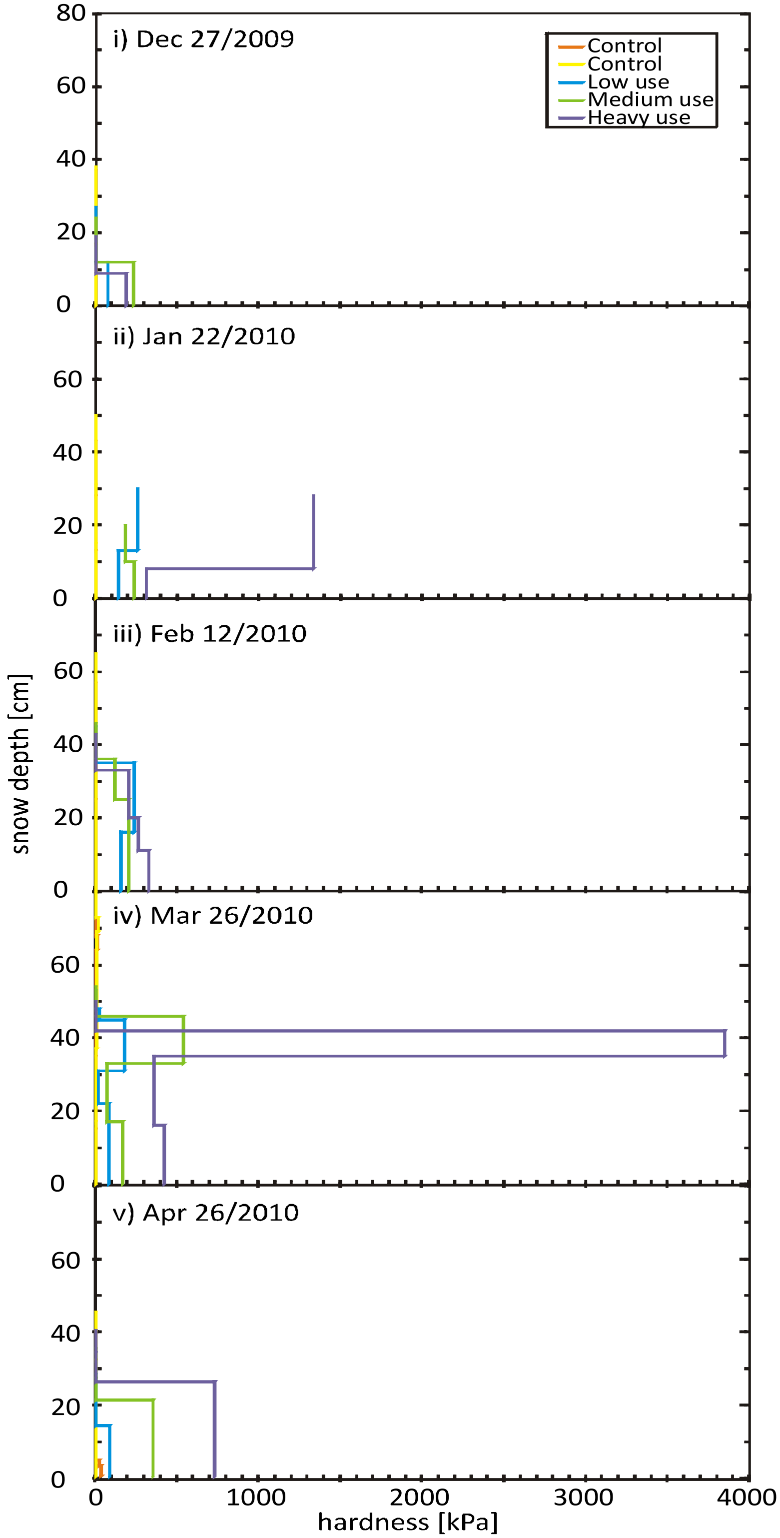

Figure 5.5c. Hardness profiles measured for no, low, medium, and heavy use snow compaction treatments beginning on 30 cm of snow at the snow compaction study plot located in Fraser Experimental Forest, Colorado during the 2009-2010 winter.

5.6 Ram Resistance

5.6.1 Shallow Snowpack Compaction Initiation (30 cm): Rabbit Ears Pass

Mean snowpack ram resistance increased as a result of low and heavy use compaction treatments beginning on 30 cm of snow at the Rabbit Ears Pass study plots (5.6a), which resulted in significant differences between treatments and the control (Table 5.1e). Low and heavy use resulted in maximum mean snowpack ram resistance measurements of 201N and 465N on 13-14 March and 6-7 February, respectively, compared to 127N for the control on 17 April (Figure 5.6a). Low and heavy use mean snowpack ram resistance experienced the largest difference compared to the control on 12 December (Figure 5.6a). Low and heavy use resulted in maximum subnivean ram resistance measurements of 614N and 1,297N on 12 December and 6-7 February, respectively, compared to 44N for the control on 13-14 March (Figure 5.6a). Mean snowpack ram resistance and subnivean ram resistance for low and heavy use treatments were greater than the control through the winter; however, there were limited differences between varying use and the control by the end of winter.

5.6.2 Deep Snowpack Compaction Initiation (120 cm): Rabbit Ears Pass

Mean snowpack ram resistance and subnivean ram resistance increased as a result of low and heavy use compaction treatments beginning on 120 cm of snow at the Rabbit Ears Pass study plot (Figure 5.6a); however these increases were not large enough to result in significant differences between varying use and the control (Table 5.1e). Low and heavy use resulted in a maximum mean snowpack ram resistance of 144N and 260N on 13-14 March, respectively, compared to 127N for the control on 17 April (Figure

5.6a). Low and heavy use mean snowpack ram resistance were greater than the control for the entire winter following the initial treatment; however, there were minimal differences by the end of winter. Low and heavy use resulted in a maximum subnivean ram resistance of 270N and 90N on 13-14 March and 6-7 February, respectively, compared to 44N for the control on 13-14 March (Figure 5.6a). Both low and heavy use subnivean ram resistance fluctuated around the control following the initial treatment and by the end of the winter there was minimal difference (Figure 5.6a).

5.6.3 Walton Creek, Dumont Lakes and Muddy Creek Trailheads: Rabbit Ears Pass

Mean snowpack ram resistance and subnivean ram resistance at Muddy Creek and Dumont Lakes were significantly different than Walton Creek (Table 5.2f). Mean snowpack ram resistance and subnivean ram resistance at Muddy Creek were greater than Dumont Lakes and Walton Creek at the beginning of the motorized winter recreation season on 11 December (Figure 5.6b). Subsequent to this date, mean ram resistance and subnivean ram resistance at Muddy Creek and Dumont Lakes were greater than Walton Creek throughout winter (Figure 5.6b). Mean ram resistance at Muddy Creek and Dumont Lakes increased to a maximum of 249N and 210N by 16 April, respectively, compared to a maximum of 82N measured at Walton Creek on 12 March (Figure 5.6b). Subnivean ram resistance increased to a maximum of 817N at Muddy Creek on 12 March and 280N at Dumont Lakes on 5 February compared to a maximum of 44N measured at Walton Creek on 16 April (Figure 5.6b). The mean ram resistance at Walton Creek decreased prior to the last sampling date, and Muddy Creek and Dumont Lakes continued to show increasing trends, while subnivean ram resistance at Muddy Creek and Dumont

Lakes were beginning to show decreasing trends to subnivean ram resistance measurements comparable to Walton Creek (Figure 5.6b).

5.6.4 Shallow Snowpack Compaction Initiation (30 cm): Fraser Experimental Forest

Low, medium and heavy use compaction treatments resulted in an increase in mean snowpack ram resistance and subnivean ram resistance following snow compaction treatments beginning on 30 cm of snow at the Fraser Experimental Forest study plots (Figure 5.6c), which resulted in significant differences between the treatments and the control (Table 5.1e). Mean snowpack ram resistance generally increased throughout the winter for all treatments (Figure 5.6c). Low and medium use resulted in a maximum mean snowpack ram resistance of 544N and 591N on 26 March, respectively, while heavy use resulted in a maximum mean snowpack ram resistance of 866N on 12 February (Figure 5.6c). Comparably, the control reached a maximum mean snowpack ram resistance of 18N on 26 March (Figure 5.6c). Subnivean ram resistance increased following the initial snow compaction treatment and continued to increase throughout the duration of the winter season. Both low and medium use resulted in a maximum subnivean ram resistance of 1,220N, while heavy use resulted in a maximum subnivean hardness of 3,220N on 12 February compared to a maximum of 28N for the control on 26 March (Figure 5.6c).

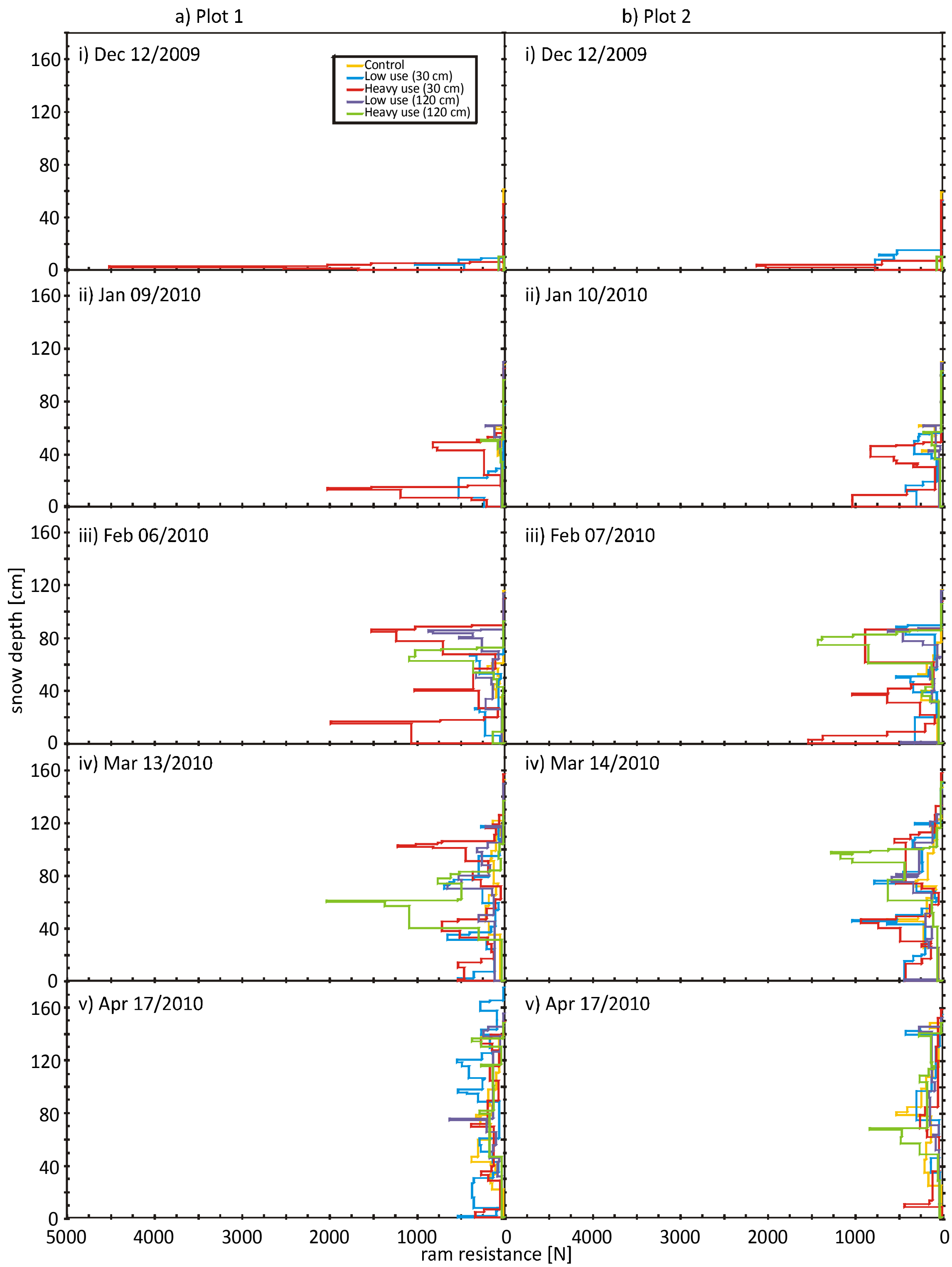

Figure 5.6a. Ram resistance profiles measured for no, low, medium, and heavy use snow compaction treatments beginning on 30 cm and 120 cm of snow at the snow compaction study plots located near Rabbit Ears Pass, Colorado during the 2009-2010 winter.

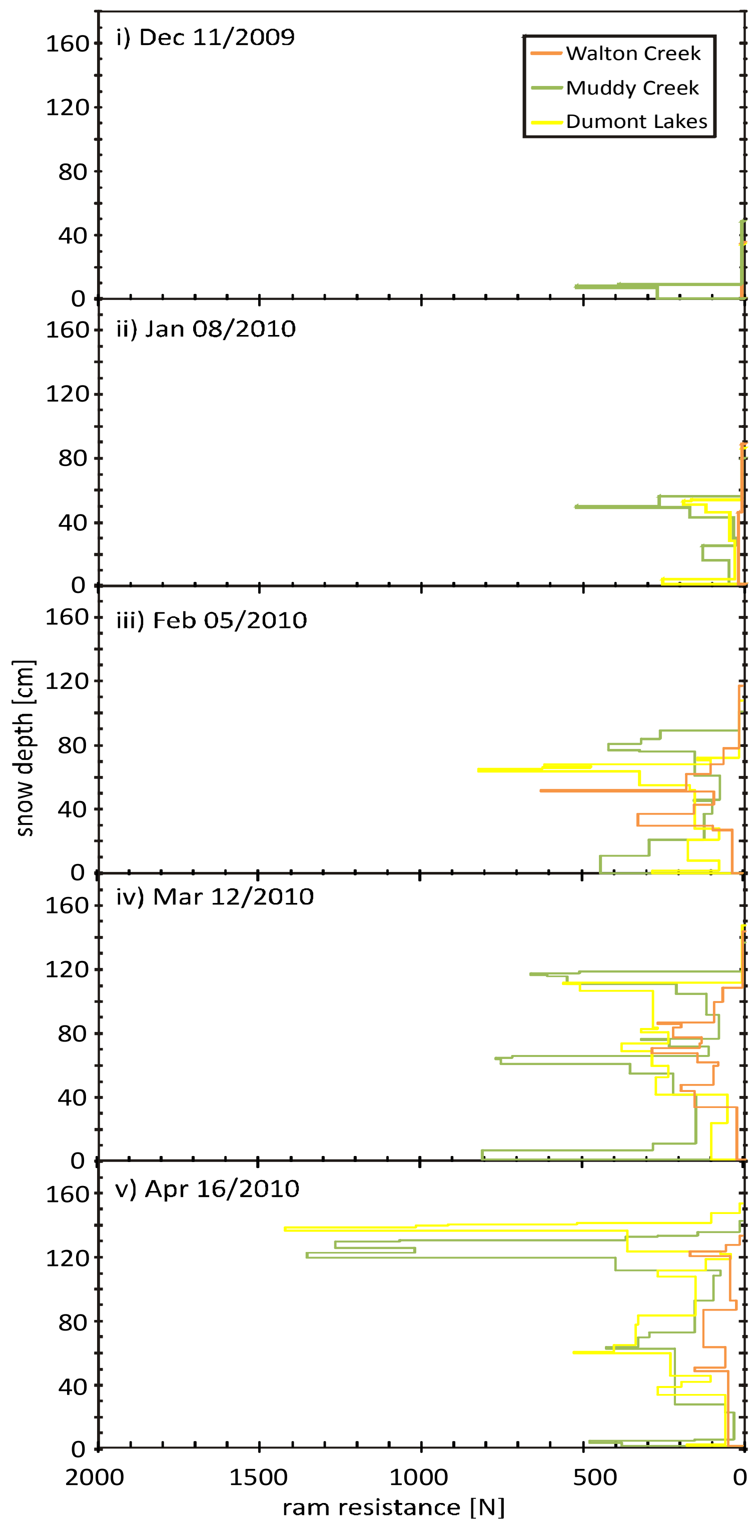

Figure 5.6b. Ram resistance profiles measured at Muddy Creek, Dumont Lakes, and Walton Creek trailheads near Rabbit Ears Pass, Colorado during the 2009-2010 winter.

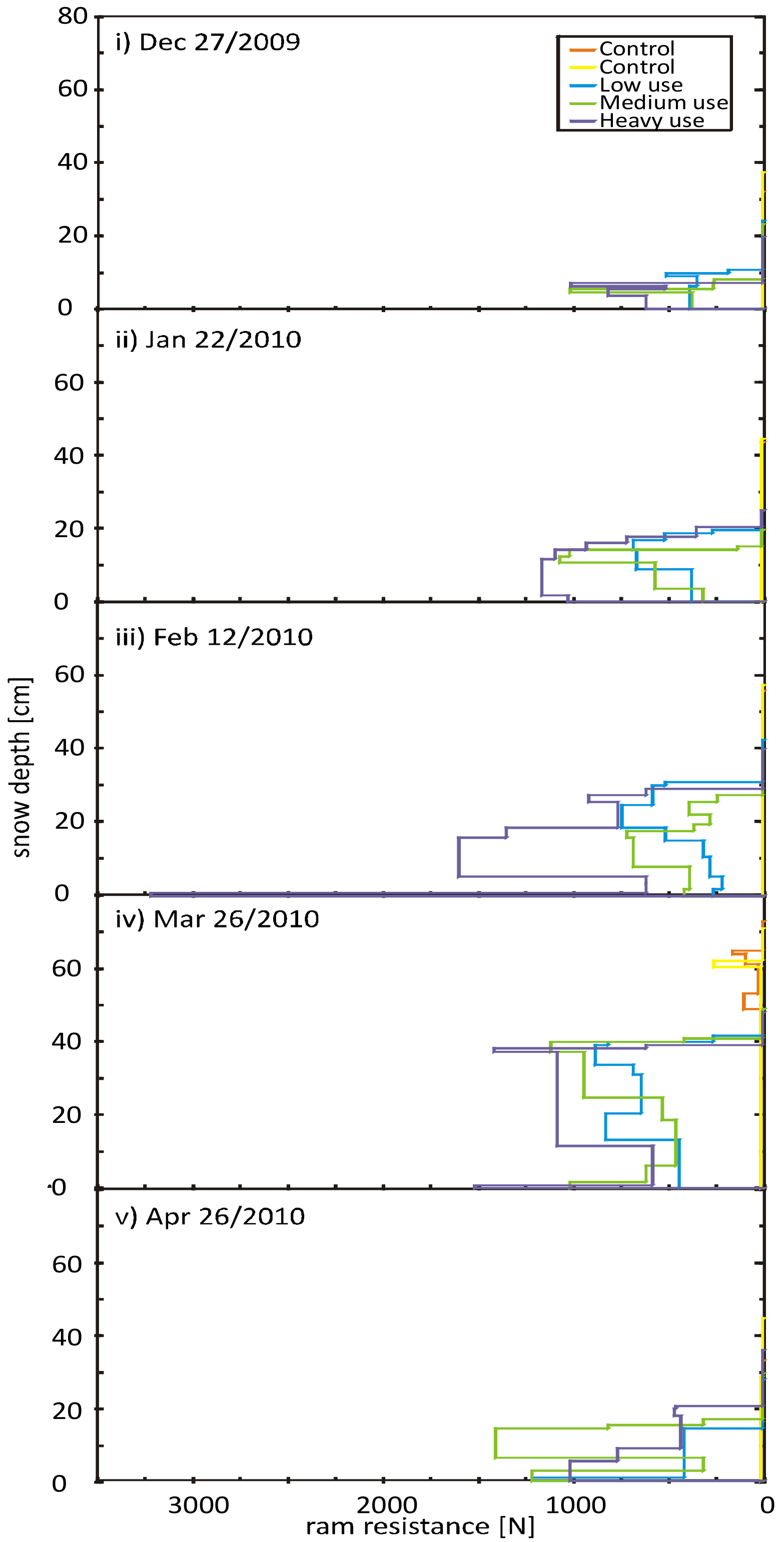

Figure 5.6c. Ram resistance profiles measured for no, low, medium, and heavy use snow compaction treatments beginning on 30 cm of snow at the snow compaction study plot located in Fraser Experimental Forest, Colorado during the 2009-2010 winter.

5.7 Heat Flow

Compaction due to motorized winter recreation increased the bulk density of the snowpack (Figures 5.1a, 5.1b and 5.1c), thus increasing the thermal conductivity (Figure 5.7a) to values comparable to those outlined by Marchand (1987). However, thermal conductivity at Fraser Experimental Forest for low, medium and heavy use was greater than the control for the entire winter. Low use thermal conductivity reached a maximum on 12 February, which was 374 percent greater than the average control, while medium and heavy use increased to as much as 174 percent and 145 percent by 26 March, respectively (Figure 5.7a). Motorized winter recreation operating on a deep snow regime, similar to Rabbit Ears Pass, has comparable influences on the thermal conductivity of the snowpack, although the changes were not as pronounced. The insulative values for low, medium and heavy use decreased by 50 percent, 51 percent and 46 percent, respectively, compared to the average control on 12 February (Figure 5.7b), when snow depth was shallower (Figure 5.3f) and bulk snowpack density had the greatest difference compared to the control (Figure 5.1c).

Motorized winter recreation operating on a deep snow regime, similar to Rabbit Ears Pass, has similar influences on the insulative value of the snowpack. However, the deeper snowpack allows for increased insulative values (Figure 5.7c) as a result of deeper snow depths and because compaction events are followed by fresh snowfall events producing a snowpack stratified with less dense layers of high insulative value and denser layers with low insulative value. The bulk snowpack density was greater than the control for the entire winter season when compaction treatments began on a shallow snowpack (Figure 5.1a) resulting in lower insulative values (Figure 5.7c). As a result, low and heavy use insulative values were 10 percent and 21 percent different than the control, respectively (Figure 5.7c), when bulk snowpack density varied the most on 6 February (Figure 5.1a).

Minor changes in bulk snowpack density were observed when motorized winter recreation began on a deep snowpack , although heavy use bulk snowpack density increased following the initial compaction treatment (Figure 5.1a), which decreased the insulative value by 20 percent of the control on 6 February (Figure 5.7c). However, heavy use bulk snowpack density recovered and by 13 March the insulative value differed by only 4 percent (Figure 5.7c). On the contrary, low use bulk snowpack density was similar to the control (Figure 5.1a), which resulted in comparable insulative values for the entire winter season even after compaction treatments were initiated (Figure 5.7c).

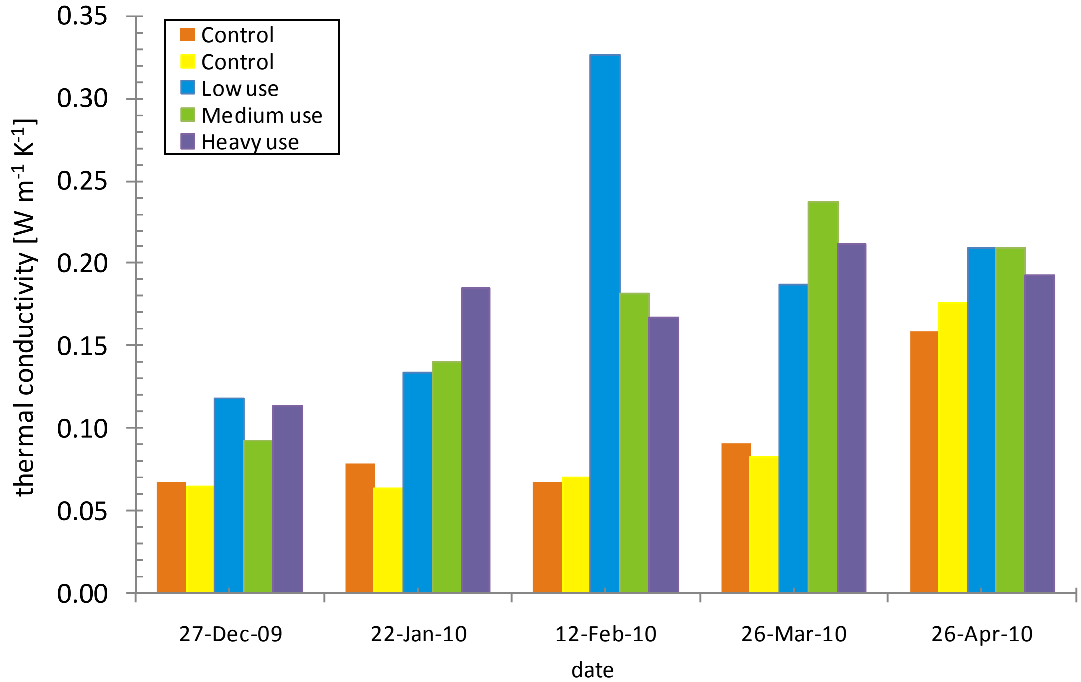

Figure 5.7a. Modeled thermal conductivity for no, low, medium and heavy use at Fraser Experimental Forest, Colorado when compaction treatments began on a shallow snowpack during the 2009-2010 winter.

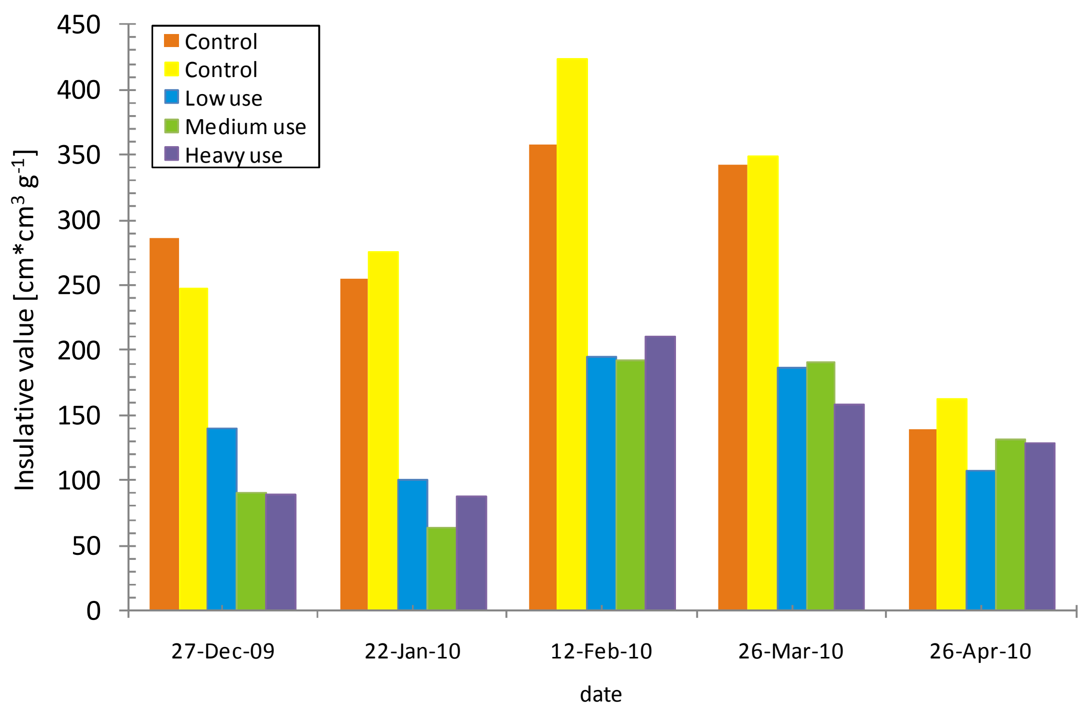

Figure 5.7b. No, low, medium and heavy use insulative value calculated using Marchand's thermal index for Fraser Experimental Forest, Colorado when compaction treatments began on a shallow snowpack during the 2009-2010 winter.

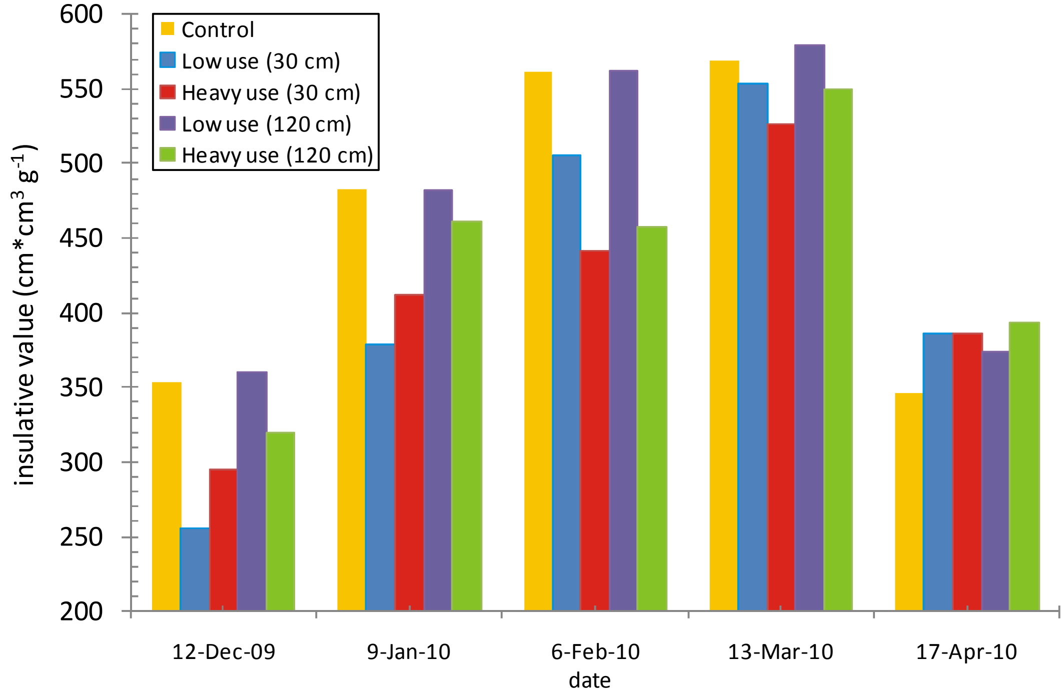

Figure 5.7c. No, low and heavy use insulative value calculated using Marchand's thermal index for Rabbit Ears Pass, Colorado when compaction treatments began on a shallow (30 cm) and deep (120 cm) snowpack during the 2009-2010 winter.

6.0 DISCUSSION

6.1 Implications

Changes to physical and mechanical properties of the snowpack were compared for varying use of motorized winter recreation beginning on different snow depths. There are a number of external and internal environmental factors that contribute to the changes in snowpack properties including gravitational force, the force exerted by the weight of air, wind, solar radiation, aspect and slope, but compression stress exerted by the weight of a motorized winter recreation vehicle can have significant effects on the physical properties of the snowpack that far exceed natural factors (Table 5.1 and Table 5.1). Motorized winter recreation vehicles exert approximately 1.15 kPa-1.78 kPa of pressure to the underlying snowpack assuming an average track dimension of approximately 50 cm x 396 cm x 3 cm and a snowmobile weight of 295-454 kg that includes the weight of a 90 kg rider (data obtained from Polaris Snowmobiles Official website at <http://www.polarisindustries.com>). In comparison, fresh snow with a density of 100 kg/m^3 exerts a pressure of 0.003 kPa to the underlying snowpack (Moynier, 2006). Needless to say, motorized winter recreation has an influence on the properties of the snowpack and the results presented in the previous chapter can be used to infer changes to the habitat conditions and the potential for mammalian movement within the subnivean environment.

6.1.1 Insulative Value

Snow density, depth, grain characteristics and temperature are important to subnivean mammals since changes to these properties can influence the insulative value of the snowpack. The density of the entire snowpack (bulk) and in the subnivean layer increased (Figures 5.1a and 5.1c) while the basal layer temperatures were significantly affected (Figures 5.2a and 5.2c) as a result of motorized winter recreation beginning on a shallow snowpack. Additionally, the decrease in snow depth (Figures 5.3b, 5.3d and 5.3f) was due to motorized winter recreation beginning on a shallow snowpack.

The insulative value of the snowpack is inversely proportional to the thermal conductivity. Marchand (1982) proposed the use a of a snow thermal index for estimating the insulative value of a snow cover that is directly related to layer thickness and inversely related to the density. Therefore, as density increases and snow depth decreases the insulative value decreases. Motorized winter recreation operating on a shallow snow regime, similar to Fraser Experimental Forest, can have a large influence on the insulative value (Figure 5.7b) of the snowpack due to increased bulk snowpack density (Figure 5.1c) and decreased snow depth (5.3f).

These results suggest that motorized winter recreation beginning on a shallow snowpack and operating on shallow and deep snow covers can have negative effects on the thermal conductivity (Figure 5.7a), thus influencing the insulative value of the snowpack (Figure 5.7b). Although the regression only explains 39 percent of the variability it is apparent that as the thermal conductivity increases the insulative value decreases (Figure 6.1). A deep snowpack is capable of decreasing the effect of compaction from motorized winter recreation vehicles reducing large increases in bulk snowpack density, thereby allowing conduction processes to proceed similar to the control and maintain insulative values that may be suitable for the survival of overwintering subnivean mammals. Conversely, shallow snow regimes are more susceptible to greater changes in these properties influencing the thermal conductivity and insulative value, thus having a greater effect on the microclimate that subnivean mammals depend on for overwintering success.

6.1.2 Impediment of Subnivean Movement

Snowpack density, hardness, and ram resistance increased as a result of motorized winter recreation for the entire snowpack and at the subnivean interface. These properties are important to subnivean mammals since changes to these snowpack properties can impede movement.

Increased subnivean density may impede subnivean mammals from moving within the snowpack because of an increase in the bonding between snow crystals leading to an overall gain in hardness and ram resistance. A sufficient layer of cohesion-less snow crystals (depth hoar) is desired for mammalian movement within the snowpack, which are strong in compression and weak in shear. These mechanical properties make it possible for the subnivean space to remain persistent throughout the winter season with the addition of snow loads by being strong in compression, while the weak shear of depth hoar crystals may provide for relatively easy movement by subnivean mammals. However, the subnivean space may collapse due to pressure from heavy overlying loads (Green, 1998).

Increased subnivean density, ram resistance and hardness are a result of changes to the grain characteristics and compaction by motorized winter recreation; as depth hoar crystals become compacted there is an increase in bonding between crystals and early compaction impedes further kinetic growth. Temperature gradients were maintained throughout the winter season ranging from $33^{o}C\ m^{-1}$ at the beginning of the season to near $0^{o}C\ m^{-1}$ by the end of the winter season. These temperature gradients were unaffected by compaction from motorized winter recreation (Figures 5.2a, 5.2b, and 5.2c) due to the edge effect of heat transfer from the warmer ground adjacent to the plots, heat transfer from the buffer areas located parallel to compaction transects and diurnal changes in ambient air temperatures. The temperature gradient was sufficient for kinetic growth metamorphism for most of the winter season ($T_G > 10^{o}C\ m^{-1}$); however increases in density suggest that kinetic growth was retarded by reduced vapor diffusion as a result of decreased porosity. Compaction increases density, hardness and ram resistance making it more difficult for subnivean mammals to move. Such increases in subnivean density, hardness and ram resistance were observed for motorized winter recreation that began on a shallow snowpack for both shallow (Figures 5.1c, 5.5c and 5.6c) and deep (Figures 5.1a, 5.5a and 5.6a) snow regimes, but was much less apparent for motorized winter recreation that began on a deep snowpack (Figures 5.1a, 5.5a and 5.6a, respectively).

Hardness is the force per unit area required to penetrate the structure of the snowpack and is a measure of strength in compression (McClung and Schaerer, 2006). Similarly, the greater the hardness of the snow, the greater resistance it has towards movement and hardness can be assessed by characterizing the microstructure and bonding characteristics of the snow crystals (Shapiro et al., 1997). Since hardness and density depend predominantly on grain characteristics, such as bonding and grain contacts (Shapiro et al., 1997) and decreasing grain size results in increased hardness and density, then motorized winter recreation beginning on a shallow snowpack could provide greater resistance to movement for subnivean mammals. Increases in both subnivean density and hardness were observed at Rabbit Ears Pass and Fraser Experimental Forest; however, these increases were more pronounced at Fraser Experimental Forest. For example, low, medium, and heavy use subnivean densities at Fraser Experimental Forest were 288 kg/m^3, 336 kg/m^3, and 330 kg/m^3, respectively (Figure 5.1c), compared to 116 kg/m^3 on 27 December following the initial snow compaction treatment. Low use subnivean hardness increased to a maximum of 138 kPa on 22 January, while medium and heavy use subnivean hardness increased to a maximum of 352 kPa and 728 kPa on 26 March, respectively, compared to 4 kPa for the control on 26 March (Figure 5.5c). The large increase in subnivean density at the beginning of the season may influence the distribution and survival of subnivean mammals by deterring them from creating subnivean tunnels, while also inducing in a substantial increase in subnivean hardness. This increase in subnivean hardness may also make it more difficult for subnivean mammals to move with ease within the snowpack.

Pruitt (2005) found that an undisturbed snowpack can have strength values that range from 0.02 to 0.5N and these values can increase to as much as 70N as a result of two passes with one person on a snowmobile. The precision of the standard ram penetrometer used in this study was 10N, which was unable to capture ram resistance values this low. For comparison, our study revealed that for a deep snow cover regime, such as Rabbit Ears Pass, motorized winter recreation that began on a shallow snowpack resulted in maximum subnivean ram resistance values of 614N and 1,297N for low and heavy compaction, respectively (Figure 5.6a). In areas that receive lower annual snowfall, such as Fraser Experimental Forest, motorized winter recreation can result in a substantial increase in bulk and subnivean ram resistance (Figure 5.6c) to the point where a compacted snowpack may exhibit relatively uniform snowpack ram resistance making movement more difficult in both the intranivean and subnivean spaces (Figure 5.6c). Conversely, in areas that receive higher annual snowfall, similar to Rabbit Ears Pass, motorized winter recreation increases bulk and subnivean ram resistance, but fresh snowfall events following compaction treatments can produce a snowpack of stratified strong and weak layers (Figure 5.6a). Subnivean mammals may select these weaker layers for movement (Green, 1998). These results suggests that a deeper snowpack is capable of decreasing the effect of motorized winter recreation on mechanical properties near the subnivean space imperative for unimpeded movement by subnivean mammals.

6.2 Future Work

This research has provided insight into the effect of compaction from motorized winter recreation on snowpack properties. Further work will provide a comprehensive understanding of the large-scale impact that this land use practice may have on snow covered ecosystems. The following lists future work that can provide more insight into the influences of motorized winter recreation:

- Determine an adequate snow depth for motorized winter recreation to begin and operate on that will minimize the influence of compaction to the physical and mechanical properties of the subnivean space;

- Evaluate the influence of motorized winter recreation on the internal energy flux of the snowpack by modeling thermal conduction and heat flux processes using SNTHERM (Jordan, 1991);
- Quantify the amount of CO_2 in a snowpack influenced by varying use of motorized winter recreation to determine the extent of CO_2 trapped within the snowpack;
- Assess the influence of compaction due to motorized winter recreation on light levels and how changes to the internal light regime can influence vegetation growth and photosynthesis;
- Assess the influence of compaction of the subnivean on habitat fragmentation and changes in predator/prey relationships

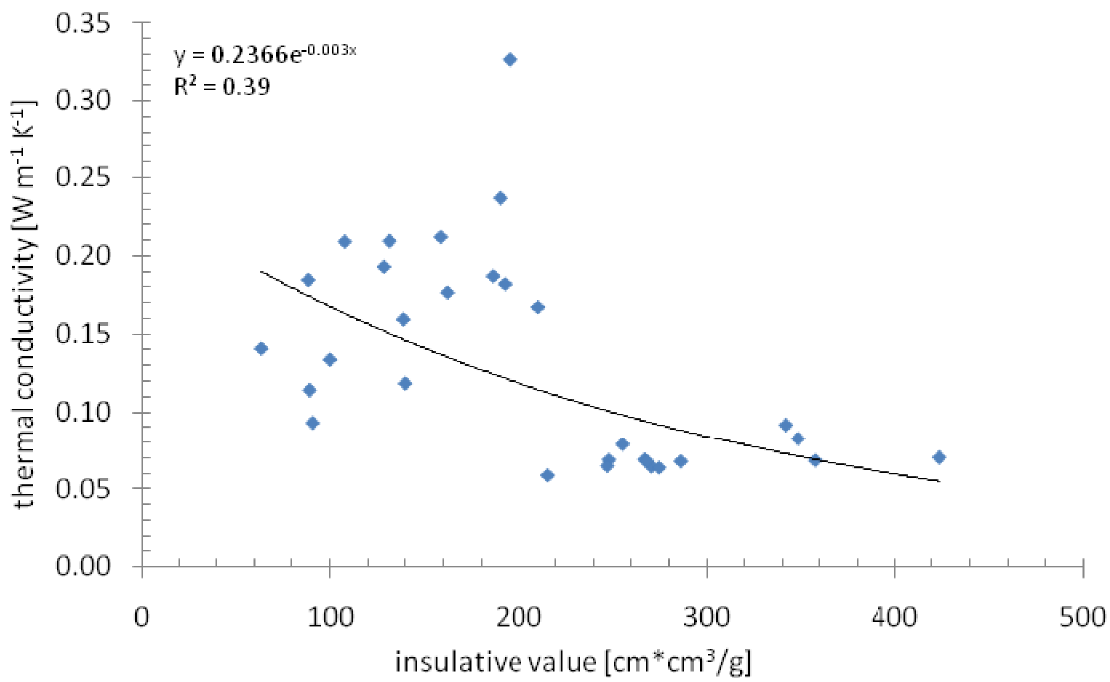

Figure 6.1. Relationship between model thermal conductivity and the insulative value calculated using Marchand's thermal index showing that the insulative value increases with decreasing thermal conductivity.

7.0 CONCLUSION

7.1 Conclusion

This study examined the effect of compaction from motorized winter recreation on snowpack properties. It showed that snowpack properties change with varying use of motorized winter recreation, with the amount of snowfall, at the initiation of use. Minimizing the effect of compaction on these properties will aid in maintaining a stable subnivean environment that promotes unimpeded subnivean movement. Land use managers may consider evaluation of these snowpack properties in consideration of management plans.

Motorized winter recreation creates compaction that influences the physical and mechanical properties of the snowpack. In particular, this increases bulk snowpack density, hardness, and ram resistance when winter recreational use occurs and decreases snow depth. The largest differences in snowpack properties are associated with motorized winter recreation beginning on a shallow snowpack (30 cm), which increases bulk snowpack and subnivean density, hardness, and ram resistance. These increases are directly related to increasing motorized winter recreation use (from low to medium to heavy). Conversely, motorized winter recreation that begins on a deep snowpack (120 cm) has a limited effect on snowpack properties as seen by bulk and subnivean densities, temperatures, hardness, and ram resistance comparable to an undisturbed snowpack.

Changes to snowpack properties near the subnivean environment could influence movement by small mammals in the subnivean space when motorized winter recreation begins operation on a shallow snowpack, due to an increase in density, hardness, and ram resistance near the subnivean space. Additionally, the insulative value decreases due to changes in density, snow depth and crystal morphology across the entire snowpack and near the subnivean space. Conversely, motorized winter recreation that begins operation on a deep snowpack reduces the effect of compaction throughout the snowpack providing a subnivean environment comparable to natural snowpack conditions, which may allow subnivean mammals to move more easily in a well-insulated environment.

Snowpack properties of varying snowpack regimes (shallow vs. deep) respond differently to motorized winter recreation. Shallow snow covers experience an increase in bulk and subnivean densities, ram resistance, and hardness and a decrease in snowpack temperatures (bulk and subnivean) and snow depth that are more pronounced than changes to these properties when motorized winter recreation operates on a deep snowpack. These changes in the physical properties of the snowpack are due to motorized winter recreation operating on an already compacted snowpack yielding thick layers of dense, strong, hard snow. Deep snow covers experience more snowfall events that create "cushions" of relatively undisturbed snow between compaction events lessening the effect of motorized winter recreation on snowpack properties. These differences between snow regimes suggest that shallow snowpacks are more susceptible to larger changes in snowpack properties, which will have greater adverse effects on the insulative value of the subnivean environment and mammalian movement within this habitat.

Field measurements and study plot observations were able to provide a good representation of the effect of compaction from motorized winter recreation on snowpack properties supporting the hypotheses. The overall objectives were attained and provide insight on the influence and implications of motorized winter recreation on snow covered areas, and the type of measurements needed in the management of motorized winter recreational areas.

8.0 LITERATURE CITED

Aitchison, C. W., 2001. The Effect of Snow Cover on Small Animals. In: G. Jones, J. W. Pomeroy, D. A. Walker and R. W. Hoham (Eds.) *Snow Ecology: An Interdiseplenary Examination of Snow Covered Ecosystems*. Cambridge University Press, Cambridge, pp. 229-265.

Auerbach, N. A. and Halpenny, J. C., 1991. Snowpack and the Subnivean Environment for Different Aspects on an Open Meadow in Jackson Hole, Wyoming, U.S. *Arctic and Alpine Research,* 23(1), 41-44.

Colbeck, S.C., 1982. An Overview of Seasonal Snow Metamorphism. *Reviews of Geophysics and Space Physics,* 20(1), 45-61.

Colbeck, S.C. 1987. A review of the metamorphism and classification of seasonal snow cover crystals. Avalanche Formation, Movement and Effects. IAHS Pub. 162. 3 – 34.

Colbeck, S.C. and 7 other, 1990. *The International Classification for Seasonal Snow on the Ground*. International Commission on Snow and Ice (IAHS), World Data Center A for Glaciology, University of Colorado, Boulder, CO, 37 pp.

Cook, B. and Borrie, W., 1995. Trends in Recreation Use and Management of Wilderness. *International Journal of Wilderness,* 1(2), 30-34.

Courtin, G. M., Kalliomaki, N. M., Hillis, T., and Robitaille, R. L., 1991. The Effect of Abiotic Factors on the Overwintering success in the Meadow Vole, *Microtus Pennsylvanicus*: Winter Redefined. *Arctic and Alpine Research,* 23(1), 45-52.

Dorrance, M. J., Savage, P. J. and Huff, D. E., 1975. Effects of Snowmobiles on White-Tailed Deer. *Journal of Wildlife Management,* 39(3), 563-569.

Diamond, M. and W.P. Lowry, 1953. Correlation of density of new snow with 700 mb temperature. Research Paper 1, Snow, Ice and Permafrost Research Establishment, US Army Corps of Engineers, 3 pp.

Dunne, T. and Leopold, L.B., 1978. *Water in Environmental Planning*. W.H. Freeman and Company, New York, pp. 466-470.

Fassnacht, S.R. and E.D. Soulis, 2002. Implications during transitional periods of improvements of snow processes in the Land Surface Scheme – Hydrological Model WATCLASS. *Atmosphere-Ocean,* 40(4), 389-403.

Formozov, A.N., 1946. *Snow Cover as an Integral Factor in the Ecology of Mammals and Birds*. Boreal Institute, Edmonton, 152 pp.

Gold, L.W. 1958. Changes in a shallow snow cover subject to a temperate climate *Journal of. Glaciology,* 3, 218–222.

Green, K., 1998. A winter niche: the subnivean space. In: Green, K. (Ed.), *Snow: A Natural History, An Uncertain Future*. Australian Alps Liaison Committee, Canberra, pp. 125-140.

Greene, E. et al., 2009. *Snow, Weather, and Avalanches: Observational Guidelines for Avalanche Programs in the United States*. American Avalanche Association and USDA Forest Service National Avalanche Center, 136 pp.

Höller, P. and R. Fromm, 2010. Quantification of the hand hardness test. *Annals of Glaciology,* 51(54), 39-44.

Jordan, R., 1991. *A one dimensional model for snow cover: technical documentation for SNTHERM89*. Special Report 91-16, US Army Cold Regions Research and Engineering Laboratory (CRREL), Hanover, NH, 49 pp.

Kolbe, J. A., Squires, J. R., Pletscher, D. H. and Ruggiero, L. F., 2007. The Effect of Snowmobile Trails on Coyote Movements Within Lynx Home Ranges. *The Journal of Wildlife Management,* 71(5), 1409-1418.

Longley, R.W. 1960. Snow depth and density at Resolute, Northwest Territories. *Journal of Glaciology,* 3, 733–738.

Marchand, P. J., 1982. An Index for Evaluating the Temperature Stability of a Subnivean Environment. *The Journal of Wildlife Management*, 46(2), 518-520.

Marchand, P. J., 1987. *Life in the cold*. University Press of New England, Hanover, New Hampshire, 176 pp.

McClung, D. and Schaerer, P., 2006. *The Avalanche Handbook, 3rd Edition*. The Mountaineers Books, Seattle, Washington, 342 pp.

Moynier, J., 2006. *Avalanche Aware: The Essential Guide to Avalanche Safety.* Morris Book Publishing, LLC, Guilford, Connecticut, 90 pp.

Pruitt, W. O., 1960. Animals in the Snow. *Scientific American,* 202(1): 60-68.

Pruitt, W. O., 1970. Some ecological aspects of snow. In: *Proceedings of the 1960 Helsinki Symposium on Ecology of the Subarctic Regions*. UNESCO, Paris, pp. 83-99.

Pruitt, W. O., 1984. Snow and small animals. In: Merritt, J.F., (Ed.), *Winter Ecology of Small Mammals*. Special publication No. 10. Carnegie Museum of Natural History, Pittsburgh, pp. 1-8.

Pruitt, W. O., 2005. Why and how to study a snowcover. *Canadian field-naturalist*, 119(1): 118-128.

Sanecki, G. M., Green, K., Wood, H., and Lindenmayer, D., 2006. The implications of snow-based recreation for small mammals in the subnivean space in south-east Australia. *Biological Conservation*, 129, 511-518.

SAS Institute Inc., 2008. *SAS/STAT® 9.2 User's Guide.* SAS Institue Inc., Cary, North Carolina, 224 pp.

Schmidt, R.A., J.R. and D.R. Gluns. 1991. Snowfall interception on branches of three conifer species. *Can. J. Forest Res.* 21, 1262–1269.

Shapiro, L. H., Johnson, J. B., Sturm, M., and Blaisdell, G. L., 1997. *Snow Mechanics: Review of the State of Knowledge and Applications*. USA Cold Regions Research and Engineering Laboratory (CRREL), Research Report 97-3.

USDA Forest Service, 2005. *Winter Recreation Management and Routt National Forest Plan Amendment*. USDA Forest Service, Medicine Bow-Routt Nationals Forests, Rocky Mountain Region, 23 pp.

USDA Forest Service Rocky Mountain Region. "Region 2 Regional Forester's Sensitive Species." United States Forest Service. http://www.fs.fed.us/r2/projects/scp/sensitivespecies/index.shtml [accessed October 1, 2010].

Wahl, K. L., 1992: Evaluation of trends in runoff in the western United States: Managing water resources during global change. *Proc. Annual Conf. and Symp.,* Reno, NV, American Water Resources Association, 701–710.

Winter Wildlands Alliance, 2006. *Winter Recreation on Western National Forest Lands: A Comprehensive Analysis of Motorized and Non-Motorized Opportunity and Access*. Winter Wildlands Alliance, Boise, Idaho, 44 pp.

US Army Cold Regions Research and Engineering Laboratory, 2005. "Thermal Conductivity Measurements." Snow Interest Group (SIG). http://snow.usace.army.mil/heat_mass_transfer/thermal_conductivity.htm [accessed October 13, 2010].

APPENDIX A

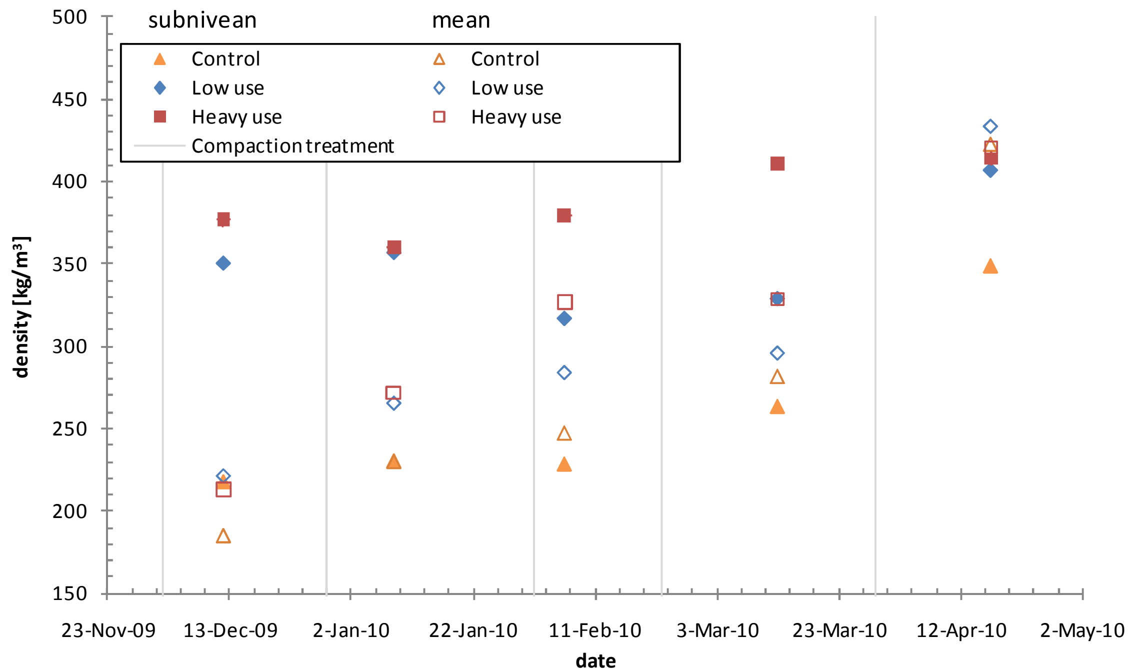

Figure A-1. No, low and heavy use bulk snowpack density and subnivean density measured at the snow compaction study plots on Rabbit Ears Pass, Colorado when compaction treatments began on a shallow snowpack during the 2009-2010 winter.

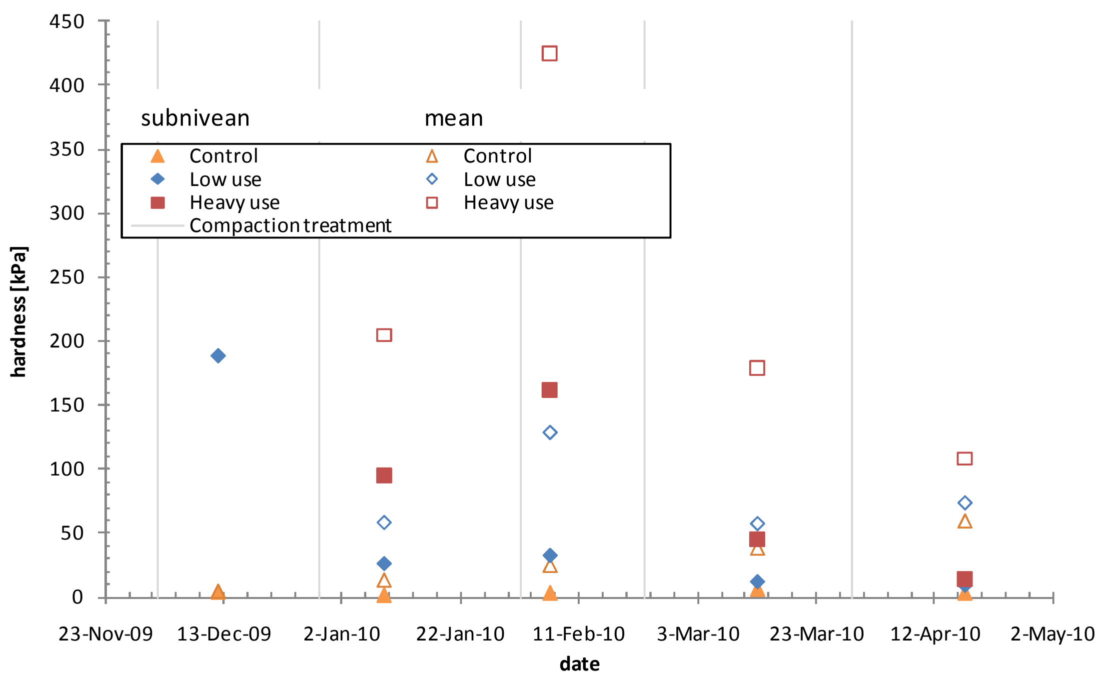

Figure A-2. No, low and heavy use mean snowpack hardness and subnivean hardness measured at the snow compaction study plots on Rabbit Ears Pass, Colorado when compaction treatments began on a shallow snowpack during the 2009-2010 winter.

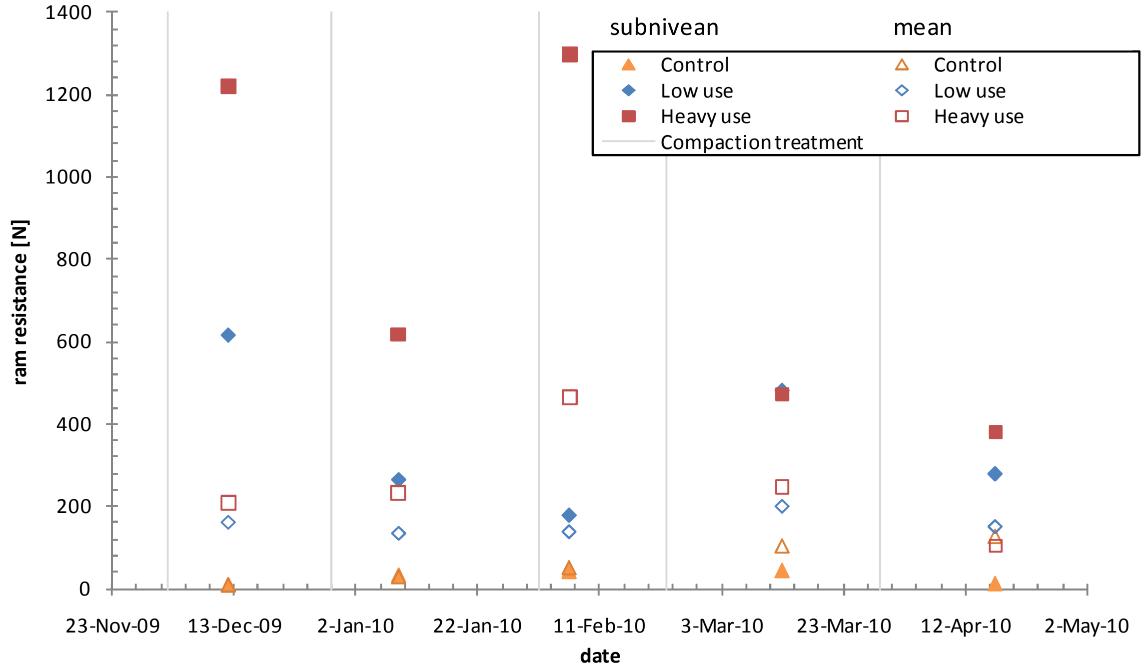

Figure A-3. No, low and heavy mean snowpack ram resistance and subnivean ram resistance measured at the snow compaction study plots on Rabbit Ears Pass, Colorado when compaction treatments began on a shallow snowpack during the 2009-2010 winter.

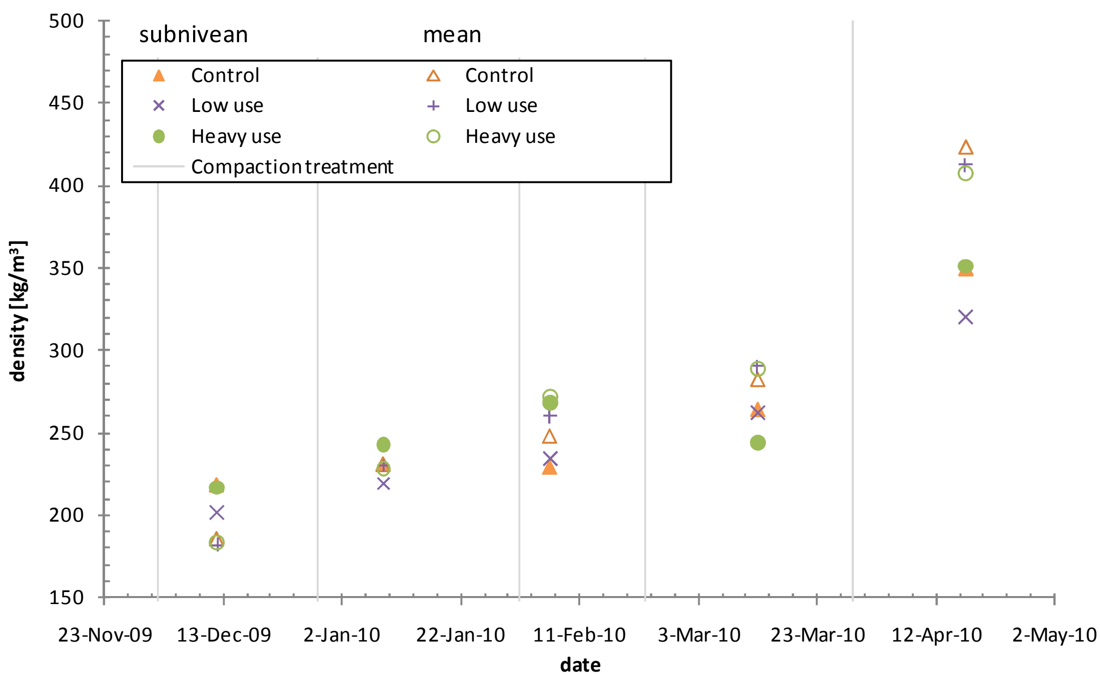

Figure A-4. No, low and heavy bulk snowpack density and subnivean density measured at the snow compaction study plots on Rabbit Ears Pass, Colorado when compaction treatments began on a deep snowpack during the 2009-2010 winter.

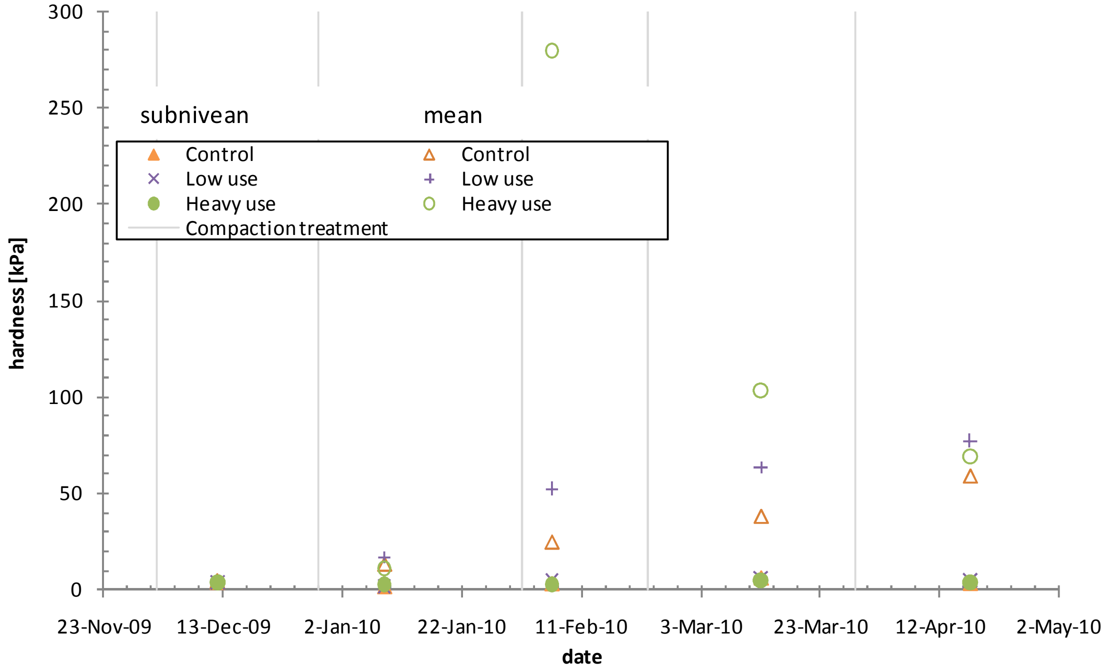

Figure A-5. No, low and heavy mean snowpack hardness and subnivean hardness measured at the snow compaction study plots on Rabbit Ears Pass, Colorado when compaction treatments began on a deep snowpack during the 2009-2010 winter.

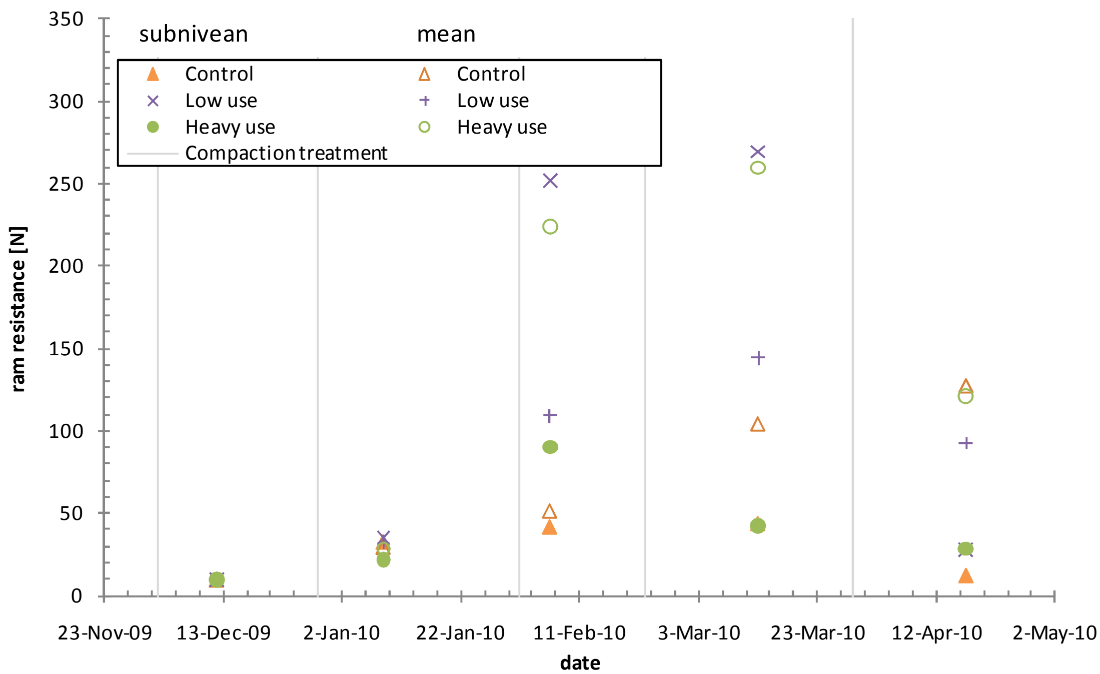

Figure A-6. No, low and heavy use mean snowpack ram resistance and subnivean ram resistance measured at the snow compaction study plots on Rabbit Ears Pass, Colorado when compaction treatments began on a deep snowpack during the 2009-2010 winter.

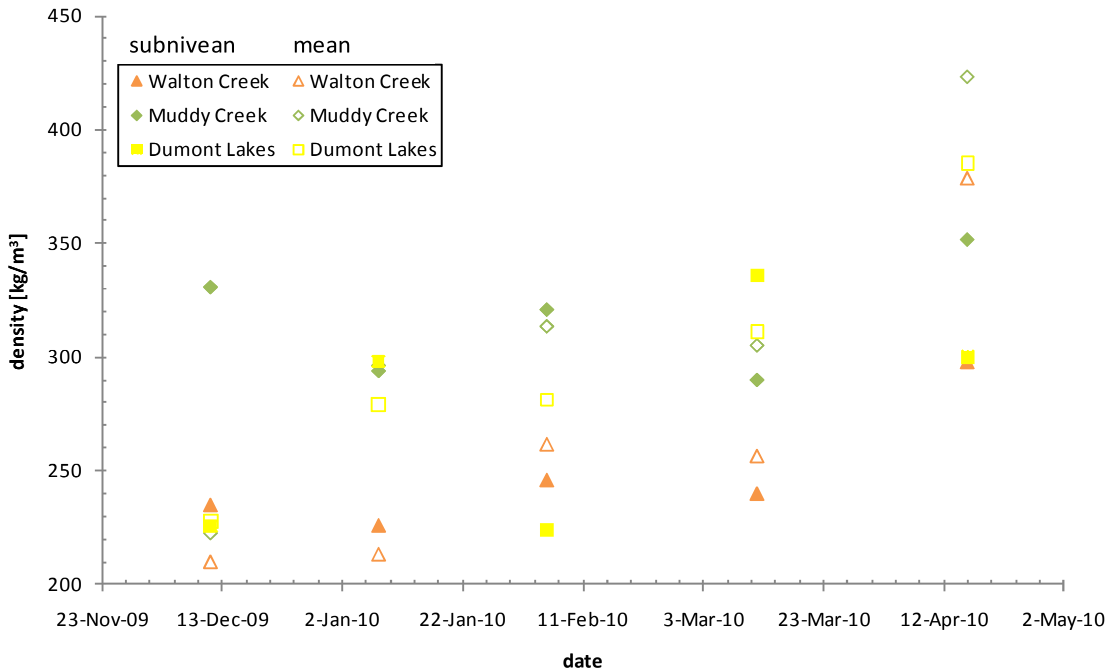

Figure A-7. Bulk snowpack density and subnivean density measured at Muddy Creek, Dumont Lakes and Walton Creek trailheads on Rabbit Ears Pass, Colorado during the 2009-2010 winter.

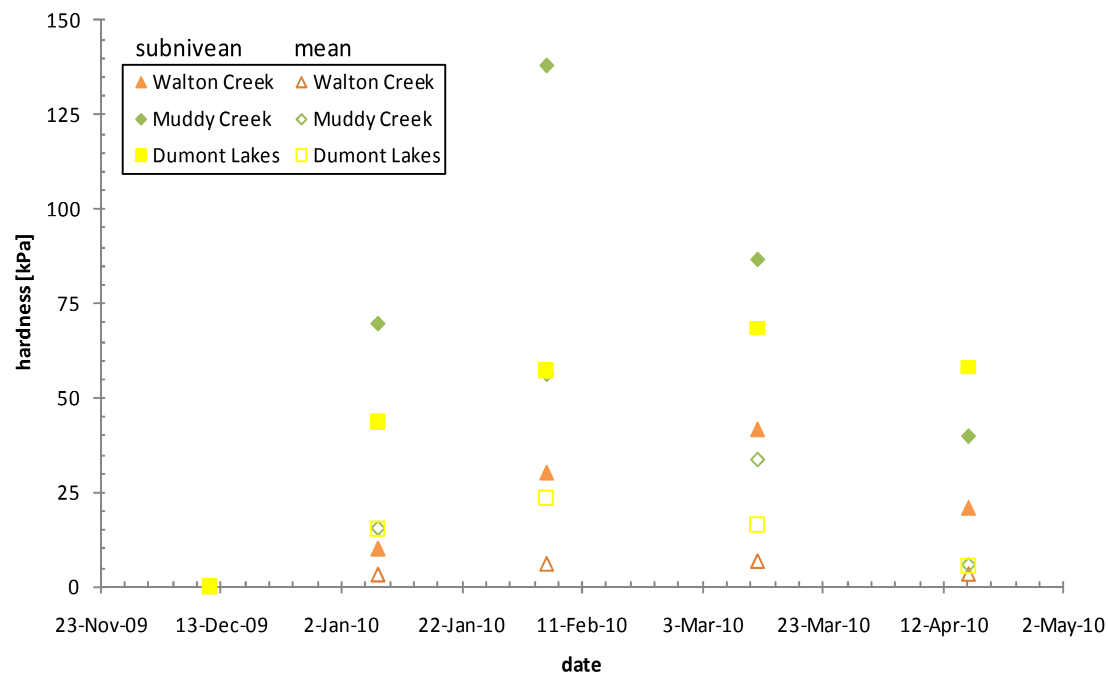

Figure A-8. Mean snowpack hardness and subnivean hardness measured at Muddy Creek, Dumont Lakes and Walton Creek trailheads on Rabbit Ears Pass, Colorado during the 2009-2010 winter.

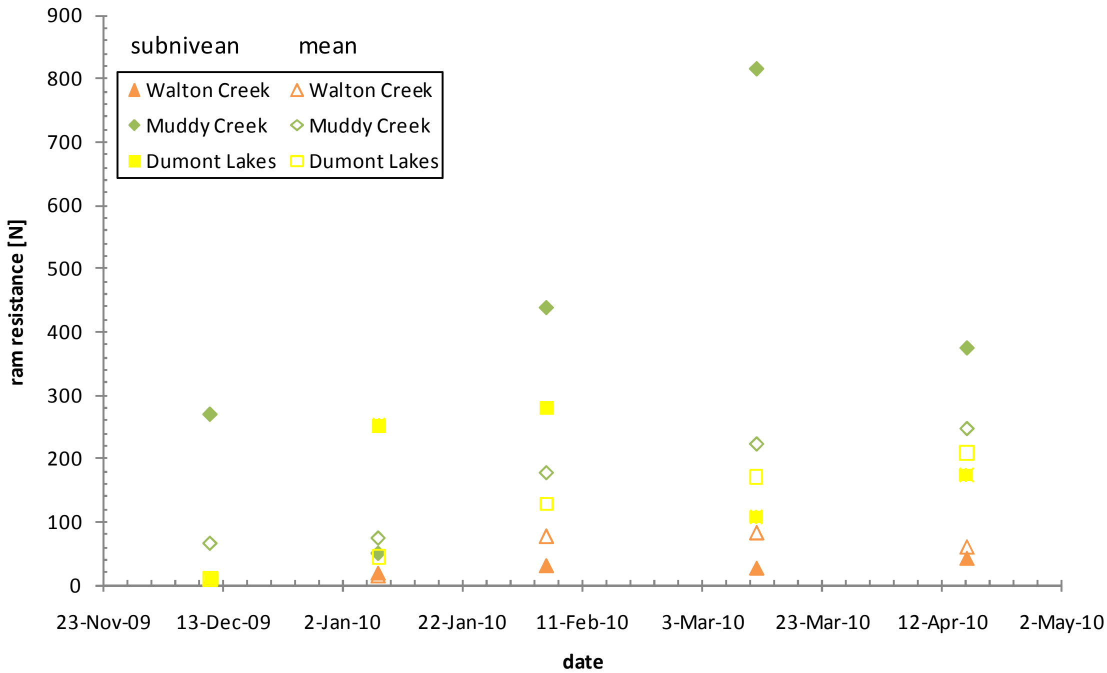

Figure A-9. Mean snowpack ram resistance and subnivean ram resistance measured at Muddy Creek, Dumont Lakes and Walton Creek trailheads on Rabbit Ears Pass, Colorado during the 2009-2010 winter.

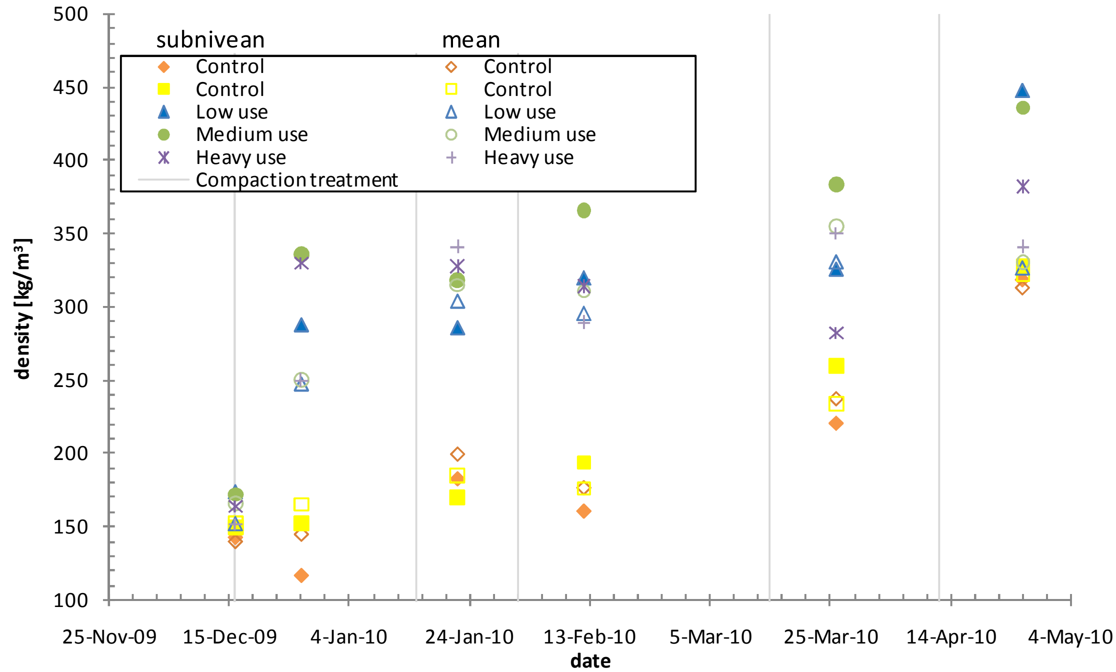

Figure A-10. No, low, medium and heavy use mean snowpack density and subnivean density measured at the snow compaction study plot in Fraser Experimental Forest, Colorado when compaction treatments began on shallow snowpack during the 2009-2010 winter.

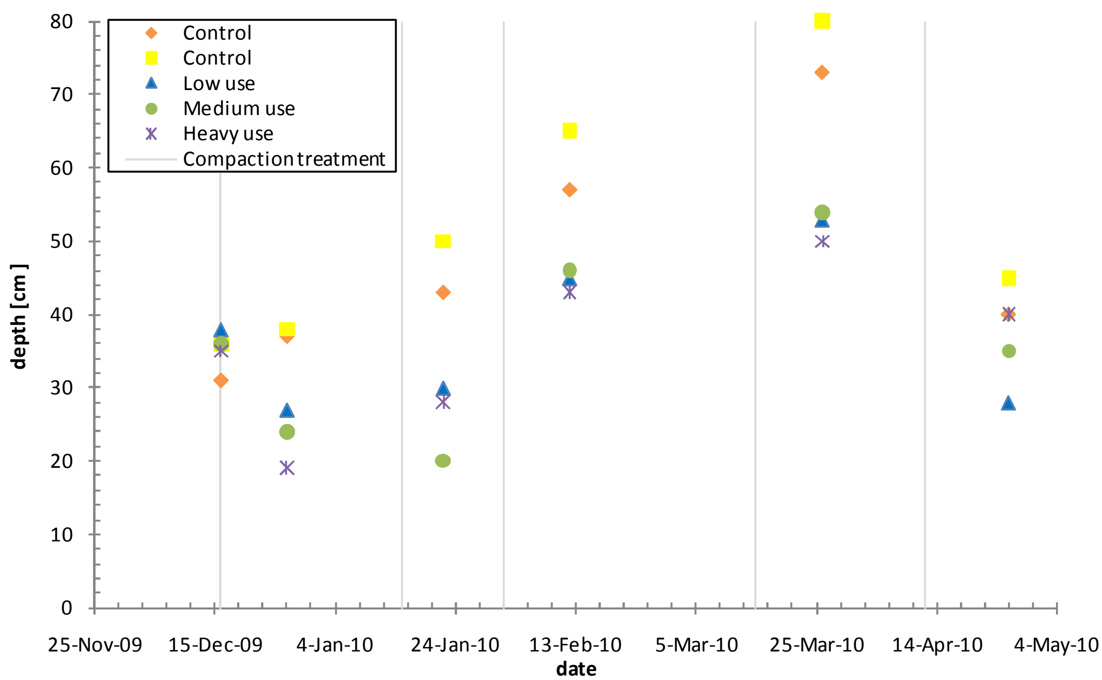

Figure A-11. No, low, medium and heavy use snow depth measured at the snow compaction study plot in Fraser Experimental Forest, Colorado when compaction treatments began on a shallow snowpack during the 2009-2010 winter.

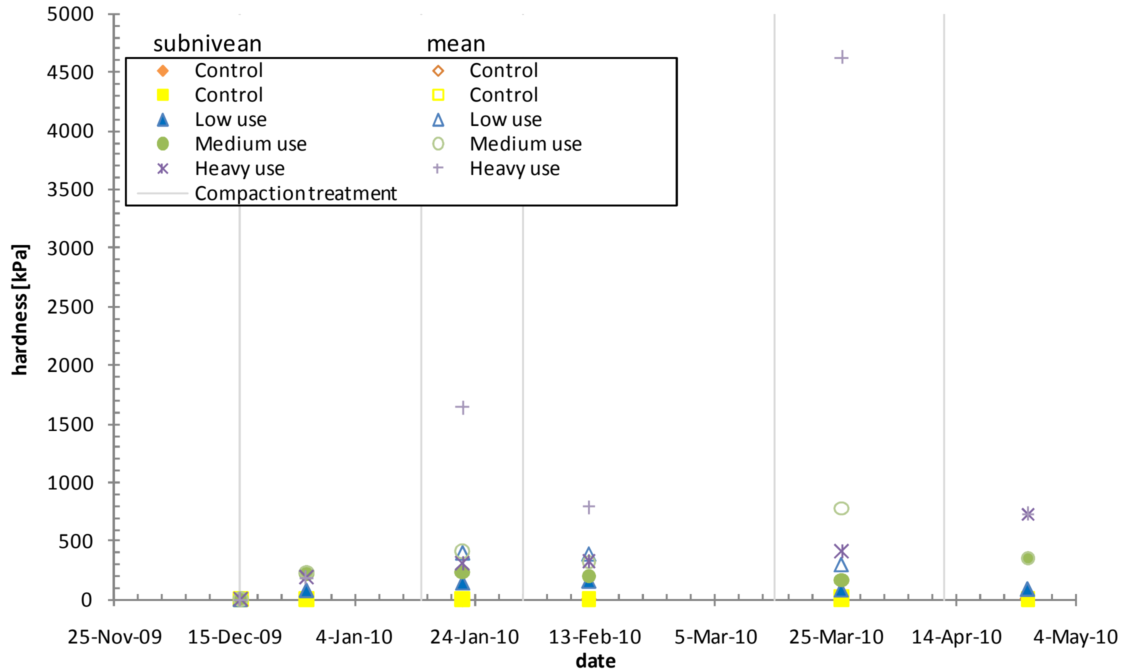

Figure A-12. No, low, medium and heavy use mean snowpack hardness and subnivean hardness measured at the snow compaction study plot in Fraser Experimental Forest, Colorado when compaction treatments began on a shallow snowpack during the 2009-2010 winter.

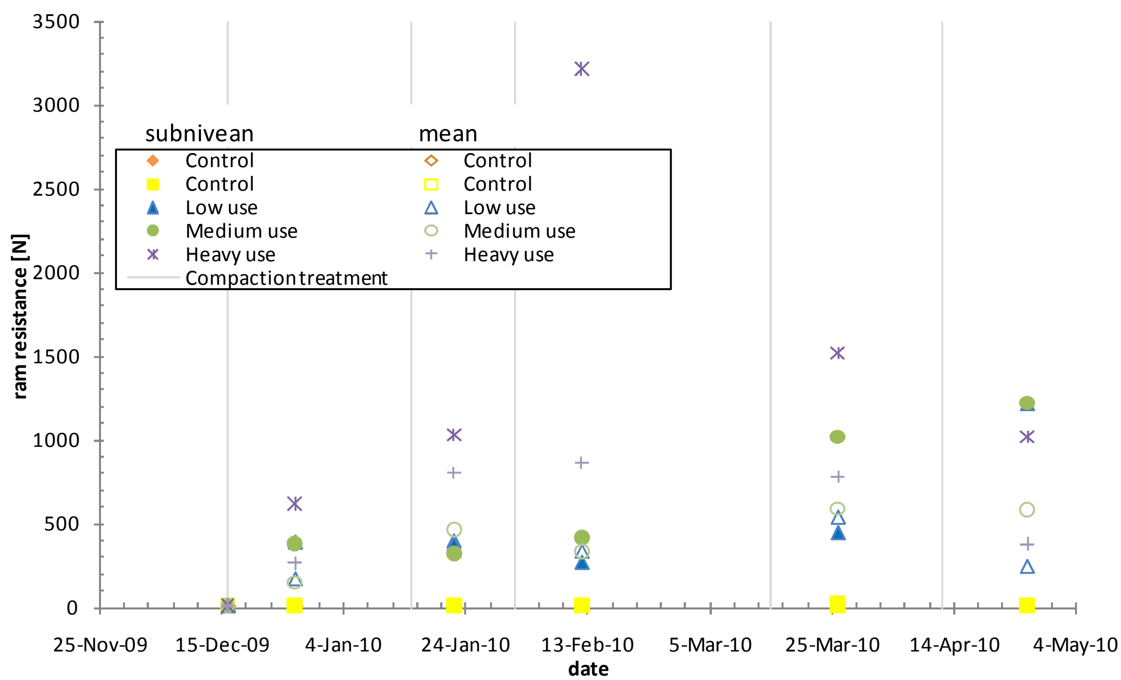

Figure A-13. No, low, medium and heavy use mean snowpack ram resistance (dashed line) and subnivean ram resistance (solid line) measured at the snow compaction study plot in Fraser Experimental Forest, Colorado when compaction treatments began on a shallow snowpack during the 2009-2010 winter.

APPENDIX B

Table B-1. Raw data collected at the snow compaction plots on Rabbit Ears Pass, Colorado during the 2009-2010 winter season.

Date	Plot	Trt.	Snow depth (cm)		ρ_{s1} (kg/m^3)	ρ_{s2} (kg/m^3)	T_d (cm)	T_s (°C)	Strat. Layer (cm)		Crystal Type	Size (mm)		Layer (cm)		Disc rad. (m)	Force (N)		
12/12/09	1	1	42	32	105	90	42	-7	42	31	N	1.0	1.0	14	0	0.011	34.00	82.00	82.00
12/12/09	1	1	32	22	199	191	40	-8	31	14	N-->F	1.0	1.5						
12/12/09	1	1	22	12	259	289	35	-11	14	0	R/Ice								
12/12/09	1	1	12	2	355	328	30	-10											
12/12/09	1	1					25	-9											
12/12/09	1	1					20	-6											
12/12/09	1	1					15	-5											
12/12/09	1	1					10	-5											
12/12/09	1	1					5	-4											
12/12/09	1	1					0	-3											
12/12/09	1	2	55	45	102	107	55	-8	55	46	N	1.0	1.5	13	0	0.023	8.50	7.75	7.83
12/12/09	1	2	45	35	154	173	50	-8	46	32	N-->F	1.0	1.5						
12/12/09	1	2	35	25	185	189	45	-9	32	13	F	1.0	2.0						
12/12/09	1	2	25	15	234	222	40	-9	13	0	DH	2.0	4.0						
12/12/09	1	2	15	5	213	210	35	-9											
12/12/09	1	2	10	0	205	212	30	-8											
12/12/09	1	2					25	-7											
12/12/09	1	2					20	-6											
12/12/09	1	2					15	-4											
12/12/09	1	2					10	-3											
12/12/09	1	2					5	-1											
12/12/09	1	2					0	-1											
12/12/09	1	3	57	47	103	98	57	-7	57	50	N	1.0	1.0	17	0	0.023	8.50	6.00	7.50
12/12/09	1	3	47	37	161	167	55	-7	50	31	R	0.3	0.5						
12/12/09	1	3	37	27	202	198	50	-11	31	17	F	1.0	1.5						
12/12/09	1	3	27	17	234	225	45	-13	17	0	DH	2.0	4.0						
12/12/09	1	3	17	7	215	225	40	-13											
12/12/09	1	3	10	0	215	206	35	-12											
12/12/09	1	3					30	-10											
12/12/09	1	3					25	-8											
12/12/09	1	3					20	-6											
12/12/09	1	3					15	-5											
12/12/09	1	3					10	-4											
12/12/09	1	3					5	-3											
12/12/09	1	3					0	-2											
12/12/09	1	4	54	44	99	89	54	-7	57	46	N	0.5	1.0	13	0	0.023	5.50	7.00	6.58
12/12/09	1	4	44	34	178	187	50	-8	46	28	N-->F	1.0	1.5						
12/12/09	1	4	34	24	183	188	45	-10	28	13	F	1.0	2.0						
12/12/09	1	4	24	14	219	217	40	-10	13	0	DH	2.0	3.5						
12/12/09	1	4	14	4	198	199	35	-10											
12/12/09	1	4	10	0	197	200	30	-8											
12/12/09	1	4					25	-7											
12/12/09	1	4					20	-6											
12/12/09	1	4					15	-5											
12/12/09	1	4					10	-3											

Date	Plot	Trt.	Snow depth (cm)		ρ_{s1} (kg/m^3)	ρ_{s2} (kg/m^3)	T_d (cm)	T_s (°C)	Strat. Layer (cm)		Crystal Type	Size (mm)		Layer (cm)		Disc rad. (m)	Force (N)		
12/12/09	1	4					5	-2											
12/12/09	1	4					0	-2											
12/12/09	1	5	50	40	98	94	50	-7	50	43	N	0.5	1.0	13	0	0.023	0.00	0.00	0.00
12/12/09	1	5	40	30	203	205	45	-8	43	21	SR	0.3	0.5						
12/12/09	1	5	30	20	200	200	40	-12	21	13	R	0.5	0.8						
12/12/09	1	5	20	10	207	218	35	-12	13	3	R	<0.25							
12/12/09	1	5	10	0	423	361	30	-11	3	0	IL								
12/12/09	1	5					25	-10											
12/12/09	1	5					20	-7											
12/12/09	1	5					15	-5											
12/12/09	1	5					10	-4											
12/12/09	1	5					5	-4											
12/12/09	1	5					0	-3											
12/12/09	2		52	42			52	-7	52	44	N-->F	1.0	2.0	20	0	0.011	57	94	80.5
12/12/09	2		42	32			50	-8	44	40	R	0.5	1.0						
12/12/09	2		32	22			45	-10	40	20	SR	0.3	0.5						
12/12/09	2		22	12			40	-11	20	0	R	1.0	1.5						
12/12/09	2		12	2			35	-11											
12/12/09	2						30	-9											
12/12/09	2						25	-7											
12/12/09	2						20	-5											
12/12/09	2						15	-5											
12/12/09	2						10	-4											
12/12/09	2						5	-4											
12/12/09							0	-3											
12/12/09	2	1	55	45			55	-6	55	48	N	0.5	1.0	15	0	0.023	6.25	4.75	6.75
12/12/09	2	1	45	35			50	-8	48	42	N-->F	0.3	0.5						
12/12/09	2	1	35	25			45	-9	42	31	F	1.0	1.5						
12/12/09	2	1	25	15			40	-10	31	15	F	1.0	1.0						
12/12/09	2	1	15	5			35	-10	15	0	DH	2.0	3.0						
12/12/09	2	1					30	-9											
12/12/09	2	1					25	-7											
12/12/09	2	1					20	-6											
12/12/09	2	1					15	-5											
12/12/09	2	1					10	-4											
12/12/09	2	1					5	-3											
12/12/09	2	1					0	-2											
12/12/09	2	2	60	50			60	-6	60	52	N	1.0	1.5	17	0	0.023	6.25	6.25	6.75
12/12/09	2	2	50	40			55	-7	52	44	N-->F	0.3	0.5						
12/12/09	2	2	40	30			50	-10	44	32	R	0.3	0.5						
12/12/09	2	2	30	20			45	-12	32	17	F	1.0	2.0						
12/12/09	2	2	20	10			40	-11	17	0	DH	2.0	3.0						
12/12/09	2	2	10	0			35	-10											
12/12/09	2	2					30	-9											
12/12/09	2	2					25	-7											

Date	Plot	Trt.	Snow depth (cm)		ρ_{s1} (kg/m^3)	ρ_{s2} (kg/m^3)	T_d (cm)	T_s (^{o}C)	Strat. Layer (cm)		Crystal Type	Size (mm)		Layer (cm)		Disc rad. (m)	Force (N)		
12/12/09	2	2					20	-6											
12/12/09	2	2					15	-4											
12/12/09	2	2					10	-2											
12/12/09	2	2					5	-2											
12/12/09	2	2					0	-2											
12/12/09	2	3	56	46			56	-6	56	48	N	1.0	1.5	15	0	0.023	8	6	5
12/12/09	2	3	46	36			55	-6	48	43	N-->F	1.0	1.0						
12/12/09	2	3	36	26			50	-8	43	31	R	0.3	0.5						
12/12/09	2	3	26	16			45	-10	31	15	F	1.0	2.0						
12/12/09	2	3	16	6			40	-10	15	0	DH	2.0	4.0						
12/12/09	2	3	10	0			35	-9											
12/12/09	2	3					30	-9											
12/12/09	2	3					25	-7											
12/12/09	2	3					20	-6											
12/12/09	2	3					15	-4											
12/12/09	2	3					10	-3											
12/12/09	2	3					5	-3											
12/12/09	2	3					0	-1											
12/12/09	2	4	53	43			50	-7	53	42	N	0.5	1.0	12	0	0.023	0	0	0
12/12/09	2	4	43	33			45	-7	43	12	N-->F	0.3	0.5						
12/12/09	2	4	33	23			40	-10	12	4	R	0.5	0.8						
12/12/09	2	4	23	13			35	-11	4	0	R	<0.25							
12/12/09	2	4	13	3			30	-10											
12/12/09	2	4					25	-9											
12/12/09	2	4					20	-6											
12/12/09	2	4					15	-4											
12/12/09	2	4					10	-4											
12/12/09	2	4					5	-3											
12/12/09	2	4					0	-2											
1/9/10	1	1	80	70	151	152	80	-21	80	77	SH/NSH	1.0	2.0	77	68	0.23	4.50	4.25	4.50
1/9/10	1	1	70	60	152	151	75	-23	77	68	N-->R	0.1	0.2	68	41	0.23	11.25	11.75	7.75
1/9/10	1	1	60	50	189	184	70	-22	68	55	F	0.2	0.5	41	33	0.011	14.75	11.75	14.50
1/9/10	1	1	50	40	210	198	65	-16	55	41	F-->R	0.2	0.5	33	17	0.006	16.00	10.75	9.25
1/9/10	1	1	40	30	290	273	60	-14	41	33	R	0.2	0.5	17	0	0.006	14.00	15.75	18.50
1/9/10	1	1	30	20	404	336	55	-11	33	17	F	1.0	1.5						
1/9/10	1	1	20	10	387	347	50	-9	17	0	DH	2.0	4.0						
1/9/10	1	1	10	0	356	352	45	-7											
1/9/10	1	1					40	-5											
1/9/10	1	1					35	-4											
1/9/10	1	1					30	-3											
1/9/10	1	1					25	-3											
1/9/10	1	1					20	-2											
1/9/10	1	1					15	-2											
1/9/10	1	1					10	-2											
1/9/10	1	1					5	-1											

Date	Plot	Trt.	Snow depth (cm)		ρ_{s1} (kg/m^3)	ρ_{s2} (kg/m^3)	T_d (cm)	T_s (^{o}C)	Strat. Layer (cm)		Crystal Type	Size (mm)		Layer (cm)		Disc rad. (m)	Force (N)		
1/9/10	1	1					0	-1											
1/9/10	1	1																	
1/9/10	1	1																	
1/9/10	1	1																	
1/9/10	1	2	97	87	143	142	97	-16	97	93	SH/NSH	0.5	1.0	97	93	0.023	0.00	0.00	0.00
1/9/10	1	2	87	77	154	167	95	-18	93	88	R	0.1	0.2	93	88	0.023	5.25	4.25	6.75
1/9/10	1	2	77	67	175	176	90	-21	88	76	R	0.1	0.2	88	76	0.023	5.25	4.50	4.75
1/9/10	1	2	67	57	199	202	85	-19	76	53	F	0.1	0.2	76	53	0.023	19.25	18.50	16.75
1/9/10	1	2	57	47	272	263	80	-15	53	33	F	0.2	0.5	53	33	0.011	10.00	6.00	8.75
1/9/10	1	2	47	37	278	284	75	-13	33	0	F/DH	1.0	2.0	33	0	0.011	4.75	4.75	4.00
1/9/10	1	2	37	27	260	298	70	-11											
1/9/10	1	2	27	17	269	244	65	-8											
1/9/10	1	2	17	7	233	263	60	-7											
1/9/10	1	2	10	0	220	256	55	-5											
1/9/10	1	2					50	-5											
1/9/10	1	2					45	-4											
1/9/10	1	2					40	-4											
1/9/10	1	2					35	-3											
1/9/10	1	2					30	-3											
1/9/10	1	2					25	-2											
1/9/10	1	2					20	-2											
1/9/10	1	2					15	-2											
1/9/10	1	2					10	-1											
1/9/10	1	2					5	-1											
1/9/10	1	2					0	-1											
1/9/10	1	3	104	94	150	144	104	-11	104	98	N	0.5	1.0	104	92	0.23	5.25	5.75	5.50
1/9/10	1	3	94	84	153	155	100	-13	98	92	R	0.1	0.2	92	60	0.23	8.75	8.00	8.25
1/9/10	1	3	84	74	173	175	95	-18	92	60	R	0.1	0.2	60	37	0.011	12.75	13.50	14.25
1/9/10	1	3	74	64	182	190	90	-18	60	37	F	1.0	1.5	37	0	0.011	3.75	3.00	3.00
1/9/10	1	3	64	54	259	240	85	-15	37	0	F/DH	1.0	3.0						
1/9/10	1	3	54	44	267	267	80	-12											
1/9/10	1	3	44	34	314	301	75	-10											
1/9/10	1	3	34	24	292	297	70	-7											
1/9/10	1	3	24	14	251	250	65	-6											
1/9/10	1	3	14	4	224	239	60	-5											
1/9/10	1	3	10	0	224	240	55	-4											
1/9/10	1	3					50	-3											
1/9/10	1	3					45	-3											
1/9/10	1	3					40	-3											
1/9/10	1	3					35	-3											
1/9/10	1	3					30	-2											
1/9/10	1	3					25	-2											
1/9/10	1	3					20	-2											
1/9/10	1	3					15	-1											
1/9/10	1	3					10	-1											

Date	Plot	Trt.	Snow depth (cm)		ρ_{s1} (kg/m^3)	ρ_{s2} (kg/m^3)	T_d (cm)	T_s (°C)	Strat. Layer (cm)		Crystal Type	Size (mm)		Layer (cm)		Disc rad. (m)	Force (N)		
1/9/10	1	3					5	-1											
1/9/10	1	3					0	-1											
1/9/10	1	4	105	95	147	139	105	-12	105	98	N-->F	0.1	0.2	105	93	0.023	4.50	4.50	4.50
1/9/10	1	4	95	85	156	148	100	-11	98	93	R	0.1	0.2	93	70	0.011	3.50	4.50	4.00
1/9/10	1	4	85	75	178	178	95	-16	93	70	R	0.2	0.5	70	50	0.011	23.00	23.00	20.75
1/9/10	1	4	75	65	193	194	90	-15	70	50	F	0.2	0.5	50	26	0.011	10.75	11.00	12.50
1/9/10	1	4	65	55	270	271	85	-9	50	26	F	0.5	1.0	26	0	0.011	3.00	3.25	4.50
1/9/10	1	4	55	45	276	274	80	-10	26	0	F/DH	2.0	4.0						
1/9/10	1	4	45	35	318	316	75	-8											
1/9/10	1	4	35	25	312	276	70	-8											
1/9/10	1	4	25	15	262	260	65	-7											
1/9/10	1	4	15	5	239	231	60	-6											
1/9/10	1	4	10	0	264	132	55	-5											
1/9/10	1	4					50	-4											
1/9/10	1	4					45	-4											
1/9/10	1	4					40	-3											
1/9/10	1	4					35	-3											
1/9/10	1	4					30	-3											
1/9/10	1	4					25	-3											
1/9/10	1	4					20	-2											
1/9/10	1	4					15	-2											
1/9/10	1	4					10	-2											
1/9/10	1	4					5	-2											
1/9/10	1	4					0	-2											
1/9/10	1	5	103	93	142	140	103	-9	103	90	N-->R	0.1	0.2	103	90	0.023	4.50	4.00	4.00
1/9/10	1	5	93	83	172	170	95	-13	90	76	N-->F	0.2	0.5	90	76	0.023	8.25	7.50	5.25
1/9/10	1	5	83	73	178	193	90	-15	76	55	F	0.5	1.0	76	55	0.023	16.50	17.75	20.50
1/9/10	1	5	73	63	188	198	85	-15	55	35	F	0.2	0.5	55	35	0.003	15.00	12.00	17.50
1/9/10	1	5	63	53	231	213	80	-13	35	15	F	1.0	1.5	35	15	0.011	10.75	11.25	15.25
1/9/10	1	5	53	43	325	377	75	-11	15	0	F	0.5	1.5	15	0	0.003	36.00	30.00	30.00
1/9/10	1	5	43	33	369	384	70	-9											
1/9/10	1	5	33	23	315	332	65	-7											
1/9/10	1	5	23	13	353	351	60	-6											
1/9/10	1	5	13	3	365	413	55	-5											
1/9/10	1	5					50	-4											
1/9/10	1	5					45	-3											
1/9/10	1	5					40	-3											
1/9/10	1	5					35	-3											
1/9/10	1	5					30	-3											
1/9/10	1	5					25	-3											
1/9/10	1	5					20	-3											
1/9/10	1	5					15	-2											
1/9/10	1	5					10	-2											
1/9/10	1	5					5	-2											
1/9/10	1	5					0	-2											

Date	Plot	Trt.	Snow depth (cm)		ρ_{s1} (kg/m^3)	ρ_{s2} (kg/m^3)	T_d (cm)	T_s (^oC)	Strat. Layer (cm)		Crystal Type	Size (mm)		Layer (cm)		Disc rad. (m)	Force (N)		
1/10/10	2	1	100	90	159	164	100	-20	100	90	N-->F	0.1	0.2	100	90	0.023	4.50	4.50	4.25
1/10/10	2	1	90	80	157	164	95	-21	90	55	F	0.2	0.5	90	55	0.023	16.00	16.00	17.50
1/10/10	2	1	80	70	203	190	90	-19	55	36	F	0.5	1.0	55	36	0.006	17.75	22.00	16.75
1/10/10	2	1	70	60	211	211	85	-12	36	17	F	1.0	2.0	36	17	0.011	8.25	8.00	7.75
1/10/10	2	1	60	50	365	293	80	-14	17	0	F	2.0	4.0	17	0	0.006	9.25	12.00	18.25
1/10/10	2	1	50	40	332	348	75	-11											
1/10/10	2	1	40	30	325	310	70	-10											
1/10/10	2	1	30	20	303	281	65	-8											
1/10/10	2	1	20	10	365	344	60	-7											
1/10/10	2	1	10	0	360	360	55	-5											
1/10/10	2	1					50	-5											
1/10/10	2	1					45	-4											
1/10/10	2	1					40	-4											
1/10/10	2	1					35	-4											
1/10/10	2	1					30	-3											
1/10/10	2	1					25	-3											
1/10/10	2	1					20	-2											
1/10/10	2	1					15	-2											
1/10/10	2	1					10	-2											
1/10/10	2	1					5	-2											
1/10/10	2	1					0	-2											
1/10/10	2	2	100	90	151	157	100	-13	100	88	N-->F	0.1	0.2	100	88	0.023	5.25	4.75	4.50
1/10/10	2	2	90	80	166	167	95	-19	88	57	F	0.2	0.3	88	57	0.023	13.00	13.00	14.50
1/10/10	2	2	80	70	191	190	90	-19	57	27	F	0.5	1.5	57	27	0.011	9.25	9.00	8.75
1/10/10	2	2	70	60	219	199	85	-17	27	0	DH	2.0	4.0	27	0	0.023	7.25	6.00	9.25
1/10/10	2	2	60	50	277	268	80	-13											
1/10/10	2	2	50	40	284	276	75	-11											
1/10/10	2	2	40	30	293	304	70	-10											
1/10/10	2	2	30	20	254	263	65	-9											
1/10/10	2	2	20	10	221	243	60	-7											
1/10/10	2	2	10	0	268	228	55	-6											
1/10/10	2	2					50	-5											
1/10/10	2	2					45	-5											
1/10/10	2	2					40	-4											
1/10/10	2	2					35	-4											
1/10/10	2	2					30	-3											
1/10/10	2	2					25	-3											
1/10/10	2	2					20	-3											
1/10/10	2	2					15	-2											
1/10/10	2	2					10	-2											
1/10/10	2	2					5	-2											
1/10/10	2	2					0	-2											
1/10/10	2	3	101	91	162	148	101	-12	101	90	N-->F	0.1	0.2	101	90	0.023	4.50	4.25	4.50
1/10/10	2	3	91	81	168	158	95	-16	90	60	N-->F	0.2	0.5	90	60	0.011	3.00	3.25	3.00
1/10/10	2	3	81	71	186	184	90	-17	60	25	F	1.0	1.5	60	25	0.011	12.00	12.25	12.25

Date	Plot	Trt.	Snow depth (cm)		ρ_{s1} (kg/m^3)	ρ_{s2} (kg/m^3)	T_d (cm)	T_s (^oC)	Strat. Layer (cm)		Crystal Type	Size (mm)		Layer (cm)		Disc rad. (m)	Force (N)		
1/10/10	2	3	71	61	201	206	85	-15	25	0	DH	2.5	4.5	25	0	0.023	7.25	6.50	6.75
1/10/10	2	3	61	51	272	264	80	-13											
1/10/10	2	3	51	41	275	277	75	-11											
1/10/10	2	3	41	31	318	328	70	-10											
1/10/10	2	3	31	21	271	284	65	-8											
1/10/10	2	3	21	11	265	261	60	-7											
1/10/10	2	3	11	1	228	232	55	-6											
1/10/10	2	3					50	-5											
1/10/10	2	3					45	-5											
1/10/10	2	3					40	-4											
1/10/10	2	3					35	-4											
1/10/10	2	3					30	-3											
1/10/10	2	3					25	-3											
1/10/10	2	3					20	-3											
1/10/10	2	3					15	-2											
1/10/10	2	3					10	-2											
1/10/10	2	3					5	-2											
1/10/10	2	3					0	-1											
1/10/10	2	4	101	91	159	155	101	-8	101	90	N-->F	0.1	0.2	101	90	0.023	3.75	3.75	3.75
1/10/10	2	4	91	81	170	173	95	-14	90	57	N-->F	0.2	0.5	90	57	0.023	14.50	16.00	14.75
1/10/10	2	4	81	71	191	190	90	-17	57	28	F	0.5	1.0	57	28	0.011	8.50	9.25	8.75
1/10/10	2	4	71	61	212	214	85	-16	28	14	F	1.0	2.0	28	0	0.023	4.50	7.25	7.00
1/10/10	2	4	61	51	278	264	80	-14	14	0	DH	2.0	4.0						
1/10/10	2	4	51	41	290	292	75	-12											
1/10/10	2	4	41	31	285	307	70	-10											
1/10/10	2	4	31	21	242	255	65	-8											
1/10/10	2	4	21	11	238	228	60	-7											
1/10/10	2	4	11	1	252	228	55	-6											
1/10/10	2	4					50	-5											
1/10/10	2	4					45	-4											
1/10/10	2	4					40	-4											
1/10/10	2	4					35	-4											
1/10/10	2	4					30	-3											
1/10/10	2	4					25	-3											
1/10/10	2	4					20	-2											
1/10/10	2	4					15	-2											
1/10/10	2	4					10	-2											
1/10/10	2	4					5	-1											
1/10/10	2	4					0	-1											
1/10/10	2	5	95	85	145	150	95	-5	95	83	N-->F	0.1	0.2	95	83	0.023	5.25	5.75	5.50
1/10/10	2	5	85	75	190	191	90	-13	83	42	F	0.2	0.5	83	42	0.023	10.75	15.00	12.50
1/10/10	2	5	75	65	195	191	85	-16	42	24	F	0.5	1.0	42	24	0.006	64.00	53.00	51.00
1/10/10	2	5	65	55	236	205	80	-15	24	5	F	1.0	1.5	24	5	0.006	5.25	6.25	5.50
1/10/10	2	5	55	45	230	237	75	-14	5	0	F	0.5	1.0	5	0	0.006	45.00	61.00	55.00
1/10/10	2	5	45	35	296	417	70	-12											

Date	Plot	Trt.	Snow depth (cm)		ρ_{s1} (kg/m^3)	ρ_{s2} (kg/m^3)	T_d (cm)	T_s (°C)	Strat. Layer (cm)		Crystal Type	Size (mm)		Layer (cm)		Disc rad. (m)	Force (N)		
1/10/10	2	5	35	25	402	395	65	-10											
1/10/10	2	5	25	15	328	317	60	-8											
1/10/10	2	5	15	5	352	325	55	-7											
1/10/10	2	5	10	0	380	283	50	-5											
1/10/10	2	5					45	-4											
1/10/10	2	5					40	-4											
1/10/10	2	5					35	-4											
1/10/10	2	5					30	-3											
1/10/10	2	5					25	-3											
1/10/10	2	5					20	-3											
1/10/10	2	5					15	-3											
1/10/10	2	5					10	-2											
1/10/10	2	5					5	-2											
1/10/10	2	5					0	-2											
2/6/10	1	1	90	80	65	60	90	-4	90	72	N	1.0	1.5	90	72	0.023	2.50	0.00	0.00
2/6/10	1	1	80	70	255	99	85	-6	72	51	F-->R	0.5	1.0	72	51	0.006	32.00	33.00	28.00
2/6/10	1	1	70	60	361	341	80	-6	51	33	F	1.0	1.5	51	33	0.011	13.00	16.00	12.00
2/6/10	1	1	60	50	267	302	75	-6	33	15	F	1.0	1.5	33	15	0.006	23.00	24.00	29.00
2/6/10	1	1	50	40	299	302	70	-7	15	0	F/DH	1.0	2.0	15	0	0.006	19.00	14.00	21.00
2/6/10	1	1	40	30	299	361	65	-6											
2/6/10	1	1	30	20	406	413	60	-6											
2/6/10	1	1	20	10	319	384	55	-6											
2/6/10	1	1	10	0	316	280	50	-6											
2/6/10	1	1					45	-5											
2/6/10	1	1					40	-5											
2/6/10	1	1					35	-4											
2/6/10	1	1					30	-4											
2/6/10	1	1					25	-3											
2/6/10	1	1					20	-3											
2/6/10	1	1					15	-3											
2/6/10	1	1					10	-3											
2/6/10	1	1					5	-3											
2/6/10	1	1					0	-2											
2/6/10	1	2	90	80	72	65	90	-4	90	75	N	1.0	1.5	90	75	0.023	3.75	2.75	3.00
2/6/10	1	2	80	70	368	307	85	-4	75	55	F-->R	1.0	1.5	75	55	0.006	88.00	99.00	93.00
2/6/10	1	2	70	60	339	395	80	-5	55	31	F	1.0	2.0	55	31	0.011	18.00	20.00	18.00
2/6/10	1	2	60	50	330	365	75	-7	31	0	F/DH	2.0	4.0	31	0	0.023	15.25	16.00	12.75
2/6/10	1	2	50	40	312	297	70	-6											
2/6/10	1	2	40	30	282	284	65	-7											
2/6/10	1	2	30	20	254	247	60	-7											
2/6/10	1	2	20	10	228	248	55	-7											
2/6/10	1	2	10	0	300	288	50	-6											
2/6/10	1	2					45	-6											
2/6/10	1	2					40	-6											
2/6/10	1	2					35	-5											

Date	Plot	Trt.	Snow depth (cm)		ρ_{s1} (kg/m^3)	ρ_{s2} (kg/m^3)	T_d (cm)	T_s (°C)	Strat. Layer (cm)		Crystal Type	Size (mm)		Layer (cm)		Disc rad. (m)	Force (N)		
2/6/10	1	2					30	-4											
2/6/10	1	2					25	-4											
2/6/10	1	2					20	-3											
2/6/10	1	2					15	-2											
2/6/10	1	2					10	-2											
2/6/10	1	2					5	-2											
2/6/10	1	2					0	-2											
2/6/10	1	3	105	95	77	80	105	-1	105	81	N	1.0	1.5	105	81	0.023	3.25	2.75	3.50
2/6/10	1	3	100	90	119	122	100	-2	81	50	F	1.0	1.5	81	50	0.023	22.00	23.25	23.00
2/6/10	1	3	90	80	205	211	95	-4	50	23	F	1.5	2.0	50	23	0.006	9.25	5.75	6.75
2/6/10	1	3	80	70	251	246	90	-5	23	0	DH	2.0	4.0	23	0	0.023	16.50	18.00	18.00
2/6/10	1	3	70	60	279	294	85	-6											
2/6/10	1	3	60	50	319	328	80	-6											
2/6/10	1	3	50	40	319	319	75	-5											
2/6/10	1	3	40	30	335	330	70	-5											
2/6/10	1	3	30	20	285	294	65	-5											
2/6/10	1	3	20	10	274	262	60	-5											
2/6/10	1	3	10	0	232	240	55	-5											
2/6/10	1	3					50	-4											
2/6/10	1	3					45	-4											
2/6/10	1	3					40	-4											
2/6/10	1	3					35	-3											
2/6/10	1	3					30	-3											
2/6/10	1	3					25	-3											
2/6/10	1	3					20	-3											
2/6/10	1	3					15	-2											
2/6/10	1	3					10	-2											
2/6/10	1	3					5	-2											
2/6/10	1	3					0	-1											
2/6/10	1	4	109	99	77	80	109	-12	109	93	N	1.0	1.5	109	93	0.023	2.75	0.00	0.00
2/6/10	1	4	100	90	93	127	105	-11	93	76	N-->R	0.2	0.5	93	76	0.006	12.75	17.50	9.75
2/6/10	1	4	90	80	300	322	100	-16	76	53	F	1.0	1.5	76	53	0.006	3.25	3.25	3.00
2/6/10	1	4	80	70	351	315	95	-15	53	28	F	0.5	1.0	53	28	0.011	14.50	15.50	15.00
2/6/10	1	4	70	60	282	294	90	-9	28	22	F	2.0	2.5	28	0	0.011	6.25	8.00	7.25
2/6/10	1	4	60	50	311	319	85	-10	22	0	DH	2.5	4.5						
2/6/10	1	4	50	40	332	319	80	-8											
2/6/10	1	4	40	30	322	336	75	-8											
2/6/10	1	4	30	20	326	303	70	-7											
2/6/10	1	4	20	10	275	261	65	-6											
2/6/10	1	4	10	0	240	232	60	-5											
2/6/10	1	4					55	-4											
2/6/10	1	4					50	-4											
2/6/10	1	4					45	-3											
2/6/10	1	4					40	-3											
2/6/10	1	4					35	-3											

Date	Plot	Trt.	Snow depth (cm)		ρ_{s1} (kg/m^3)	ρ_{s2} (kg/m^3)	T_d (cm)	T_s (°C)	Strat. Layer (cm)		Crystal Type	Size (mm)		Layer (cm)		Disc rad. (m)	Force (N)		
2/6/10	1	4					30	-3											
2/6/10	1	4					25	-2											
2/6/10	1	4					20	-2											
2/6/10	1	4					15	-2											
2/6/10	1	4					10	-2											
2/6/10	1	4					5	-2											
2/6/10	1	4					0	-2											
2/6/10	1	5	107	97	84	67	107	-2	107	95	N	1.0	1.5	107	95	0.023	0.00	0.00	0.00
2/6/10	1	5	100	90	345	148	100	-2	95	71	F	0.2	0.5	95	71	0.006	94.00	95.00	95.00
2/6/10	1	5	90	80	358	367	95	-5	71	46	F-->R	1.0	1.5	71	46	0.011	24.00	23.00	17.00
2/6/10	1	5	80	70	413	384	90	-7	46	28	F	0.5	1.0	46	28	0.011	67.00	64.00	56.00
2/6/10	1	5	70	60	295	303	85	-7	28	16	F	1.0	2.0	28	16	0.011	18.00	14.00	12.00
2/6/10	1	5	60	50	319	360	80	-7	16	0	F	0.5	1.0	16	0	0.003	45.00	39.00	60.00
2/6/10	1	5	50	40	415	445	75	-7											
2/6/10	1	5	40	30	365	387	70	-6											
2/6/10	1	5	30	20	320	336	65	-6											
2/6/10	1	5	20	10	325	408	60	-5											
2/6/10	1	5	10	0	403	359	55	-5											
2/6/10	1	5					50	-5											
2/6/10	1	5					45	-4											
2/6/10	1	5					40	-4											
2/6/10	1	5					35	-4											
2/6/10	1	5					30	-4											
2/6/10	1	5					25	-3											
2/6/10	1	5					20	-3											
2/6/10	1	5					15	-3											
2/6/10	1	5					10	-2											
2/6/10	1	5					5	-2											
2/6/10	1	5					0	-2											
2/7/10	2	1	112	102	76	79	112	-2	112	91	N	1.0	1.5	112	91	0.023	0.00	0.00	5.50
2/7/10	2	1	110	100	78	71	105	-2	91	72	F-->R	0.2	0.5	91	72	0.006	27.00	28.00	31.00
2/7/10	2	1	100	90	189	241	100	-5	72	52	F	0.5	1.0	72	52	0.011	15.00	15.50	17.75
2/7/10	2	1	90	80	368	356	95	-6	52	35	F	1.0	1.5	52	35	0.006	19.00	16.00	13.00
2/7/10	2	1	80	70	275	321	90	-6	35	18	F	1.0	2.0	35	18	0.011	11.25	12.75	11.50
2/7/10	2	1	70	60	285	291	85	-6	18	0	F	1.5	2.0	18	0	0.006	38.00	23.00	18.00
2/7/10	2	1	60	50	372	367	80	-6											
2/7/10	2	1	50	40	341	364	75	-6											
2/7/10	2	1	40	30	313	319	70	-6											
2/7/10	2	1	30	20	325	315	65	-6											
2/7/10	2	1	20	10	380	389	60	-5											
2/7/10	2	1	10	0	336	336	55	-5											
2/7/10	2	1					50	-4											
2/7/10	2	1					45	-4											
2/7/10	2	1					40	-4											
2/7/10	2	1					35	-4											

Date	Plot	Trt.	Snow depth (cm)		ρ_{s1} (kg/m^3)	ρ_{s2} (kg/m^3)	T_d (cm)	T_s (^{o}C)	Strat. Layer (cm)		Crystal Type	Size (mm)		Layer (cm)		Disc rad. (m)	Force (N)		
2/7/10	2	1					30	-4											
2/7/10	2	1					25	-3											
2/7/10	2	1					20	-3											
2/7/10	2	1					15	-2											
2/7/10	2	1					10	-2											
2/7/10	2	1					5	-2											
2/7/10	2	1					0	-2											
2/7/10	2	2	100	90	85	83	100	-4	100	92	N	1.0	2.0	100	92	0.023	0.00	0.00	0.00
2/7/10	2	2	90	80	85	85	95	-7	92	81	N-->R	1.0	1.5	92	81	0.023	5.25	4.75	15.50
2/7/10	2	2	80	70	417	367	90	-8	81	58	F-->R	0.5	1.0	81	58	0.003	41.00	39.00	44.00
2/7/10	2	2	70	60	346	332	85	-6	58	41	F	1.0	1.5	58	41	0.011	36.00	27.00	38.00
2/7/10	2	2	60	50	339	347	80	-7	41	25	F	1.0	2.0	41	25	0.011	13.00	12.00	13.00
2/7/10	2	2	50	40	309	311	75	-7	25	0	DH	2.5	4.5	25	0	0.023	15.00	14.75	13.25
2/7/10	2	2	40	30	330	329	70	-7											
2/7/10	2	2	30	20	274	275	65	-7											
2/7/10	2	2	20	10	259	277	60	-6											
2/7/10	2	2	10	0	232	252	55	-6											
2/7/10	2	2					50	-6											
2/7/10	2	2					45	-5											
2/7/10	2	2					40	-5											
2/7/10	2	2					35	-5											
2/7/10	2	2					30	-4											
2/7/10	2	2					25	-4											
2/7/10	2	2					20	-4											
2/7/10	2	2					15	-3											
2/7/10	2	2					10	-3											
2/7/10	2	2					5	-2											
2/7/10	2	2					0	-2											
2/7/10	2	3	112	102	90	88	112	-3	112	99	N	1.0	2.0	112	99	0.023	0.00	2.50	0.00
2/7/10	2	3	110	100	91	108	105	-5	99	79	N-->R	1.0	1.5	99	79	0.023	20.50	20.25	18.75
2/7/10	2	3	100	90	182	196	100	-7	79	57	F	0.5	1.0	79	57	0.011	11.50	11.00	9.75
2/7/10	2	3	90	80	244	260	95	-7	57	23	F	1.0	1.5	57	23	0.011	17.00	15.50	16.50
2/7/10	2	3	80	70	260	271	90	-7	23	0	DH	2.0	4.0	23	0	0.011	7.50	9.75	8.75
2/7/10	2	3	70	60	299	299	85	-6											
2/7/10	2	3	60	50	317	330	80	-6											
2/7/10	2	3	50	40	319	312	75	-5											
2/7/10	2	3	40	30	349	349	70	-5											
2/7/10	2	3	30	20	302	327	65	-5											
2/7/10	2	3	20	10	267	273	60	-4											
2/7/10	2	3	10	0	220	224	55	-4											
2/7/10	2	3					50	-4											
2/7/10	2	3					45	-4											
2/7/10	2	3					40	-4											
2/7/10	2	3					35	-3											
2/7/10	2	3					30	-3											

Date	Plot	Trt.	Snow depth (cm)		ρ_{s1} (kg/m^3)	ρ_{s2} (kg/m^3)	T_d (cm)	T_s (°C)	Strat. Layer (cm)		Crystal Type	Size (mm)		Layer (cm)		Disc rad. (m)	Force (N)		
2/7/10	2	3					25	-3											
2/7/10	2	3					20	-3											
2/7/10	2	3					15	-2											
2/7/10	2	3					10	-2											
2/7/10	2	3					5	-2											
2/7/10	2	3					0	-2											
2/7/10	2	4	115	105	85	79	115	-4	115	90	N	1.0	2.0	115	90	0.023	0.00	3.25	3.00
2/7/10	2	4	110	100	94	92	110	-5	90	76	F-->R	0.2	0.5	90	76	0.006	41.00	39.00	48.00
2/7/10	2	4	100	90	132	127	105	-5	76	50	F	1.0	1.5	76	50	0.011	12.75	13.25	14.00
2/7/10	2	4	90	80	366	341	100	-6	50	26	F	1.0	2.0	50	26	0.011	15.00	15.25	10.25
2/7/10	2	4	80	70	347	335	95	-7	26	0	DH	2.0	4.0	26	0	0.011	7.75	7.50	8.25
2/7/10	2	4	70	60	296	295	90	-7											
2/7/10	2	4	60	50	338	340	85	-7											
2/7/10	2	4	50	40	311	312	80	-6											
2/7/10	2	4	40	30	336	333	75	-6											
2/7/10	2	4	30	20	279	267	70	-6											
2/7/10	2	4	20	10	288	274	65	-5											
2/7/10	2	4	10	0	240	224	60	-5											
2/7/10	2	4					55	-5											
2/7/10	2	4					50	-5											
2/7/10	2	4					45	-4											
2/7/10	2	4					40	-4											
2/7/10	2	4					35	-4											
2/7/10	2	4					30	-3											
2/7/10	2	4					25	-3											
2/7/10	2	4					20	-3											
2/7/10	2	4					15	-3											
2/7/10	2	4					10	-2											
2/7/10	2	4					5	-2											
2/7/10	2	4					0	-2											
2/7/10	2	5	105	95	80	85	105	-2	105	90	N	1.0	1.5	105	90	0.023	2.75	0.00	2.75
2/7/10	2	5	100	90	94	110	100	-1	90	63	F-->R	0.2	0.5	90	63	0.003	20.00	20.00	25.00
2/7/10	2	5	90	80	368	402	95	-3	63	45	F	1.0	1.5	63	45	0.011	21.00	20.00	19.00
2/7/10	2	5	80	70	368	401	90	-6	45	29	F	0.5	1.0	45	29	0.006	77.00	37.00	59.00
2/7/10	2	5	70	60	294	392	85	-6	29	7	F	1.0	2.0	29	7	0.011	17.00	15.00	17.00
2/7/10	2	5	60	50	320	344	80	-6	7	0	F-->R	0.5	1.0	7	0	0.003	29.00	23.00	36.00
2/7/10	2	5	50	40	443	419	75	-6											
2/7/10	2	5	40	30	439	426	70	-6											
2/7/10	2	5	30	20	377	371	65	-6											
2/7/10	2	5	20	10	336	339	60	-5											
2/7/10	2	5	10	0	376	380	55	-5											
2/7/10	2	5					50	-5											
2/7/10	2	5					45	-5											
2/7/10	2	5					40	-4											
2/7/10	2	5					35	-4											

Date	Plot	Trt.	Snow depth (cm)		ρ_{s1} (kg/m^3)	ρ_{s2} (kg/m^3)	T_d (cm)	T_s (^oC)	Strat. Layer (cm)		Crystal Type	Size (mm)		Layer (cm)		Disc rad. (m)	Force (N)		
2/7/10	2	5					30	-4											
2/7/10	2	5					25	-4											
2/7/10	2	5					20	-3											
2/7/10	2	5					15	-3											
2/7/10	2	5					10	-3											
2/7/10	2	5					5	-3											
2/7/10	2	5					0	-2											
3/13/10	1	1	142	132	138	116	142	-4	142	140	N	1.0	2.0	142	129	0.023	3.25	3.25	3.50
3/13/10	1	1	140	130	150	148	135	-6	140	140	MF	-	-	129	111	0.023	19.00	17.25	18.75
3/13/10	1	1	130	120	224	215	130	-9	140	129	N-->R	1.0	1.5	111	85	0.011	11.50	19.00	24.00
3/13/10	1	1	120	110	219	215	125	-9	129	127	F	1.0	2.0	85	63	0.011	14.00	19.00	17.75
3/13/10	1	1	110	100	277	234	120	-7	127	112	R	0.2	0.5	63	35	0.011	12.75	12.75	12.25
3/13/10	1	1	100	90	352	309	115	-6	112	111	F-->Ice	0.5	1.0	35	0	0.011	16.00	14.00	14.25
3/13/10	1	1	90	80	305	350	110	-5	111	85	R	0.5	1.0						
3/13/10	1	1	80	70	324	303	105	-5	85	63	F-->R	0.5	1.0						
3/13/10	1	1	70	60	375	382	100	-5	63	35	F-->R	1.0	1.5						
3/13/10	1	1	60	50	328	300	95	-4	35	0	DH	2.0	4.0						
3/13/10	1	1	50	40	330	309	90	-4											
3/13/10	1	1	40	30	333	374	85	-4											
3/13/10	1	1	30	20	341	426	80	-4											
3/13/10	1	1	20	10	314	320	75	-3											
3/13/10	1	1	10	0	320	336	70	-3											
3/13/10	1	1					65	-3											
3/13/10	1	1					60	-3											
3/13/10	1	1					50	-3											
3/13/10	1	1					40	-3											
3/13/10	1	1					30	-2											
3/13/10	1	1					25	-2											
3/13/10	1	1					20	-2											
3/13/10	1	1					15	-2											
3/13/10	1	1					10	-2											
3/13/10	1	1					5	-2											
3/13/10	1	1					0	-1											
3/13/10	1	2	138	128	141	151	138	-1	138	136	N	1.0	2.0	138	123	0.023	4.50	4.00	3.75
3/13/10	1	2	130	120	187	173	130	-3	136	136	MF	-	-	123	100	0.023	19.00	21.00	24.00
3/13/10	1	2	120	110	202	195	125	-7	136	123	N-->R	1.0	1.5	100	88	0.011	8.50	6.00	15.25
3/13/10	1	2	110	100	214	195	120	-7	123	100	R	0.2	0.5	88	63	0.006	33.00	30.00	30.00
3/13/10	1	2	100	90	218	228	115	-6	100	97	F	1.0	1.5	63	40	0.006	51.00	51.00	60.00
3/13/10	1	2	90	80	361	372	110	-5	97	88	R	0.2	0.5	40	0	0.011	12.00	10.50	8.75
3/13/10	1	2	80	70	392	362	105	-5	88	63	R	0.5	1.0						
3/13/10	1	2	70	60	400	384	100	-4	63	40	F-->R	1.0	1.5						
3/13/10	1	2	60	50	438	404	95	-4	40	0	DH	3.0	4.0						
3/13/10	1	2	50	40	374	344	90	-4											
3/13/10	1	2	40	30	293	287	80	-4											
3/13/10	1	2	30	20	269	258	70	-4											

Date	Plot	Trt.	Snow depth (cm)		ρ_{s1} (kg/m^3)	ρ_{s2} (kg/m^3)	T_d (cm)	T_s (^oC)	Strat. Layer (cm)		Crystal Type	Size (mm)		Layer (cm)		Disc rad. (m)	Force (N)		
3/13/10	1	2	20	10	253	262	60	-3											
3/13/10	1	2	10	0	272	224	50	-3											
3/13/10	1	2					40	-3											
3/13/10	1	2					30	-2											
3/13/10	1	2					25	-2											
3/13/10	1	2					20	-2											
3/13/10	1	2					15	-2											
3/13/10	1	2					10	-2											
3/13/10	1	2					5	-1											
3/13/10	1	2					0	-1											
3/13/10	1	3	148	138	148	130	152	-1	148	146	N	1.0	2.0	148	132	0.023	3.25	4.50	3.25
3/13/10	1	3	140	130	172	171	145	-1	146	146	MF	-	-	132	120	0.023	16.00	17.50	19.75
3/13/10	1	3	130	120	201	185	140	-3	146	132	N-->R	1.0	1.5	120	84	0.011	17.75	15.50	15.00
3/13/10	1	3	120	110	226	225	135	-4	132	129	F	1.0	1.5	84	32	0.011	20.00	19.00	19.50
3/13/10	1	3	110	100	245	263	130	-7	129	120	R	0.2	0.5	32	0	0.011	11.25	12.00	16.75
3/13/10	1	3	100	90	304	311	125	-6	120	117	F	1.0	2.0						
3/13/10	1	3	90	80	311	314	120	-6	117	84	R	0.5	1.0						
3/13/10	1	3	80	70	316	313	115	-5	84	32	F-->R	1.0	1.5						
3/13/10	1	3	70	60	329	328	110	-5	32	0	DH	2.0	4.0						
3/13/10	1	3	60	50	350	362	105	-4											
3/13/10	1	3	50	40	360	344	100	-4											
3/13/10	1	3	40	30	357	365	90	-4											
3/13/10	1	3	30	20	337	322	80	-3											
3/13/10	1	3	20	10	281	290	70	-3											
3/13/10	1	3	10	0	256	252	60	-3											
3/13/10	1	3					50	-3											
3/13/10	1	3					40	-2											
3/13/10	1	3					30	-2											
3/13/10	1	3					25	-2											
3/13/10	1	3					20	-2											
3/13/10	1	3					15	-2											
3/13/10	1	3					10	-2											
3/13/10	1	3					5	-1											
3/13/10	1	3					0	-1											
3/13/10	1	4	152	142	129	141	152	-1	152	150	N	1.0	2.0	152	136	0.023	3.75	3.25	3.50
3/13/10	1	4	150	140	143	135	145	-1	150	150	MF	-	-	136	121	0.011	7.00	6.75	12.50
3/13/10	1	4	140	130	198	205	140	-4	150	136	N-->R	1.0	1.5	121	108	0.011	9.25	9.75	8.75
3/13/10	1	4	130	120	213	218	135	-5	136	134	F	1.0	2.0	108	90	0.006	18.50	20.00	20.50
3/13/10	1	4	120	110	214	246	130	-6	134	121	Ring	0.1	0.2	90	72	0.011	52.00	53.00	56.00
3/13/10	1	4	110	100	324	317	125	-6	121	118	F	0.5	2.0	72	48	0.011	21.00	22.00	20.00
3/13/10	1	4	100	90	290	296	120	-5	118	108	R	0.2	0.5	48	22	0.006	10.25	9.75	10.50
3/13/10	1	4	90	80	310	347	115	-5	108	90	R	0.2	0.5	22	0	0.006	5.75	5.25	5.50
3/13/10	1	4	80	70	383	376	110	-4	90	72	R	1.0	1.5						
3/13/10	1	4	70	60	336	325	105	-4	72	48	R	1.0	1.5						
3/13/10	1	4	60	50	350	340	100	-4	48	22	Ring	1.0	1.5						

Date	Plot	Trt.	Snow depth (cm)		ρ_{s1} (kg/m^3)	ρ_{s2} (kg/m^3)	T_d (cm)	T_s (°C)	Strat. Layer (cm)		Crystal Type	Size (mm)		Layer (cm)		Disc rad. (m)	Force (N)		
3/13/10	1	4	50	40	348	360	90	-4	22	0	DH	2.0	4.0						
3/13/10	1	4	40	30	341	342	80	-4											
3/13/10	1	4	30	20	347	314	70	-3											
3/13/10	1	4	20	10	295	276	60	-3											
3/13/10	1	4	10	0	284	268	50	-3											
3/13/10	1	4					40	-2											
3/13/10	1	4					30	-2											
3/13/10	1	4					25	-2											
3/13/10	1	4					20	-2											
3/13/10	1	4					15	-2											
3/13/10	1	4					10	-2											
3/13/10	1	4					5	-1											
3/13/10	1	4					0	-1											
3/13/10	1	5	153	143	156	154	153	-1	153	152	N	1.0	2.0	153	141	0.023	3.00	2.75	3.75
3/13/10	1	5	150	140	140	168	145	-2	152	141	N--R	1.0	1.5	141	115	0.011	10.25	9.25	10.00
3/13/10	1	5	140	130	204	207	140	-5	141	139	MF	-	-	115	105	0.011	8.75	7.00	7.75
3/13/10	1	5	130	120	214	211	135	-5	139	115	N-->R	1.0	1.5	105	88	0.006	32.00	41.00	47.00
3/13/10	1	5	120	110	241	221	130	-6	115	112	F	1.0	2.0	88	62	0.006	28.00	25.00	35.00
3/13/10	1	5	110	100	300	359	125	-6	112	105	R	0.2	0.5	62	40	0.011	20.00	22.00	24.00
3/13/10	1	5	100	90	353	355	120	-6	105	88	R	0.2	0.5	40	16	0.023	48.00	46.00	43.00
3/13/10	1	5	90	80	373	377	115	-5	88	62	R	0.5	1.0	16	0	0.006	74.00	63.00	60.00
3/13/10	1	5	80	70	436	404	110	-4	62	40	F-->R	1.0	1.5						
3/13/10	1	5	70	60	424	377	105	-4	40	16	F-->R	1.0	1.5						
3/13/10	1	5	60	50	339	334	100	-4	16	0	F	0.5	1.0						
3/13/10	1	5	50	40	425	432	90	-4											
3/13/10	1	5	40	30	420	424	80	-3											
3/13/10	1	5	30	20	359	369	70	-3											
3/13/10	1	5	20	10	405	436	60	-3											
3/13/10	1	5	10	0	420	428	50	-3											
3/13/10	1	5					40	-2											
3/13/10	1	5					30	-2											
3/13/10	1	5					25	-2											
3/13/10	1	5					20	-2											
3/13/10	1	5					15	-2											
3/13/10	1	5					10	-2											
3/13/10	1	5					5	-2											
3/13/10							0	-2											
3/14/10	2	1	145	135	160	164	145	-5	145	142	MF	-	-	145	133	0.023	3.75	4.00	3.50
3/14/10	2	1	140	130	197	183	140	-6	142	133	N-->R	1.0	1.5	133	117	0.011	9.75	7.25	8.00
3/14/10	2	1	130	120	209	214	135	-8	133	131	MF	-	-	117	88	0.006	11.75	14.25	12.00
3/14/10	2	1	120	110	226	236	130	-7	131	117	N-->R	0.0	1.0	88	67	0.011	56.00	59.00	45.00
3/14/10	2	1	110	100	275	228	125	-6	117	114	MF	-	-	67	41	0.011	16.00	15.00	19.00
3/14/10	2	1	100	90	357	353	120	-6	114	88	R	0.2	0.5	41	13	0.011	23.00	30.00	34.00
3/14/10	2	1	90	80	341	310	115	-5	88	67	F-->R	1.0	0.5	13	0	0.011	60.00	46.00	64.00
3/14/10	2	1	80	70	392	336	110	-5	67	41	F-->R	1.0	2.0						

Date	Plot	Trt.	Snow depth (cm)		ρ_{s1} (kg/m^3)	ρ_{s2} (kg/m^3)	T_d (cm)	T_s (°C)	Strat. Layer (cm)		Crystal Type	Size (mm)		Layer (cm)		Disc rad. (m)	Force (N)		
3/14/10	2	1	70	60	356	308	105	-4	41	13	F	1.0	2.0						
3/14/10	2	1	60	50	332	325	100	-4	13	0	DH	2.0	3.0						
3/14/10	2	1	50	40	383	376	90	-4											
3/14/10	2	1	40	30	424	380	80	-4											
3/14/10	2	1	30	20	327	320	70	-3											
3/14/10	2	1	20	10	352	348	60	-3											
3/14/10	2	1	10	0	336	324	50	-3											
3/14/10	2	1					40	-3											
3/14/10	2	1					30	-2											
3/14/10	2	1					25	-2											
3/14/10	2	1					20	-2											
3/14/10	2	1					15	-2											
3/14/10	2	1					10	-2											
3/14/10	2	1					5	-2											
3/14/10	2	1					0	-2											
3/14/10	2	2	147	137	162	149	147	-2	147	144	MF	-	-	147	132	0.023	5.75	5.50	5.50
3/14/10	2	2	140	130	191	183	140	-5	144	132	N-->R	1.0	1.5	132	111	0.011	9.00	7.75	9.00
3/14/10	2	2	130	120	214	208	135	-6	132	131	MF	-	-	111	86	0.006	4.00	4.50	4.25
3/14/10	2	2	120	110	248	212	130	-6	131	111	R	0.2	0.5	86	70	0.006	31.00	36.00	40.00
3/14/10	2	2	110	100	230	253	125	-6	111	109	MF	-	-	70	23	0.023	95.00	100.00	85.00
3/14/10	2	2	100	90	365	371	120	-5	109	86	R	0.2	0.5	23	0	0.023	23.00	23.00	23.00
3/14/10	2	2	90	80	381	379	115	-5	86	70	F-->R	1.0	1.5						
3/14/10	2	2	80	70	420	396	110	-5	70	23	F-->R	1.0	1.5						
3/14/10	2	2	70	60	432	378	105	-4	23	0	DH	2.0	4.0						
3/14/10	2	2	60	50	363	329	100	-4											
3/14/10	2	2	50	40	346	327	90	-4											
3/14/10	2	2	40	30	338	334	80	-4											
3/14/10	2	2	30	20	343	298	70	-3											
3/14/10	2	2	20	10	294	282	60	-3											
3/14/10	2	2	10	0	220	260	50	-3											
3/14/10	2	2					40	-3											
3/14/10	2	2					30	-2											
3/14/10	2	2					20	-2											
3/14/10	2	2					10	-2											
3/14/10	2	2					0	-1											
3/14/10	2	3	145	135	156	154	145	-2	145	143	MF	-	-	145	134	0.023	4.00	3.75	3.50
3/14/10	2	3	140	130	194	196	140	-3	143	134	N-->R	1.0	1.5	134	117	0.023	21.50	21.00	22.50
3/14/10	2	3	130	120	211	218	135	-5	134	133	MF	-	-	117	81	0.011	12.75	14.00	14.25
3/14/10	2	3	120	110	236	238	130	-5	133	117	N-->R	0.5	1.0	81	40	0.011	17.75	16.25	18.75
3/14/10	2	3	110	100	259	251	125	-6	117	115	MF	-	-	40	19	0.006	7.00	7.00	8.25
3/14/10	2	3	100	90	304	302	120	-5	115	81	R	0.2	0.5	19	0	0.006	5.25	5.25	3.50
3/14/10	2	3	90	80	300	316	115	-5	81	40	F-->R	0.5	1.0						
3/14/10	2	3	80	70	341	330	110	-5	40	19	F-->R	1.0	1.5						
3/14/10	2	3	70	60	316	328	105	-5	19	0	DH	2.0	4.0						
3/14/10	2	3	60	50	346	340	100	-5											

Date	Plot	Trt.	Snow depth (cm)		ρ_{s1} (kg/m^3)	ρ_{s2} (kg/m^3)	T_d (cm)	T_s (°C)	Strat. Layer (cm)		Crystal Type	Size (mm)		Layer (cm)		Disc rad. (m)	Force (N)		
3/14/10	2	3	50	40	342	368	90	-4											
3/14/10	2	3	40	30	338	345	80	-4											
3/14/10	2	3	30	20	362	362	70	-3											
3/14/10	2	3	20	10	286	286	60	-3											
3/14/10	2	3	10	0	280	268	50	-3											
3/14/10	2	3					40	-2											
3/14/10	2	3					30	-2											
3/14/10	2	3					20	-2											
3/14/10	2	3					10	-2											
3/14/10	2	3					0	-1											
3/14/10	2	4	150	140	163	168	150	-1	150	148	MF	-	-	150	139	0.023	3.75	3.25	4.00
3/14/10	2	4	140	130	213	207	145	-1	148	139	N-->R	0.2	0.5	139	118	0.023	17.25	16.00	15.75
3/14/10	2	4	130	120	212	219	140	-4	139	138	MF	-	-	118	102	0.006	3.75	3.50	3.50
3/14/10	2	4	120	110	229	235	135	-5	138	118	R	0.2	0.5	102	93	0.006	14.50	16.50	17.25
3/14/10	2	4	110	100	359	313	130	-5	118	116	MF	-	-	93	77	0.006	4.00	6.75	5.50
3/14/10	2	4	100	90	338	320	125	-5	116	102	R	0.2	0.5	77	67	0.011	57.00	71.00	83.00
3/14/10	2	4	90	80	336	350	120	-5	102	93	F-->R	0.5	1.0	67	40	0.011	22.00	20.00	18.00
3/14/10	2	4	80	70	349	395	115	-5	93	77	F-->R	0.5	1.0	40	22	0.011	26.00	26.00	26.00
3/14/10	2	4	70	60	328	369	110	-5	77	67	F-->R	0.5	1.0	22	0	0.011	12.00	16.00	15.00
3/14/10	2	4	60	50	340	366	105	-4	67	40	F-->R	1.0	1.5						
3/14/10	2	4	50	40	371	350	100	-4	40	22	F-->R	1.0	1.5						
3/14/10	2	4	40	30	340	341	90	-4	22	0	DH	2.0	4.0						
3/14/10	2	4	30	20	356	349	80	-4											
3/14/10	2	4	20	10	262	287	70	-4											
3/14/10	2	4	10	0	240	256	60	-3											
3/14/10	2	4					50	-3											
3/14/10	2	4					40	-3											
3/14/10	2	4					30	-2											
3/14/10	2	4					20	-2											
3/14/10	2	4					10	-2											
3/14/10	2	4					0	-2											
3/14/10	2	5	150	140	149	164	150	-1	150	149	MF	-	-	150	139	0.023	2.25	3.25	3.50
3/14/10	2	5	140	130	222	220	145	-1	149	139	N-->R	1.0	1.5	139	115	0.011	12.00	12.75	12.00
3/14/10	2	5	130	120	221	204	140	-2	139	137	MF	-	-	115	100	0.011	9.75	7.00	8.00
3/14/10	2	5	120	110	228	236	135	-4	137	115	N-->R	1.0	1.5	100	85	0.006	48.00	55.00	47.00
3/14/10	2	5	110	100	271	233	130	-5	115	113	MF	-	-	85	60	0.006	49.00	56.00	67.00
3/14/10	2	5	100	90	389	359	125	-4	113	100	R	0.2	0.5	60	40	0.011	23.00	23.00	23.00
3/14/10	2	5	90	80	389	354	120	-4	100	85	R	0.2	0.5	40	10	0.011	48.00	40.00	39.00
3/14/10	2	5	80	70	411	389	115	-4	85	60	F-->R	1.0	1.5	10	0	0.006	52.00	52.00	42.00
3/14/10	2	5	70	60	426	421	110	-4	60	40	F-->R	1.0	1.5						
3/14/10	2	5	60	50	340	330	105	-4	40	10	F	1.0	2.0						
3/14/10	2	5	50	40	364	394	100	-4	10	0	F-->R	1.0	1.5						
3/14/10	2	5	40	30	469	445	90	-4											
3/14/10	2	5	30	20	378	410	80	-4											
3/14/10	2	5	20	10	353	343	70	-3											

Date	Plot	Trt.	Snow depth (cm)		ρ_{s1} (kg/m^3)	ρ_{s2} (kg/m^3)	T_d (cm)	T_s (^{o}C)	Strat. Layer (cm)		Crystal Type	Size (mm)		Layer (cm)		Disc rad. (m)	Force (N)		
3/14/10	2	5	10	0	396	400	60	-3											
3/14/10	2	5					50	-3											
3/14/10	2	5					40	-3											
3/14/10	2	5					30	-3											
3/14/10	2	5					20	-2											
3/14/10	2	5					10	-2											
3/14/10	2	5					0	-2											
4/17/10	1	1	174	164	316	291	174	0	174	170	N-->R	1.0	1.5	174	170	0.011	3.50	3.25	4.25
4/17/10	1	1	170	160	405	415	170	0	170	161	R	0.5	1.0	170	161	0.006	29.00	36.00	19.00
4/17/10	1	1	160	150	413	385	160	0	161	148	R	0.2	0.5	161	148	0.011	31.00	27.00	24.00
4/17/10	1	1	150	140	441	440	150	0	148	140	R	1.0	1.5	148	140	0.011	16.00	17.00	13.00
4/17/10	1	1	140	130	443	447	140	0	140	128	R	1.0	1.5	140	128	0.011	13.00	15.00	13.00
4/17/10	1	1	130	120	362	492	130	0	128	123	F	2.0	2.5	128	123	0.006	14.00	14.00	15.00
4/17/10	1	1	120	110	434	472	120	0	123	92	R	0.5	1.0	123	92	0.011	19.00	16.00	18.00
4/17/10	1	1	110	100	395	473	110	0	92	30	R	1.0	1.5	92	30	0.011	30.00	28.00	41.00
4/17/10	1	1	100	90	442	487	100	0	30	0	F-->R	1.0	2.0	30	0	0.011	22.00	36.00	17.00
4/17/10	1	1	90	80	431	424	90	0											
4/17/10	1	1	80	70	407	430	80	0											
4/17/10	1	1	70	60	365	421	70	0											
4/17/10	1	1	60	50	480	394	60	0											
4/17/10	1	1	50	40	408	398	50	0											
4/17/10	1	1	40	30	432	453	40	0											
4/17/10	1	1	30	20	496	460	30	0											
4/17/10	1	1	20	10	416	429	20	0											
4/17/10	1	1	10	0	364	348	10	0											
4/17/10	1	1					0	0											
4/17/10	1	2	143	133	175	190	140	-1	143	138	N-->R	1.0	2.0	143	138	0.023	2.50	2.50	2.50
4/17/10	1	2	140	130	369	381	130	-2	138	125	F-->R	1.0	2.0	138	125	0.006	40.00	35.00	37.00
4/17/10	1	2	130	120	353	297	120	-2	125	115	R	1.0	1.5	125	115	0.011	10.25	9.75	8.50
4/17/10	1	2	120	110	496	476	110	-1	115	108	R	1.0	2.0	115	108	0.006	21.00	22.00	23.00
4/17/10	1	2	110	100	540	520	100	-1	108	100	R	1.0	2.0	108	100	0.011	31.00	36.00	24.00
4/17/10	1	2	100	90	453	440	90	-1	100	78	R	0.5	1.0	100	78	0.011	39.00	33.00	23.00
4/17/10	1	2	90	80	432	465	80	-1	78	71	R	0.5	1.0	78	71	0.011	14.00	21.00	46.00
4/17/10	1	2	80	70	516	463	70	-1	71	58	R	0.5	1.0	71	57	0.011	48.00	46.00	53.00
4/17/10	1	2	70	60	448	487	60	-1	58	57	IL	-	-	57	30	0.011	13.00	18.00	23.00
4/17/10	1	2	60	50	448	449	50	-1	57	30	R	1.0	1.5	30	0	0.011	3.75	5.75	10.25
4/17/10	1	2	50	40	386	453	40	-1	30	0	F-->R	1.0	2.0						
4/17/10	1	2	40	30	381	436	30	-1											
4/17/10	1	2	30	20	407	384	20	-1											
4/17/10	1	2	20	10	402	404	10	-1											
4/17/10	1	2	10	0	360	400	0	-1											
4/17/10	1	3	138	128	412	462	138	-1	138	133	N-->R	0.5	1.0	138	133	0.023	2.50	2.50	2.50
4/17/10	1	3	130	120	490	455	130	-1	133	120	R	0.5	1.0	133	120	0.011	75.00	80.00	82.00
4/17/10	1	3	120	110	470	504	120	-1	120	95	R	1.0	1.5	120	95	0.011	4.50	9.75	12.50
4/17/10	1	3	110	100	457	421	110	-1	95	72	R	0.2	0.5	95	72	0.011	41.00	56.00	40.00

Date	Plot	Trt.	Snow depth (cm)		ρ_{s1} (kg/m^3)	ρ_{s2} (kg/m^3)	T_d (cm)	T_s (^{o}C)	Strat. Layer (cm)		Crystal Type	Size (mm)		Layer (cm)		Disc rad. (m)	Force (N)		
4/17/10	1	3	100	90	437	429	100	-2	72	59	R	0.5	1.0	72	59	0.011	41.00	38.00	28.00
4/17/10	1	3	90	80	512	423	90	-2	59	20	R	1.0	1.5	59	20	0.011	37.00	31.00	33.00
4/17/10	1	3	80	70	421	417	80	-1	20	0	F-->R	1.0	2.0	20	0	0.011	11.75	9.75	14.00
4/17/10	1	3	70	60	429	383	70	-1											
4/17/10	1	3	60	50	428	400	60	-1											
4/17/10	1	3	50	40	466	411	50	-1											
4/17/10	1	3	40	30	401	405	40	-1											
4/17/10	1	3	30	20	369	368	30	-1											
4/17/10	1	3	20	10	359	336	20	-1											
4/17/10	1	3	10	0	345	372	10	-1											
4/17/10	1	3					0	-1											
4/17/10	1	4	150	140	297	233	150	1	150	144	N-->R	1.0	1.5	150	144	0.023	4.00	3.25	0.00
4/17/10	1	4	140	130	362	397	140	0	144	133	R	0.5	1.0	144	133	0.006	42.00	38.00	45.00
4/17/10	1	4	130	120	322	392	130	0	133	119	R	1.0	1.5	133	119	0.011	46.00	36.00	58.00
4/17/10	1	4	120	110	434	395	120	0	119	85	R	0.2	0.5	119	85	0.011	20.00	25.00	22.00
4/17/10	1	4	110	100	388	442	110	0	85	67	R	0.2	0.5	85	67	0.011	33.00	31.00	39.00
4/17/10	1	4	100	90	368	411	100	0	67	25	R	0.5	1.0	67	25	0.011	27.00	23.00	20.00
4/17/10	1	4	90	80	397	468	90	0	25	0	F-->R	1.0	2.0	25	0	0.011	16.25	16.75	17.25
4/17/10	1	4	80	70	381	436	80	0											
4/17/10	1	4	70	60	361	367	70	0											
4/17/10	1	4	60	50	432	387	60	0											
4/17/10	1	4	50	40	372	374	50	0											
4/17/10	1	4	40	30	387	409	40	0											
4/17/10	1	4	30	20	356	343	30	0											
4/17/10	1	4	20	10	300	376	20	0											
4/17/10	1	4	10	0	284	280	10	0											
4/17/10	1	4					0	0											
4/17/10	1	5	150	140	308	370	150	0	150	144	N-->R	1.0	1.5	150	144	0.023	2.75	2.75	2.75
4/17/10	1	5	140	130	385	404	140	0	144	130	R	2.0	2.5	144	130	0.006	30.00	30.00	28.00
4/17/10	1	5	130	120	437	489	130	0	130	115	R	1.0	1.5	130	115	0.011	22.00	22.00	21.00
4/17/10	1	5	120	110	358	420	120	0	115	103	R	1.0	1.5	115	103	0.011	28.00	24.00	15.00
4/17/10	1	5	110	100	509	487	110	0	103	54	R	0.5	1.0	103	54	0.011	20.00	26.00	30.00
4/17/10	1	5	100	90	419	412	100	0	54	38	R	1.0	1.5	54	38	0.011	17.00	16.00	12.00
4/17/10	1	5	90	80	465	547	90	0	38	27	R	0.5	1.0	38	27	0.011	61.00	67.00	73.00
4/17/10	1	5	80	70	443	490	80	0	27	0	F-->R	1.0	1.5	27	0	0.011	21.00	26.00	20.00
4/17/10	1	5	70	60	492	511	70	0											
4/17/10	1	5	60	50	515	454	60	0											
4/17/10	1	5	50	40	414	443	50	0											
4/17/10	1	5	40	30	543	504	40	0											
4/17/10	1	5	30	20	441	431	30	0											
4/17/10	1	5	20	10	438	433	20	0											
4/17/10	1	5	10	0	400	372	10	0											
4/17/10	1	5					0	0											
4/17/10	2	1	150	140	332	396	150	-1	150	145	N-->R	1.0	1.5	150	145	0.023	3.50	4.75	3.00
4/17/10	2	1	140	130	408	421	140	-1	145	133	R	1.5	2.0	145	133	0.006	26.00	28.00	18.00

Date	Plot	Trt.	Snow depth (cm)		ρ_{s1} (kg/m^3)	ρ_{s2} (kg/m^3)	T_d (cm)	T_s (^oC)	Strat. Layer (cm)		Crystal Type	Size (mm)		Layer (cm)		Disc rad. (m)	Force (N)		
4/17/10	2	1	130	120	450	504	130	-1	133	112	R	1.5	2.0	133	112	0.011	23.00	16.00	17.00
4/17/10	2	1	120	110	517	482	120	-1	112	89	R	0.2	0.5	112	89	0.011	37.00	37.00	37.00
4/17/10	2	1	110	100	451	391	110	-1	89	71	R	0.5	1.0	89	71	0.011	38.00	40.00	36.00
4/17/10	2	1	100	90	500	534	100	-1	71	30	R	1.0	1.5	71	30	0.011	17.00	14.00	11.00
4/17/10	2	1	90	80	383	493	90	-1	30	10	R	1.0	1.5	30	10	0.011	10.50	9.25	10.00
4/17/10	2	1	80	70	489	484	80	-1	10	0	F-->R	1.0	2.0	10	0	0.011	32.00	28.00	38.00
4/17/10	2	1	70	60	482	481	70	-1											
4/17/10	2	1	60	50	417	429	60	-1											
4/17/10	2	1	50	40	520	478	50	-1											
4/17/10	2	1	40	30	431	376	40	-1											
4/17/10	2	1	30	20	415	409	30	-1											
4/17/10	2	1	20	10	418	437	20	-1											
4/17/10	2	1	10	0	448	468	10	-1											
4/17/10	2	1					0	-1											
4/17/10	2	2	152	142	365	366	152	2	152	148	F-->R	1.0	1.5	152	148	0.011	5.75	2.75	0.00
4/17/10	2	2	150	140	344	342	150	0	148	140	R	1.0	1.5	148	140	0.011	55.00	52.00	57.00
4/17/10	2	2	140	130	375	362	140	0	140	127	R	1.0	1.5	140	127	0.011	13.00	11.00	14.00
4/17/10	2	2	130	120	456	393	130	0	127	116	R	1.0	2.0	127	116	0.011	24.00	39.00	40.00
4/17/10	2	2	120	110	503	432	120	0	116	107	R	1.0	1..5	116	107	0.011	25.00	31.00	28.00
4/17/10	2	2	110	100	388	400	110	0	107	107	IL	-	-	107	93	0.011	15.00	26.00	19.00
4/17/10	2	2	100	90	479	441	100	0	107	93	R	1.0	1.5	93	72	0.011	17.00	14.00	27.00
4/17/10	2	2	90	80	416	412	90	0	93	72	R	1.0	2.0	72	57	0.011	39.00	43.00	48.00
4/17/10	2	2	80	70	452	478	80	0	72	58	R	1.0	1.5	57	35	0.011	5.50	5.25	4.25
4/17/10	2	2	70	60	387	494	70	0	58	57	IL	-	-	35	0	0.011	6.25	7.75	5.50
4/17/10	2	2	60	50	445	392	60	0	57	35	R	0.5	1.0						
4/17/10	2	2	50	40	412	377	50	0	35	0	F-->R	1.5	2.5						
4/17/10	2	2	40	30	451	370	40	0											
4/17/10	2	2	30	20	368	362	30	0											
4/17/10	2	2	20	10	377	370	20	0											
4/17/10	2	2	10	0	324	320	10	0											
4/17/10	2	2					0	0											
4/17/10	2	3	150	140	358	360	150	-1	155	152	N-->R	1.0	1.5	155	152	0.011	2.50	0.00	0.00
4/17/10	2	3	140	130	467	499	140	-1	152	142	R	1.0	1.5	152	142	0.011	22.00	25.00	18.00
4/17/10	2	3	130	120	432	448	130	-1	142	134	R	1.0	1.5	142	134	0.023	25.00	25.00	25.00
4/17/10	2	3	120	110	402	417	120	-1	134	118	R	1.0	2.0	134	118	0.023	29.00	29.00	28.00
4/17/10	2	3	110	100	410	471	110	-1	118	112	R	1.0	1.5	118	112	0.011	15.00	14.00	10.00
4/17/10	2	3	100	90	417	399	100	-1	112	87	R	0.5	1.0	112	87	0.011	13.00	20.00	19.00
4/17/10	2	3	90	80	531	514	90	-1	87	71	R	0.5	1.0	87	71	0.011	22.00	28.00	34.00
4/17/10	2	3	80	70	456	439	80	-1	71	48	R	0.5	1.0	71	48	0.011	16.00	14.00	15.00
4/17/10	2	3	70	60	413	413	70	-1	48	30	R	1.0	2.0	48	30	0.011	14.00	11.00	16.00
4/17/10	2	3	60	50	410	408	60	-1	30	0	F-->R	1.5	2.5	30	0	0.023	21.00	23.00	30.00
4/17/10	2	3	50	40	407	456	50	-1											
4/17/10	2	3	40	30	466	422	40	-1											
4/17/10	2	3	30	20	485	382	30	-1											
4/17/10	2	3	20	10	409	376	20	-1											

Date	Plot	Trt.	Snow depth (cm)		ρ_{s1} (kg/m^3)	ρ_{s2} (kg/m^3)	T_d (cm)	T_s (^{o}C)	Strat. Layer (cm)		Crystal Type	Size (mm)		Layer (cm)		Disc rad. (m)	Force (N)		
4/17/10	2	3	10	0	348	332	10	-1											
4/17/10	2	3					0	-1											
4/17/10	2	4	148	138	404	469	148	-1	148	143	N-->R	1.0	1.5	148	132	0.011	43.00	43.00	63.00
4/17/10	2	4	140	130	458	425	140	-1	143	132	R	1.0	1.5	132	124	0.023	25.00	32.00	38.00
4/17/10	2	4	130	120	390	405	130	-1	132	124	R	1.0	1.5	124	110	0.011	27.00	33.00	31.00
4/17/10	2	4	120	110	532	528	120	-1	124	110	R	0.2	0.5	110	86	0.011	35.00	39.00	45.00
4/17/10	2	4	110	100	448	408	110	-1	110	86	R	0.2	0.5	86	70	0.011	34.00	38.00	42.00
4/17/10	2	4	100	90	548	530	100	-1	86	70	R	1.0	1.5	70	50	0.011	16.00	17.00	18.00
4/17/10	2	4	90	80	407	398	90	-1	70	50	R	1.0	1.5	50	25	0.011	20.00	20.00	21.00
4/17/10	2	4	80	70	512	464	80	-1	50	25	R	1.0	1.5	25	0	0.023	17.00	20.00	14.00
4/17/10	2	4	70	60	444	425	70	-1	25	0	F-->R	1.0	2.0						
4/17/10	2	4	60	50	552	529	60	-1											
4/17/10	2	4	50	40	447	406	50	-1											
4/17/10	2	4	40	30	525	464	40	-1											
4/17/10	2	4	30	20	428	460	30	-1											
4/17/10	2	4	20	10	445	428	20	-1											
4/17/10	2	4	10	0	332	384	10	-1											
4/17/10	2	4					0	-1											
4/17/10	2	5	150	140	380	404	150	-1	150	149	-	-	-	150	136	0.011	43.00	38.00	3.50
4/17/10	2	5	140	130	441	400	140	-1	150	148	N-->R	1.0	1.5	136	129	0.011	47.00	45.00	41.00
4/17/10	2	5	130	120	358	344	130	-1	148	136	R	1.0	1.5	129	119	0.011	34.00	29.00	42.00
4/17/10	2	5	120	110	384	409	120	-1	136	129	R	1.0	1.5	119	109	0.011	22.00	27.00	40.00
4/17/10	2	5	110	100	410	427	110	-1	129	119	F-->R	2.0	4.0	109	90	0.011	16.00	18.00	15.00
4/17/10	2	5	100	90	424	476	100	-1	119	109	R	0.2	0.5	90	78	0.011	18.00	19.00	14.00
4/17/10	2	5	90	80	378	430	90	-1	109	90	R	0.2	0.5	78	55	0.011	48.00	62.00	16.00
4/17/10	2	5	80	70	482	455	80	-1	90	78	R	0.2	0.5	55	36	0.011	21.00	19.00	54.00
4/17/10	2	5	70	60	393	415	70	-1	78	55	R	0.5	1.0	36	15	0.006	41.00	42.00	21.00
4/17/10	2	5	60	50	406	404	60	-1	55	36	R	1.0	1.5	15	0	0.006	20.00	22.00	43.00
4/17/10	2	5	50	40	401	407	50	-1	36	15	F-->R	1.0	2.0						
4/17/10	2	5	40	30	439	417	40	-1	15	0	F-->R	1.0	1.5						
4/17/10	2	5	30	20	427	417	30	-1											
4/17/10	2	5	20	10	352	416	20	-1											
4/17/10	2	5	10	0	404	480	10	-1											
4/17/10	2	5					0	-1											

Table B-2. Standard ram penetrometer data measured at the snow compaction plots on Rabbit Ears Pass, Colorado during the 2009-2010 winter season.

Date	Plot	Trt.	Tube weight (kg)	Hammer weight (kg)	Tube and hammer T+H (kg)	# of falls n	Fall height f (cm)	Location of point L (cm)	Penetration *p* (cm)	*(nfH)/p* (kg)	RN (kg)	RR (N)	Height above ground (cm)
12/12/09	1	1											41
12/12/09	1	1	1	0	1	0	0	32	15	0	1	10	9
12/12/09	1	1	1	0.5	1.5	0	0	32	0				9
12/12/09	1	1	1	0.5	1.5	10	5	33	1	25	27	265	8
12/12/09	1	1	1	1	2	0	0	33	0				8
12/12/09	1	1	1	1	2	10	5	34	1	50	52	520	7
12/12/09	1	1	1	1	2	10	10	36	2	50	52	520	5
12/12/09	1	1	1	1	2	5	20	37	1	100	102	1020	4
12/12/09	1	1	1	1	2	7	25	41	4	44	46	458	0
12/12/09	1	2											63
12/12/09	1	2	1	0	1	0	0	63	63	0	1	10	0
12/12/09	1	3											61
12/12/09	1	3	1	0	1	0	0	61	61	0	1	10	0
12/12/09	1	4											60
12/12/09	1	4	1	0	1	0	0	60	60	0	1	10	0
12/12/09	1	5											50
12/12/09	1	5	1	0	1	0	0	44	44	0	1	10	6
12/12/09	1	5	1	0.5	1.5	0	0	44	0				6
12/12/09	1	5	1	0.5	1.5	15	5	45	1	38	39	390	5
12/12/09	1	5	1	1	2	0	0	45	0				5
12/12/09	1	5	1	1	2	15	10	46	1	150	152	1520	4
12/12/09	1	5	1	1	2	10	20	47	1	200	202	2020	3
12/12/09	1	5	1	1	2	15	30	48	1	450	452	4520	2
12/12/09	1	5	1	1	2	5	50	49	1	250	252	2520	1
12/12/09	1	5	1	1	2	3	55	50	1	165	167	1670	0
12/12/09	2	1											52
12/12/09	2	1	1	0	1	0	0	37	15	0	1	10	15
12/12/09	2	1	1	0.5	1.5	0	0	37	0				15
12/12/09	2	1	1	0.5	1.5	10	10	38	1	50	52	515	14
12/12/09	2	1	1	0.5	1.5	10	20	40	2	50	52	515	12
12/12/09	2	1	1	1	2	0	0	40	0				12
12/12/09	2	1	1	1	2	7	10	41	1	70	72	720	11
12/12/09	2	1	1	1	2	8	20	44	3	53	55	553	8
12/12/09	2	1	1	1	2	20	30	52	8	75	77	770	0
12/12/09	2	2											59
12/12/09	2	2	1	0	1	0	0	59	59	0	1	10	0
12/12/09	2	3											59
12/12/09	2	3	1	0	1	0	0	59	59	0	1	10	0
12/12/09	2	4											60
12/12/09	2	4	1	0	1	0	0	60	60	0	1	10	0
12/12/09	2	5											53
12/12/09	2	5	1	0	1	0	0	45	45	0	1	10	8
12/12/09	2	5	1	0.5	1.5	0	0	45	0				8
12/12/09	2	5	1	0.5	1.5	1	5	45	0				8
12/12/09	2	5	1	0.5	1.5	10	10	45	0				8

Date	Plot	Trt.	Tube weight (kg)	Hammer weight (kg)	Tube and hammer T+H (kg)	# of falls n	Fall height f (cm)	Location of point L (cm)	Penetration *p* (cm)	*(nfH)/p* (kg)	RN (kg)	RR (N)	Height above ground (cm)
12/12/09	2	5	1	1	2	0	0	46	1	0	2	20	7
12/12/09	2	5	1	1	2	10	10	46	0				7
12/12/09	2	5	1	1	2	10	20	49	3	67	69	687	4
12/12/09	2	5	1	1	2	7	30	50	1	210	212	2120	3
12/12/09	2	5	1	1	2	5	40	51	1	200	202	2020	2
12/12/09	2	5	1	1	2	3	50	53	2	75	77	770	0
1/9/10	1	1											77
1/9/10	1	1	1	0	1	0	0	48	48	0	1	10	29
1/9/10	1	1	1	0.5	1.5	0	0	48	0				29
1/9/10	1	1	1	0.5	1.5	6	5	50	2	8	9	90	27
1/9/10	1	1	1	0.5	1.5	10	10	53	3	17	18	182	24
1/9/10	1	1	1	1	2	7	5	55	2	18	20	195	22
1/9/10	1	1	1	1	2	10	10	57	2	50	52	520	20
1/9/10	1	1	1	1	2	10	20	61	4	50	52	520	16
1/9/10	1	1	1	1	2	15	30	70	9	50	52	520	7
1/9/10	1	1	1	1	2	15	10	77	7	21	23	234	0
1/9/10	1	2											96
1/9/10	1	2	1	0	1	0	0	45	45	0	1	10	51
1/9/10	1	2	1	0.5	1.5	0	0	45	0				51
1/9/10	1	2	1	0.5	1.5	10	5	46	1	25	27	265	50
1/9/10	1	2	1	0.5	1.5	7	10	52	6	6	7	73	44
1/9/10	1	2	1	0.5	1.5	11	5	62	10	3	4	43	34
1/9/10	1	2	1	0.5	1.5	4	10	96	34	1	2	21	0
1/9/10	1	3											108
1/9/10	1	3	1	0	1	0	0	47	47	0	1	10	61
1/9/10	1	3	1	0.5	1.5	0	0	47	0				61
1/9/10	1	3	1	0.5	1.5	7	5	49	2	9	10	103	59
1/9/10	1	3	1	0.5	1.5	2	10	62	13	1	2	23	46
1/9/10	1	3	1	0.5	1.5	16	5	69	7	6	7	72	39
1/9/10	1	3	2	0	2	0	0	69	0				39
1/9/10	1	3	2	0.5	2.5	0	0	69	0				39
1/9/10	1	3	2	0.5	2.5	5	5	108	39	0	3	28	0
1/9/10	1	4											110
1/9/10	1	4	1	0	1	0	0	48	48	0	1	10	62
1/9/10	1	4	1	0.5	1.5	0	0	48	0				62
1/9/10	1	4	1	0.5	1.5	8	5	49	1	20	22	215	61
1/9/10	1	4	1	0.5	1.5	16	10	57	8	10	12	115	53
1/9/10	1	4	2	0	2	0	0	57	0				53
1/9/10	1	4	2	0.5	2.5	0	0	57	0				53
1/9/10	1	4	2	0.5	2.5	10	5	69	12	2	5	46	41
1/9/10	1	4	2	0.5	2.5	10	10	110	41	1	4	37	0
1/9/10	1	5											105
1/9/10	1	5	1	0	1	0	0	49	49	0	1	10	56
1/9/10	1	5	1	0.5	1.5	0	0	49	0				56
1/9/10	1	5	1	0.5	1.5	10	5	52	3	8	10	98	53

Date	Plot	Trt.	Tube weight (kg)	Hammer weight (kg)	Tube and hammer T+H (kg)	# of falls n	Fall height f (cm)	Location of point L (cm)	Penetration *p* (cm)	*(nfH)/p* (kg)	RN (kg)	RR (N)	Height above ground (cm)
1/9/10	1	5	1	0.5	1.5	7	10	54	2	18	19	190	51
1/9/10	1	5	1	0.5	1.5	3	20	55	1	30	32	315	50
1/9/10	1	5	1	1	2	0	0	55	0				50
1/9/10	1	5	1	1	2	5	5	56	1	25	27	270	49
1/9/10	1	5	1	1	2	8	10	57	1	80	82	820	48
1/9/10	1	5	1	1	2	12	20	60	3	80	82	820	45
1/9/10	1	5	1	1	2	5	30	62	2	75	77	770	43
1/9/10	1	5	1	1	2	10	40	81	19	21	23	231	24
1/9/10	1	5	1	1	2	4	5	89	8	3	5	45	16
1/9/10	1	5	1	1	2	2	20	90	1	40	42	420	15
1/9/10	1	5	1	1	2	5	30	91	1	150	152	1520	14
1/9/10	1	5	1	1	2	5	40	92	1	200	202	2020	13
1/9/10	1	5	1	1	2	14	50	98	6	117	119	1187	7
1/9/10	1	5	2	0	2	0	0	98	0				7
1/9/10	1	5	2	0.5	2.5	1	5	98	0				7
1/9/10	1	5	2	0.5	2.5	7	20	100	2	35	38	375	5
1/9/10	1	5	2	0.5	2.5	6	30	105	5	18	21	205	0
1/10/10	2	1											100
1/10/10	2	1	1	0	1	0	0	44	44	0	1	10	56
1/10/10	2	1	1	0.5	1.5	0	0	44	0				56
1/10/10	2	1	1	0.5	1.5	5	5	45	1	13	14	140	55
1/10/10	2	1	1	0.5	1.5	10	10	47	2	25	27	265	53
1/10/10	2	1	1	1	2	0	0	47	0				53
1/10/10	2	1	1	1	2	5	5	48	1	25	27	270	52
1/10/10	2	1	1	1	2	5	10	50	2	25	27	270	50
1/10/10	2	1	1	1	2	15	20	60	10	30	32	320	40
1/10/10	2	1	1	1	2	3	10	63	3	10	12	120	37
1/10/10	2	1	1	1	2	14	5	81	18	4	6	59	19
1/10/10	2	1	1	1	2	6	10	84	3	20	22	220	16
1/10/10	2	1	1	1	2	8	20	88	4	40	42	420	12
1/10/10	2	1	1	1	2	11	30	100	12	28	30	295	0
1/10/10	2	2											103
1/10/10	2	2	1	0	1	0	0	46	46	0	1	10	57
1/10/10	2	2	1	0.5	1.5	0	0	46	0				57
1/10/10	2	2	1	0.5	1.5	3	5	46	0				57
1/10/10	2	2	1	0.5	1.5	4	10	47	1	20	22	215	56
1/10/10	2	2	1	0.5	1.5	9	20	56	9	10	12	115	47
1/10/10	2	2	1	0.5	1.5	14	10	67	11	6	8	79	36
1/10/10	2	2	1	0.5	1.5	3	20	103	36	1	2	23	0
1/10/10	2	3											110
1/10/10	2	3	1	0	1	0	0	48	48	0	1	10	62
1/10/10	2	3	1	0.5	1.5	0	0	48	0				62
1/10/10	2	3	1	0.5	1.5	4	5	48	0				62
1/10/10	2	3	1	0.5	1.5	5	10	49	1	25	27	265	61
1/10/10	2	3	1	0.5	1.5	5	20	56	7	7	9	86	54

Date	Plot	Trt.	Tube weight (kg)	Hammer weight (kg)	Tube and hammer T+H (kg)	# of falls n	Fall height f (cm)	Location of point L (cm)	Penetration *p* (cm)	*(nfH)/p* (kg)	RN (kg)	RR (N)	Height above ground (cm)
1/10/10	2	3	1	0.5	1.5	9	10	64	8	6	7	71	46
1/10/10	2	3	2	0	2	0	0	64	0				46
1/10/10	2	3	2	0.5	2.5	0	0	64	0				46
1/10/10	2	3	2	0.5	2.5	7	5	67	3	6	8	83	43
1/10/10	2	3	2	0.5	2.5	4	10	68	1	20	23	225	42
1/10/10	2	3	2	0.5	2.5	5	20	110	42	1	4	37	0
1/10/10	2	4											109
1/10/10	2	4	1	0	1	0	0	47	47	0	1	10	62
1/10/10	2	4	1	0.5	1.5	0	0	47	0				62
1/10/10	2	4	1	0.5	1.5	8	5	48	1	20	22	215	61
1/10/10	2	4	1	0.5	1.5	18	10	63	15	6	8	75	46
1/10/10	2	4	2	0	2	0	0	63	0				46
1/10/10	2	4	2	0.5	2.5	0	0	66	3	0	3	25	43
1/10/10	2	4	2	0.5	2.5	5	5	67	1	13	15	150	42
1/10/10	2	4	2	0.5	2.5	7	10	109	42	1	3	33	0
1/10/10	2	5											103
1/10/10	2	5	1	0	1	0	0	54	54	0	1	10	49
1/10/10	2	5	1	0.5	1.5	0	0	54	0				49
1/10/10	2	5	1	0.5	1.5	8	5	55	1	20	22	215	48
1/10/10	2	5	1	0.5	1.5	6	10	56	1	30	32	315	47
1/10/10	2	5	1	1	2	0	0	56	0				47
1/10/10	2	5	1	1	2	2	5	56	0				47
1/10/10	2	5	1	1	2	5	10	57	1	50	52	520	46
1/10/10	2	5	1	1	2	8	20	59	2	80	82	820	44
1/10/10	2	5	1	1	2	16	30	65	6	80	82	820	38
1/10/10	2	5	1	1	2	4	40	68	3	53	55	553	35
1/10/10	2	5	1	1	2	5	20	70	2	50	52	520	33
1/10/10	2	5	2	0	2	0	0	70	0				33
1/10/10	2	5	2	0.5	2.5	0	0	70	0				33
1/10/10	2	5	2	0.5	2.5	4	5	70	0				33
1/10/10	2	5	2	1	3	0	0	70	0				33
1/10/10	2	5	2	1	3	5	5	71	1	25	28	280	32
1/10/10	2	5	2	1	3	6	10	73	2	30	33	330	30
1/10/10	2	5	2	1	3	4	20	90	17	5	8	77	13
1/10/10	2	5	2	1	3	5	30	94	4	38	41	405	9
1/10/10	2	5	2	1	3	10	40	98	4	100	103	1030	5
1/10/10	2	5	2	1	3	10	50	103	5	100	103	1030	0
2/6/10	1	1											93
2/6/10	1	1	1	0	1	0	0	25	25	0	1	10	68
2/6/10	1	1	1	0.5	1.5	0	0	25	0				68
2/6/10	1	1	1	0.5	1.5	15	5	26	1	38	39	390	67
2/6/10	1	1	1	1	2	0	0	26	0				67
2/6/10	1	1	1	1	2	12	10	30	4	30	32	320	63
2/6/10	1	1	1	1	2	13	20	40	10	26	28	280	53
2/6/10	1	1	1	1	2	1	10	44	4	3	5	45	49

Date	Plot	Trt.	Tube weight (kg)	Hammer weight (kg)	Tube and hammer T+H (kg)	# of falls n	Fall height f (cm)	Location of point L (cm)	Penetration *p* (cm)	*(nfH)/p* (kg)	RN (kg)	RR (N)	Height above ground (cm)
2/6/10	1	1	1	1	2	20	5	66	22	5	7	65	27
2/6/10	1	1	2	0	2	0	0	66	0				27
2/6/10	1	1	2	1	3	0	0	66	0				27
2/6/10	1	1	2	1	3	6	5	67	1	30	33	330	26
2/6/10	1	1	2	1	3	5	10	69	2	25	28	280	24
2/6/10	1	1	2	1	3	17	20	87	18	19	22	219	6
2/6/10	1	1	2	1	3	1	10	93	6	2	5	47	0
2/6/10	1	2											93
2/6/10	1	2	1	0	1	0	0	20	20	0	1	10	73
2/6/10	1	2	1	0.5	1.5	0	0	20	0				73
2/6/10	1	2	1	0.5	1.5	12	5	21	1	30	32	315	72
2/6/10	1	2	1	1	2	0	0	21	0				72
2/6/10	1	2	1	1	2	7	10	22	1	70	72	720	71
2/6/10	1	2	1	1	2	10	20	24	2	100	102	1020	69
2/6/10	1	2	1	1	2	10	30	27	3	100	102	1020	66
2/6/10	1	2	1	1	2	8	40	30	3	107	109	1087	63
2/6/10	1	2	1	1	2	10	30	39	9	33	35	353	54
2/6/10	1	2	1	1	2	1	20	41	2	10	12	120	52
2/6/10	1	2	1	1	2	3	10	44	3	10	12	120	49
2/6/10	1	2	1	1	2	8	5	50	6	7	9	87	43
2/6/10	1	2	2	0	2	0	0	56	6	0	2	20	37
2/6/10	1	2	2	0.5	2.5	0	0	56	0				37
2/6/10	1	2	2	0.5	2.5	1	5	84	28	0	3	26	9
2/6/10	1	2	2	0.5	2.5	20	10	93	9	11	14	136	0
2/6/10	1	3											116
2/6/10	1	3	1	0	1	0	0	55	55	0	1	10	61
2/6/10	1	3	1	0.5	1.5	0	0	55	0				61
2/6/10	1	3	1	0.5	1.5	10	5	57	2	13	14	140	59
2/6/10	1	3	1	0.5	1.5	7	10	59	2	18	19	190	57
2/6/10	1	3	1	0.5	1.5	3	20	64	5	6	8	75	52
2/6/10	1	3	2	0	2	0	0	64	0				52
2/6/10	1	3	2	0.5	2.5	0	0	64	0				52
2/6/10	1	3	2	0.5	2.5	8	5	71	7	3	5	54	45
2/6/10	1	3	2	0.5	2.5	8	10	75	4	10	13	125	41
2/6/10	1	3	2	0.5	2.5	4	20	81	6	7	9	92	35
2/6/10	1	3	2	0.5	2.5	1	10	116	35	0	3	26	0
2/6/10	1	4											114
2/6/10	1	4	1	0	1	0	0	27	27	0	1	10	87
2/6/10	1	4	1	0.5	1.5	0	0	27	0				87
2/6/10	1	4	1	0.5	1.5	10	5	28	1	25	27	265	86
2/6/10	1	4	1	0.5	1.5	17	10	29	1	85	87	865	85
2/6/10	1	4	1	0.5	1.5	8	20	30	1	80	82	815	84
2/6/10	1	4	1	0.5	1.5	7	30	33	3	35	37	365	81
2/6/10	1	4	1	0.5	1.5	10	10	34	1	50	52	515	80
2/6/10	1	4	1	0.5	1.5	12	40	44	10	24	26	255	70

Date	Plot	Trt.	Tube weight (kg)	Hammer weight (kg)	Tube and hammer T+H (kg)	# of falls n	Fall height f (cm)	Location of point L (cm)	Penetration *p* (cm)	*(nfH)/p* (kg)	RN (kg)	RR (N)	Height above ground (cm)
2/6/10	1	4	1	0.5	1.5	2	30	50	6	5	7	65	64
2/6/10	1	4	1	0.5	1.5	12	20	60	10	12	14	135	54
2/6/10	1	4	2	0	2	0	0	60	0				54
2/6/10	1	4	2	0.5	2.5	0	0	60	0				54
2/6/10	1	4	2	0.5	2.5	12	20	64	4	30	33	325	50
2/6/10	1	4	2	0.5	2.5	4	30	69	5	12	15	145	45
2/6/10	1	4	2	0.5	2.5	12	20	80	11	11	13	134	34
2/6/10	1	4	2	0.5	2.5	10	30	88	8	19	21	213	26
2/6/10	1	4	2	0.5	2.5	1	20	114	26	0	3	29	0
2/6/10	1	5											110
2/6/10	1	5	1	0	1	0	0	20	20	0	1	10	90
2/6/10	1	5	1	1	2	0	0	20	0				90
2/6/10	1	5	1	1	2	7	5	21	1	35	37	370	89
2/6/10	1	5	1	1	2	10	20	23	2	100	102	1020	87
2/6/10	1	5	1	1	2	10	30	25	2	150	152	1520	85
2/6/10	1	5	1	1	2	17	50	32	7	121	123	1234	78
2/6/10	1	5	1	1	2	17	40	42	10	68	70	700	68
2/6/10	1	5	1	1	2	3	30	53	11	8	10	102	57
2/6/10	1	5	1	1	2	27	20	69	16	34	36	358	41
2/6/10	1	5	2	0	2	0	0	69	0				41
2/6/10	1	5	2	0	2	0	0	69	0				41
2/6/10	1	5	2	1	3	10	10	70	1	100	103	1030	40
2/6/10	1	5	2	1	3	17	20	83	13	26	29	292	27
2/6/10	1	5	2	1	3	3	10	90	7	4	7	73	20
2/6/10	1	5	2	1	3	8	5	92	2	20	23	230	18
2/6/10	1	5	2	1	3	7	10	93	1	70	73	730	17
2/6/10	1	5	2	1	3	13	30	95	2	195	198	1980	15
2/6/10	1	5	2	1	3	31	50	110	15	103	106	1063	0
2/7/10	2	1											116
2/7/10	2	1	1	0	1	0	0	26	26	0	1	10	90
2/7/10	2	1	1	0.5	1.5	0	0	26	0				90
2/7/10	2	1	1	0.5	1.5	15	5	27	1	38	39	390	89
2/7/10	2	1	1	1	2	0	0	27	0				89
2/7/10	2	1	1	1	2	10	5	28	1	50	52	520	88
2/7/10	2	1	1	1	2	20	10	33	5	40	42	420	83
2/7/10	2	1	1	1	2	6	20	52	19	6	8	83	64
2/7/10	2	1	1	1	2	3	10	60	8	4	6	58	56
2/7/10	2	1	1	1	2	13	5	65	5	13	15	150	51
2/7/10	2	1	2	0	2	0	0	65	0				51
2/7/10	2	1	2	1	3	0	0	65	0				51
2/7/10	2	1	2	1	3	10	5	66	1	50	53	530	50
2/7/10	2	1	2	1	3	10	10	69	3	33	36	363	47
2/7/10	2	1	2	1	3	12	20	77	8	30	33	330	39
2/7/10	2	1	2	1	3	6	10	96	19	3	6	62	20
2/7/10	2	1	2	1	3	28	20	116	20	28	31	310	0

Date	Plot	Trt.	Tube weight (kg)	Hammer weight (kg)	Tube and hammer T+H (kg)	# of falls n	Fall height f (cm)	Location of point L (cm)	Penetration *p* (cm)	*(nfH)/p* (kg)	RN (kg)	RR (N)	Height above ground (cm)
2/7/10	2	2											106
2/7/10	2	2	1	0	1	0	0	20	20	0	1	10	86
2/7/10	2	2	1	1	2	0	0	20	0				86
2/7/10	2	2	1	1	2	7	5	21	1	35	37	370	85
2/7/10	2	2	1	1	2	10	10	23	2	50	52	520	83
2/7/10	2	2	1	1	2	10	20	25	2	100	102	1020	81
2/7/10	2	2	1	1	2	9	30	27	2	135	137	1370	79
2/7/10	2	2	1	1	2	14	40	31	4	140	142	1420	75
2/7/10	2	2	1	1	2	23	50	45	14	82	84	841	61
2/7/10	2	2	1	1	2	1	40	49	4	10	12	120	57
2/7/10	2	2	1	1	2	10	10	60	11	9	11	111	46
2/7/10	2	2	2	0	2	0	0	60	0				46
2/7/10	2	2	2	0.5	2.5	0	0	60	0				46
2/7/10	2	2	2	0.5	2.5	10	5	63	3	8	11	108	43
2/7/10	2	2	2	0.5	2.5	10	10	66	3	17	19	192	40
2/7/10	2	2	2	0.5	2.5	8	20	70	4	20	23	225	36
2/7/10	2	2	2	0.5	2.5	3	30	74	4	11	14	138	32
2/7/10	2	2	2	0.5	2.5	6	20	106	32	2	4	44	0
2/7/10	2	3											117
2/7/10	2	3	1	0	1	0	0	40	40	0	1	10	77
2/7/10	2	3	1	0.5	1.5	0	0	40	0				77
2/7/10	2	3	1	0.5	1.5	16	5	50	10	4	6	55	67
2/7/10	2	3	1	0.5	1.5	10	10	56	6	8	10	98	61
2/7/10	2	3	1	0.5	1.5	13	20	64	8	16	18	178	53
2/7/10	2	3	2	0	2	0	0	64	0				53
2/7/10	2	3	2	0.5	2.5	0	0	64	0				53
2/7/10	2	3	2	0.5	2.5	5	10	65	1	25	28	275	52
2/7/10	2	3	2	0.5	2.5	5	20	70	5	10	13	125	47
2/7/10	2	3	2	0.5	2.5	11	10	77	7	8	10	104	40
2/7/10	2	3	2	0.5	2.5	15	20	84	7	21	24	239	33
2/7/10	2	3	2	0.5	2.5	7	30	117	33	3	6	57	0
2/7/10	2	4											116
2/7/10	2	4	1	0	1	0	0	28	28	0	1	10	88
2/7/10	2	4	1	1	2	0	0	28	0				88
2/7/10	2	4	1	1	2	10	5	30	2	25	27	270	86
2/7/10	2	4	1	1	2	6	10	31	1	60	62	620	85
2/7/10	2	4	1	1	2	15	20	38	7	43	45	449	78
2/7/10	2	4	1	1	2	2	30	41	3	20	22	220	75
2/7/10	2	4	1	1	2	6	5	50	9	3	5	53	66
2/7/10	2	4	2	0	2	0	0	50	0				66
2/7/10	2	4	2	0.5	2.5	0	0	51	1	0	3	25	65
2/7/10	2	4	2	0.5	2.5	10	5	58	7	4	6	61	58
2/7/10	2	4	2	0.5	2.5	10	20	67	9	11	14	136	49
2/7/10	2	4	2	0.5	2.5	4	30	76	9	7	9	92	40
2/7/10	2	4	2	0.5	2.5	16	10	85	9	9	11	114	31

Date	Plot	Trt.	Tube weight (kg)	Hammer weight (kg)	Tube and hammer T+H (kg)	# of falls n	Fall height f (cm)	Location of point L (cm)	Penetration *p* (cm)	*(nfH)/p* (kg)	RN (kg)	RR (N)	Height above ground (cm)
2/7/10	2	4	2	0.5	2.5	5	20	115	30	2	4	42	1
2/7/10	2	4	2	0.5	2.5	3	30	116	1	45	48	475	0
2/7/10	2	5											108
2/7/10	2	5	1	0	1	0	0	21	21	0	1	10	87
2/7/10	2	5	1	1	2	0	0	21	0				87
2/7/10	2	5	1	1	2	43	50	46	25	86	88	880	62
2/7/10	2	5	1	1	2	27	5	63	17	8	10	99	45
2/7/10	2	5	1	1	2	10	10	66	3	33	35	353	42
2/7/10	2	5	1	1	2	12	20	70	4	60	62	620	38
2/7/10	2	5	2	0	2	0	0	70	0				38
2/7/10	2	5	2	1	3	0	0	70	0				38
2/7/10	2	5	2	1	3	10	10	71	1	100	103	1030	37
2/7/10	2	5	2	1	3	12	30	77	6	60	63	630	31
2/7/10	2	5	2	1	3	5	40	86	9	22	25	252	22
2/7/10	2	5	2	1	3	2	20	93	7	6	9	87	15
2/7/10	2	5	2	1	3	10	10	99	6	17	20	197	9
2/7/10	2	5	2	1	3	9	20	102	3	60	63	630	6
2/7/10	2	5	2	1	3	10	40	105	3	133	136	1363	3
2/7/10	2	5	2	1	3	9	50	108	3	150	153	1530	0
3/13/10	1	1											150
3/13/10	1	1	1	0	1	0	0	32	32	0	1	10	118
3/13/10	1	1	1	0.5	1.5	0	0	32	0				118
3/13/10	1	1	1	0.5	1.5	10	5	33	1	25	27	265	117
3/13/10	1	1	1	0.5	1.5	3	10	36	3	5	7	65	114
3/13/10	1	1	1	0.5	1.5	13	5	42	6	5	7	69	108
3/13/10	1	1	1	0.5	1.5	11	10	55	13	4	6	57	95
3/13/10	1	1	1	0.5	1.5	42	20	70	15	28	30	295	80
3/13/10	1	1	2	0	2	0	0	70	0				80
3/13/10	1	1	2	0.5	2.5	0	0	70	0				80
3/13/10	1	1	2	0.5	2.5	6	5	71	1	15	18	175	79
3/13/10	1	1	2	0.5	2.5	13	10	73	2	33	35	350	77
3/13/10	1	1	2	0.5	2.5	11	20	75	2	55	58	575	75
3/13/10	1	1	2	0.5	2.5	8	30	77	2	60	63	625	73
3/13/10	1	1	2	0.5	2.5	10	40	80	3	67	69	692	70
3/13/10	1	1	2	0.5	2.5	10	50	91	11	23	25	252	59
3/13/10	1	1	2	0.5	2.5	1	40	96	5	4	7	65	54
3/13/10	1	1	2	0.5	2.5	7	30	109	13	8	11	106	41
3/13/10	1	1	2	0.5	2.5	10	10	113	4	13	15	150	37
3/13/10	1	1	2	0.5	2.5	5	30	115	2	38	40	400	35
3/13/10	1	1	2	0.5	2.5	10	50	119	4	63	65	650	31
3/13/10	1	1	2	1	3	0	0	119	0				31
3/13/10	1	1	2	1	3	12	10	126	7	17	20	201	24
3/13/10	1	1	2	1	3	29	5	143	17	9	12	115	7
3/13/10	1	1	2	1	3	16	10	148	5	32	35	350	2
3/13/10	1	1	2	1	3	5	20	150	2	50	53	530	0

Date	Plot	Trt.	Tube weight (kg)	Hammer weight (kg)	Tube and hammer T+H (kg)	# of falls n	Fall height f (cm)	Location of point L (cm)	Penetration *p* (cm)	*(nfH)/p* (kg)	RN (kg)	RR (N)	Height above ground (cm)
3/13/10	1	2											137
3/13/10	1	2	1	0	1	0	0	33	5	0	1	10	104
3/13/10	1	2	1	0.5	1.5	0	0	33	0				104
3/13/10	1	2	1	0.5	1.5	10	5	39	6	4	6	57	98
3/13/10	1	2	1	0.5	1.5	5	10	44	5	5	7	65	93
3/13/10	1	2	1	0.5	1.5	10	5	53	9	3	4	43	84
3/13/10	1	2	1	0.5	1.5	3	10	54	1	15	17	165	83
3/13/10	1	2	1	0.5	1.5	10	20	56	2	50	52	515	81
3/13/10	1	2	1	0.5	1.5	12	30	59	3	60	62	615	78
3/13/10	1	2	1	0.5	1.5	15	40	63	4	75	77	765	74
3/13/10	1	2	1	0.5	1.5	23	50	75	12	48	49	494	62
3/13/10	1	2	2	0	2	0	0	75	0				62
3/13/10	1	2	2	1	3	0	0	75	0				62
3/13/10	1	2	2	1	3	10	5	76	1	50	53	530	61
3/13/10	1	2	2	1	3	10	20	77	1	200	203	2030	60
3/13/10	1	2	2	1	3	10	40	80	3	133	136	1363	57
3/13/10	1	2	2	1	3	36	50	97	17	106	109	1089	40
3/13/10	1	2	2	1	3	8	30	106	9	27	30	297	31
3/13/10	1	2	2	1	3	1	5	137	31	0	3	32	0
3/13/10	1	3											153
3/13/10	1	3	1	0	1	0	0	31	24	0	1	10	122
3/13/10	1	3	1	0.5	1.5	0	0	31	0				122
3/13/10	1	3	1	0.5	1.5	7	10	34	3	12	13	132	119
3/13/10	1	3	1	0.5	1.5	14	5	43	9	4	5	54	110
3/13/10	1	3	1	0.5	1.5	18	10	54	11	8	10	97	99
3/13/10	1	3	1	0.5	1.5	8	20	60	6	13	15	148	93
3/13/10	1	3	2	0	2	0	0	60	0				93
3/13/10	1	3	2	0.5	2.5	0	0	60	0				93
3/13/10	1	3	2	0.5	2.5	10	5	62	2	13	15	150	91
3/13/10	1	3	2	0.5	2.5	16	20	79	17	9	12	119	74
3/13/10	1	3	2	0.5	2.5	4	5	81	2	5	8	75	72
3/13/10	1	3	2	0.5	2.5	10	10	88	7	7	10	96	65
3/13/10	1	3	2	0.5	2.5	12	20	96	8	15	18	175	57
3/13/10	1	3	2	0.5	2.5	15	30	108	12	19	21	213	45
3/13/10	1	3	2	0.5	2.5	15	20	118	10	15	18	175	35
3/13/10	1	3	2	0.5	2.5	5	30	153	35	2	5	46	0
3/13/10	1	4											150
3/13/10	1	4	1	0	1	0	0	32	32	0	1	10	118
3/13/10	1	4	1	0.5	1.5	0	0	32	0				118
3/13/10	1	4	1	0.5	1.5	8	5	33	1	20	22	215	117
3/13/10	1	4	1	0.5	1.5	2	20	45	12	2	3	32	105
3/13/10	1	4	1	0.5	1.5	14	10	49	4	18	19	190	101
3/13/10	1	4	1	0.5	1.5	9	20	52	3	30	32	315	98
3/13/10	1	4	1	0.5	1.5	16	30	62	10	24	26	255	88
3/13/10	1	4	2	0	2	0	0	62	0				88

Date	Plot	Trt.	Tube weight (kg)	Hammer weight (kg)	Tube and hammer T+H (kg)	# of falls n	Fall height f (cm)	Location of point L (cm)	Penetration *p* (cm)	*(nfH)/p* (kg)	RN (kg)	RR (N)	Height above ground (cm)
3/13/10	1	4	2	0.5	2.5	0	0	62	0				88
3/13/10	1	4	2	0.5	2.5	11	10	66	4	14	16	163	84
3/13/10	1	4	2	0.5	2.5	6	20	70	4	15	18	175	80
3/13/10	1	4	2	0.5	2.5	10	30	73	3	50	53	525	77
3/13/10	1	4	2	0.5	2.5	7	40	76	3	47	49	492	74
3/13/10	1	4	2	0.5	2.5	10	50	80	4	63	65	650	70
3/13/10	1	4	2	1	3	0	0	80	0				70
3/13/10	1	4	2	1	3	11	5	85	5	11	14	140	65
3/13/10	1	4	2	0.5	2.5	0	0	85	0				65
3/13/10	1	4	2	0.5	2.5	15	20	100	15	10	13	125	50
3/13/10	1	4	2	0.5	2.5	9	30	105	5	27	30	295	45
3/13/10	1	4	2	0.5	2.5	19	40	150	45	8	11	109	0
3/13/10	1	5											157
3/13/10	1	5	1	0	1	0	0	31	31	0	1	10	126
3/13/10	1	5	1	0.5	1.5	0	0	31	0				126
3/13/10	1	5	1	0.5	1.5	6	10	38	7	4	6	58	119
3/13/10	1	5	1	0.5	1.5	9	5	40	2	11	13	128	117
3/13/10	1	5	1	0.5	1.5	4	10	41	1	20	22	215	116
3/13/10	1	5	1	0.5	1.5	4	20	46	5	8	10	95	111
3/13/10	1	5	1	0.5	1.5	10	10	51	5	10	12	115	106
3/13/10	1	5	1	0.5	1.5	7	20	52	1	70	72	715	105
3/13/10	1	5	1	0.5	1.5	5	30	53	1	75	77	765	104
3/13/10	1	5	1	0.5	1.5	5	40	54	1	100	102	1015	103
3/13/10	1	5	1	1	2	0	0	54	0				103
3/13/10	1	5	1	1	2	12	10	55	1	120	122	1220	102
3/13/10	1	5	1	1	2	4	20	56	1	80	82	820	101
3/13/10	1	5	1	1	2	14	30	66	10	42	44	440	91
3/13/10	1	5	1	1	2	13	10	74	8	16	18	183	83
3/13/10	1	5	2	0	2	0	0	74	0				83
3/13/10	1	5	2	1	3	0	0	74	0				83
3/13/10	1	5	2	1	3	10	10	77	3	33	36	363	80
3/13/10	1	5	2	1	3	5	20	80	3	33	36	363	77
3/13/10	1	5	2	1	3	4	30	85	5	24	27	270	72
3/13/10	1	5	2	1	3	1	10	95	10	1	4	40	62
3/13/10	1	5	2	1	3	10	5	102	7	7	10	101	55
3/13/10	1	5	2	1	3	14	10	110	8	18	21	205	47
3/13/10	1	5	2	1	3	5	20	112	2	50	53	530	45
3/13/10	1	5	2	1	3	16	30	119	7	69	72	716	38
3/13/10	1	5	2	1	3	6	40	124	5	48	51	510	33
3/13/10	1	5	2	1	3	4	20	129	5	16	19	190	28
3/13/10	1	5	2	1	3	7	10	135	6	12	15	147	22
3/13/10	1	5	2	1	3	9	5	140	5	9	12	120	17
3/13/10	1	5	2	1	3	7	10	143	3	23	26	263	14
3/13/10	1	5	2	1	3	10	20	147	4	50	53	530	10
3/13/10	1	5	2	1	3	13	30	156	9	43	46	463	1

Date	Plot	Trt.	Tube weight (kg)	Hammer weight (kg)	Tube and hammer T+H (kg)	# of falls n	Fall height f (cm)	Location of point L (cm)	Penetration *p* (cm)	*(nfH)/p* (kg)	RN (kg)	RR (N)	Height above ground (cm)
3/13/10	1	5	2	1	3	5	10	157	1	50	53	530	0
3/14/10	2	1											150
3/14/10	2	1	1	0	1	0	0	5	5	0	1	10	145
3/14/10	2	1	1	0.5	1.5	0	0	5	0				145
3/14/10	2	1	1	0.5	1.5	1	5	30	25	0	2	16	120
3/14/10	2	1	1	0.5	1.5	6	10	31	1	30	32	315	119
3/14/10	2	1	1	0.5	1.5	2	20	34	3	7	8	82	116
3/14/10	2	1	1	0.5	1.5	10	10	41	7	7	9	86	109
3/14/10	2	1	1	0.5	1.5	6	20	43	2	30	32	315	107
3/14/10	2	1	1	0.5	1.5	13	30	49	6	33	34	340	101
3/14/10	2	1	1	0.5	1.5	12	40	60	11	22	23	233	90
3/14/10	2	1	1	0.5	1.5	10	30	67	7	21	23	229	83
3/14/10	2	1	1	0.5	1.5	15	40	74	7	43	44	444	76
3/14/10	2	1	2	0	2	0	0	74	0				76
3/14/10	2	1	2	0.5	2.5	0	0	74	0				76
3/14/10	2	1	2	0.5	2.5	10	30	76	2	75	78	775	74
3/14/10	2	1	2	0.5	2.5	8	40	82	6	27	29	292	68
3/14/10	2	1	2	0.5	2.5	2	30	87	5	6	9	85	63
3/14/10	2	1	2	0.5	2.5	5	5	90	3	4	7	67	60
3/14/10	2	1	2	0.5	2.5	10	10	95	5	10	13	125	55
3/14/10	2	1	2	0.5	2.5	7	30	100	5	21	24	235	50
3/14/10	2	1	2	0.5	2.5	10	40	104	4	50	53	525	46
3/14/10	2	1	2	0.5	2.5	4	50	105	1	100	103	1025	45
3/14/10	2	1	2	1	3	0	0	105	0				45
3/14/10	2	1	2	1	3	10	5	106	1	50	53	530	44
3/14/10	2	1	2	1	3	6	10	107	1	60	63	630	43
3/14/10	2	1	2	1	3	19	20	130	23	17	20	195	20
3/14/10	2	1	2	1	3	4	5	131	1	20	23	230	19
3/14/10	2	1	2	1	3	12	10	135	4	30	33	330	15
3/14/10	2	1	2	1	3	30	20	150	15	40	43	430	0
3/14/10	2	2											151
3/14/10	2	2	1	0	1	0	0	5	5	0	1	10	146
3/14/10	2	2	1	0.5	1.5	0	0	5	0				146
3/14/10	2	2	1	0.5	1.5	1	5	35	30	0	2	16	116
3/14/10	2	2	1	0.5	1.5	12	10	49	14	4	6	58	102
3/14/10	2	2	1	0.5	1.5	5	5	50	1	13	14	140	101
3/14/10	2	2	1	0.5	1.5	4	10	51	1	20	22	215	100
3/14/10	2	2	1	0.5	1.5	4	30	52	1	60	62	615	99
3/14/10	2	2	1	0.5	1.5	4	40	53	1	80	82	815	98
3/14/10	2	2	1	0.5	1.5	5	50	54	1	125	127	1265	97
3/14/10	2	2	2	0	2	0	0	54	0				97
3/14/10	2	2	2	1	3	0	0	54	0				97
3/14/10	2	2	2	1	3	20	5	55	1	100	103	1030	96
3/14/10	2	2	2	1	3	17	20	58	3	113	116	1163	93
3/14/10	2	2	2	1	3	10	30	61	3	100	103	1030	90

Date	Plot	Trt.	Tube weight (kg)	Hammer weight (kg)	Tube and hammer T+H (kg)	# of falls n	Fall height f (cm)	Location of point L (cm)	Penetration *p* (cm)	*(nfH)/p* (kg)	RN (kg)	RR (N)	Height above ground (cm)
3/14/10	2	2	2	1	3	13	40	74	13	40	43	430	77
3/14/10	2	2	2	1	3	19	50	90	16	59	62	624	61
3/14/10	2	2	2	1	3	15	5	99	9	8	11	113	52
3/14/10	2	2	2	1	3	8	10	110	11	7	10	103	41
3/14/10	2	2	2	1	3	19	5	151	41	2	5	53	0
3/14/10	2	3											147
3/14/10	2	3	1	0	1	0	0	24	24	0	1	10	123
3/14/10	2	3	1	0.5	1.5	0	0	24	0				123
3/14/10	2	3	1	0.5	1.5	10	5	30	6	4	6	57	117
3/14/10	2	3	1	0.5	1.5	6	10	33	3	10	12	115	114
3/14/10	2	3	1	0.5	1.5	12	5	40	7	4	6	58	107
3/14/10	2	3	1	0.5	1.5	16	10	50	10	8	10	95	97
3/14/10	2	3	1	0.5	1.5	30	20	70	20	15	17	165	77
3/14/10	2	3	2	0	2	0	0	70	0				77
3/14/10	2	3	2	0.5	2.5	0	0	70	0				77
3/14/10	2	3	2	0.5	2.5	5	10	71	1	25	28	275	76
3/14/10	2	3	2	0.5	2.5	11	20	75	4	28	30	300	72
3/14/10	2	3	2	0.5	2.5	30	1	78	3	5	8	75	69
3/14/10	2	3	2	0.5	2.5	10	10	84	6	8	11	108	63
3/14/10	2	3	2	0.5	2.5	20	20	97	13	15	18	179	50
3/14/10	2	3	2	0.5	2.5	5	30	100	3	25	28	275	47
3/14/10	2	3	2	0.5	2.5	6	40	102	2	60	63	625	45
3/14/10	2	3	2	0.5	2.5	15	50	122	20	19	21	213	25
3/14/10	2	3	2	0.5	2.5	4	20	147	25	2	4	41	0
3/14/10	2	4											151
3/14/10	2	4	1	0	1	0	0	24	24	0	1	10	127
3/14/10	2	4	1	0.5	1.5	0	0	24	0				127
3/14/10	2	4	1	0.5	1.5	11	5	30	6	5	6	61	121
3/14/10	2	4	1	0.5	1.5	7	10	33	3	12	13	132	118
3/14/10	2	4	1	0.5	1.5	12	20	46	13	9	11	107	105
3/14/10	2	4	1	0.5	1.5	8	30	50	4	30	32	315	101
3/14/10	2	4	2	0.5	2.5	24	40	70	20	24	27	265	81
3/14/10	2	4	2	0	2	0	0	70	0				81
3/14/10	2	4	2	0.5	2.5	0	0	70	0				81
3/14/10	2	4	2	0.5	2.5	5	20	71	1	50	53	525	80
3/14/10	2	4	2	1	3	0	0	71	0				80
3/14/10	2	4	2	1	3	5	5	72	1	25	28	280	79
3/14/10	2	4	2	1	3	11	20	76	4	55	58	580	75
3/14/10	2	4	2	1	3	8	30	84	8	30	33	330	67
3/14/10	2	4	2	1	3	15	10	100	16	9	12	124	51
3/14/10	2	4	2	1	3	8	20	110	10	16	19	190	41
3/14/10	2	4	2	1	3	8	10	119	9	9	12	119	32
3/14/10	2	4	2	1	3	6	5	121	2	15	18	180	30
3/14/10	2	4	2	1	3	6	10	126	5	12	15	150	25
3/14/10	2	4	2	1	3	8	5	150	24	2	5	47	1

Date	Plot	Trt.	Tube weight (kg)	Hammer weight (kg)	Tube and hammer T+H (kg)	# of falls n	Fall height f (cm)	Location of point L (cm)	Penetration *p* (cm)	*(nfH)/p* (kg)	RN (kg)	RR (N)	Height above ground (cm)
3/14/10	2	4	2	1	3	4	10	151	1	40	43	430	0
3/14/10	2	5											158
3/14/10	2	5	1	0	1	0	0	25	25	0	1	10	133
3/14/10	2	5	1	0.5	1.5	0	0	25	0				133
3/14/10	2	5	1	0.5	1.5	16	5	32	7	6	7	72	126
3/14/10	2	5	1	0.5	1.5	17	10	45	13	7	8	80	113
3/14/10	2	5	1	0.5	1.5	5	20	47	2	25	27	265	111
3/14/10	2	5	1	0.5	1.5	7	30	50	3	35	37	365	108
3/14/10	2	5	1	0.5	1.5	8	40	53	3	53	55	548	105
3/14/10	2	5	1	0.5	1.5	48	50	83	30	40	42	415	75
3/14/10	2	5	2	0	2	0	0	83	0				75
3/14/10	2	5	2	1	3	0	0	83	0				75
3/14/10	2	5	2	1	3	5	10	84	1	50	53	530	74
3/14/10	2	5	2	1	3	4	20	88	4	20	23	230	70
3/14/10	2	5	2	1	3	2	10	91	3	7	10	97	67
3/14/10	2	5	2	1	3	2	5	100	9	1	4	41	58
3/14/10	2	5	2	1	3	10	10	109	9	11	14	141	49
3/14/10	2	5	2	1	3	5	20	111	2	50	53	530	47
3/14/10	2	5	2	1	3	9	30	114	3	90	93	930	44
3/14/10	2	5	2	1	3	7	40	118	4	70	73	730	40
3/14/10	2	5	2	1	3	9	50	128	10	45	48	480	30
3/14/10	2	5	2	1	3	1	20	130	2	10	13	130	28
3/14/10	2	5	2	1	3	4	10	132	2	20	23	230	26
3/14/10	2	5	2	1	3	3	30	141	9	10	13	130	17
3/14/10	2	5	2	1	3	4	5	142	1	20	23	230	16
3/14/10	2	5	2	1	3	6	10	145	3	20	23	230	13
3/14/10	2	5	2	1	3	25	20	158	13	38	41	415	0
4/17/10	1	1											175
4/17/10	1	1	1	0	1	0	0	10	10	0	1	10	165
4/17/10	1	1	1	0.5	1.5	0	0	10	0				165
4/17/10	1	1	1	0.5	1.5	3	10	11	1	15	17	165	164
4/17/10	1	1	1	0.5	1.5	12	30	18	7	26	27	272	157
4/17/10	1	1	1	0.5	1.5	5	20	25	7	7	9	86	150
4/17/10	1	1	1	0.5	1.5	10	10	32	7	7	9	86	143
4/17/10	1	1	1	0.5	1.5	10	20	36	4	25	27	265	139
4/17/10	1	1	1	0.5	1.5	10	30	46	10	15	17	165	129
4/17/10	1	1	1	0.5	1.5	10	10	50	4	13	14	140	125
4/17/10	1	1	1	0.5	1.5	12	20	55	5	24	26	255	120
4/17/10	1	1	1	0.5	1.5	7	30	57	2	53	54	540	118
4/17/10	1	1	1	0.5	1.5	7	40	60	3	47	48	482	115
4/17/10	1	1	1	0.5	1.5	14	50	69	9	39	40	404	106
4/17/10	1	1	2	0	2	0	0	69	0				106
4/17/10	1	1	2	0.5	2.5	0	0	69	0				106
4/17/10	1	1	2	0.5	2.5	2	20	70	1	20	23	225	105
4/17/10	1	1	2	0.5	2.5	12	30	78	8	23	25	250	97

Date	Plot	Trt.	Tube weight (kg)	Hammer weight (kg)	Tube and hammer T+H (kg)	# of falls n	Fall height f (cm)	Location of point L (cm)	Penetration *p* (cm)	*(nfH)/p* (kg)	RN (kg)	RR (N)	Height above ground (cm)
4/17/10	1	1	2	0.5	2.5	4	50	80	2	50	53	525	95
4/17/10	1	1	2	1	3	0	0	80	0				95
4/17/10	1	1	2	1	3	4	10	81	1	40	43	430	94
4/17/10	1	1	2	1	3	8	20	87	6	27	30	297	88
4/17/10	1	1	2	1	3	9	10	115	28	3	6	62	60
4/17/10	1	1	2	1	3	5	5	116	1	25	28	280	59
4/17/10	1	1	2	1	3	10	10	120	4	25	28	280	55
4/17/10	1	1	2	1	3	6	20	125	5	24	27	270	50
4/17/10	1	1	2	1	3	17	5	133	8	11	14	136	42
4/17/10	1	1	2	1	3	3	10	141	8	4	7	68	34
4/17/10	1	1	2	0.5	2.5	0	0	141	0				34
4/17/10	1	1	2	0.5	2.5	8	10	145	4	10	13	125	30
4/17/10	1	1	2	0.5	2.5	13	20	149	4	33	35	350	26
4/17/10	1	1	2	0.5	2.5	25	30	160	11	34	37	366	15
4/17/10	1	1	2	0.5	2.5	13	40	168	8	33	35	350	7
4/17/10	1	1	2	0.5	2.5	1	20	170	2	5	8	75	5
4/17/10	1	1	2	0.5	2.5	5	10	174	4	6	9	88	1
4/17/10	1	1	2	0.5	2.5	5	20	175	1	50	53	525	0
4/17/10	1	2											148
4/17/10	1	2	1	0	1	0	0	12	12	0	1	10	136
4/17/10	1	2	1	0.5	1.5	0	0	12	0				136
4/17/10	1	2	1	0.5	1.5	7	20	14	2	35	37	365	134
4/17/10	1	2	1	0.5	1.5	5	40	18	4	25	27	265	130
4/17/10	1	2	1	0.5	1.5	2	30	32	14	2	4	36	116
4/17/10	1	2	1	0.5	1.5	5	10	33	1	25	27	265	115
4/17/10	1	2	1	0.5	1.5	12	30	48	15	12	14	135	100
4/17/10	1	2	1	0.5	1.5	20	20	67	19	11	12	120	81
4/17/10	1	2	2	0	2	0	0	67	0				81
4/17/10	1	2	2	1	3	0	0	67	0				81
4/17/10	1	2	2	1	3	5	10	69	2	25	28	280	79
4/17/10	1	2	2	1	3	23	20	102	33	14	17	169	46
4/17/10	1	2	2	0.5	2.5	0	0	102	0				46
4/17/10	1	2	2	0.5	2.5	10	5	148	46	1	3	30	0
4/17/10	1	3											148
4/17/10	1	3	1	0	1	0	0	10	10	0	1	10	138
4/17/10	1	3	1	0.5	1.5	0	0	10	0				138
4/17/10	1	3	1	0.5	1.5	10	10	12	2	25	27	265	136
4/17/10	1	3	1	0.5	1.5	8	30	38	26	5	6	61	110
4/17/10	1	3	1	0.5	1.5	20	10	51	13	8	9	92	97
4/17/10	1	3	1	0.5	1.5	15	20	60	9	17	18	182	88
4/17/10	1	3	1	0.5	1.5	3	30	63	3	15	17	165	85
4/17/10	1	3	1	0.5	1.5	17	10	70	7	12	14	136	78
4/17/10	1	3	2	0	2	0	0	70	0				78
4/17/10	1	3	2	0.5	2.5	0	0	70	0				78
4/17/10	1	3	2	0.5	2.5	6	20	72	2	30	33	325	76

Date	Plot	Trt.	Tube weight (kg)	Hammer weight (kg)	Tube and hammer T+H (kg)	# of falls n	Fall height f (cm)	Location of point L (cm)	Penetration *p* (cm)	*(nfH)/p* (kg)	RN (kg)	RR (N)	Height above ground (cm)
4/17/10	1	3	2	0.5	2.5	5	50	77	5	25	28	275	71
4/17/10	1	3	2	0.5	2.5	16	20	89	12	13	16	158	59
4/17/10	1	3	2	0.5	2.5	24	30	102	13	28	30	302	46
4/17/10	1	3	2	0.5	2.5	7	40	106	4	35	38	375	42
4/17/10	1	3	2	0.5	2.5	10	5	108	2	13	15	150	40
4/17/10	1	3	2	0.5		14	10	115	7	10	10	100	33
4/17/10	1	3	2	0.5		11	20	122	7	16	16	157	26
4/17/10	1	3	2	0.5		14	10	127	5	14	14	140	21
4/17/10	1	3	2	0.5		10	5	148	21	1	1	12	0
4/17/10	1	4											155
4/17/10	1	4	1	0	1	0	0	10	10	0	1	10	145
4/17/10	1	4	1	0.5	1.5	0	0	10	0				145
4/17/10	1	4	1	0.5	1.5	10	10	13	3	17	18	182	142
4/17/10	1	4	1	0.5	1.5	6	30	17	4	23	24	240	138
4/17/10	1	4	1	0.5	1.5	4	20	29	12	3	5	48	126
4/17/10	1	4	1	0.5	1.5	38	30	80	51	11	13	127	75
4/17/10	1	4	2	0	2	0	0	80	0				75
4/17/10	1	4	2	0.5	2.5	0	0	80	0				75
4/17/10	1	4	2	0.5	2.5	4	30	81	1	60	63	625	74
4/17/10	1	4	2	0.5	2.5	8	40	90	9	18	20	203	65
4/17/10	1	4	2	0.5	2.5	7	20	100	10	7	10	95	55
4/17/10	1	4	2	0.5	2.5	10	10	105	5	10	13	125	50
4/17/10	1	4	2	0.5	2.5	7	20	110	5	14	17	165	45
4/17/10	1	4	2	0.5	2.5	2	10	113	3	3	6	58	42
4/17/10	1	4	2	0.5	2.5	15	5	120	7	5	8	79	35
4/17/10	1	4	2	0.5	2.5	4	10	124	4	5	8	75	31
4/17/10	1	4	2	0.5	2.5	3	5	155	31	0	3	27	0
4/17/10	1	5											149
4/17/10	1	5	1	0	1	0	0	10	10	0	1	10	139
4/17/10	1	5	1	1	2	0	0	10	0				139
4/17/10	1	5	1	1	2	8	5	13	3	13	15	153	136
4/17/10	1	5	1	1	2	10	10	17	4	25	27	270	132
4/17/10	1	5	1	1	2	3	20	22	5	12	14	140	127
4/17/10	1	5	1	1	2	10	5	34	12	4	6	62	115
4/17/10	1	5	1	1	2	16	10	45	11	15	17	165	104
4/17/10	1	5	1	1	2	14	5	60	15	5	7	67	89
4/17/10	1	5	1	1	2	30	10	78	18	17	19	187	71
4/17/10	1	5	2	0	2	0	0	78	0				71
4/17/10	1	5	2	1	3	0	0	78	0				71
4/17/10	1	5	2	1	3	7	10	80	2	35	38	380	69
4/17/10	1	5	2	1	3	14	20	110	30	9	12	123	39
4/17/10	1	5	2	1	3	9	5	114	4	11	14	143	35
4/17/10	1	5	2	1	3	7	10	117	3	23	26	263	32
4/17/10	1	5	2	1	3	3	20	121	4	15	18	180	28
4/17/10	1	5	2	1	3	4	10	143	22	2	5	48	6

Date	Plot	Trt.	Tube weight (kg)	Hammer weight (kg)	Tube and hammer T+H (kg)	# of falls n	Fall height f (cm)	Location of point L (cm)	Penetration *p* (cm)	*(nfH)/p* (kg)	RN (kg)	RR (N)	Height above ground (cm)
4/17/10	1	5	2	1	3	8	5	145	2	20	23	230	4
4/17/10	1	5	2	1	3	12	10	149	4	30	33	330	0
4/17/10	2	1											154
4/17/10	2	1	1	0	1	0	0	9	9	0	1	10	145
4/17/10	2	1	1	1	2	0	0	9	0				145
4/17/10	2	1	1	1	2	7	10	12	3	23	25	253	142
4/17/10	2	1	1	1	2	6	20	15	3	40	42	420	139
4/17/10	2	1	1	1	2	2	5	24	9	1	3	31	130
4/17/10	2	1	1	1	2	12	10	48	24	5	7	70	106
4/17/10	2	1	1	1	2	20	5	58	10	10	12	120	96
4/17/10	2	1	1	1	2	30	20	80	22	27	29	293	74
4/17/10	2	1	2	0	2	0	0	80	0				74
4/17/10	2	1	2	1	3	0	0	80	0				74
4/17/10	2	1	2	1	3	2	5	109	29	0	3	33	45
4/17/10	2	1	2	1	3	6	5	112	3	10	13	130	42
4/17/10	2	1	2	1	3	8	10	120	8	10	13	130	34
4/17/10	2	1	2	0.5	2.5	0	0	120	0				34
4/17/10	2	1	2	0.5	2.5	9	5	154	34	1	3	32	0
4/17/10	2	2											148
4/17/10	2	2	1	0	1	0	0	8	8	0	1	10	140
4/17/10	2	2	1	0.5	1.5	0	0	8	0				140
4/17/10	2	2	1	0.5	1.5	10	10	10	2	25	27	265	138
4/17/10	2	2	1	0.5	1.5	23	20	30	20	12	13	130	118
4/17/10	2	2	1	0.5	1.5	2	30	33	3	10	12	115	115
4/17/10	2	2	1	0.5	1.5	3	10	35	2	8	9	90	113
4/17/10	2	2	1	0.5	1.5	7	20	40	5	14	16	155	108
4/17/10	2	2	1	0.5	1.5	8	30	45	5	24	26	255	103
4/17/10	2	2	1	0.5	1.5	27	40	80	35	15	17	169	68
4/17/10	2	2	2	0	2	0	0	80	0				68
4/17/10	2	2	2	0.5	2.5	0	0	80	0				68
4/17/10	2	2	2	0.5	2.5	8	20	81	1	80	83	825	67
4/17/10	2	2	2	0.5	2.5	13	40	87	6	43	46	458	61
4/17/10	2	2	2	0.5	2.5	9	50	92	5	45	48	475	56
4/17/10	2	2	2	1	3	0	0	92	0				56
4/17/10	2	2	2	1	3	9	20	100	8	23	26	255	48
4/17/10	2	2	2	1	3	7	5	120	20	2	5	48	28
4/17/10	2	2	2	0.5	2.5	0	0	120	0				28
4/17/10	2	2	2	0.5	2.5	2	5	148	28	0	3	27	0
4/17/10	2	3											154
4/17/10	2	3	1	0	1	0	0	6	6	0	1	10	148
4/17/10	2	3	1	0.5	1.5	0	0	6	0				148
4/17/10	2	3	1	0.5	1.5	10	10	10	4	13	14	140	144
4/17/10	2	3	1	0.5	1.5	9	20	40	30	3	5	45	114
4/17/10	2	3	1	0.5	1.5	13	10	47	7	9	11	108	107
4/17/10	2	3	1	0.5	1.5	15	20	56	9	17	18	182	98

Date	Plot	Trt.	Tube weight (kg)	Hammer weight (kg)	Tube and hammer T+H (kg)	# of falls n	Fall height f (cm)	Location of point L (cm)	Penetration *p* (cm)	*(nfH)/p* (kg)	RN (kg)	RR (N)	Height above ground (cm)
4/17/10	2	3	1	0.5	1.5	21	30	70	14	23	24	240	84
4/17/10	2	3	2	0	2	0	0	70	0				84
4/17/10	2	3	2	0.5	2.5	0	0	70	0				84
4/17/10	2	3	2	0.5	2.5	10	30	74	4	38	40	400	80
4/17/10	2	3	2	0.5	2.5	5	40	76	2	50	53	525	78
4/17/10	2	3	2	1	3	0	0	76	0				78
4/17/10	2	3	2	1	3	5	5	77	1	25	28	280	77
4/17/10	2	3	2	1	3	20	10	97	20	10	13	130	57
4/17/10	2	3	2	1	3	10	20	110	13	15	18	184	44
4/17/10	2	3	2	0.5	2.5	0	0	110	0				44
4/17/10	2	3	2	0.5	2.5	18	20	120	10	18	21	205	34
4/17/10	2	3	2	0.5	2.5	9	30	130	10	14	16	160	24
4/17/10	2	3	2	0.5		12	5	154	24	1	1	13	0
4/17/10	2	4											152
4/17/10	2	4	1	0	1	0	0	7	7	0	1	10	145
4/17/10	2	4	1	0.5	1.5	0	0	7	0				145
4/17/10	2	4	1	0.5	1.5	10	20	11	4	25	27	265	141
4/17/10	2	4	1	0.5	1.5	20	30	39	28	11	12	122	113
4/17/10	2	4	1	0.5	1.5	5	40	49	10	10	12	115	103
4/17/10	2	4	1	0.5	1.5	10	10	56	7	7	9	86	96
4/17/10	2	4	1	0.5	1.5	7	20	61	5	14	16	155	91
4/17/10	2	4	1	0.5	1.5	18	30	82	21	13	14	144	70
4/17/10	2	4	2	0	2	0	0	82	0				70
4/17/10	2	4	2	0.5	2.5	0	0	82	0				70
4/17/10	2	4	2	0.5	2.5	1	20	89	7	1	4	39	63
4/17/10	2	4	2	0.5	2.5	3	5	90	1	8	10	100	62
4/17/10	2	4	2	0.5	2.5	10	10	101	11	5	7	70	51
4/17/10	2	4	2	0.5	2.5	5	20	142	41	1	4	37	10
4/17/10	2	4	2	0.5	2.5	1	5	152	10	0	3	28	0
4/17/10	2	5											158
4/17/10	2	5	1	0	1	0	0	6	25	0	1	10	152
4/17/10	2	5	1	1	2	0	0	6	0				152
4/17/10	2	5	1	1	2	13	5	28	22	3	5	50	130
4/17/10	2	5	1	1	2	5	10	39	11	5	7	65	119
4/17/10	2	5	1	1	2	18	5	74	35	3	5	46	84
4/17/10	2	5	2	0	2	0	0	74	0				84
4/17/10	2	5	2	1	3	0	0	74	0				84
4/17/10	2	5	2	1	3	10	10	80	6	17	20	197	78
4/17/10	2	5	2	1	3	11	20	90	10	22	25	250	68
4/17/10	2	5	2	1	3	6	5	92	2	15	18	180	66
4/17/10	2	5	2	1	3	7	10	97	5	14	17	170	61
4/17/10	2	5	2	1	3	3	5	123	26	1	4	36	35
4/17/10	2	5	2	1	3	17	10	145	22	8	11	107	13
4/17/10	2	5	2	1	3	7	5	148	3	12	15	147	10
4/17/10	2	5	2	1	3	8	10	150	2	40	43	430	8

Table B-3. Raw data collected at Muddy Creek, Dumont Lakes, and Walton Creek near Rabbit Ears Pass, Colorado during the 2009-2010 winter season.

Date	Site	Snow depth (cm)		ρ_{s1} (kg/m^3)	ρ_{s2} (kg/m^3)	T_d (cm)	T_s (^{o}C)	Strat. Layer (cm)		Crystal Type	Size (mm)		Layer (cm)		Disc rad. (m)	Force (N)		
12/11/09	MC	49	39	189	193	49	-19	49	40	F-->R	0.5	1.0	14	0	0.023	10.00	8.30	6.20
12/11/09	MC	39	29	170	178	45	-22	40	28	R-->S	0.5	1.0						
12/11/09	MC	29	19	210	213	40	-21	28	14	F	1.0	1.5						
12/11/09	MC	19	9	207	205	35	-17	14	0	DH	2.0	4.0						
12/11/09	MC	10	0	351	311	30	-13											
12/11/09	MC					25	-9											
12/11/09	MC					20	-6											
12/11/09	MC					15	-4											
12/11/09	MC					10	-3											
12/11/09	MC					5	-2											
12/11/09	MC					0	-1											
12/11/09	DL	32	22	202	208	32	-12	32	20	N-->R	0.3	0.5	20	0	0.023	13.00	12.50	11.50
12/11/09	DL	22	12	279	226	30	-13	20	0	F	1.0	2.0						
12/11/09	DL	12	2	222	229	25	-11											
12/11/09	DL					20	-9											
12/11/09	DL					15	-7											
12/11/09	DL					10	-5											
12/11/09	DL					5	-4											
12/11/09	DL					0	-2											
12/11/09	WC	33	23	189	171	33	-8	33	28	N-->R	0.5	1.0	15	0	0.023	8.00	8.50	9.50
12/11/09	WC	23	13	217	212	30	-11	28	15	F	1.0	2.0						
12/11/09	WC	13	3	220	250	25	-14	15	0	F	2.0	3.0						
12/11/09	WC					20	-12											
12/11/09	WC					15	-7											
12/11/09	WC					10	-7											
12/11/09	WC					5	-5											
12/11/09	WC					0	-2											
1/8/10	MC	80	70	156	168	80	-20	80	72	N	0.5	1.0	80	68	0.023	4.50	6.00	5.50
1/8/10	MC	70	60	164	188	75	-22	72	68	N-->F	0.5	0.5	68	42	0.006	10.50	10.50	6.25
1/8/10	MC	60	50	304	340	70	-20	68	58	R	0.2	0.5	42	33	0.006	9.50	9.00	12.00
1/8/10	MC	50	40	368	400	65	-15	58	42	R	0.5	0.8	33	12	0.006	7.00	6.00	9.75
1/8/10	MC	40	30	340	352	60	-10	42	33	F	1.0	1.5	12	0	0.006	10.25	13.50	11.25
1/8/10	MC	30	20	360	364	55	-7	33	12	F	1.0	2.0						
1/8/10	MC	20	10	328	324	50	-6	12	0	DH	2.5	4.5						
1/8/10	MC	10	0	292	296	45	-5											
1/8/10	MC					40	-5											
1/8/10	MC					35	-4											
1/8/10	MC					30	-3											
1/8/10	MC					25	-3											
1/8/10	MC					20	-2											
1/8/10	MC					15	-2											
1/8/10	MC					10	-2											
1/8/10	MC					5	-1											
1/8/10	MC					0	-1											
1/8/10	DL	94	84	171	157	94	-15	94	87	R	0.1	0.1	94	80	0.023	4.25	4.75	4.75

Date	Site	Snow depth (cm)		ρ_{s1} (kg/m^3)	ρ_{s2} (kg/m^3)	T_d (cm)	T_s (^oC)	Strat. Layer (cm)		Crystal Type	Size (mm)		Layer (cm)		Disc rad. (m)	Force (N)		
1/8/10	DL	84	74	169	181	90	-18	87	80	R	0.2	0.2	80	49	0.006	6.00	5.00	3.25
1/8/10	DL	74	64	276	227	85	-19	80	70	R	0.2	0.3	49	28	0.006	8.00	6.75	6.25
1/8/10	DL	64	54	290	286	80	-16	70	57	R	0.2	0.3	28	0	0.006	6.75	4.25	6.75
1/8/10	DL	54	44	337	378	75	-14	57	49	R	0.2	0.4						
1/8/10	DL	44	34	365	326	70	-11	49	28	F	1.0	1.5						
1/8/10	DL	34	24	313	255	65	-8	28	0	F	2.0	4.0						
1/8/10	DL	24	14	314	385	60	-7											
1/8/10	DL	14	4	304	292	55	-5											
1/8/10	DL					50	-4											
1/8/10	DL					45	-3											
1/8/10	DL					40	-3											
1/8/10	DL					35	-3											
1/8/10	DL					30	-3											
1/8/10	DL					25	-2											
1/8/10	DL					20	-2											
1/8/10	DL					15	-2											
1/8/10	DL					10	-1											
1/8/10	DL					5	-1											
1/8/10	DL					0	-1											
1/8/10	WC	85	75	136	143	85	-12	85	78	N-->F	0.2	0.5	85	64	0.023	4.00	3.75	5.00
1/8/10	WC	75	65	151	153	80	-12	78	64	N-->F	0.5	1.0	64	48	0.011	6.25	6.00	5.75
1/8/10	WC	65	55	182	181	75	-16	64	48	R	0.2	0.3	48	25	0.011	4.25	4.50	4.75
1/8/10	WC	55	45	219	235	70	-15	48	25	F	0.5	1.0	25	0	0.011	4.50	4.25	3.75
1/8/10	WC	45	35	255	253	65	-13	25	0	F/DH	2.0	4.0						
1/8/10	WC	35	25	248	234	60	-10											
1/8/10	WC	25	15	241	230	55	-7											
1/8/10	WC	15	5	256	268	50	-6											
1/8/10	WC	10	0	224	228	45	-4											
1/8/10	WC					40	-4											
1/8/10	WC					35	-3											
1/8/10	WC					30	-3											
1/8/10	WC					25	-2											
1/8/10	WC					20	-2											
1/8/10	WC					15	-2											
1/8/10	WC					10	-1											
1/8/10	WC					5	-1											
1/8/10	WC					0	-1											
2/5/10	MC	100	90	124	100	100	-12	100	91	N	1.0	1.5	100	91	0.023	0.00	0.00	0.00
2/5/10	MC	90	80	303	276	95	-8	91	80	F	0.3	0.5	91	80	0.006	36.00	36.00	24.00
2/5/10	MC	80	70	307	302	90	-9	80	63	F-->R	0.2	0.5	80	63	0.011	17.00	17.00	19.00
2/5/10	MC	70	60	352	375	85	-9	63	52	F-->R	0.2	0.5	63	52	0.011	27.00	24.00	19.00
2/5/10	MC	60	50	339	358	80	-9	52	30	F	1.0	1.5	52	30	0.011	15.00	17.00	26.00
2/5/10	MC	50	40	363	329	75	-8	30	0	F	2.0	2.5	30	0	0.011	34.00	39.00	22.00
2/5/10	MC	40	30	336	343	70	-7						30	0	0.011	75.00	78.00	61.00
2/5/10	MC	30	20	373	354	65	-6											

Date	Site	Snow depth (cm)		ρ_{s1} (kg/m^3)	ρ_{s2} (kg/m^3)	T_d (cm)	T_s (^oC)	Strat. Layer (cm)		Crystal Type	Size (mm)		Layer (cm)		Disc rad. (m)	Force (N)		
2/5/10	MC	20	10	339	359	60	-6											
2/5/10	MC	10	0	305	337	55	-6											
2/5/10	MC					50	-5											
2/5/10	MC					45	-5											
2/5/10	MC					40	-5											
2/5/10	MC					35	-4											
2/5/10	MC					30	-4											
2/5/10	MC					25	-4											
2/5/10	MC					20	-3											
2/5/10	MC					15	-3											
2/5/10	MC					10	-3											
2/5/10	MC					5	-3											
2/5/10	MC					0	-2											
2/5/10	DL	103	93	116	126	103	-5	103	98	N	0.5	1.0	103	98	0.023	0.00	0.00	0.00
2/5/10	DL	100	90	173	162	100	-5	98	75	N-->F	0.2	0.5	98	75	0.023	18.25	20.25	19.00
2/5/10	DL	90	80	226	216	95	-8	75	61	F-->R	0.2	0.5	75	61	0.011	8.00	10.50	10.50
2/5/10	DL	80	70	275	285	90	-8	61	50	F-->R	1.0	1.5	61	50	0.011	57.00	40.00	46.00
2/5/10	DL	70	60	328	383	85	-8	50	30	F-->R	0.5	1.0	50	30	0.011	40.00	20.00	24.00
2/5/10	DL	60	50	392	361	80	-7	30	0	F/DH	2.0	3.5	30	0	0.011	30.00	24.00	39.00
2/5/10	DL	50	40	385	336	75	-7											
2/5/10	DL	40	30	341	351	70	-6											
2/5/10	DL	30	20	331	355	65	-6											
2/5/10	DL	20	10	275	322	60	-6											
2/5/10	DL	10	0	236	212	55	-5											
2/5/10	DL					50	-5											
2/5/10	DL					45	-5											
2/5/10	DL					40	-4											
2/5/10	DL					35	-4											
2/5/10	DL					30	-3											
2/5/10	DL					25	-3											
2/5/10	DL					20	-3											
2/5/10	DL					15	-3											
2/5/10	DL					10	-3											
2/5/10	DL					5	-2											
2/5/10	DL					0	-2											
2/5/10	WC	114	104	93	100	114	-4	114	107	N	1.0	2.0	114	107	0.023	0.00	0.00	0.00
2/5/10	WC	110	100	127	128	110	-4	107	83	F-->R	0.5	1.0	107	80	0.011	9.00	9.25	8.75
2/5/10	WC	100	90	242	229	105	-4	83	80	SH/F	0.5	1.5	80	60	0.011	8.75	9.75	13.00
2/5/10	WC	90	80	250	258	100	-5	80	60	F-->R	0.5	1.0	60	50	0.011	20.00	20.50	22.50
2/5/10	WC	80	70	285	283	95	-7	60	50	R	0.2	0.5	50	30	0.011	17.50	23.50	16.00
2/5/10	WC	70	60	305	294	90	-7	50	30	F	1.0	1.5	30	0	0.011	8.50	8.75	9.00
2/5/10	WC	60	50	340	342	85	-7	30	0	DH	2.0	4.0						
2/5/10	WC	50	40	320	324	80	-6											
2/5/10	WC	40	30	356	365	75	-5											
2/5/10	WC	30	20	296	299	70	-5											

Date	Site	Snow depth (cm)		ρ_{s1} (kg/m^3)	ρ_{s2} (kg/m^3)	T_d (cm)	T_s (°C)	Strat. Layer (cm)		Crystal Type	Size (mm)		Layer (cm)		Disc rad. (m)	Force (N)		
2/5/10	WC	20	10	269	280	65	-4											
2/5/10	WC	10	0	240	252	60	-4											
2/5/10	WC					55	-4											
2/5/10	WC					50	-3											
2/5/10	WC					45	-3											
2/5/10	WC					40	-3											
2/5/10	WC					35	-3											
2/5/10	WC					30	-3											
2/5/10	WC					25	-3											
2/5/10	WC					20	-2											
2/5/10	WC					15	-2											
2/5/10	WC					10	-2											
2/5/10	WC					5	-2											
2/5/10	WC					0	-1											
3/12/10	MC	134	124	68	62	134	-2	134	121	N	2.0	4.0	134	121	0.023	5.25	2.50	0.00
3/12/10	MC	130	120	89	82	130	-2	121	100	R	0.5	1.0	121	100	0.006	8.75	16.75	12.25
3/12/10	MC	120	110	270	302	125	-5	100	77	R	1.0	1.5	100	77	0.006	12.75	10.25	6.50
3/12/10	MC	110	100	325	324	120	-5	77	61	R	1.0	2.0	77	61	0.006	17.25	7.00	9.00
3/12/10	MC	100	90	368	329	115	-6	61	36	F	1.0	2.0	61	36	0.011	19.75	16.25	18.50
3/12/10	MC	90	80	334	332	110	-6	36	0	DH	2.0	4.0	36	0	0.006	16.25	18.00	8.25
3/12/10	MC	80	70	366	370	105	-6											
3/12/10	MC	70	60	385	370	100	-6											
3/12/10	MC	60	50	382	355	90	-5											
3/12/10	MC	50	40	362	343	80	-5											
3/12/10	MC	40	30	370	352	70	-5											
3/12/10	MC	30	20	406	336	60	-4											
3/12/10	MC	20	10	349	338	50	-4											
3/12/10	MC	10	0	300	280	40	-4											
3/12/10	MC					30	-3											
3/12/10	MC					25	-3											
3/12/10	MC					20	-3											
3/12/10	MC					15	-3											
3/12/10	MC					10	-2											
3/12/10	MC					5	-2											
3/12/10	MC					0	-2											
3/12/10	DL	140	130	99	79	140	-4	140	131	N	2.0	4.0	140	131	0.023	3.25	3.00	2.75
3/12/10	DL	130	120	173	139	135	-4	131	112	N-->R	1.0	1.5	131	112	0.011	3.25	4.00	3.25
3/12/10	DL	120	110	221	234	130	-5	112	87	R	0.5	1.0	112	87	0.011	13.00	15.25	16.75
3/12/10	DL	110	100	310	314	125	-5	87	55	R	0.5	1.0	87	55	0.006	8.75	18.00	11.75
3/12/10	DL	100	90	338	342	120	-5	55	50	R	0.5	1.0	50	30	0.006	11.50	7.50	11.75
3/12/10	DL	90	80	345	341	115	-5	50	30	F	1.0	1.5	30	15	0.011	21.50	15.00	13.75
3/12/10	DL	80	70	364	369	110	-5	30	15	F	2.0	2.5	15	0	0.006	14.00	18.00	20.00
3/12/10	DL	70	60	341	370	100	-5	15	0	DH	2.0	4.0						
3/12/10	DL	60	50	382	400	90	-5											
3/12/10	DL	50	40	398	379	80	-4											

Date	Site	Snow depth (cm)		ρ_{s1} (kg/m^3)	ρ_{s2} (kg/m^3)	T_d (cm)	T_s (^{o}C)	Strat. Layer (cm)		Crystal Type	Size (mm)		Layer (cm)		Disc rad. (m)	Force (N)		
3/12/10	DL	40	30	384	350	70	-4											
3/12/10	DL	30	20	376	370	60	-4											
3/12/10	DL	20	10	312	313	50	-4											
3/12/10	DL	10	0	320	352	40	-3											
3/12/10	DL					30	-3											
3/12/10	DL					25	-3											
3/12/10	DL					20	-3											
3/12/10	DL					15	-3											
3/12/10	DL					10	-2											
3/12/10	DL					5	-2											
3/12/10	DL					0	-2											
3/12/10	WC	143	133	89	84	143	-2	143	127	N	2.0	4.0	143	127	0.023	2.75	2.75	2.75
3/12/10	WC	140	130	110	107	135	-1	127	110	N-->R	1.0	1.5	127	110	0.011	6.25	6.75	6.00
3/12/10	WC	130	120	186	184	130	-3	110	109	Ice/F	1.0	2.0	109	63	0.006	9.00	8.50	9.00
3/12/10	WC	120	110	197	196	125	-4	109	63	R	1.0	1.5	63	40	0.006	5.50	5.00	5.25
3/12/10	WC	110	100	239	235	120	-5	63	40	R	1.0	2.0	40	25	0.006	7.00	7.75	7.25
3/12/10	WC	100	90	272	261	115	-5	40	25	F	1.0	2.0	25	0	0.006	3.00	3.25	2.50
3/12/10	WC	90	80	302	307	110	-4	25	0	DH	2.0	4.0						
3/12/10	WC	80	70	311	299	105	-4											
3/12/10	WC	70	60	341	333	100	-4											
3/12/10	WC	60	50	315	310	95	-4											
3/12/10	WC	50	40	338	330	90	-4											
3/12/10	WC	40	30	356	331	80	-4											
3/12/10	WC	30	20	317	305	70	-3											
3/12/10	WC	20	10	266	290	60	-3											
3/12/10	WC	10	0	236	244	50	-3											
3/12/10	WC					40	-3											
3/12/10	WC					30	-2											
3/12/10	WC					25	-2											
3/12/10	WC					20	-2											
3/12/10	WC					15	-2											
3/12/10	WC					10	-2											
3/12/10	WC					5	-1											
3/12/10	WC					0	-1											
4/16/10	MC	140	130	383	348	140	0	140	139	R	1.0	2.0	140	129	0.011	16.00	14.75	17.50
4/16/10	MC	130	120	398	418	130	-2	139	129	R	0.5	1.0	129	100	0.011	20.00	16.00	15.00
4/16/10	MC	120	110	412	358	120	-2	129	100	R	0.5	1.0	100	93	0.011	27.00	33.00	50.00
4/16/10	MC	110	100	483	460	110	-1	100	93	R	1.0	1.5	93	60	0.011	24.00	14.00	20.00
4/16/10	MC	100	90	406	450	100	-1	93	60	R	1.0	2.0	60	40	0.011	13.00	14.00	11.00
4/16/10	MC	90	80	502	414	90	-1	60	40	R	1.0	2.0	40	0	0.011	8.00	9.50	5.50
4/16/10	MC	80	70	448	411	80	-1	40	0	F-->R	1.5	2.5						
4/16/10	MC	70	60	432	423	70	-1											
4/16/10	MC	60	50	484	442	60	-1											
4/16/10	MC	50	40	437	428	50	-1											
4/16/10	MC	40	30	447	454	40	-1											

Date	Site	Snow depth (cm)		ρ_{s1} (kg/m^3)	ρ_{s2} (kg/m^3)	T_d (cm)	T_s (°C)	Strat. Layer (cm)		Crystal Type	Size (mm)		Layer (cm)		Disc rad. (m)	Force (N)		
4/16/10	MC	30	20	426	432	30	-1											
4/16/10	MC	20	10	385	475	20	-1											
4/16/10	MC	10	0	324	380	10	-1											
4/16/10	MC					0	-1											
4/16/10	DL	150	140	364	369	150	0	150	147	R	1.0	2.0	150	147	0.011	8.50	9.50	5.00
4/16/10	DL	140	130	428	398	140	-2	147	137	R	1.0	1.5	147	136	0.011	60.00	50.00	36.00
4/16/10	DL	130	120	384	388	130	-2	137	136	Ice layer	-	-	136	131	0.011	65.00	72.00	75.00
4/16/10	DL	120	110	378	374	120	-1	136	131	R	1.0	1.5	131	85	0.011	22.00	24.00	15.00
4/16/10	DL	110	100	404	438	110	-1	131	85	R	1.0	1.5	85	67	0.011	38.00	36.00	37.00
4/16/10	DL	100	90	409	481	100	-1	85	67	R	1.0	1.5	67	40	0.011	20.00	19.00	15.00
4/16/10	DL	90	80	384	383	90	-1	67	40	R	1.0	1.5	40	0	0.011	8.00	9.00	7.00
4/16/10	DL	80	70	422	394	80	-1	40	10	F-->R	2.0	4.0						
4/16/10	DL	70	60	451	417	70	-1	10	0	F-->R	2.0	4.0						
4/16/10	DL	60	50	414	399	60	-1											
4/16/10	DL	50	40	383	365	50	-1											
4/16/10	DL	40	30	402	387	40	-1											
4/16/10	DL	30	20	372	349	30	-1											
4/16/10	DL	20	10	305	309	20	-1											
4/16/10	DL	10	0	280	320	10	-1											
4/16/10	DL					0	-1											
4/16/10	WC	130	120	396	405	130	-1	130	121	R	1.0	2.0	130	121	0.011	31.00	19.00	21.00
4/16/10	WC	120	110	409	395	120	-2	121	119	IL	-	-	121	106	0.011	6.25	4.25	9.25
4/16/10	WC	110	100	378	348	110	-1	119	106	R	0.5	1.0	106	100	0.011	10.75	8.50	13.75
4/16/10	WC	100	90	361	395	100	-1	106	105	IL	-	-	100	75	0.011	11.00	10.00	12.00
4/16/10	WC	90	80	386	375	90	-1	105	100	R	1.0	1.5	75	40	0.011	5.00	6.75	6.25
4/16/10	WC	80	70	414	420	80	-1	100	98	IL	-	-	40	0	0.011	3.75	4.00	4.75
4/16/10	WC	70	60	420	411	70	-1	98	75	R	0.2	0.5						
4/16/10	WC	60	50	375	394	60	-1	75	73	R	-	-						
4/16/10	WC	50	40	379	377	50	-1	73	40	IL	1.0	1.5						
4/16/10	WC	40	30	383	383	40	-1	40	0	F-->R	2.0	4.0						
4/16/10	WC	30	20	364	393	30	-1											
4/16/10	WC	20	10	348	337	20	-1											
4/16/10	WC	10	0	284	312	10	-1											
4/16/10	WC					0	-1											

Table B-4. Standard ram penetrometer data for Muddy Creek, Dumont Lakes, and Walton Creek near Rabbit Ears Pass, Colorado during the 2009-2010 winter season.

Date	Site	Tube weight (kg)	Hammer weight (kg)	Tube and hammer T+H (kg)	# of falls n	Fall height f (cm)	Location of point L (cm)	Penetration *p* (cm)	*(nfH)/p* (kg)	RN (kg)	RR (N)	Height above ground (cm)
12/11/09	MC											48
12/11/09	MC	1	0	1	0	0	39	39	0	1	10	9
12/11/09	MC	1	0.5	1.5	0	0	39	0				9
12/11/09	MC	1	0.5	1.5	10	1	39	0				9
12/11/09	MC	1	0.5	1.5	15	5	40	1	38	39	390	8
12/11/09	MC	1	1	2	0	0	40	0				8
12/11/09	MC	1	1	2	10	5	41	1	50	52	520	7
12/11/09	MC	1	1	2	10	10	45	4	25	27	270	3
12/11/09	MC	1	1	2	5	15	48	3	25	27	270	0
12/11/09	DL											34
12/11/09	DL	1	0	1	0	0	34	34	0	1	10	0
12/11/09	WC											35
12/11/09	WC	1	0	1	0	0	35	35	0	1	10	0
1/8/10	MC											79
1/8/10	MC	1	0	1	0	0	24	32	0	1	10	55
1/8/10	MC	1	0.5	1.5	0	0	24	0				55
1/8/10	MC	1	0.5	1.5	5	5	24	0				55
1/8/10	MC	1	0.5	1.5	10	10	26	2	25	27	265	53
1/8/10	MC	1	0.5	1.5	10	20	30	4	25	27	265	49
1/8/10	MC	1	1	2	0	0	30	0				49
1/8/10	MC	1	1	2	10	5	31	1	50	52	520	48
1/8/10	MC	1	1	2	9	10	37	6	15	17	170	42
1/8/10	MC	1	1	2	4	5	50	13	2	4	35	29
1/8/10	MC	1	1	2	6	5	55	33	1	3	29	24
1/8/10	MC	1	1	2	10	10	64	9	11	13	131	15
1/8/10	MC	1	1	2	3	15	79	15	3	5	50	0
1/8/10	DL											85
1/8/10	DL	1	0	1	0	0	32	32	0	1	10	53
1/8/10	DL	1	0.5	1.5	0	0	32	0				53
1/8/10	DL	1	0.5	1.5	6	5	33	1	15	17	165	52
1/8/10	DL	1	0.5	1.5	7	10	35	2	18	19	190	50
1/8/10	DL	1	1	2	0	0	35	0				50
1/8/10	DL	1	1	2	10	5	40	5	10	12	120	45
1/8/10	DL	1	1	2	5	10	58	18	3	5	48	27
1/8/10	DL	1	1	2	6	5	82	24	1	3	33	3
1/8/10	DL	1	1	2	7	10	85	3	23	25	253	0
1/8/10	WC											88
1/8/10	WC	1	0	1	0	0	43	43	0	1	10	45
1/8/10	WC	1	0.5	1.5	0	0	43	0				45
1/8/10	WC	1	0.5	1.5	9	5	88	45	1	2	20	0
2/5/10	MC											101
2/5/10	MC	1	0	1	0	0	12	12	0	1	10	89
2/5/10	MC	1	0.5	1.5	0	0	12	0				89
2/5/10	MC	1	0.5	1.5	3	5	12	0				89
2/5/10	MC	1	0.5	1.5	12	20	17	5	24	26	255	84

Date	Site	Tube weight (kg)	Hammer weight (kg)	Tube and hammer T+H (kg)	# of falls n	Fall height f (cm)	Location of point L (cm)	Penetration *p* (cm)	*(nfH)/p* (kg)	RN (kg)	RR (N)	Height above ground (cm)
2/5/10	MC	1	0.5	1.5	6	30	20	3	30	32	315	81
2/5/10	MC	1	0.5	1.5	8	40	24	4	40	42	415	77
2/5/10	MC	1	1	2	0	0	24	0				77
2/5/10	MC	1	1	2	6	5	25	1	30	32	320	76
2/5/10	MC	1	1	2	19	10	40	15	13	15	147	61
2/5/10	MC	1	1	2	15	5	55	15	5	7	70	46
2/5/10	MC	2	0	2	0	0	55	0				46
2/5/10	MC	2	0.5	2.5	0	0	55	0				46
2/5/10	MC	2	0.5	2.5	5	5	56	1	13	15	150	45
2/5/10	MC	2	1	3	0	0	56	0				45
2/5/10	MC	2	1	3	10	5	64	8	6	9	93	37
2/5/10	MC	2	1	3	14	10	80	16	9	12	118	21
2/5/10	MC	2	1	3	13	20	90	10	26	29	290	11
2/5/10	MC	2	1	3	15	30	101	11	41	44	439	0
2/5/10	DL											108
2/5/10	DL	1	0	1	0	0	36	36	0	1	10	72
2/5/10	DL	1	0.5	1.5	0	0	36	0				72
2/5/10	DL	1	0.5	1.5	5	5	37	1	13	14	140	71
2/5/10	DL	1	0.5	1.5	5	10	40	3	8	10	98	68
2/5/10	DL	1	0.5	1.5	6	20	41	1	60	62	615	67
2/5/10	DL	1	1	2	0	0	41	0				67
2/5/10	DL	1	1	2	9	5	42	1	45	47	470	66
2/5/10	DL	1	1	2	6	10	43	1	60	62	620	65
2/5/10	DL	1	1	2	4	20	44	1	80	82	820	64
2/5/10	DL	1	1	2	9	30	53	9	30	32	320	55
2/5/10	DL	2	0	2	0	0	53	0				55
2/5/10	DL	2	1	3	0	0	53	0				55
2/5/10	DL	2	1	3	8	5	56	3	13	16	163	52
2/5/10	DL	2	1	3	28	10	80	24	12	15	147	28
2/5/10	DL	2	1	3	6	5	87	7	4	7	73	21
2/5/10	DL	2	1	3	18	10	100	13	14	17	168	8
2/5/10	DL	2	1	3	5	5	106	6	4	7	72	2
2/5/10	DL	2	1	3	5	10	108	2	25	28	280	0
2/5/10	WC											117
2/5/10	WC	1	0	1	0	0	39	36	0	1	10	78
2/5/10	WC	1	0.5	1.5	0	0	39	0				78
2/5/10	WC	1	0.5	1.5	17	5	49	10	4	6	58	68
2/5/10	WC	1	0.5	1.5	10	10	55	6	8	10	98	62
2/5/10	WC	1	0.5	1.5	16	20	65	10	16	18	175	52
2/5/10	WC	2	0	2	0	0	65	0				52
2/5/10	WC	2	0.5	2.5	0	0	65	0				52
2/5/10	WC	2	0.5	2.5	12	10	66	1	60	63	625	51
2/5/10	WC	2	0.5	2.5	5	20	74	8	6	9	88	43
2/5/10	WC	2	0.5	2.5	15	10	80	6	13	15	150	37
2/5/10	WC	2	0.5	2.5	12	20	84	4	30	33	325	33

Date	Site	Tube weight (kg)	Hammer weight (kg)	Tube and hammer T+H (kg)	# of falls n	Fall height f (cm)	Location of point L (cm)	Penetration *p* (cm)	*(nfH)/p* (kg)	RN (kg)	RR (N)	Height above ground (cm)
2/5/10	WC	2	0.5	2.5	6	30	87	3	30	33	325	30
2/5/10	WC	2	0.5	2.5	2	20	90	3	7	9	92	27
2/5/10	WC	2	0.5	2.5	4	10	117	27	1	3	32	0
3/12/10	MC											136
3/12/10	MC	1	0	1	0	0	18	18	0	1	10	118
3/12/10	MC	1	0.5	1.5	0	0	18	0				118
3/12/10	MC	1	0.5	1.5	20	5	19	1	50	52	515	117
3/12/10	MC	1	0.5	1.5	13	10	20	1	65	67	665	116
3/12/10	MC	1	0.5	1.5	6	20	21	1	60	62	615	115
3/12/10	MC	1	0.5	1.5	18	30	26	5	54	56	555	110
3/12/10	MC	1	0.5	1.5	6	40	32	6	20	22	215	104
3/12/10	MC	1	0.5	1.5	14	20	45	13	11	12	123	91
3/12/10	MC	1	0.5	1.5	21	10	60	15	7	9	85	76
3/12/10	MC	2	0	2	0	0	60	0				76
3/12/10	MC	2	0.5	2.5	0	0	60	0				76
3/12/10	MC	2	0.5	2.5	12	5	61	1	30	33	325	75
3/12/10	MC	2	0.5	2.5	17	10	65	4	21	24	238	71
3/12/10	MC	2	0.5	2.5	11	10	71	6	9	12	117	65
3/12/10	MC	2	0.5	2.5	7	20	72	1	70	73	725	64
3/12/10	MC	2	0.5	2.5	5	30	73	1	75	78	775	63
3/12/10	MC	2	0.5	2.5	11	40	76	3	73	76	758	60
3/12/10	MC	2	0.5	2.5	8	50	82	6	33	36	358	54
3/12/10	MC	2	0.5	2.5	13	40	95	13	20	23	225	41
3/12/10	MC	2	0.5	2.5	16	50	126	31	13	15	154	10
3/12/10	MC	2	0.5	2.5	7	30	130	4	26	29	288	6
3/12/10	MC	2	0.5	2.5	19	50	136	6	79	82	817	0
3/12/10	DL											147
3/12/10	DL	1	0	1	0	0	36	36	0	1	10	111
3/12/10	DL	1	0.5	1.5	0	0	36	0				111
3/12/10	DL	1	0.5	1.5	22	5	37	1	55	57	565	110
3/12/10	DL	1	0.5	1.5	20	20	41	4	50	52	515	106
3/12/10	DL	1	0.5	1.5	42	30	64	23	27	29	289	83
3/12/10	DL	2	0	2	0	0	64	0				83
3/12/10	DL	2	0.5	2.5	0	0	64	0				83
3/12/10	DL	2	0.5	2.5	10	5	65	1	25	28	275	82
3/12/10	DL	2	0.5	2.5	12	10	67	2	30	33	325	80
3/12/10	DL	2	0.5	2.5	15	20	74	7	21	24	239	73
3/12/10	DL	2	0.5	2.5	12	30	79	5	36	39	385	68
3/12/10	DL	2	0.5	2.5	12	40	88	9	27	29	292	59
3/12/10	DL	2	0.5	2.5	10	30	95	7	21	24	239	52
3/12/10	DL	2	0.5	2.5	14	40	106	11	25	28	280	41
3/12/10	DL	2	0.5	2.5	4	30	124	18	3	6	58	23
3/12/10	DL	2	0.5	2.5	19	20	147	23	8	11	108	0
3/12/10	WC											143
3/12/10	WC	1	0	1	0	0	35	35	0	1	10	108

Date	Site	Tube weight (kg)	Hammer weight (kg)	Tube and hammer T+H (kg)	# of falls n	Fall height f (cm)	Location of point L (cm)	Penetration *p* (cm)	*(nfH)/p* (kg)	RN (kg)	RR (N)	Height above ground (cm)
3/12/10	WC	1	0.5	1.5	0	0	35	0				108
3/12/10	WC	1	0.5	1.5	20	5	44	9	6	7	71	99
3/12/10	WC	1	0.5	1.5	22	10	57	13	8	10	100	86
3/12/10	WC	2	0	2	0	0	57	0				86
3/12/10	WC	2	0.5	2.5	0	0	57	0				86
3/12/10	WC	2	0.5	2.5	10	5	58	1	25	28	275	85
3/12/10	WC	2	0.5	2.5	7	10	60	2	18	20	200	83
3/12/10	WC	2	0.5	2.5	12	20	66	6	20	23	225	77
3/12/10	WC	2	0.5	2.5	3	30	70	4	11	14	138	73
3/12/10	WC	2	0.5	2.5	7	10	73	3	12	14	142	70
3/12/10	WC	2	0.5	2.5	8	20	76	3	27	29	292	67
3/12/10	WC	2	0.5	2.5	5	30	82	6	13	15	150	61
3/12/10	WC	2	0.5	2.5	5	5	84	2	6	9	88	59
3/12/10	WC	2	0.5	2.5	18	10	96	12	8	10	100	47
3/12/10	WC	2	0.5	2.5	7	20	100	4	18	20	200	43
3/12/10	WC	2	0.5	2.5	9	30	110	10	14	16	160	33
3/12/10	WC	2	0.5	2.5	1	20	143	33	0	3	28	0
4/16/10	MC											141
4/16/10	MC	1	0	1	0	0	7	7	0	1	10	134
4/16/10	MC	1	0.5	1.5	0	0	7	0				134
4/16/10	MC	1	0.5	1.5	10	5	9	2	13	14	140	132
4/16/10	MC	1	0.5	1.5	5	10	10	1	25	27	265	131
4/16/10	MC	1	0.5	1.5	7	20	12	2	35	37	365	129
4/16/10	MC	1	0.5	1.5	7	30	13	1	105	107	1065	128
4/16/10	MC	1	0.5	1.5	20	50	17	4	125	127	1265	124
4/16/10	MC	1	1	2	0	0	17	0				124
4/16/10	MC	1	1	2	15	20	20	3	100	102	1020	121
4/16/10	MC	1	1	2	10	40	23	3	133	135	1353	118
4/16/10	MC	1	1	2	6	50	31	8	38	40	395	110
4/16/10	MC	1	1	2	3	5	34	3	5	7	70	107
4/16/10	MC	1	0.5	1.5	0	0	34	0				107
4/16/10	MC	1	0.5	1.5	24	10	50	16	8	9	90	91
4/16/10	MC	1	0.5	1.5	27	20	70	20	14	15	150	71
4/16/10	MC	2	0	2	0	0	70	0				71
4/16/10	MC	2	0.5	2.5	0	0	70	0				71
4/16/10	MC	2	0.5	2.5	8	20	73	3	27	29	292	68
4/16/10	MC	2	0.5	2.5	12	30	79	6	30	33	325	62
4/16/10	MC	2	0.5	2.5	2	40	80	1	40	43	425	61
4/16/10	MC	2	0.5	2.5	26	50	115	35	19	21	211	26
4/16/10	MC	2	0.5	2.5	6	5	120	5	3	6	55	21
4/16/10	MC	2	0.5	2.5	1	10	137	17	0	3	28	4
4/16/10	MC	2	0.5	2.5	5	5	138	1	13	15	150	3
4/16/10	MC	2	0.5	2.5	9	10	139	1	45	48	475	2
4/16/10	MC	2	0.5	2.5	7	20	141	2	35	38	375	0
4/16/10	DL											152

Date	Site	Tube weight (kg)	Hammer weight (kg)	Tube and hammer T+H (kg)	# of falls n	Fall height f (cm)	Location of point L (cm)	Penetration *p* (cm)	*(nfH)/p* (kg)	RN (kg)	RR (N)	Height above ground (cm)
4/16/10	DL	1	0	1	0	0	6	6	0	1	10	146
4/16/10	DL	1	0.5	1.5	0	0	6	0				146
4/16/10	DL	1	0.5	1.5	10	10	12	6	8	10	98	140
4/16/10	DL	1	0.5	1.5	5	20	13	1	50	52	515	139
4/16/10	DL	1	0.5	1.5	6	30	14	1	90	92	915	138
4/16/10	DL	1	0.5	1.5	5	40	15	1	100	102	1015	137
4/16/10	DL	1	1	2	0	0	15	0				137
4/16/10	DL	1	1	2	14	20	17	2	140	142	1420	135
4/16/10	DL	1	1	2	11	40	30	13	34	36	358	122
4/16/10	DL	1	1	2	1	10	32	2	5	7	70	120
4/16/10	DL	1	1	2	1	5	35	3	2	4	37	117
4/16/10	DL	1	0.5	1.5	0	0	35	0				117
4/16/10	DL	1	0.5	1.5	14	10	42	7	10	12	115	110
4/16/10	DL	1	0.5	1.5	10	20	46	4	25	27	265	106
4/16/10	DL	1	0.5	1.5	21	30	70	24	13	15	146	82
4/16/10	DL	2	0	2	0	0	70	0				82
4/16/10	DL	2	0.5	2.5	0	0	70	0				82
4/16/10	DL	2	0.5	2.5	3	20	71	1	30	33	325	81
4/16/10	DL	2	0.5	2.5	10	30	76	5	30	33	325	76
4/16/10	DL	2	0.5	2.5	20	40	89	13	31	33	333	63
4/16/10	DL	2	0.5	2.5	6	50	93	4	38	40	400	59
4/16/10	DL	2	0.5	2.5	5	20	94	1	50	53	525	58
4/16/10	DL	2	0.5	2.5	14	40	108	14	20	23	225	44
4/16/10	DL	2	0.5	2.5	12	5	112	4	8	10	100	40
4/16/10	DL	2	0.5	2.5	10	10	115	3	17	19	192	37
4/16/10	DL	2	0.5	2.5	12	20	120	5	24	27	265	32
4/16/10	DL	2	0.5	2.5	6	30	151	31	3	5	54	1
4/16/10	DL	2	0.5	2.5	6	5	152	1	15	18	175	0
4/16/10	WC											132
4/16/10	WC	1	0	1	0	0	6	6	0	1	10	126
4/16/10	WC	1	0.5	1.5	6	5	10	4	4	5	53	122
4/16/10	WC	1	0.5	1.5	9	10	13	3	15	17	165	119
4/16/10	WC	1	0.5	1.5	7	20	41	28	3	4	40	91
4/16/10	WC	2	0	2	17	5	47	6	0	2	20	85
4/16/10	WC	2	0.5	2.5	45	10	70	23	10	12	123	62
4/16/10	WC	2	0.5	2.5	0	0	70	0				62
4/16/10	WC	2	0.5	2.5	0	0	70	0				62
4/16/10	WC	2	0.5	2.5	15	5	83	13	3	5	54	49
4/16/10	WC	2	0.5	2.5	5	10	85	2	13	15	150	47
4/16/10	WC	2	0.5	2.5	9	20	132	47	2	4	44	0

Table B-5. Raw data collected at the snow compaction study plot at Fraser Experimental Forest, Colorado during the 2009-2010 winter season.

Date	Trt.	Snow depth (cm)		ρ_{s1} (kg/m^3)	ρ_{s2} (kg/m^3)	T_d (cm)	T_s (°C)	Strat. Layer (cm)		Crystal Type	Size (mm)		Layer (cm)		Disc rad. (m)	Force (N)		
12/27/09	1	27	17	136	136	27	-13	27	21	N-->R	1.0	1.0	27	12	0.023	7.50	5.75	8.25
12/27/09	1	17	7	324	312	25	-15	21	12	F	1.0	2.0	12	0	0.006	18.00	20.00	19.75
12/27/09	1	10	0	292	284	20	-7	12	5	F-->R	1.0	1.5						
12/27/09	1					15	-7	5	0	F	2.0	4.0						
12/27/09	1					10	-6											
12/27/09	1					5	-5											
12/27/09	1					0	-5											
12/27/09	2	24	14	164	164	24	-11	24	16	N-->F	0.2	0.5	24	12	0.023	5.75	3.00	2.50
12/27/09	2	14	4	344	328	20	-9	16	12	F	1.0	3.0	12	0	0.003	14.50	12.00	12.75
12/27/09	2					15	-7	12	0	F	1.0	1.5						
12/27/09	2					10	-6											
12/27/09	2					5	-5											
12/27/09	2					0	-4											
12/27/09	3	37	27	140	128	37	-15	37	31	N-->F	1.0	3.0	37	17	0.023	3.00	3.75	3.50
12/27/09	3	27	17	204	188	35	-16	31	17	N-->F	0.2	0.5	17	0	0.023	4.25	4.00	5.00
12/27/09	3	17	7	128	140	30	-13	17	0	F/DH	4.0	6.0						
12/27/09	3	10	0	116	116	25	-11											
12/27/09	3					20	-10											
12/27/09	3					15	-9											
12/27/09	3					10	-6											
12/27/09	3					5	-5											
12/27/09	3					0	-4											
12/27/09	4	19	9	176	164	19	-15	19	12	N-->F	0.2	0.5	19	9	0.023	0.00	0.00	0.00
12/27/09	4	10	0	348	312	15	-8	12	9	F	1.0	1.5	9	0	0.003	9.00	13.00	11.50
12/27/09	4					10	-7	9	0	F-->R	0.5	1.0						
12/27/09	4					5	-6											
12/27/09	4					0	-5											
12/27/09	5	38	28	132	144	38	-15	38	30	N-->F	0.5	1.0	38	17	0.023	3.75	3.25	4.00
12/27/09	5	28	18	208	200	35	-15	30	17	F	0.2	0.5	17	0	0.023	4.25	2.75	2.75
12/27/09	5	18	8	164	168	30	-13	17	0	F-->DH	2.0	4.0						
12/27/09	5	10	0	148	156	25	-12											
12/27/09	5					20	-11											
12/27/09	5					15	-9											
12/27/09	5					10	-7											
12/27/09	5					5	-7											
12/27/09	5					0	-5											
12/27/09	5																	
1/22/10	1	30	20	260	288	30	-6	30	26	N-->R	0.2	0.5	30	13	0.006	42.00	53.00	59.00
1/22/10	1	20	10	372	332	25	-6	26	13	F	0.5	1.0	13	0	0.006	38.00	33.00	37.00
1/22/10	1	10	0	256	316	20	-7	13	0	F	1.0	1.5						
1/22/10	1					15	-6											
1/22/10	1					10	-6											
1/22/10	1					5	-6											
1/22/10	1					0	-5											
1/22/10	2	20	10	312	312	20	-5	20	16	N-->F	0.2	0.5	20	10	0.006	32.00	41.00	51.00

Date	Trt.	Snow depth (cm)		ρ_{s1} (kg/m^3)	ρ_{s2} (kg/m^3)	T_d (cm)	T_s (^{o}C)	Strat. Layer (cm)		Crystal Type	Size (mm)		Layer (cm)		Disc rad. (m)	Force (N)		
1/22/10	2	10	0	312	324	15	-6	16	10	F	1.0	1.5	10	0	0.006	45.00	63.00	50.00
1/22/10	2					10	-6	10	0	F	1.0	3.0						
1/22/10	2					5	-6											
1/22/10	2					0	-6											
1/22/10	3	43	33	148	164	43	-3	43	28	N-->F	0.2	0.5	43	28	0.023	2.50	2.75	2.75
1/22/10	3	40	30	212	212	40	-5	28	13	F	1.0	2.0	28	13	0.023	3.50	3.75	2.50
1/22/10	3	30	20	208	224	35	-7	13	0	F/DH	2.0	4.0	13	0	0.023	0.00	0.00	0.00
1/22/10	3	20	10	220	244	30	-5											
1/22/10	3	10	0	184	180	25	-5											
1/22/10	3					20	-5											
1/22/10	3					15	-5											
1/22/10	3					10	-4											
1/22/10	3					5	-4											
1/22/10	3					0	-4											
1/22/10	4	28	18	316	320	19	-5	28	26	N-->F	0.2	0.5	28	8	0.003	61.00	36.00	61.00
1/22/10	4	20	10	384	372	15	-8	26	8	F	1.0	1.5	8	0	0.003	33.00	30.00	29.00
1/22/10	4	10	0	340	316	10	-7	8	0	F	1.0	2.0						
1/22/10	4					5	-6											
1/22/10	4					0	-5											
1/22/10	4																	
1/22/10	5	50	40	152	148	50	-3	50	45	N-->F	0.2	0.5	50	31	0.023	3.00	2.50	2.50
1/22/10	5	40	30	196	176	45	-6	45	31	F	1.0	1.5	31	15	0.023	6.25	7.00	6.50
1/22/10	5	30	20	208	208	40	-6	31	15	F	1.5	2.5	15	0	0.023	5.25	4.00	4.00
1/22/10	5	20	10	200	220	35	-6	15	0	DH	2.5	4.5						
1/22/10	5	10	0	168	172	30	-6											
1/22/10	5					25	-5											
1/22/10	5					20	-5											
1/22/10	5					15	-5											
1/22/10	5					10	-4											
1/22/10	5					5	-3											
1/22/10	5					0	-3											
2/12/10	1	45	35	108	160	45	-3	45	35	N	1.0	1.5	45	35	0.023	0.00	0.00	0.00
2/12/10	1	40	30	284	284	40	-7	35	16	F-->R	0.5	1.0	35	16	0.006	60.00	60.00	67.00
2/12/10	1	30	20	392	388	35	-8	16	0	F	1.5	2.5	16	0	0.006	35.00	60.00	51.00
2/12/10	1	20	10	352	348	30	-7											
2/12/10	1	10	0	308	332	25	-7											
2/12/10	1					20	-6											
2/12/10	1					15	-6											
2/12/10	1					10	-5											
2/12/10	1					5	-5											
2/12/10	1					0	-5											
2/12/10	2	46	36	128	124	46	-1	46	36	N	0.2	0.5	46	36	0.023	0.00	0.00	0.00
2/12/10	2	40	30	288	304	40	-6	36	25	F-->R	1.0	1.5	36	25	0.006	60.00	64.00	46.00
2/12/10	2	30	20	384	376	35	-7	25	0	F	1.0	3.0	25	0	0.006	45.00	36.00	44.00
2/12/10	2	20	10	380	392	30	-7											

Date	Trt.	Snow depth (cm)		ρ_{s1} (kg/m^3)	ρ_{s2} (kg/m^3)	T_d (cm)	T_s (^oC)	Strat. Layer (cm)		Crystal Type	Size (mm)		Layer (cm)		Disc rad. (m)	Force (N)		
2/12/10	2	10	0	360	372	25	-6											
2/12/10	2					20	-6											
2/12/10	2					15	-6											
2/12/10	2					10	-5											
2/12/10	2					5	-5											
2/12/10	2					0	-4											
2/12/10	3	57	47	100	120	57	-1	57	39	N	1.0	2.5	57	39	0.023	0.00	0.00	0.00
2/12/10	3	50	40	176	184	50	-5	39	25	F	1.0	2.0	39	25	0.023	4.50	3.75	4.00
2/12/10	3	40	30	188	188	45	-8	25	0	DH	3.0	5.0	25	0	0.023	5.00	4.50	4.00
2/12/10	3	30	20	188	196	40	-7											
2/12/10	3	20	10	240	220	35	-7											
2/12/10	3	10	0	152	168	30	-6											
2/12/10	3					25	-6											
2/12/10	3					20	-5											
2/12/10	3					15	-5											
2/12/10	3					10	-4											
2/12/10	3					5	-3											
2/12/10	3					0	-3											
2/12/10	4	43	33	104	116	43	-2	43	33	N	1.0	1.5	43	33	0.023	0.00	0.00	0.00
2/12/10	4	40	30	336	300	35	-5	33	20	F-->R	0.5	1.5	33	20	0.006	85.00	74.00	70.00
2/12/10	4	30	20	368	336	30	-6	20	11	F-->R	1.0	1.5	20	11	0.003	33.00	44.00	28.00
2/12/10	4	20	10	352	356	25	-6	11	0	F	1.0	2.0	11	0	0.003	39.00	35.00	34.00
2/12/10	4	10	0	304	324	20	-6											
2/12/10	4					15	-6											
2/12/10	4					10	-5											
2/12/10	4					5	-5											
2/12/10	4					0	-4											
2/12/10	5	65	55	96	100	65	-1	65	46	N	1.0	1.5	65	46	0.023	2.75	2.50	0.00
2/12/10	5	60	50	148	136	60	-4	46	20	F	1.5	2.5	46	20	0.023	4.25	4.25	4.00
2/12/10	5	50	40	196	192	55	-7	20	0	DH	4.0	6.0	20	0	0.023	4.50	3.50	4.50
2/12/10	5	40	30	208	208	50	-7											
2/12/10	5	30	20	212	192	45	-7											
2/12/10	5	20	10	196	196	40	-7											
2/12/10	5	10	0	208	180	35	-6											
2/12/10	5					30	-5											
2/12/10	5					25	-5											
2/12/10	5					20	-4											
2/12/10	5					15	-3											
2/12/10	5					10	-3											
2/12/10	5					5	-3											
2/12/10	5					0	-3											
3/26/10	1	53	43	212	248	53	-1	53	48	N-->R	0.5	1.0	53	48	0.011	8.25	9.75	6.75
3/26/10	1	50	40	364	396	50	0	48	45	F-->I	1.0	2.0	48	45	0.006	58.00	36.00	42.00
3/26/10	1	40	30	344	372	45	-7	45	31	F-->R	1.0	2.0	45	31	0.006	82.00	78.00	64.00
3/26/10	1	30	20	348	354	40	-5	31	22	F	1.0	1.5	31	22	0.011	29.00	29.00	63.00

Date	Trt.	Snow depth (cm)		ρ_{s1} (kg/m^3)	ρ_{s2} (kg/m^3)	T_d (cm)	T_s (°C)	Strat. Layer (cm)		Crystal Type	Size (mm)		Layer (cm)		Disc rad. (m)	Force (N)		
3/26/10	1	20	10	344	336	35	-5	22	0	F	1.0	1.5	22	0	0.011	74.00	73.00	71.00
3/26/10	1	10	0	352	300	30	-4											
3/26/10	1					25	-4											
3/26/10	1					20	-4											
3/26/10	1					15	-3											
3/26/10	1					10	-3											
3/26/10	1					5	-2											
3/26/10	1					0	-2											
3/26/10	2	54	44	172	144	54	-2	54	46	N-->F	0.2	0.5	54	46	0.006	3.25	3.50	3.25
3/26/10	2	50	40	368	368	50	-1	46	33	F-->R	0.2	0.5	46	33	0.003	66.00	70.00	53.00
3/26/10	2	40	30	380	442	45	-7	33	17	F	1.0	1.5	33	17	0.006	28.00	32.00	21.00
3/26/10	2	30	20	425	406	40	-7	17	0	F	2.0	3.0	17	0	0.006	52.00	63.00	66.00
3/26/10	2	20	10	380	411	35	-6											
3/26/10	2	10	0	388	380	30	-6											
3/26/10	2					25	-5											
3/26/10	2					20	-4											
3/26/10	2					15	-4											
3/26/10	2					10	-4											
3/26/10	2					5	-4											
3/26/10	2					0	-4											
3/26/10	3	73	63	204	184	73	-1	73	68	N-->F	0.5	1.0	73	68	0.023	0.00	0.00	0.00
3/26/10	3	70	60	248	218	70	0	68	64	F-->I	1.0	1.5	68	64	0.006	20.00	34.00	24.00
3/26/10	3	60	50	312	300	65	-7	64	48	F	1.0	1.5	64	48	0.011	7.25	7.75	8.00
3/26/10	3	50	40	268	244	60	-7	48	35	F	1.0	2.0	48	35	0.023	16.50	14.25	16.00
3/26/10	3	40	30	232	232	55	-7	35	15	F	1.0	2.0	35	15	0.023	4.50	5.25	6.50
3/26/10	3	30	20	220	236	50	-6	15	0	DH	8.0	10.0	15	0	0.023	8.75	13.75	9.75
3/26/10	3	20	10	228	232	45	-6											
3/26/10	3	10	0	228	212	40	-6											
3/26/10	3					35	-5											
3/26/10	3					30	-4											
3/26/10	3					25	-4											
3/26/10	3					20	-3											
3/26/10	3					15	-3											
3/26/10	3					10	-2											
3/26/10	3					5	-2											
3/26/10	3					0	-2											
3/26/10	4	50	40	180	200	50	-2	50	42	N-->F	0.5	1.0	50	42	0.023	3.75	3.50	3.25
3/26/10	4	40	30	453	447	45	-4	42	35	F	0.5	1.0	42	35	0.001	81.00	87.00	91.00
3/26/10	4	30	20	418	419	40	-5	35	16	F	1.0	1.5	35	16	0.003	23.00	29.00	28.00
3/26/10	4	20	10	411	409	35	-6	16	0	F	1.0	2.0	16	0	0.003	35.00	38.00	38.00
3/26/10	4	10	0	284	280	30	-5											
3/26/10	4					25	-5											
3/26/10	4					20	-5											
3/26/10	4					15	-4											
3/26/10	4					10	-4											

Date	Trt.	Snow depth (cm)		ρ_{s1} (kg/m^3)	ρ_{s2} (kg/m^3)	T_d (cm)	T_s (^{o}C)	Strat. Layer (cm)		Crystal Type	Size (mm)		Layer (cm)		Disc rad. (m)	Force (N)		
3/26/10	4					5	-3											
3/26/10	4					0	-3											
3/26/10	5	80	70	196	172	80	-1	80	73	N-->F	0.5	1.0	80	73	0.023	3.50	4.25	3.75
3/26/10	5	70	60	240	272	75	-4	73	69	F-->I	1.0	2.0	73	69	0.006	48.00	31.00	32.00
3/26/10	5	60	50	272	320	70	-6	69	37	F	1.0	1.5	69	37	0.011	4.75	5.75	7.00
3/26/10	5	50	40	228	232	65	-7	37	17	F	2.0	4.0	37	17	0.011	4.25	3.25	5.75
3/26/10	5	40	30	184	212	60	-7	17	0	DH	8.0	10.0	17	0	0.011	5.25	5.25	8.00
3/26/10	5	30	20	224	228	55	-6											
3/26/10	5	20	10	228	220	50	-6											
3/26/10	5	10	0	240	280	45	-5											
3/26/10	5					40	-5											
3/26/10	5					35	-5											
3/26/10	5					30	-4											
3/26/10	5					25	-4											
3/26/10	5					20	-3											
3/26/10	5					15	-3											
3/26/10	5					10	-2											
3/26/10	5					5	-2											
3/26/10	5					0	-2											
4/26/10	1	28	18	176	172	28	0	28	21	N	1.0	1.5	28	21	0.023	2.75	4.50	3.00
4/26/10	1	20	10	336	380	25	-1	21	14	F-->R	1.0	1.5	21	14	0.011	5.00	5.25	5.75
4/26/10	1	10	0	436	460	20	-1	14	0	F-->R	1.0	2.0	14	0	0.011	72.00	74.00	49.00
4/26/10	1					15	-1											
4/26/10	1					10	-1											
4/26/10	1					5	-1											
4/26/10	1					0	-1											
4/26/10	2	35	25	212	208	35	0	35	27	N	1.0	1.5	35	27	0.023	4.75	6.50	3.50
4/26/10	2	30	20	296	268	30	-2	27	21	F-->R	0.5	1.0	27	21	0.011	4.50	3.25	3.25
4/26/10	2	20	10	412	376	25	-1	21	0	F-->R	2.0	4.0	21	0	0.006	67.00	71.00	61.00
4/26/10	2	10	0	444	428	20	-1											
4/26/10	2					15	-1											
4/26/10	2					10	-1											
4/26/10	2					5	-1											
4/26/10						0	-1											
4/26/10	3	40	30	180	196	40	-1	40	34	N-->R	1.0	1.5	40	34	0.023	3.00	3.25	0.00
4/26/10	3	30	20	320	352	35	-1	34	25	F-->R	1.0	2.0	34	25	0.011	4.50	7.25	3.25
4/26/10	3	20	10	416	404	30	-1	25	0	F-->R	2.0	6.0	25	0	0.023	14.50	13.25	8.50
4/26/10	3	10	0	308	328	25	-1											
4/26/10	3					20	-1											
4/26/10	3					15	-1											
4/26/10	3					10	-1											
4/26/10	3					5	-1											
4/26/10	3					0	-1											
4/26/10	4	40	30	200	188	40	-1	40	34	N-->R	1.0	1.5	40	34	0.023	5.25	6.50	5.75
4/26/10	4	30	20	404	376	35	-1	34	26	F-->R	0.2	0.5	34	26	0.011	8.75	4.75	7.25

Date	Trt.	Snow depth (cm)		ρ_{s1} (kg/m^3)	ρ_{s2} (kg/m^3)	T_d (cm)	T_s (°C)	Strat. Layer (cm)		Crystal Type	Size (mm)		Layer (cm)		Disc rad. (m)	Force (N)		
4/26/10	4	20	10	404	392	30	-1	26	0	F-->R	2.0	4.0	26	0	0.003	27.00	37.00	31.00
4/26/10	4	10	0	368	396	25	-1											
4/26/10	4					20	-1											
4/26/10	4					15	-1											
4/26/10	4					10	-1											
4/26/10	4					5	-1											
4/26/10						0	-1											
4/26/10	5	45	35	204	216	45	-1	45	40	N-->R	1.0	1.5	45	40	0.023	3.00	4.00	3.00
4/26/10	5	40	30	356	328	40	-1	40	32	F-->R	1.0	1.5	40	32	0.011	3.00	4.00	4.75
4/26/10	5	30	20	380	348	35	-1	32	0	F-->R	4.0	8.0	32	0	0.023	8.00	8.50	6.00
4/26/10	5	20	10	380	352	30	-1											
4/26/10	5	10	0	320	336	25	-1											
4/26/10	5					20	-1											
4/26/10	5					15	-1											
4/26/10	5					10	-1											
4/26/10	5					5	-1											
4/26/10	5					0	-1											

Table B-6. Standard ram penetrometer data collected at the snow compaction study plot at Fraser Experimental Forest, Colorado during the 2009-2010 winter season.

Date	Trt.	Tube weight (kg)	Hammer weight (kg)	Tube and hammer T+H (kg)	# of falls n	Fall height f (cm)	Location of point L (cm)	Penetration *p* (cm)	*(nfH)/p* (kg)	RN (kg)	RR (N)	Height above ground (cm)
12/27/09	1											27
12/27/09	1	1	0	1	0	0	15	15	0	1	10	12
12/27/09	1	1	0.5	1.5	0	0	15	0				12
12/27/09	1	1	0.5	1.5	7	5	16	1	18	19	190	11
12/27/09	1	1	0.5	1.5	10	10	17	1	50	52	515	10
12/27/09	1	1	1	2	0	0	17	0				10
12/27/09	1	1	1	2	10	10	20	3	33	35	353	7
12/27/09	1	1	1	2	13	20	27	7	37	39	391	0
12/27/09	2											26
12/27/09	2	1	0	1	0	0	17	17	0	1	10	9
12/27/09	2	1	0.5	1.5	0	0	17	0				9
12/27/09	2	1	0.5	1.5	10	5	18	1	25	27	265	8
12/27/09	2	1	0.5	1.5	10	10	18	0				8
12/27/09	2	1	1	2	0	0	18	0				8
12/27/09	2	1	1	2	10	5	20	2	25	27	270	6
12/27/09	2	1	1	2	10	10	21	1	100	102	1020	5
12/27/09	2	1	1	2	9	20	26	5	36	38	380	0
12/27/09	3											36
12/27/09	3	1	0	1	0	0	36	36	0	1	10	0
12/27/09	4											22
12/27/09	4	1	0	1	0	0	14	17	0	1	10	8
12/27/09	4	1	0.5	1.5	10	20	15	1	100	102	1015	7
12/27/09	4	1	1	2	0	0	15	0				7
12/27/09	4	1	1	2	10	5	16	1	50	52	520	6
12/27/09	4	1	1	2	16	10	18	2	80	82	820	4
12/27/09	4	1	1	2	12	20	22	4	60	62	620	0
12/27/09	5											42
12/27/09	5	1	0	1	0	0	42	42	0	1	10	0
1/22/10	1											28
1/22/10	1	1	0	1	0	0	6	6	0	1	10	22
1/22/10	1	1	0.5	1.5	0	0	6	0				22
1/22/10	1	1	0.5	1.5	3	5	6	0				22
1/22/10	1	1	1	2	0	0	6	0				22
1/22/10	1	1	1	2	5	5	7	1	25	27	270	21
1/22/10	1	1	1	2	10	10	9	2	50	52	520	19
1/22/10	1	1	1	2	10	20	12	3	67	69	687	16
1/22/10	1	1	1	2	13	30	18	6	65	67	670	10
1/22/10	1	1	1	2	18	20	28	10	36	38	380	0
1/22/10	2											22
1/22/10	2	1	0	1	0	0	5	5	0	1	10	17
1/22/10	2	1	0.5	1.5	0	0	5	0				17
1/22/10	2	1	0.5	1.5	5	5	6	1	13	14	140	16
1/22/10	2	1	1	2	0	0	6	0				16
1/22/10	2	1	1	2	4	5	6	0				16
1/22/10	2	1	1	2	5	10	7	1	50	52	520	15

Date	Trt.	Tube weight (kg)	Hammer weight (kg)	Tube and hammer T+H (kg)	# of falls n	Fall height f (cm)	Location of point L (cm)	Penetration *p* (cm)	*(nfH)/p* (kg)	RN (kg)	RR (N)	Height above ground (cm)
1/22/10	2	1	1	2	5	20	8	1	100	102	1020	14
1/22/10	2	1	1	2	7	30	10	2	105	107	1070	12
1/22/10	2	1	1	2	11	40	18	8	55	57	570	4
1/22/10	2	1	1	2	4	30	22	4	30	32	320	0
1/22/10	3											49
1/22/10	3	1	0	1	0	0	49	49	0	1	10	0
1/22/10	4											28
1/22/10	4	1	0	1	0	0	5	5	0	1	10	23
1/22/10	4	1	1	2	0	0	5	0				23
1/22/10	4	1	1	2	10	10	8	3	33	35	353	20
1/22/10	4	1	1	2	7	20	10	2	70	72	720	18
1/22/10	4	2	1	3	6	30	12	2	90	93	930	16
1/22/10	4	2	1	3	8	40	15	3	107	110	1097	13
1/22/10	4	2	1	3	25	50	26	11	114	117	1166	2
1/22/10	4	2	1	3	5	40	28	2	100	103	1030	0
1/22/10	5											50
1/22/10	5	1	0	1	0	0	50	50	0	1	10	0
2/12/10	1											48
2/12/10	1	1	0	1	0	0	13	6	0	1	10	35
2/12/10	1	1	1	2	0	0	13	0				35
2/12/10	1	1	1	2	10	5	14	1	50	52	520	34
2/12/10	1	1	1	2	17	20	20	6	57	59	587	28
2/12/10	1	1	1	2	17	30	27	7	73	75	749	21
2/12/10	1	1	1	2	5	40	31	4	50	52	520	17
2/12/10	1	1	1	2	5	30	36	5	30	32	320	12
2/12/10	1	1	1	2	8	20	42	6	27	29	287	6
2/12/10	1	1	1	2	8	10	46	4	20	22	220	2
2/12/10	1	1	1	2	10	5	48	2	25	27	270	0
2/12/10	2											45
2/12/10	2	1	0	1	0	0	14	5	0	1	10	31
2/12/10	2	1	1	2	0	0	14	0				31
2/12/10	2	1	1	2	9	5	16	2	23	25	245	29
2/12/10	2	1	1	2	15	10	20	4	38	40	395	25
2/12/10	2	1	1	2	4	20	23	3	27	29	287	22
2/12/10	2	1	1	2	7	10	25	2	35	37	370	20
2/12/10	2	1	1	2	7	20	27	2	70	72	720	18
2/12/10	2	1	1	2	20	30	36	9	67	69	687	9
2/12/10	2	1	1	2	13	20	43	7	37	39	391	2
2/12/10	2	1	1	2	8	10	45	2	40	42	420	0
2/12/10	3											63
2/12/10	3	1	0	1	0	0	63	63	0	1	10	0
2/12/10	4											45
2/12/10	4	1	0	1	0	0	12	5	0	1	10	33
2/12/10	4	1	1	2	0	0	12	0				33
2/12/10	4	1	1	2	12	10	14	2	60	62	620	31

Date	Trt.	Tube weight (kg)	Hammer weight (kg)	Tube and hammer T+H (kg)	# of falls n	Fall height f (cm)	Location of point L (cm)	Penetration *p* (cm)	*(nfH)/p* (kg)	RN (kg)	RR (N)	Height above ground (cm)
2/12/10	4	1	1	2	9	20	16	2	90	92	920	29
2/12/10	4	1	1	2	20	30	24	8	75	77	770	21
2/12/10	4	1	1	2	10	40	27	3	133	135	1353	18
2/12/10	4	1	1	2	38	50	39	12	158	160	1603	6
2/12/10	4	1	1	2	3	40	41	2	60	62	620	4
2/12/10	4	1	1	2	6	30	44	3	60	62	620	1
2/12/10	4	1	1	2	8	40	45	1	320	322	3220	0
2/12/10	5											65
2/12/10	5	1	0	1	0	0	65	65	0	1	10	0
3/26/10	1											55
3/26/10	1	1	0	1	0	0	8	8	0	1	10	47
3/26/10	1	1	1	2	0	0	8	0				47
3/26/10	1	1	1	2	10	5	10	2	25	27	270	45
3/26/10	1	1	1	2	8	10	11	1	80	82	820	44
3/26/10	1	1	1	2	13	40	17	6	87	89	887	38
3/26/10	1	1	1	2	10	20	20	3	67	69	687	35
3/26/10	1	1	1	2	25	30	32	12	63	65	645	23
3/26/10	1	1	1	2	13	50	40	8	81	83	833	15
3/26/10	1	1	1	2	32	20	55	15	43	45	447	0
3/26/10	2											55
3/26/10	2	1	0	1	0	0	9	9	0	1	10	46
3/26/10	2	1	1	2	0	0	9	0				46
3/26/10	2	1	1	2	4	10	10	1	40	42	420	45
3/26/10	2	1	1	2	11	30	13	3	110	112	1120	42
3/26/10	2	1	1	2	26	50	27	14	93	95	949	28
3/26/10	2	1	1	2	9	40	34	7	51	53	534	21
3/26/10	2	1	1	2	31	20	48	14	44	46	463	7
3/26/10	2	1	1	2	10	30	53	5	60	62	620	2
3/26/10	2	1	1	2	5	40	55	2	100	102	1020	0
3/26/10	3											82
3/26/10	3	1	0	1	0	0	9	9	0	1	10	73
3/26/10	3	1	0.5	1.5	0	0	9	0				73
3/26/10	3	1	0.5	1.5	6	5	10	1	15	17	165	72
3/26/10	3	1	0.5	1.5	5	10	13	3	8	10	98	69
3/26/10	3	1	0.5	1.5	6	5	22	9	2	3	32	60
3/26/10	3	1	0.5	1.5	9	10	27	5	9	11	105	55
3/26/10	3	1	0.5	1.5	2	20	82	55	0	2	19	0
3/26/10	4											54
3/26/10	4	1	0	1	0	0	10	10	0	1	10	44
3/26/10	4	1	1	2	0	0	10	0				44
3/26/10	4	1	1	2	6	10	11	1	60	62	620	43
3/26/10	4	1	1	2	7	20	12	1	140	142	1420	42
3/26/10	4	1	1	2	62	50	41	29	107	109	1089	13
3/26/10	4	1	1	2	17	40	53	12	57	59	587	1
3/26/10	4	1	1	2	3	50	54	1	150	152	1520	0

Date	Trt.	Tube weight (kg)	Hammer weight (kg)	Tube and hammer T+H (kg)	# of falls n	Fall height f (cm)	Location of point L (cm)	Penetration *p* (cm)	*(nfH)/p* (kg)	RN (kg)	RR (N)	Height above ground (cm)
3/26/10	5											80
3/26/10	5	1	0	1	0	0	10	10	0	1	10	70
3/26/10	5	1	0.5	1.5	0	0	10	0				70
3/26/10	5	1	0.5	1.5	10	10	12	2	25	27	265	68
3/26/10	5	1	0.5	1.5	3	5	80	68	0	2	16	0
4/26/10	1											31
4/26/10	1	1	0	1	0	0	15	15	0	1	10	16
4/26/10	1	1	1	2	0	0	15	0				16
4/26/10	1	1	1	2	20	30	30	15	40	42	420	1
4/26/10	1	1	1	2	3	40	31	1	120	122	1220	0
4/26/10	2											33
4/26/10	2	1	0	1	0	0	14	14	0	1	10	19
4/26/10	2	1	1	2	0	0	14	0				19
4/26/10	2	1	1	2	12	5	16	2	30	32	320	17
4/26/10	2	1	1	2	8	10	17	1	80	82	820	16
4/26/10	2	1	1	2	25	50	26	9	139	141	1409	7
4/26/10	2	1	1	2	4	30	30	4	30	32	320	3
4/26/10	2	1	1	2	6	20	31	1	120	122	1220	2
4/26/10	2	1	1	2	8	30	33	2	120	122	1220	0
4/26/10	3											37
4/26/10	3	1	0	1	0	0	19	19	0	1	10	18
4/26/10	3	1	0.5	1.5	0	0	19	0				18
4/26/10	3	1	0.5	1.5	1	5	37	18	0	2	16	0
4/26/10	4											40
4/26/10	4	1	0	1	0	0	17	17	0	1	10	23
4/26/10	4	1	0.5	1.5	0	0	17	0				23
4/26/10	4	1	0.5	1.5	18	5	18	1	45	47	465	22
4/26/10	4	1	1	2	0	0	18	0				22
4/26/10	4	1	1	2	9	10	20	2	45	47	470	20
4/26/10	4	1	1	2	21	20	30	10	42	44	440	10
4/26/10	4	1	1	2	10	30	34	4	75	77	770	6
4/26/10	4	1	1	2	15	40	40	6	100	102	1020	0
4/26/10	5											50
4/26/10	5	1	0	1	0	0	18	10	0	1	10	32
4/26/10	5	1	0.5	1.5	0	0	18	0				32
4/26/10	5	1	0.5	1.5	1	5	50	32	0	2	16	0